OXYTOCIN MEDIATES NEUROENDOCRINE REPROGRAMMING OF THE EPICARDIUM IN HEART REGENERATION

Ву

Aaron Howard Wasserman

A DISSERTATION

Submitted to
Michigan State University
in partial fulfillment of the requirements
for the degree of

Cell and Molecular Biology – Doctor of Philosophy

2022

ABSTRACT

Cardiovascular disease (CVD) is the leading cause of mortality in the United States and the rest of the developed world. Individuals with CVD often suffer massive heart injuries, leading to the loss of billions of cardiac muscle cells and associated vasculature. Critical work published in the last two decades demonstrated that these lost cells can be partially regenerated by the epicardium, the outermost mesothelial layer of the heart, in a process that highly recapitulates its role in heart development. Upon cardiac injury, mature epicardial cells activate and undergo an epithelial-to-mesenchymal transition (EMT) to form epicardium-derived progenitor cells (EpiPCs), multipotent progenitors that can differentiate into several important cardiac lineages, including cardiomyocytes and vascular cells. In mammals, this process alone is insufficient for significant regeneration, but it may be possible to prime it by administering specific reprogramming factors, leading to enhanced EpiPC function.

Here, I differentiated a mature-like model of human induced pluripotent stem cell (hiPSC)-derived epicardial cells (hEpiCs) and used it to conduct a screening of 15 candidate neuroendocrine hormones that may be involved in the epicardial activation process. I identified oxytocin (OXT) as the compound that most strongly induced epicardial cell proliferation, EMT, and dedifferentiation to a progenitor-like state. In addition, I demonstrated that OXT is produced after cardiac cryoinjury in zebrafish, a naturally regenerating animal model. This increased OXT elicited significant epicardial activation, cardiomyocyte proliferation, and neovascularization, thereby promoting heart regeneration. I also found that oxytocin signaling was critical for proper epicardium development in zebrafish embryos. Finally, I differentiated a three-dimensional hiPSC-

derived human heart organoid (hHO) model and used it to develop a cryoinjury protocol that simulated cardiac injury. Again, I found that OXT induced cellular proliferation and epicardial activation, features that were consistent with a pro-regenerative phenotype.

Remarkably, all the above processes were significantly impaired when OXT signaling was inhibited chemically through receptor antagonism or genetically through RNA interference. RNA sequencing data suggested that the transforming growth factor beta (TGF-β) pathway was the primary mediator of OXT-induced epicardial activation. My research combines a naturally regenerating animal model with multiple *in vitro* models of the human heart to reveal for the first time an evolutionary conserved brain-controlled mechanism that induces cellular reprogramming and regeneration of the injured heart. These findings could yield significant translational advances for the treatment of cardiac injuries and CVD.

ACKNOWLEDGEMENTS

Carrying out a dissertation project and earning a Ph.D. is a highly collaborative process, and I am thankful to have had the help and support of numerous advisors, faculty members, lab mates, family, and friends throughout my journey. First off, I would like to thank my mentor, Dr. Aitor Aguirre, for giving me a home in his lab, allowing me to design a thesis based on my research passions, and pushing me to conduct great science every step of the way. I would also like to thank my graduate committee members (Dr. Kyle Miller, Dr. Sangbum Park, Dr. Amy Ralston, and Dr. Dana Spence) for their thoughtful contributions and guidance over the last few years and for ensuring that I stayed on track towards graduation. Special shout outs go to Dr. William Jackson for granting me ample access to his confocal microscope and to Dr. Assaf Gilad and the ADDRC (Assay Development and Drug Repurposing Core) for allowing me to use their automated cell imaging/counting equipment. Finally, I would like to express my gratitude towards Dr. Donna Koslowsky, Dr. Michael Bachmann, Dr. Steve DiCarlo, and Dr. Heidi Lujan for their lessons and advice on teaching, mentorship, and career planning, all of which have helped to make me a more well-rounded scientist.

Being a part of the Cell and Molecular Biology (CMB) graduate program at MSU has been a terrific experience. I am forever grateful to Dr. Susan Conrad for convincing me to join CMB at the start of my Ph.D. And I am especially appreciative of Dr. Peggy Petroff, the current director of the CMB program. I would like to thank her for always having my best interests at heart and for giving me support and encouragement throughout my time at MSU. Dr. Petroff has done an excellent job with the CMB program,

and it is in good hands with her. I would also like to thank Alaina Burghardt for her tireless dedication to CMB, it has been a pleasure to work with her.

On a personal level, the support I have received from my fellow lab mates has been instrumental towards my success. A special thank you goes to Mani, Amanda, and Yoni for helping me with cell/organoid culture, zebrafish work, experiments, and data analysis, and for being great friends. I would also like to thank Brett, Colin, Jesús, Kristen, Sasha, Priya, and Mishref for their suggestions and feedback and for making the Aguirre lab an enjoyable place to work. In addition, I would like to acknowledge McKenna and Allison for being enthusiastic and reliable undergraduate students and outstanding mentees. And a big shout out to all the graduate students, postdoctoral fellows, and staff members at the IQ institute whom I have had the pleasure of getting to know throughout my Ph.D. Finally, I would like to save the biggest and most important thank you for my family. Thank you to Mom and Dad for being an unconditional source of love and support while also challenging me to be my best self. Thank you to Ben and Eli for being amazing brothers and best friends and for making my life infinitely more enjoyable. And thank you to Annah for your endless words of encouragement and for always being there when I need someone to talk to. I love you all and I am so grateful to have you in my life!

TABLE OF CONTENTS

LIST OF TABLES	viii
LIST OF FIGURES	ix
LIST OF ABBREVIATIONS	xii
Chapter 1: Introduction	1
1.1: Background on cardiovascular disease and cardiac regeneration	1
1.2: The epicardium is a source of cardiac progenitor cells	
1.3: The neuroendocrine signaling axis affects regeneration	13
1.4: Induced pluripotent stem cells have numerous applications in pred	clinical
research	15
Chapter 2: Materials and Methods	20
2.1: Stem cell culture	
2.2: hiPSC differentiation to hiPSC-derived epicardial cells (hEpiCs)	
2.3: hiPSC lentiviral transduction	
2.4: hiPSC differentiation to hiPSC-derived human heart organoids (hi	
2.5: Organoid maturation and cryoinjury	
2.6: Organoid single-cell dissociation	
2.7: Zebrafish cardiac cryoinjury/injections	27
2.8: Zebrafish embryo experiments	
2.9: Gene expression analysis	30
2.10: RNA sequencing	31
2.11: Sample preparation for histology/immunofluorescence	32
2.12: Histology	32
2.13: Immunofluorescence	
2.14: Confocal microscopy and image analysis	
2.15: Statistical analysis	37
Chapter 3: Oxytocin Induces a Pro-Regenerative Phenotype in hiPSC-Do	erived
Epicardial Cells	
3.1: Introduction	
3.2: Results	
3.3: Discussion	
3.4: Future Directions	
Chapter 4: Oxytocin Signaling is Necessary for Heart Regeneration in	
Zebrafish	84
4.1: Introduction	
4.2: Results.	
4.3: Discussion	
4.4: Future Directions	

Chapter 5: Oxytocin Induces a Pro-Regenerative Phenotype in	
Three-Dimensional Human Heart Organoids	118
5.1: Introduction	118
5.2: Results	120
5.3: Discussion	139
5.4: Future Directions	140
Chapter 6: Conclusions and Perspectives	142
6.1: Main Findings	142
6.2: Limitations	
6.3: Significance and Broader Implications	145

LIST OF TABLES

Table 2.1: Step-by-step protocol for lentiviral production and hiPSC transduction	23
Table 3.1: Neuroendocrine candidate list for screening in hEpiCs	56

LIST OF FIGURES

Figure 1.1: Overview of epicardial activation	11
Figure 1.2: Overview of epithelial-to-mesenchymal transition	12
Figure 1.3: Applications of induced pluripotent stem cells (iPSCs)	19
Figure 2.1: Plasmids used for short hairpin RNA (shRNA)-mediated knockdown of <i>OXTR</i> in hiPSCs	22
Figure 2.2: Schematic of protocol used for hHO differentiation	25
Figure 2.3: Schematic of protocol used for hHO cryoinjury	26
Figure 2.4: Overview of zebrafish cardiac cryoinjury	29
Figure 2.5: Overview of immunofluorescence protocol	35
Figure 3.1: Schematic of protocol used for hEpiC differentiation	42
Figure 3.2: hEpiCs display epithelial cell morphology	43
Figure 3.3: hEpiCs express epicardial cell markers	44
Figure 3.4: Differentiating hEpiCs increase expression of epicardial markers	45
Figure 3.5: Matured hEpiCs retain their epithelial nature	46
Figure 3.6: Matured hEpiCs do not undergo EMT	46
Figure 3.7: Matured hEpiCs decrease their proliferation rates	47
Figure 3.8: Matured hEpiCs display a quiescent transcriptional phenotype short-term	48
Figure 3.9: Matured hEpiCs display a quiescent transcriptional phenotype long-term	49
Figure 3.10: Neuroendocrine screening results	57
Figure 3.11: OXT induces hEpiC proliferation	60
Figure 3.12: OXT displays more potent effects than thymosin β4	61
Figure 3.13: 100 nM OXT induces optimal hEpiC proliferation	62

Figure 3.14: Vitamin C masks the proliferative effects of OXT	62
Figure 3.15: OXT induces hEpiC activation	64
Figure 3.16: Identification of differentially expressed genes	67
Figure 3.17: Gene ontology analysis	68
Figure 3.18: OXT increases expression of TGF- β and BMP signaling markers	69
Figure 3.19: OXT acts through a receptor-mediated mechanism	73
Figure 3.20: hEpiCs do not express AVP receptors	74
Figure 3.21: hEpiCs express OXT receptor	75
Figure 3.22: Confirmation of successful <i>OXTR</i> knockdown	76
Figure 3.23: OXTR knockdown prevents hEpiC proliferation in response to OXT	77
Figure 3.24: OXTR knockdown does not affect hEpiC differentiation efficiency	78
Figure 3.25: OXTR knockdown prevents hEpiC activation in response to OXT	79
Figure 3.26: OXTR analogs increase hEpiC proliferation	80
Figure 4.1: Cardiac cryoinjury induces OXT release	87
Figure 4.2: Cardiac cryoinjury induces epicardial activation	87
Figure 4.3: Cardiac cryoinjury induces OXTR expression	88
Figure 4.4: OXTR inhibition increases myocardial scar size	91
Figure 4.5: OXTR inhibition increases fibrosis accumulation	92
Figure 4.6: OXTR inhibition decreases expression of EpiPC markers	95
Figure 4.7: OXTR inhibition decreases epicardial activation	96
Figure 4.8: OXTR inhibition decreases epicardial proliferation	97
Figure 4.9: OXTR inhibition decreases expression of EMT markers	98
Figure 4.10: OXTR inhibition decreases cardiomyocyte proliferation	. 101

Figure 4.11: OXTR inhibition decreases cardiomyocyte proliferation	102
Figure 4.12: OXTR inhibition decreases vasculature formation	103
Figure 4.13: OXTR inhibition increases oxytocin release	104
Figure 4.14: OXTR inhibition disrupts ventricular epicardium formation	108
Figure 4.15: OXTR inhibition disrupts ventricular epicardium formation	109
Figure 4.16: OXTR inhibition disrupts ventricular epicardium formation	110
Figure 4.17: OXTR inhibition disrupts atrial epicardium formation	111
Figure 4.18: OXTR inhibition disrupts epicardium formation	112
Figure 5.1: Visualization of cryoinjured organoids	124
Figure 5.2: Cryoinjury decreases nuclei staining in hHOs	124
Figure 5.3: Cryoinjury increases trypan blue staining in hHOs	125
Figure 5.4: Cryoinjury decreases cellular viability in hHOs	126
Figure 5.5: Cryoinjury increases cellular apoptosis in hHOs	127
Figure 5.6: Cryoinjury decreases hHO size	128
Figure 5.7: Cryoinjury does not affect extracellular matrix deposition in hHOs	129
Figure 5.8: OXTR knockdown decreases hHO size	133
Figure 5.9: OXTR knockdown decreases epicardial activity after cryoinjury	134
Figure 5.10: OXT induces modest cellular proliferation before OXTR knockdown	135
Figure 5.11: OXT does not induce cellular proliferation after OXTR knockdown	136
Figure 5.12: OXT induces modest epicardial activation before OXTR knockdown	137
Figure 5.13: OXT does not induce epicardial activation after OXTR knockdown	138
Figure 5.14: hHO maturation increases OXT production	139
Figure 6.1: Proposed model for neuroendocrine reprogramming of the epicardium in heart regeneration	143

LIST OF ABBREVIATIONS

ACTA2 Alpha Smooth Muscle Actin

ACTH Adrenocorticotropic Hormone

AJ Adherens Junction

AMPK 5' Adenosine Monophosphate-Activated Protein Kinase

ANOVA Analysis of Variance

ANP Atrial Natriuretic Peptide

AVP Arginine Vasopressin

AVPR Arginine Vasopressin Receptor

BDNF Brain-Derived Neurotrophic Factor

BM Basement Membrane

BMP Bone Morphogenetic Protein

BNP Brain Natriuretic Peptide

BSA Bovine Serum Albumin

CDC Centers for Disease Control and Prevention

CDH1 Cadherin 1/Epithelial Cadherin

cGMP Cyclic Guanosine Monophosphate

CHIR CHIR99021

CI Cryoinjury

CM Cardiomyocyte

CNN1 Calponin 1

CRISPR Clustered Regularly Interspaced Short Palindromic Repeats

CT Cycle Threshold

cTnl Cardiac Troponin I

cTnT Cardiac Troponin T

CVD Cardiovascular Disease

Cy3 Cyanine 3

DAG Diacylglycerol

DAPI 4'6-Diamidino-2-Phenylindole

DI H₂O Deionized Water

DMEM/F12 Dulbecco's Modified Eagle Medium/Nutrient Mixture F-12

DPF Days Post-Fertilization

DPI Days Post-Injury

DREADD Designer Receptor Exclusively Activated by Designer Drugs

EAT Epicardial Adipose Tissue

EC Endothelial Cell

ECM Extracellular Matrix

EDTA Ethylenediaminetetraacetic Acid

eGFP Enhanced Green Fluorescent Protein

ELISA Enzyme-Linked Immunosorbent Assay

EMT Epithelial-to-Mesenchymal Transition

EPI Epicardium

EpiC Epicardial Cell

EpiPC Epicardium-Derived Progenitor Cell

ERK Extracellular Signal-Regulated Kinase

ESC Embryonic Stem Cell

E8 Essential 8 Medium

FDR False Discovery Rate

FGF Fibroblast Growth Factor

FSTL1 Follistatin-Like 1

GDF15 Growth Differentiation Factor 15

GH Growth Hormone

GHIH Growth Hormone-Inhibiting Hormone/Somatostatin

GHRH Growth Hormone-Releasing Hormone

GO Gene Ontology

GPCR G Protein-Coupled Receptor

GSK Glycogen Synthase Kinase

HCM Hypertrophic Cardiomyopathy

HEK Human Embryonic Kidney

hEpiC Human iPSC-Derived Epicardial Cell

HGF Hepatocyte Growth Factor

hHO Human Heart Organoid

hiPSC Human Induced Pluripotent Stem Cell

HPF Hours Post-Fertilization

HUVEC Human Umbilical Vein Endothelial Cell

H3P Phosphorylated Histone H3

IA Injured Area

IGF Insulin-Like Growth Factor

IgG Immunoglobulin G

INHBB Inhibin Subunit Beta B

iPSC Induced Pluripotent Stem Cell

IP₃ Inositol Trisphosphate

I/R Ischemia-Reperfusion

JAK Janus Kinase

KCNQ1 Potassium Voltage-Gated Channel Subfamily Q Member 1

KLF4 Kruppel-Like Factor 4

LAD Left Anterior Descending

LB Luria-Bertani

LEFTY2 Left-Right Determination Factor 2

MCH Melanin-Concentrating Hormone

MC4R Melanocortin Receptor 4

MHC Myosin Heavy Chain

MI Myocardial Infarction

MS-222 Tricaine Methanesulfonate

MTZ Metronidazole

MYH1E Myosin Heavy Chain 1E

MYO Myocardium

NFAT Nuclear Factor of Activated T-Cells

NLS Nuclear Localization Signal

NO Nitric Oxide

NPY Neuropeptide Y

NTR Nitroreductase

NT5E 5'-Nucleotidase

OCT Optimal Cutting Temperature

OCT-4 Octamer-Binding Transcription Factor 4

OXT Oxytocin

OXTR Oxytocin Receptor

PACAP Pituitary Adenylate Cyclase Activating Polypeptide

PBS Phosphate-Buffered Saline

PCNA Proliferating Cell Nuclear Antigen

PDGF Platelet-Derived Growth Factor

PE/PEO Proepicardial Organ

PFA Paraformaldehyde

PI3K Phosphatidylinositol-3-Kinase

PKC Protein Kinase C

PLC Phospholipase C

PND Postnatal Day

POMC Pro-Opiomelanocortin

PORCN Porcupine O-Acyltransferase

PRL Prolactin

PVN Paraventricular Nucleus

qRT-PCR Quantitative Reverse Transcription Polymerase Chain Reaction

RALDH2 Retinaldehyde Dehydrogenase 2

RNA-Seq RNA Sequencing

ROCK Rho-Associated Protein Kinase

RPM Revolutions Per Minute

RPMI Roswell Park Memorial Institute

SB SB431542

SE Subepicardium

shOXTR OXTR Knockdown hEpiC/hHO Line

shRNA Short Hairpin RNA

SNAI Snail Family Transcriptional Repressor

SOX2 Sex Determining Region Y-Box Transcription Factor 2

STAT Signal Transducer and Activator of Transcription

TAC Trans-Ascending Aortic Constriction

TBX18 T-Box Transcription Factor 18

TCF21 Transcription Factor 21

TF Transcription Factor

TGF- β Transforming Growth Factor β

TJP1 Tight Junction Protein 1

TMEM100 Transmembrane Protein 100

TNNT2 Cardiac Troponin T

TRH Thyrotropin-Releasing Hormone

TSH Thyroid Stimulating Hormone

TZV Thiazovivin

VEGF Vascular Endothelial Growth Factor

VIM Vimentin

Vit. C Vitamin C

WT1 Wilms Tumor 1

ZO-1 Zonula Occludens 1

 $\alpha\text{-MSH} \qquad \quad \alpha\text{-Melanocyte Stimulating Hormone}$

 $\beta\text{-End} \qquad \quad \beta\text{-Endorphin}$

Chapter 1: Introduction

1.1: Background on cardiovascular disease and cardiac regeneration

Cardiovascular disease (CVD) is the leading cause of mortality in the United States and the rest of the developed world (Virani et al., 2020). According to the Centers for Disease Control and Prevention (CDC), ~20% of all deaths in the U.S. are attributable to heart disease, and CVD kills more people annually than respiratory disease, stroke, Alzheimer's disease, and diabetes combined. In addition, the direct medical costs of treating CVD are projected to increase steadily throughout the next decade to nearly 1 trillion dollars in 2030, an increase of ~200% since 2010 (Heidenreich et al., 2011; Knapper et al., 2015). Clearly, heart disease is a major public health problem that needs to be addressed, both in the clinic and via cutting-edge preclinical research. One of the major types of CVD that is of relevance to this project is myocardial infarction (MI), commonly known as a heart attack. MI occurs when blood flow to the heart is decreased or prevented entirely, typically due to an obstruction in one of the coronary vessels. If this impairment in perfusion lasts for long enough, the heart muscle underneath the vessel becomes ischemic due to a lack of blood and oxygen delivery to the infarcted area (Thygesen et al., 2018). Ultimately, the cardiomyocytes (CMs) in this region of the myocardium will be unable to produce sufficient ATP to sustain basic functions and will undergo necrosis and apoptosis in response (Heusch, 2020). A single MI can result in the loss of ~25% of CMs, which are the chief contractile cells of the heart. If left untreated, this condition can lead to heart failure (Laflamme & Murry, 2011).

In humans, the extreme loss of cardiomyocytes that occurs after MI is mostly permanent. Human CMs are terminally differentiated cells, and as such, their innate

regenerative capacity is extremely limited, with an annual physiological turnover of less than 1% (Bergmann et al., 2009). Recent evidence suggests that over half of adult human CMs are polyploid in nature, with some even containing multiple nuclei, thereby presenting natural barriers to mitosis and cytokinesis (Bergmann et al., 2015; Derks & Bergmann, 2020). Because adult mammalian CMs are unable to regenerate, the injured heart instead typically resorts to a process of wound repair. Cardiac fibroblasts activate and migrate to the injured area, where they secrete type I collagen to fill in the void left behind by cardiomyocyte death. The resulting fibrotic scar has limited contractile ability, as it is composed of stiff extracellular matrix (ECM) proteins that impede the activity of the ventricle (Fan et al., 2012; Hinderer & Schenke-Layland, 2019). Unfortunately, our ability to treat this clinical outcome is limited. Current therapies for CVD include thrombolytics, blood thinners, and beta blockers to relax the heart (American Heart Association). However, these medications merely serve to ameliorate or slow the progression of heart attack symptoms, and they do not address the underlying loss of cardiac tissue or fibrosis accumulation. In addition, compliance is not guaranteed (Cramer, 2002). As MI patients progress to end-stage heart failure, their best option becomes organ transplantation, however, the availability of donor hearts is limited (Page et al., 2018). Therefore, the ability to induce heart regeneration, which results in growth and proliferation of endogenous diseased cells (and subsequent restoration of cardiac function) would be paramount in the discovery of new therapeutic strategies for the successful treatment of MI and other types of CVD (Laflamme & Murry, 2011; Uygur & Lee, 2016).

While not known to occur in humans, cardiac regeneration has been reported in several animal models such as zebrafish (Jopling et al., 2010; Poss et al., 2002), newts (Witman et al., 2011), salamanders (Becker et al., 1974), and frogs (Liao et al., 2017). In addition, the mouse heart has some transient regenerative potential up until ~7 days of age, suggesting that the mammalian heart may have an innate regenerative mechanism that becomes dormant in adults (Porrello et al., 2011, 2013). As discussed in more detail below, after cardiac injury, zebrafish hearts regenerate through dedifferentiation of preexisting cardiomyocytes to a stem cell-like state, and proliferation of those CMs to fill in the infarcted area (Jopling et al., 2010). And recent evidence shows that neonatal mouse hearts regenerate in a similar way. After resection of the left ventricular apex, injured neonatal CMs disassemble their sarcomeres and re-enter the cell cycle (as demonstrated by immunofluorescence for phosphorylated histone H3 and aurora B kinase), leading to regeneration. Genetic fate mapping approaches show that the newly formed CMs arise from pre-existing CMs (Porrello et al., 2011). While these findings have proven difficult to reproduce (Andersen et al., 2014; Cai et al., 2019), it is generally accepted that the ability of mammalian hearts to regenerate decreases as they age. Indeed, a recent study utilizing stable isotope labeling of cardiomyocytes shows that after myocardial injury, only ~3% of adult mammalian CMs in the infarct zone undergo cell division, with the rest being polyploid and/or binucleated (Senyo et al., 2013). Naturally, this limited ability of CMs to divide is insufficient to restore lost function to the myocardium after MI. zebrafish, amphibians, and neonatal mice clearly share numerous molecular mechanisms that allow for regeneration (Uygur & Lee, 2016). In contrast, adult mammalian hearts present several obstacles that prevent regeneration, such as a limited

vascular supply to the site of injury and a significant fibroblast population that lays down collagen, thereby taking away space for CM proliferation (Tzahor & Poss, 2017). And because adult cardiomyocytes are mostly unable to dedifferentiate after injury, then perhaps the most effective way to unlock the cardiac regenerative mechanisms described above would be through identifying and activating a stem cell-like population derived from an entirely different layer of the heart.

1.2: The epicardium is a source of cardiac progenitor cells

The epicardium is the outermost mesothelial layer of the heart that surrounds the myocardium and serves a structural and protective role. It is a relatively quiescent structure in healthy adults, with most of its activity occurring after injury (Riley, 2012). The steps involved in the formation of this cell layer have only recently come into focus in the last ~30-40 years (Carmona et al., 2010). The embryonic epicardium originates from an extra-cardiac cell cluster known as the proepicardium (PE). In the zebrafish, this transient structure appears around 48 hours post-fertilization (hpf) and in the mouse, it appears around embryonic day 8.5 (E8.5) (Simões & Riley, 2018). Zebrafish PE clusters form in two locations, one at the boundary between the atrium and ventricle (the main source of epicardial cells) and the other at the venous pole of the ventricle (Peralta et al., 2014). Over the course of the next ~12-24 hours, PE cell clusters are gradually released into the pericardial cavity and float towards the myocardium, with their movements being driven by the heartbeat (Peralta et al., 2013, 2014). Once these cells reach the myocardial surface, they adhere tightly, flatten, and subsequently proliferate to cover the entire heart by about 6 days post-fertilization (Peralta et al., 2014; Simões & Riley, 2018). These processes occur in a similar manner in mouse hearts, although there is evidence that the

PE cluster and myocardial surface make direct contact with each other, resulting in the immediate transfer of proepicardial cells to the developing heart (Andrés-Delgado & Mercader, 2016; Rodgers et al., 2008).

Once the epicardium forms, its activity levels generally decrease as development proceeds. However, a small subset of these cells undergoes epithelial-to-mesenchymal transition (EMT) to aid in the formation of the developing heart. To undergo EMT, epicardial cells disassemble their cell-cell junctions and lose their apical-basal polarity. The basement membrane upon which epithelial cells sit then breaks down, thereby allowing the spindle-shaped, motile mesenchymal cells to migrate into the subepicardial space (Von Gise & Pu, 2012). At the molecular level, EMT events are typically regulated by expression of the *snail*, *slug*, and *twist* gene families, leading to a decrease in epithelial cadherin production (Von Gise & Pu, 2012). The transcription factors Wt1 (Wilms tumor 1) and Tcf21 (transcription factor 21), which are highly expressed in PE and epicardial cells, are also implicated in regulating epicardial EMT (Acharya et al., 2012; Martínez-Estrada et al., 2010; Quijada et al., 2020; Von Gise et al., 2011). Epicardial cells that undergo EMT are known as epicardium-derived progenitor cells (EpiPCs), which are multipotent cardiac progenitors that contribute to multiple different cell lineages in the developing heart. It is well accepted that EpiPCs can differentiate into vascular smooth muscle cells and cardiac fibroblasts in zebrafish and mice (Acharya et al., 2012; Kikuchi, Gupta, et al., 2011), and there is evidence to suggest they can differentiate into endothelial cells as well (Zhou et al., 2008). Importantly, several reports utilizing genetic lineage tracing have suggested that mouse EpiPCs can also differentiate into cardiomyocytes (Cai et al., 2008; Zhou et al., 2008). However, there is a lack of

consensus regarding this hypothesis because the genes driving Cre recombinase activity in these studies (*Tbx18* and *Wt1*) are also expressed at certain points throughout CM development (Christoffels et al., 2009; Rudat & Kispert, 2012). Regardless, the embryonic epicardium is essential for proper development of the heart and its resident cell populations.

The adult epicardium is a mostly quiescent single-cell layer, as demonstrated by studies in the mouse heart showing that expression levels of key genes involved in epicardial activation decrease throughout development to the point where they are barely detectable by 3 months of age (Smart et al., 2011; Smits et al., 2018; Zhou et al., 2011). The role the epicardium plays in cardiac homeostasis maintenance in adult mammals remains incompletely characterized (Masters & Riley, 2014). However, it regularly contributes cells to the ventricle in adult zebrafish in a process that depends on fibroblast growth factor (FGF) signaling. It is believed that this epicardial activity is involved in maintaining growth and homeostasis of the zebrafish heart (Wills et al., 2008). The importance of the epicardium is significantly magnified after cardiac injury, such as MI. After the heart encounters damage or insult, the epicardial layer activates and largely recapitulates its embryonic phenotype (Riley, 2012). In mice, one of the first steps involved in this process is a transient upregulation of Wt1, Tbx18, and Raldh2 levels, all of which are expressed in the fetal epicardium. Expression levels of these genes peak around 3 days post-MI and remain elevated in the majority of epicardial cells until 14 days post-MI, after which time they begin to decrease (Limana et al., 2010; Van Wijk et al., 2012; Zhou et al., 2011). After injury, the damaged epicardium is regenerated by nearby intact epicardial cells within 3 days (Van Wijk et al., 2012). These cells maintain their

proliferative potential, thereby causing a thickening of the epicardial layer in the region surrounding the infarct (Zhou et al., 2011). Similar to the process that occurs in heart development, a subset of the activated epicardial cells in the injured area increase their expression of snail, slug, and twist genes and undergo EMT to form EpiPCs (Van Wijk et al., 2012; Zhou et al., 2011). They then migrate into the subepicardial space, where they can contribute to several cardiac cell lineages. As is the case during cardiogenesis, it is widely accepted that adult EpiPCs contribute to the newly forming fibroblast and smooth muscle cell populations (Russell et al., 2011; Zhou et al., 2011, 2012). In addition, recent studies have shown that epicardial activation post injury can induce angiogenesis in the adult heart (Smart et al., 2010; Zangi et al., 2013). There is also evidence that mouse epicardial cells can convert to adipocytes after MI, a process that is enhanced by insulinlike growth factor 1 (IGF-1) activity (Zangi et al., 2017). This finding is important to CVD research because the balance between the physiological and pathological effects of epicardial adipose tissue (EAT), a layer of cardiac fat derived from the epicardium (Yamaguchi et al., 2015), is delicate. While normally cardioprotective in humans, as EAT volume accumulates, the incidence of coronary artery disease, inflammation, and metabolic syndrome increases (lacobellis, 2015; Patel et al., 2017). Taken together, the above studies demonstrate that EpiPCs contribute to the majority of cell types in the heart after injury, which could have beneficial or deleterious effects depending on which lineage predominates.

While there is a consensus that the majority of adult EpiPCs differentiate to cardiac fibroblasts and smooth muscle cells, there is also evidence that they can replenish the lost cardiomyocyte population after injury, which has relevance for cardiac regeneration

studies. One early mouse study described a population of stem cell-like precursor cells in the epicardium after injury, which migrate towards the injury site and start to express myocardial markers (Limana et al., 2007). Another study utilized genetic lineage tracing to show EpiPCs co-expressing the reporter protein and cardiac troponin I (cTnI). Although these cells had migrated to the infarcted area, their number was still too low for significant regeneration (Van Wijk et al., 2012). Importantly, this process of EpiPC differentiation to CMs after injury can be made more efficient. In one landmark study, Smart and colleagues identified a Wt1+ stem cell population in mice. After MI, lineage tracing experiments showed that some of these EpiPCs differentiated into cells expressing cardiac troponin T (cTnT) and α-sarcomeric actin, a process that was enhanced by application of thymosin β4 (a regulator of actin polymerization) before injury. These new CMs integrated structurally and functionally with native myocardial tissue (Smart et al., 2011). While these reports provide significant evidence that epicardial progenitor cells can differentiate into cardiomyocytes, it is important to note that as is the case in heart development, these findings are somewhat controversial. Indeed, similar studies using lineage tracing have demonstrated that EpiPCs only differentiate into fibroblasts and smooth muscle cells, and not CMs (Zhou et al., 2011, 2012). Regardless, it is apparent that the activated epicardium at least has the potential to replenish lost CMs after MI via its resident stem cell population. In addition to mouse studies, other regenerating model organisms have been used in recent years to investigate the activity of EpiPCs after cardiac injury. Importantly, genetic ablation of the epicardium reduces the regenerative capacity of the zebrafish heart (Wang et al., 2015). Adult EpiPCs have been shown to give rise to at least cardiac fibroblasts and perivascular cells after injury (González-Rosa et al., 2012; Kikuchi, Gupta, et al., 2011). The potential may also exist for them to contribute new cardiomyocytes to the regenerating heart, as a recent lineage tracing study in salamanders revealed adult EpiPCs transitioning into *de novo* CMs in a manner dependent upon tight junctions (Eroglu et al., 2022). For an overview of the processes involved in epicardial regeneration, see **Figure 1.1**. For an overview of epithelial-to-mesenchymal transition, see **Figure 1.2**.

Notably, the activated epicardium is not just a source of progenitor cells that can replenish lost CMs after injury, but a source of paracrine signals that may contribute to heart regeneration. In one landmark study from 2011, Zhou et al. isolated EpiPCs from injured adult mice, expanded them in culture, and collected the media. Injection of this EpiPC-conditioned medium into infarcted mouse hearts stimulated significant growth and proliferation of endothelial cells and subsequent blood vessel assembly. application of the progenitor cell media reduced infarct size and improved ventricular function at 1 week post-MI. Gene expression analyses demonstrated that EpiPCs secrete several pro-angiogenic factors, with vascular endothelial growth factor A (Vegfa) and fibroblast growth factor 2 (Fgf2) being the main proteins that mediate the above effects (Zhou et al., 2011). And these are not the only factors that mediate angiogenesis after injury, as similar findings have been observed when human EpiPC-conditioned medium is injected into infarcted rat hearts after ischemia-reperfusion injury. However, these beneficial effects were attributed to the presence of hepatocyte growth factor (HGF) and immunoglobulin G (IgG) complexes in the media (Rao et al., 2015). Finally, there is also evidence that epicardial-secreted factors may stimulate cardiomyocyte regeneration. Wei et al. found that the glycoprotein follistatin-like 1 (Fstl1) is produced by the epicardium

and can induce CMs to re-enter the cell cycle and divide. In addition, application of an epicardial patch containing recombinant human FSTL1 at the time of MI improved mouse survival, increased CM proliferation, reduced cardiac fibrosis accumulation, and improved cardiac function (Wei et al., 2015). Overall, it is apparent that the activated epicardium plays a massively important role after cardiac injury, both through stem cell-mediated and paracrine pathways. Therefore, this cell layer might be the key to eventually unlocking innate cardiac regeneration pathways in humans (Quijada et al., 2020; Rao & Spees, 2017; Simões & Riley, 2018; Smits et al., 2018).

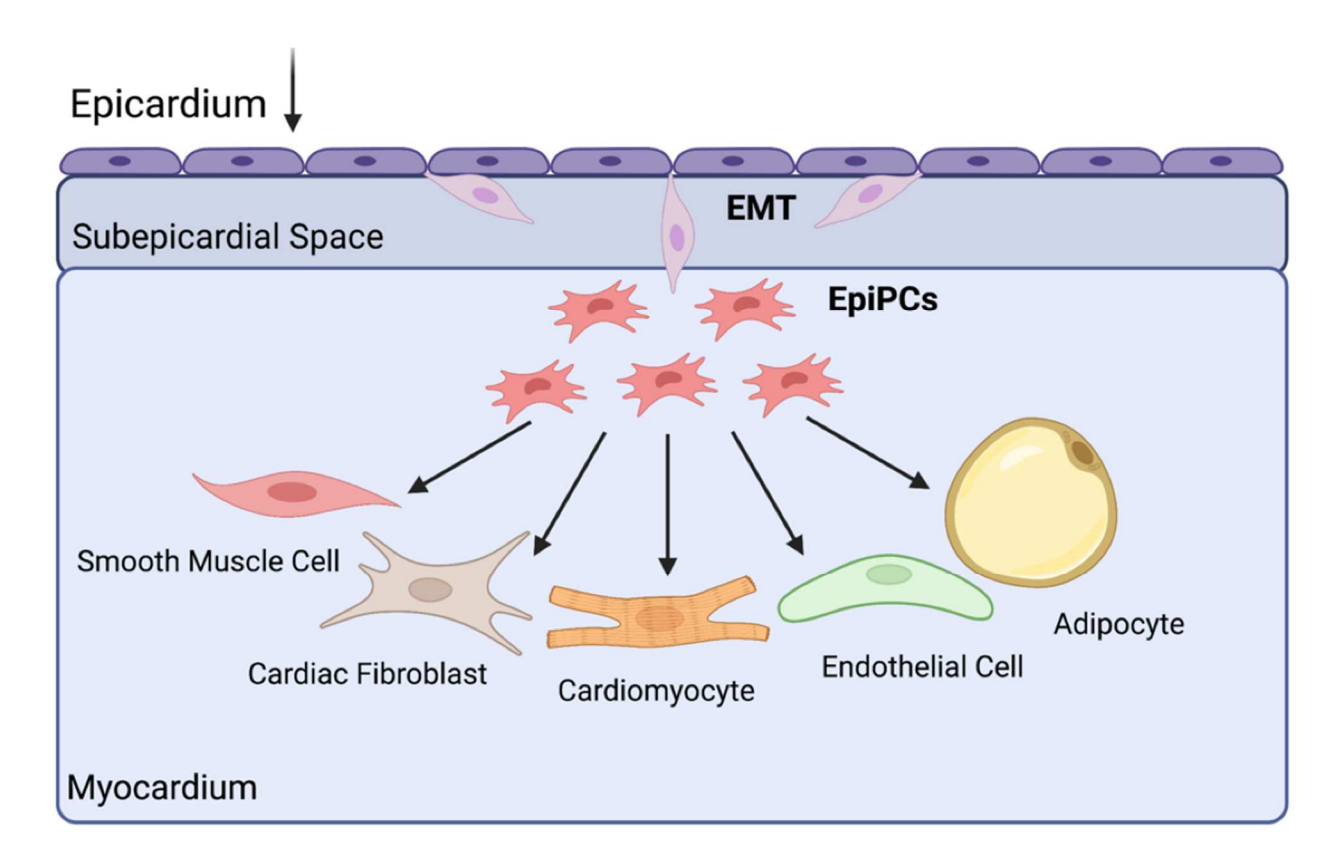


Figure 1.1: Overview of epicardial activation. In healthy adult hearts, the epicardium (purple cells) is a quiescent single cell layer of mesothelial cells. In response to cardiac injury, a subset of epicardial cells activate, migrate into the subepicardial space (gray), and undergo epithelial-to-mesenchymal transition (EMT) to form epicardium-derived progenitor cells (EpiPCs). These EpiPCs can then go on to invade the damaged myocardium (blue) and differentiate into smooth muscle cells, fibroblasts, cardiomyocytes, endothelial cells, and adipocytes, thereby replacing some of the cells that were lost after the initial injury. Image created with BioRender.com.

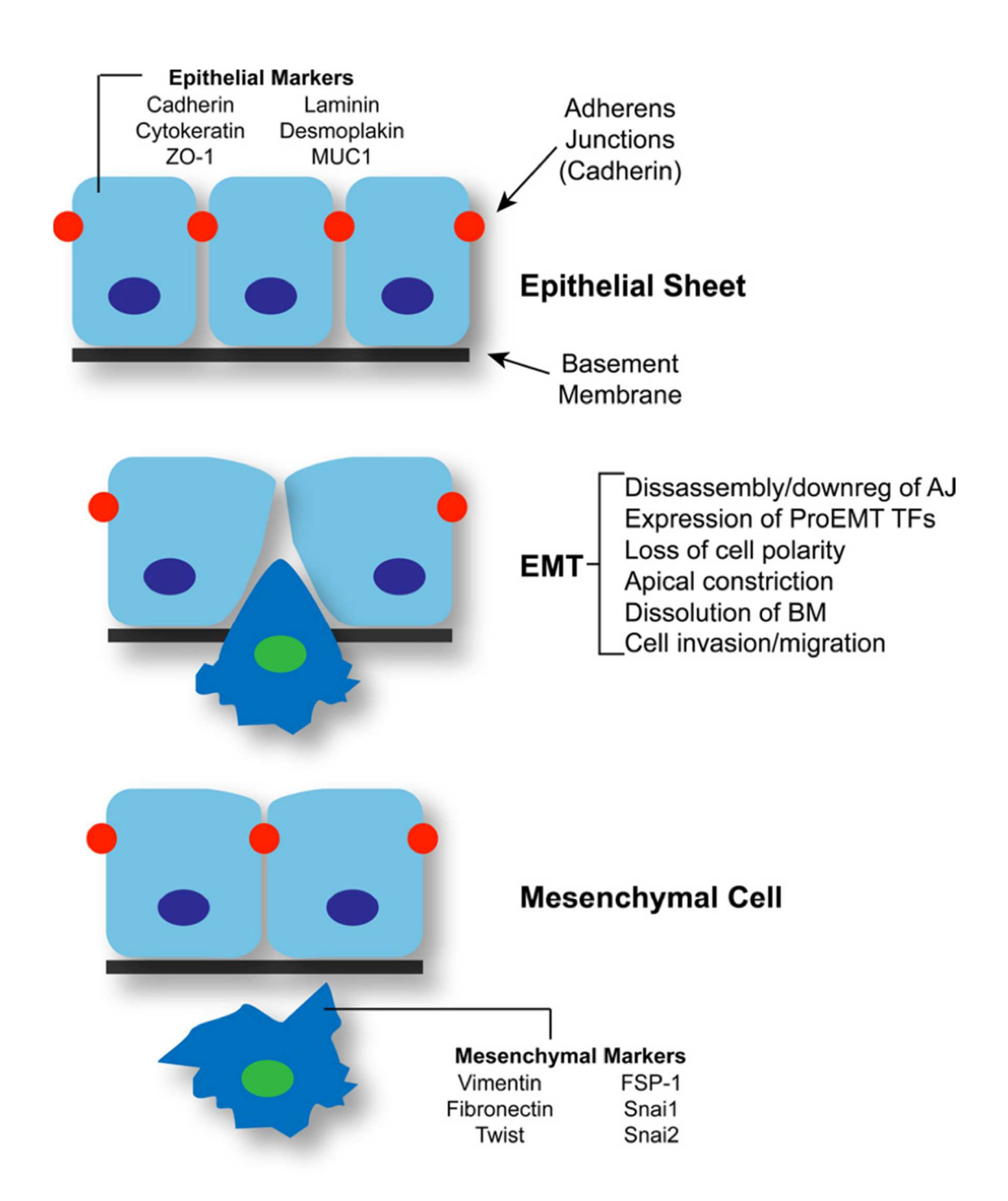


Figure 1.2: Overview of epithelial-to-mesenchymal transition. Polarized epithelial cells are typically held together by adherens junctions atop a basement membrane. Upon initiation of EMT, these cells increase their expression of EMT genes, lose their apical-basal polarity, disassemble their adherens junctions, and dissolve their basement membranes. Newly formed mesenchymal cells are motile and spindle-shaped and can migrate through the basement membrane to invade underlying tissue. These processes occur in the epicardium to contribute new mesenchymal cells in development and in response to injury; AJ: Adherens Junctions, BM: Basement Membrane, EMT: Epithelial-

Figure 1.2 (cont'd)

to-Mesenchymal Transition, TF: Transcription Factor. Image re-produced from Von Gise A and Pu WT, *Circ Res.* 2012.

1.3: The neuroendocrine signaling axis affects regeneration

While evidence suggests that epicardial progenitor cells may be able to replenish lost cardiomyocytes after cardiac injury, it should be noted that this activity is insufficient for significant regeneration in mammals. Importantly, the process of epicardial activation leading to heart regeneration can be "primed" or made more efficient by signaling factors present within the body, such as thymosin β4 (Smart et al., 2007, 2011; Wang et al., 2021) and brain natriuretic peptide (BNP) (Li et al., 2020). Identifying the source of these factors and their mechanisms of action will be paramount in advancing the potential therapeutic applications of epicardial stem cells in cardiac regeneration research. The hypothesis upon which this project is based is that the brain is the ultimate source of critical peptides and proteins that can enhance epicardial activation and heart regeneration after MI. The rationale for these studies is that the brain plays a central role in several energetically demanding processes that serve to maintain body homeostasis. For example, the cardiovascular and respiratory control centers are located in the brainstem (Dampney, 2016; Guyenet & Bayliss, 2015) and energy balance and thermoregulation are mediated by the hypothalamus (Morrison, 2016; Roh et al., 2016). In addition, the brain-heart signaling axis regulates heart rate, blood pressure, and systolic and diastolic function (Dampney, 2016; Palma & Benarroch, 2014). Cardiac regeneration is also a biologically and energetically demanding process, and it is unlikely that is completely autonomous. It stands to be reasoned that this phenomenon is under some degree of central control.

Ultimately, proving this hypothesis would uncover a novel mechanism to induce regeneration of the injured heart.

If it is truly the case that the brain regulates heart regeneration to some extent, then one question worth exploring is which region of the brain is mainly responsible and what factor(s) it releases to the heart after injury. The neural endocrine structures, such as the hypothalamus and pituitary, play a particularly important role in maintaining normal cardiovascular function through the release of various hormones (Gordan et al., 2015; Rhee & Pearce, 2011). Interestingly, recent evidence suggests that damage to the hypothalamus inhibits endogenous regenerative processes in vertebrates. In this study, Zhang et al. utilize electrocautery to ablate the basal hypothalamus in regenerationcompetent tadpoles and subsequently amputate their limbs. While the majority of shamoperated animals displayed fully regenerated limbs one month later, the hypothalamusinjured animals showed little or no digit restoration, thereby suggesting at least one critical factor is released by this brain structure that regulates regeneration. Indeed, loss-offunction studies demonstrated that α -melanocyte stimulating hormone (α -MSH) and melanocortin receptor 4 (Mc4r) signaling are required for limb regeneration at this stage of development (Zhang et al., 2018). And the concept of hormonal control of regeneration extends further than just limb studies. In fact, there is evidence that several hormones affect cardiac regeneration (Amram et al., 2021). A recent study found that estrogen can accelerate zebrafish heart regeneration, in part by inducing an immune response (Xu et al., 2020). In addition, exogenous thyroid hormone application inhibits zebrafish heart regeneration. Conversely, when thyroid hormone signaling is inhibited, adult mouse cardiomyocytes continue to progress through the cell cycle, thereby enhancing their proliferative potential (Hirose et al., 2019). Finally, there is evidence that induction of acute daily stress in zebrafish, as accomplished by exposure to heat shock, caffeine, and overcrowded tanks, leads to increased cortisol secretion and impaired heart regeneration (Sallin & Jaźwińska, 2016). Taken together, these studies suggest that hormones are critical for regulating regeneration after cardiac injury. However, as of now, there are no reports of neuroendocrine hormones being directly involved in this process. In addition, their ability to prime epicardial cell activation and differentiation to new cardiac cells after injury has not been studied. Proper identification and characterization of these hormones will be critical in advancing the clinical potential of cardiac regeneration research. Demonstrating this potential using several different model systems would uncover for the first time a direct neuroendocrine mechanism that induces regeneration of the injured heart. In addition, it could yield significant translational advances in the treatment of cardiovascular disease by expanding our understanding of cardiac reprogramming mechanisms in vitro and in vivo.

1.4: Induced pluripotent stem cells have numerous applications in preclinical research

Induced pluripotent stem cells (iPSCs) were first derived directly from mouse fibroblasts and characterized in 2006 (Takahashi & Yamanaka, 2006). The following year, the same group generated iPSCs from adult human dermal fibroblasts by retroviral-mediated transduction of a combination of four transcription factors (OCT-4, SOX2, KLF4, and c-MYC) into the somatic cells (Takahashi et al., 2007). The resulting stem cells demonstrated pluripotency, as they had the ability to self-renew and could be differentiated into any specialized cell type deriving from the ectoderm, mesoderm, or endoderm (Romito & Cobellis, 2016). iPSCs present many potential clinical advantages

compared to other stem cell types, especially as it relates to transplantation potential. These cells can be created from tissues of the same patient that will receive the transplant, thereby avoiding the immune rejection that would occur upon introduction of "non-self" entities (Kiskinis & Eggan, 2010). In addition, iPSCs advance the field of personalized medicine, as patient-specific lines can be derived from individuals with different disorders and subsequently used for disease modeling, drug discovery, and toxicity testing. (Bellin et al., 2012). Findings from these studies could greatly enhance the ability to diagnose and treat numerous conditions, particularly those that affect organs from which it is difficult to obtain primary tissue, such as the brain and heart (Bellin et al., 2012). One more benefit of iPSCs is that they solve some of the ethical issues associated with the use of embryonic stem cells (ESCs), which are derived from early human embryos and require their destruction to generate cell lines (Lengner, 2010; Takahashi, 2010). Indeed, in just 15 short years, induced pluripotent stem cells have completely revolutionized preclinical research.

The ability to make iPSCs specific to particular diseases has been instrumental in advancing understanding of their pathogenesis and progression. To date, there are iPSC lines for modeling numerous disorders affecting the nervous, muscular, metabolic, cardiovascular, and pulmonary systems, among others (Park et al., 2008; Singh et al., 2015). And these stem cells have proven valuable in recapitulating key aspects of many common diseases. In one early study, iPSC lines were generated from patients with mutations in the presenilin genes, and neurons differentiated from these cells secreted increased levels of amyloid β 42, a hallmark feature of Alzheimer's disease (Yagi et al., 2011). Patient-specific iPSCs have also been utilized to model Parkinson's disease

(Jiang et al., 2012) and Huntington's disease (Mattis et al., 2012). Pluripotent stem cell modeling extends to the cardiovascular system as well, as iPSC-derived cardiomyocytes from patients with mutations in the KCNQ1 gene displayed increased action potential durations as a result of reduced outward potassium currents. This phenotype recapitulates a type of arrhythmia known as long QT syndrome (Moretti et al., 2010). Another study showed that cardiomyocytes from patients with hypertrophic cardiomyopathy (HCM) responded to endothelin-1, a peptide associated with vasoconstriction, with increased growth and myocardial disarray, thereby contributing to contractile dysfunction (Tanaka et al., 2014). In addition, other common disorders such as cystic fibrosis (Crane et al., 2015), Duchenne muscular dystrophy (Kazuki et al., 2010), and hemophilia A (Jia et al., 2014) have all been successfully modelled using iPSCs in the last 10-15 years. And these pluripotent cells are increasingly being utilized as screening platforms for the development and validation of drugs and therapeutics, as well a means to study the toxicity and side effects of these drugs (Shi et al., 2017; Singh et al., 2015). Clearly, iPSC research has great benefit for the treatment of human disease.

Importantly, iPSCs may also play a role in regenerative medicine, as the potential exists for them to be reprogrammed from the somatic cells of a patient, differentiated into a new cell type, and transplanted back into the same patient at the site of injury or degeneration (Singh et al., 2015). In fact, in recent years, several preclinical studies have demonstrated this potential. Evidence suggests that iPSCs can be differentiated into cardiac myocytes to replace cardiac tissue after myocardial infarction (Masumoto et al., 2014), hepatocytes to regenerate liver damage caused by cirrhosis (Liu et al., 2011), pancreatic β-cell cells to treat type 1 diabetes (Jeon et al., 2012), neurons and astrocytes

to improve function after spinal cord injury (Nori et al., 2011), and progenitor cells to ameliorate muscular dystrophy (Tedesco et al., 2012). Encouraging results such as these increase the likelihood that human clinical trials studying the effects of iPSC transplantation after injury or disease will be successful. In fact, over 100 clinical trials involving pluripotent stem cells are currently in progress, with the majority focused on ophthalmic, cardiovascular, neurological, and metabolic disorders (Deinsberger et al., 2020). However, less than 25% of these trials incorporate the actual transplant of cells into patients, suggesting that some of the drawbacks of iPSCs, such as the possibility of carcinogenicity, must be overcome before their full potential can be realized (Deinsberger et al., 2020). Regardless, iPSCs clearly present many applications for preclinical research (Figure 1.3). Here, I leveraged these applications by differentiating human iPSCs into two-dimensional (Chapter 3) and three-dimensional (Chapter 5) cardiac cells. These systems, combined with zebrafish, a naturally regenerating animal model (Chapter 4), allowed me to thoroughly document the effects the neuroendocrine axis has on epicardial activation and heart regeneration.

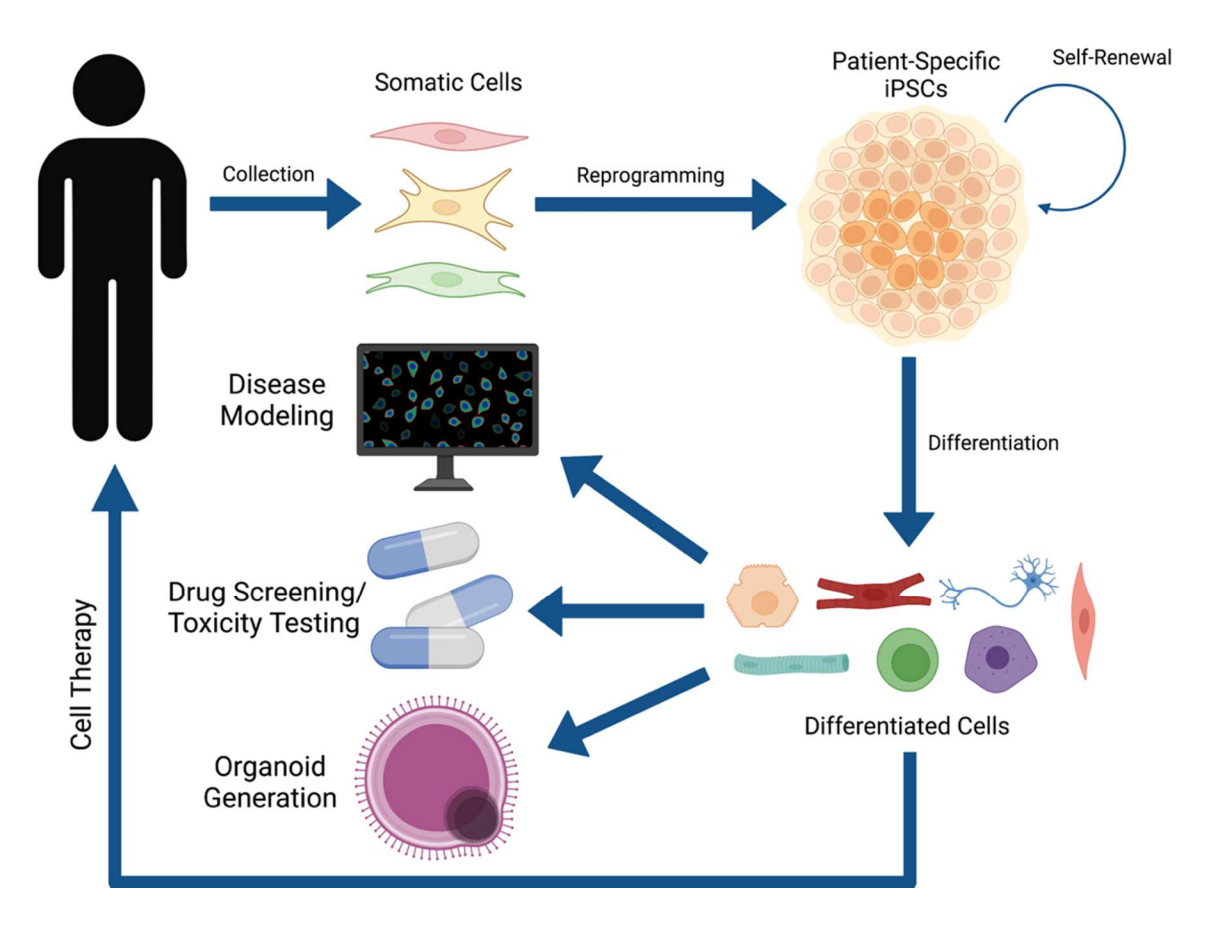


Figure 1.3: Applications of induced pluripotent stem cells (iPSCs). Generation of iPSCs is achieved by introduction of reprogramming factors (OCT-4, SOX2, KLF4, c-MYC) into somatic cells. The resulting cells are pluripotent, as they can self-renew and differentiate into any cell type found in the body. iPSCs reprogrammed from individuals with various disorders can be "patient-specific", and their differentiation products can be used in disease modeling, drug screening, toxicity testing, and three-dimensional organoid generation. They may also have applications for cell-based therapies and regenerative medicine through autologous cell transplants directly into patients after injury or disease. Image created with BioRender.com.

Chapter 2: Materials and Methods

2.1: Stem cell culture

Human induced pluripotent stem cells (hiPSCs; Cell line L1) were cultured on 6 well plates coated with growth factor-reduced Matrigel (Corning) in an incubator at 37°C, 5% CO₂. Stem cell media was changed every other day with Essential 8 Flex medium (E8 Flex; Thermo Fisher Scientific) containing 1% penicillin/streptomycin, preceded by a wash with Dulbecco's Modified Eagle Medium/Nutrient Mixture F-12 (DMEM/F12; Thermo Fisher Scientific) to remove dead cells. hiPSCs were maintained in E8 Flex until ~70% confluency was reached, at which point cells were split into new wells using ReLeSR passaging reagent (STEMCELL Technologies) with 2 μM Thiazovivin (TZV; Selleck Chemicals), a rho-associated protein kinase (ROCK) inhibitor. This reagent was added to prevent cells from undergoing apoptosis while in suspension. All hiPSC lines were periodically validated for pluripotency and genomic stability.

2.2: hiPSC differentiation to hiPSC-derived epicardial cells (hEpiCs)

hiPSCs were differentiated to epicardial monolayers using a modified version of a previously described protocol (Bao et al., 2016, 2017). Cells were dissociated using Accutase (Innovative Cell Technologies), re-plated on Matrigel coated plates, and incubated overnight in E8 Flex + 2 μ M TZV. The basal medium used for epicardial differentiation was Roswell Park Memorial Institute (RPMI) 1640 (Thermo Fisher Scientific) with B-27 supplement (with/without insulin; Gibco) added. Once passaged hiPSC monolayers reached ~90% confluence, differentiation was started via the addition of 12 μ M CHIR99021 (CHIR; Selleck Chemicals) in RPMI/B-27 minus insulin (Day 0) for 24 hours. Medium was then changed on Day 1 to remove CHIR. On Day 3, cells were

exposed to 2 µM Wnt-C59 (Selleck Chemicals) in RPMI/B-27 minus insulin for 48 hours, followed by a medium change on Day 5 to remove it. On Day 6, cardiac progenitors were then re-plated in RPMI/B-27 (Gibco) with 100 µg/mL Vitamin C (Vit. C) using Accutase and TZV. Cells were directed down the epicardial lineage by the consecutive addition of 9 µM CHIR99021 on Days 7 and 8, followed by RPMI/B-27/Vit. C changes on Days 9 and 11. All media were added to cells as gently as possible to prevent disruption of the epicardial monolayers. On Day 12, hEpiCs were again re-plated using Accutase and TZV and 2 μM SB431542 (TGF-β receptor inhibitor; Selleck Chemicals) was added to prevent cells from spontaneously undergoing EMT. Epicardial cells were cultured long-term in RPMI/B-27/Vit. C + 2 µM SB431542 and split when full confluence was reached. To ensure that hEpiCs were as mature as possible for experiments, Vitamin C and SB431542 were removed from the culture system 5 days prior to sample collection. OXT and other compounds were added directly to the media 2 days later, for a total exposure time of 3 days, unless otherwise indicated. Automated cell counting was conducted using the Cytation 3 and Cytation 5 Cell Imaging Multi-Mode Readers (Biotek).

2.3: hiPSC lentiviral transduction

Bacteria carrying the plasmid for short hairpin RNA (shRNA)-mediated knockdown of *OXTR* and a scrambled plasmid (both designed with VectorBuilder, see **Figure 2.1**) were grown on LB agar plates and isolated colonies were expanded in LB broth, both containing ampicillin. The plasmids carried an ampicillin resistance cassette, allowing for their growth. Plasmid DNA was isolated from the bacteria by midiprep (Zymo Research), and purified DNA was transfected into 40% confluent HEK293T cells using Lipofectamine (Invitrogen). Lentiviral packaging plasmids (pVSVg, psPAX2) were also transfected at

this time, thereby allowing the generation of a functional lentivirus containing the shRNA molecules of interest. Viral supernatant was collected and concentrated after 48 hours in culture and transduced directly into hiPSCs at low to mid-confluency along with 8 μg/mL polybrene (Fisher Scientific). Because all plasmids contained puromycin-resistance cassettes, the stem cell media was changed the next day to E8 Flex containing 0.5 μg/mL puromycin (Thermo Fisher Scientific) to facilitate colony selection. hiPSCs were maintained in puromycin for 5 days and surviving monoclonal colonies were re-plated and expanded to generate new hiPSC lines. These cell lines were differentiated into two-dimensional hEpiCs and three-dimensional human heart organoids as described in Sections 2.2 and 2.4. For a step-by-step description of the techniques and methodologies involved in this protocol, see **Table 2.1**.

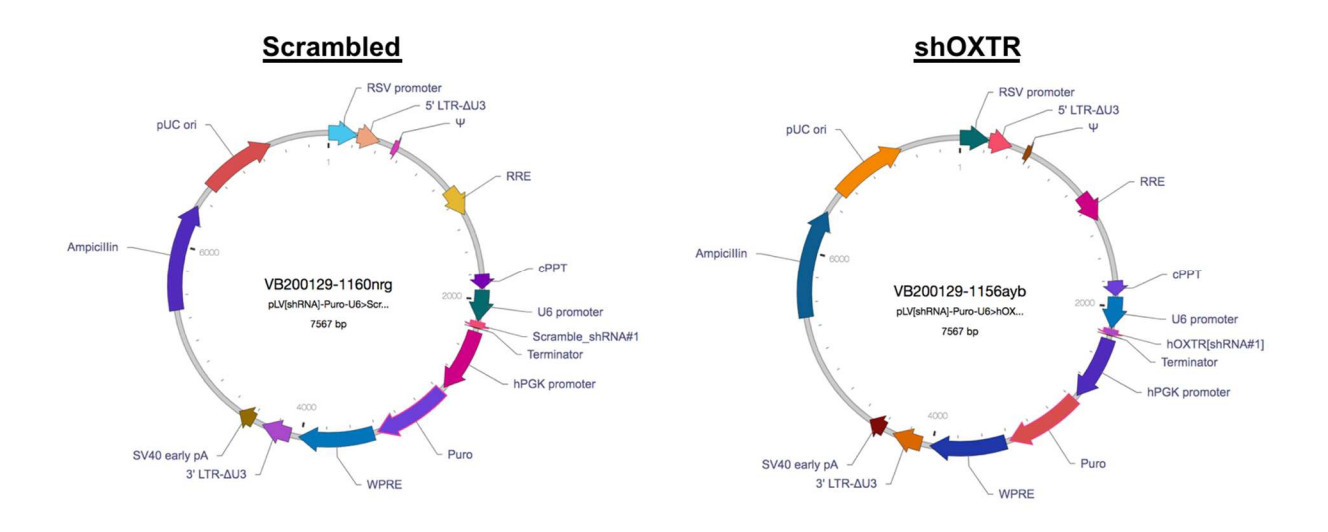


Figure 2.1: Plasmids used for short hairpin RNA (shRNA)-mediated knockdown of *OXTR* in hiPSCs.

Table 2.1: Step-by-step protocol for lentiviral production and hiPSC transduction.

Step	Time to Complete	Purpose
Design plasmid	~10 minutes	Manipulation of gene expression in target cells
Order plasmid in a bacterial glycerol stock	~1-2 weeks for shipping	Stabilizes plasmid DNA in competent bacteria cells frozen in glycerol for long-term storage
Streak plasmid-containing bacteria on petri dish containing LB agar + ampicillin	Protocol: ~10 minutes Incubation: Overnight at 37°C	Isolates single bacteria colonies that contain plasmid of interest, which has an ampicillin resistance cassette
Select colonies and grow plasmid- containing bacteria in small volume of LB broth + ampicillin	Protocol: ~5 minutes Incubation: 8 hours at 37°C and shaking at 200 rpm	Allows for growth and expansion of bacteria containing plasmid of interest, which has an ampicillin resistance cassette
Transfer ~25% of solution of plasmid- containing bacteria into large volume of LB broth + ampicillin	Protocol: ~5 minutes Incubation: Overnight at 37°C and shaking at 200 rpm	Allows for large-scale expansion of bacteria containing plasmid of interest, which has an ampicillin resistance cassette
Centrifuge bacteria and perform DNA Midiprep on pellet	~1 hour	Purifies plasmid DNA of interest from bacteria
Transfect plasmid DNA and other lentiviral components into HEK293T cells using Lipofectamine	Protocol: ~1.5 hours Incubation: 6 hours for transfection, 48-60 hours for viral assembly	Introduces plasmid DNA into packaging cells, allowing for assembly of a complete lentivirus
Harvest/filter/centrifuge lentiviral supernatant	~2 hours	Collects and concentrates complete lentiviral particles for transduction
Transduce virus into hiPSCs using polybrene	Protocol: ~30 minutes Incubation: Overnight at 37°C, 5% CO ₂	Allows lentiviral particles to infect hiPSCs efficiently
Add puromycin to hiPSC culture medium	Protocol: ~5 minutes Incubation: ~3-5 days at 37°C, 5% CO ₂	Permits only transduced hiPSCs to grow, as plasmid of interest has a puromycin resistance cassette
Select/expand surviving hiPSC colonies	Protocol: ~ 2 hours Incubation: ~1-2 weeks at 37°C, 5% CO ₂	Scales up multiple transduced hiPSC clones for downstream experiments
Differentiate new hiPSC lines to hEpiCs and organoids	Varies	Study epicardial activation in heart regeneration

2.4: hiPSC differentiation to hiPSC-derived human heart organoids (hHOs)

hiPSCs were differentiated to three-dimensional human heart organoids (hHOs) as previously described (Lewis-Israeli, Volmert, et al., 2021; Lewis-Israeli, Wasserman, Gabalski, et al., 2021) and as summarized in Figure 2.2. Briefly, Accutase was used to dissociate hiPSCs for spheroid formation. After dissociation, cells were centrifuged at 300 x g for 5 minutes and resuspended in E8 Flex medium containing 2 µM TZV. Cells were then counted using a Moxi Cell Counter (Orflo Technologies) and seeded at 10,000 cells/well in round bottom ultra-low attachment 96-well culture plates (Costar) on Day -2 at a volume of 100 µL per well. The plate was centrifuged at 100 x g for 3 minutes and incubated overnight. After 24 hours (Day -1), 50 µL of media was carefully removed from each well, and 200 µL fresh E8 Flex was added for a final volume of 250 µL per well. On Day 0, 166 μL (~2/3 total well volume) media was removed and 166 μL RPMI/B-27 minus insulin containing 4 µM CHIR99021, 0.36 pM (1.25 ng/mL) bone morphogenetic protein 4 (BMP-4), and 0.08 pM (1 ng/mL) Activin A was added for 24 hours. On Day 1, 166 µL of this media was replaced with fresh RPMI/B-27 minus insulin. On Day 2, RPMI/B-27 minus insulin containing 2 µM Wnt-C59 was added for 48 hours, followed by media changes on Day 4 and Day 6. On Day 7, a second CHIR99021 exposure (2 µM) was conducted for 1 hour in RPMI/B-27 to induce epicardium formation. Organoid medium was then replaced with fresh RPMI/B-27 every other day until Day 20. All media changes were conducted as carefully as possible using multichannel pipettes to prevent disturbance to the hHOs. In addition, conditioned media changes ensured that organoids were not accidentally aspirated and remained intact throughout differentiation.

Human Heart Organoid (hHO) Differentiation

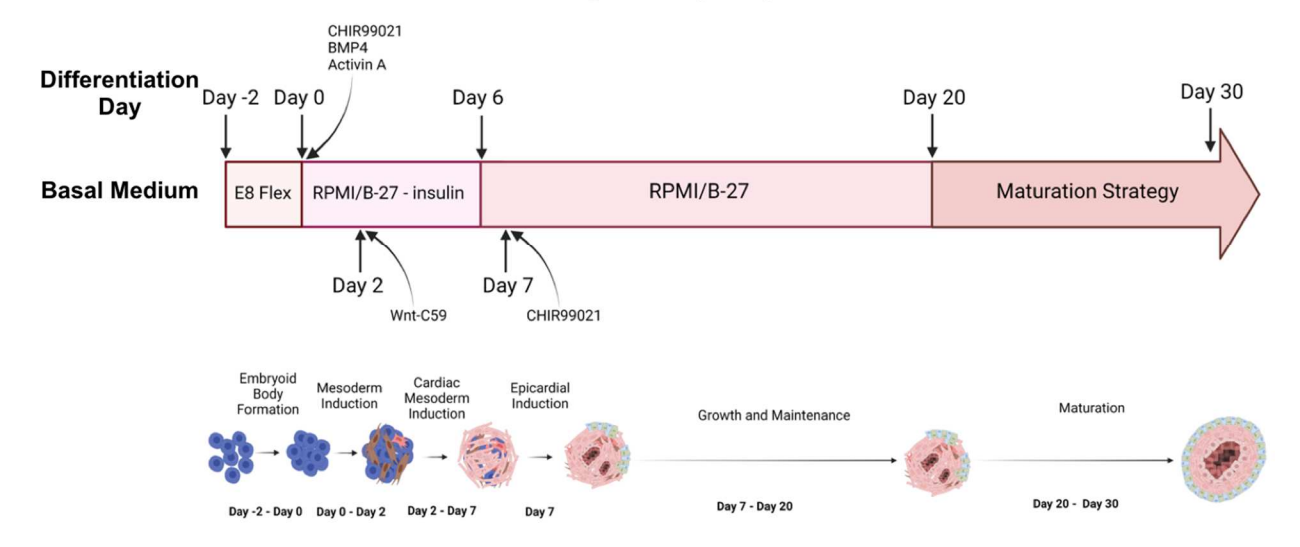


Figure 2.2: Schematic of protocol used for hHO differentiation. Image courtesy of Brett Volmert and created with BioRender.com.

2.5: Organoid maturation and cryoinjury

On Day 20 of the hHO differentiation protocol, 52.5 µM palmitate-BSA (bovine serum albumin), 40.5 µM oleate-BSA, 22.5 µM linoleate-BSA, 120 µM L-carnitine, and 30 nM T₃ thyroid hormone were added to the basal differentiation medium to increase fatty acid metabolism as previously described (Yang et al., 2014, 2019). hHOs were maintained in this "maturation medium" until ready for experiments (**Figure 2.2**). On Day 30, cryoinjury was performed by applying a liquid nitrogen cooled metal probe directly to the hHO surface (protocol modified from (Hofbauer et al., 2021; Voges et al., 2017), summarized in **Figure 2.3**). Briefly, organoids were removed from the incubator, placed in a petri dish, and visualized with a Leica M165 FC stereomicroscope under ~4.0x magnification. Residual media was removed and the tip of the metal probe was slowly lowered to the hHO surface until direct contact was made. Each cryoinjury lasted ~8-10 seconds, long enough for the wavefront of freezing tissue to be visible. Cryoinjured

organoids were then gently transferred back to wells containing 166 µL of fresh maturation medium with oxytocin added as needed. For sham injuries, hHOs were simply pipetted up from their wells, placed on a petri dish, and transferred back into fresh medium. All samples were collected 72 hours later for analysis unless otherwise indicated.

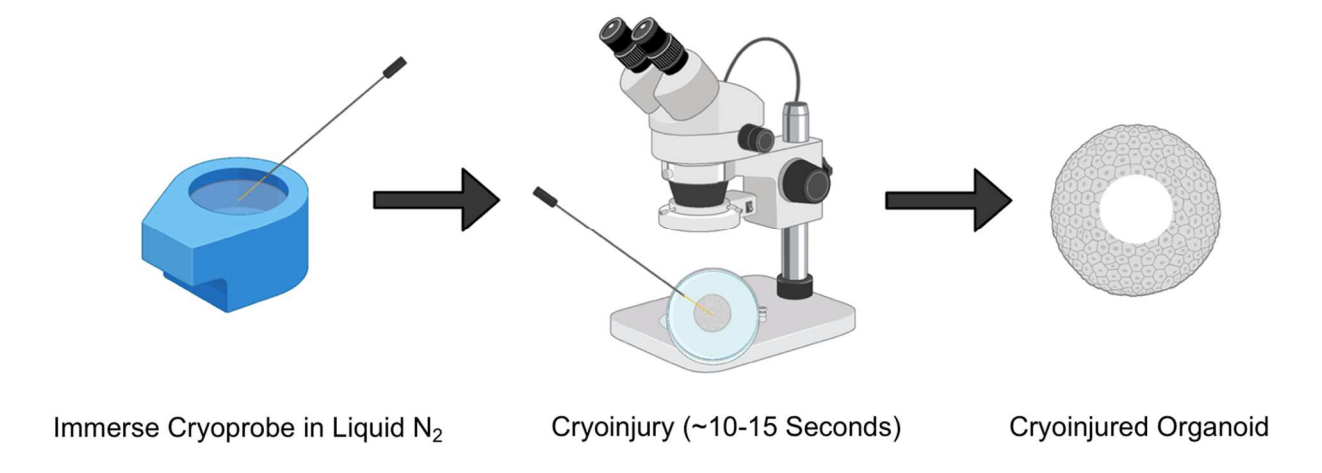


Figure 2.3: Schematic of protocol used for hHO cryoinjury. Image created with BioRender.com.

2.6: Organoid single-cell dissociation

To quantify cell viability before and after cryoinjury, matured hHOs were dissociated to single cells or small aggregates using the Stemdiff Cardiomyocyte dissociation kit (STEMCELL Technologies). First, organoids were transferred to 1.5 mL Eppendorf tubes and washed with PBS (phosphate-buffered saline). Excess media was removed and hHOs were incubated in 200 µL dissociation media for 5 minutes at 37°C on a thermal cycler (Thermo Fisher Scientific) shaking at 300 RPM (revolutions per minute). The supernatant containing dissociated cells was then transferred to a 15 mL centrifuge tube with 5 mL RPMI/B-27 and stored at room temperature. Warmed dissociation media was again added to the hHOs, incubated on a thermal cycler, and

transferred to the centrifuge tube as described above, with this process being repeated a total of 3-4 times. Once the majority of the organoids were broken up, the remaining cells were added to the tube and centrifuged at 300 x g for 5 minutes. After spinning, the supernatant was discarded and the pellet was resuspended in RPMI/B-27. Finally, cell viability was quantified via a hemocytometer.

2.7: Zebrafish cardiac cryoinjury/injections

Adult zebrafish hearts were subjected to cardiac cryoinjury as described previously (González-Rosa et al., 2011; González-Rosa & Mercader, 2012). Briefly, fish were anesthetized in a petri dish with 0.65 mM tricaine methanesulfonate (MS-222; Sigma-Aldrich) by pipetting it directly through the gills. Once operculum movement and reflex activities had ceased, fish were placed on a wet sponge ventral side up under a stereomicroscope at 1.25x magnification (Leica). The chest cavity was then opened by cutting through the pericardium until the point where the beating heart was clearly visible. Slight pressure was maintained on the abdomen to make the heart more easily accessible. For cryoinjury, a liquid nitrogen cooled metal probe was gently placed on the apex of the ventricle for ~45 seconds. Injured fish were then transferred into a recovery tank and water was pipetted into their gills until they woke from anesthesia (~30 seconds). Sham operations were carried out by simply opening the chest cavity without inducing injury. For a step-by-step summary of the cryoinjury procedure, see Figure 2.4. All fish were closely monitored for the first 2 hours after surgery and twice daily thereafter until ready for organ collection. Pharmacological inhibition of oxytocin signaling was achieved by injecting 2-3 µL of water or 1 µM L-368,899 (a non-peptide OXTR antagonist) directly into the intrathoracic cavity of anesthetized zebrafish, as described previously (Bise &

Jaźwińska, 2019). Initial injections were administered 24 hours after cryoinjury with repeat injections every 1-2 days throughout the experiment. Injections were carried out using a 25 µL gastight Neuros syringe (Hamilton), with movements controlled through the use of a manual micromanipulator (World Precision Instruments). All zebrafish were maintained in a dedicated facility between 27-28°C on a 14-hour light/10-hour dark cycle. Equal numbers of male and female fish were used for cryoinjuries.

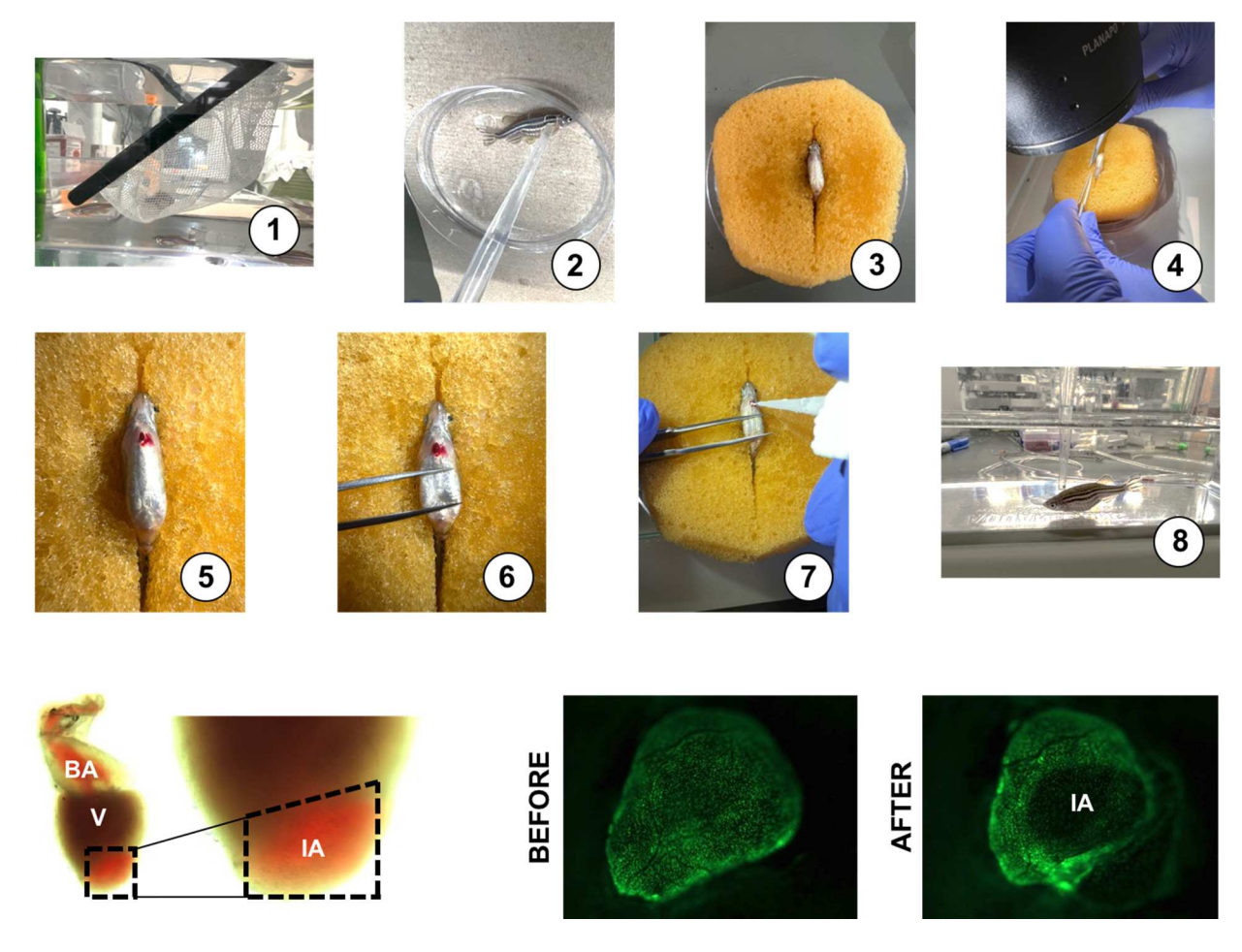


Figure 2.4: Overview of zebrafish cardiac cryoinjury. <u>TOP</u>: Step-by-step summary of the procedure used for zebrafish cryoinjury. 1) One adult zebrafish is selected from its tank using a net; 2) The fish is placed into a petri dish and tricaine is slowly pipetted into the gills to anesthetize it; 3) A spoon is used to transfer the animal ventral side up onto a wet sponge, which will hold it in place during the procedure; 4) Forceps are used to cut through the skin and the underlying pericardium, with visualization achieved via a stereomicroscope; 5) The incision is widened and the zebrafish is positioned so that the beating heart is clearly visible; 6) Pressure is applied to the abdomen to slightly elevate the heart out of the chest cavity, making it more accessible; 7) Cryoinjury is induced by gently applying a liquid nitrogen cooled metal probe to the apex of the ventricle for ~45 seconds; 8) The injured fish is transferred to a recovery tank and water is slowly pipetted into the gills to wake it from anesthesia. <u>BOTTOM</u>: Examples of freshly cryoinjured zebrafish hearts, dashed lines demarcate injured area, images on bottom right are from a transgenic strain that labels epicardial cell nuclei green; BA: Bulbus arteriosus, IA: Injured area, V: Ventricle.

2.8: Zebrafish embryo experiments

One female and one male adult fish were placed in specialized breeding tanks with a partition between them the night before experiments. The partition was removed early the next morning and fish were given ~15 minutes to breed. Fertilized embryos were collected and placed in embryo medium containing 4.96 mM NaCl, 0.179 mM KCl, 0.329 mM CaCl₂ • 2H₂O, and 0.401 mM MgCl₂ • 6H₂O dissolved in water. The appropriate concentration of L-368,899 (non-peptide OXTR antagonist) or atosiban (competitive OXTR antagonist) was added directly to the medium and embryos were placed in 6 well plates (20 per well) in an incubator at 28°C for the duration of the experiment. Dead embryos and discarded chorions were removed daily. Developing fish were imaged at 1, 2, 3, 5, and 7 days post-fertilization (dpf) with the Leica M165 FC stereomicroscope with a DFC7000 T fluorescence camera so that epicardium and myocardium formation could be observed in real time. Once the fish hatched from their chorions (~2-3 dpf), they were immobilized with 0.65 mM tricaine so that they could be manipulated into the same position for imaging, with the ventricle facing up. After imaging, fish were immediately reanimated in embryo medium and returned to the incubator until the next session. For analysis, epicardial cell number covering the ventricle and the atrium was counted manually at 3, 5, and 7 dpf for at least eight embryos per condition.

2.9: Gene expression analysis

Total RNA was extracted from samples using the RNeasy Mini Kit (Qiagen). Cells were lysed directly in their culture wells and tissues and organoids were lysed and homogenized using the Bead Mill 4 Homogenizer (Fisher Scientific). Once extracted, RNA was quantified using a NanoDrop (Mettler Toledo), with a concentration of at least

10 ng/µL being required to proceed with reverse transcription. All samples were then diluted down to the same concentration using H_2O to ensure the same amount of starting material in future steps. cDNA was synthesized using the Quantitect Reverse Transcription Kit (Qiagen) and stored at -20°C for further use. Primers for qRT-PCR were designed using the Primer Quest tool (Integrated DNA Technologies) and SYBR Green (Qiagen) was used as the DNA intercalating dye. qRT-PCR plates were run using the QuantStudio 5 Real-Time PCR system (Applied Biosystems) with a total reaction volume of 20 µL. Each well contained 10 µL SYBR Green, 6 µL H_2O , 2 µL primer mix (50 nM), and 2 µL cDNA. For analysis, expression levels of genes of interest were normalized to HPRT1 levels and fold change values were obtained using the $2^{-\Delta\Delta CT}$ method. At least 3-5 independent samples were run for each gene expression assay.

2.10: RNA sequencing

RNA was extracted from 3 control and 3 hEpiC samples treated with 100 nM OXT as described above. RNA was quantified using a Qubit Fluorometer (Thermo Fisher Scientific) and samples were sent to the MSU Genomics core, where their quality was tested using the Agilent 2100 Bioanalyzer. Samples were sequenced using the Illumina HiSeq 4000 instrument. For RNA-seq sample processing, a pipeline was created in Galaxy. Briefly, sample run quality was assessed with FASTQC and alignment to hg38 was carried out using HISAT2. Counts were obtained using featureCounts and differential expression analysis was performed with EdgeR. Further downstream bioinformatic analysis performed using **Phantasus** 1.11.0 was (artyomovlab.wustl.edu/phantasus), ToppGene Suite (http://toppgene.cchmc.org), and

Enrichr (https://maayanlab.cloud/Enrichr/). All RNA-seq datasets are deposited in Gene Expression Omnibus under GSE199427.

2.11: Sample preparation for histology/immunofluorescence

For hEpiC samples, cells were first transferred onto Millicell EZ slides (MilliporeSigma), fixed in 4% paraformaldehyde (PFA) solution for ~7 minutes, washed with PBS + 1.5 g/L glycine, and stored at 4°C for further use. hHO samples were transferred to 1.5 mL Eppendorf tubes where they were fixed in 4% PFA for ~40 minutes and washed with PBS-glycine. After extraction, zebrafish hearts were immediately washed in PBS + 0.5 mM ethylenediaminetetraacetic acid (EDTA) solution to remove excess blood, fixed in 4% PFA for ~1 hour, and washed with PBS-glycine. If needed for cryosectioning, hHO and zebrafish samples were transferred into a PBS + 30% sucrose solution for at least 48 hours or until they sank to the bottom of the tube. Tissues were then embedded in Optimal Cutting Temperature (OCT) compound (Electron Microscopy Sciences), frozen in a mold, and sectioned at 10 μm thickness onto Superfrost Plus microscope slides (Fisher Scientific) using the Leica CM3050 S cryostat. Sectioned tissue was stored at 4°C for further use.

2.12: Histology

Masson's trichrome staining was carried out using a kit from IMEB Inc. and following manufacturer's instructions. Briefly, sectioned tissue was immersed in Bouin's solution for ~50 minutes at 56-64°C to improve staining quality and washed in tap water until the yellow color was fully removed from the hearts. Slides were then stained with Biebrich's scarlet/acid fuchsin solution for 7 minutes to label muscle tissue, washed in deionized (DI) H₂O, and immersed in phosphomolybdic/phosphotungstic acid solution for

18 minutes to decolorize fibrous tissue. Next, slides were transferred directly to aniline blue solution for 12 minutes to stain collagen fibers, washed in DI H₂O, and immersed in 1% acetic acid for 3 minutes to stabilize the staining. After washing, tissue was dehydrated by successive exposure to 95% ethanol, 100% ethanol, and xylene and coverslips were added using Eukitt quick-hardening mounting medium (Sigma-Aldrich). For zebrafish tissue, brightfield images were taken of the entire ventricle, taking care to use the same exposure and intensity settings for all hearts. The injury zone was defined as the area of thickened or if applicable, fibrotic tissue. Scar size was quantified manually by tracing the injured myocardial area in ImageJ and dividing it by the total myocardial area. At least 2 sections from at least 3 independent hearts were analyzed for each condition at each time point.

2.13: Immunofluorescence

Before beginning the staining protocol, zebrafish tissues were subject to antigen retrieval by immersing slides in a sodium citrate buffer (10 mM sodium citrate, 0.05% Tween 20, pH 6.0) for ~50 minutes at 95-100°C. To start the process, all samples (cells and tissues) were blocked and permeabilized with 10% normal donkey serum, 0.5% BSA (bovine serum albumin), and 0.5% Triton X-100 in PBS for 1 hour at room temperature. After washing, primary antibodies were diluted in antibody solution (1% normal donkey serum, 0.5% BSA, 0.5% Triton X-100 for tissues and hHOs, 0.05% Triton X-100 for hEpiCs, all dissolved in PBS), added to the samples, and incubated overnight at 4°C. The next day, cells and tissues were washed, and secondary antibodies were diluted in antibody solution (with 0.05% Triton X-100) and added for 2 hours at room temperature. 4'6-diamidino-2-phenylindole (DAPI, Thermo Fisher Scientific) was then added

immediately at a concentration of 1:1000 to label DNA. Stained slides were washed 3 times in PBS and No.1 coverslips (VWR) were added using ProLong Gold Antifade Mountant (Thermo Fisher Scientific). If organoids had been used for whole-mount staining, they were first placed on 90 µm Polybead microspheres (Polysciences, Inc.) on microscope slides to ensure that they would not be deformed by the glass coverslips. When ready, coverslips were added using Vectashield antifade mounting medium (Vector Laboratories). All stained slides were allowed to cure overnight at room temperature and were stored long-term at 4°C until ready for imaging. For an overview of the general principles of immunofluorescence, see **Figure 2.5**.

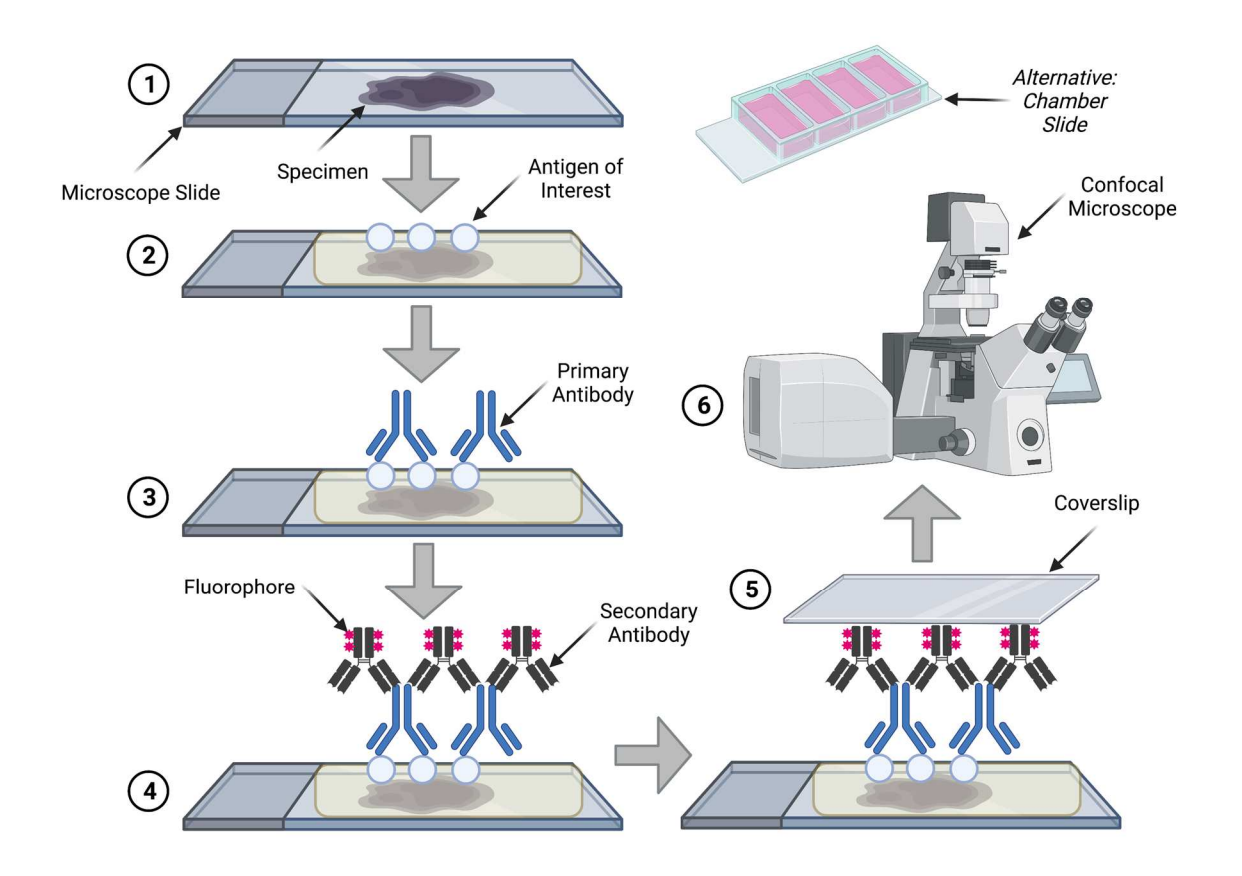


Figure 2.5: Overview of immunofluorescence protocol. 1) Cell or tissue specimens are fixed onto a microscope slide; 2) Slides are immersed in blocking solution to prevent non-specific antibody binding, leaving the antigen of interest exposed; 3) Primary antibodies are added and bind specifically to the antigen of interest; 4) Secondary antibodies are typically conjugated to a fluorophore, which allows for visualization under fluorescent light; 5) A glass coverslip is placed on top of stained slides to prepare them for imaging and to preserve samples long-term; 6) Specimens are imaged under fluorescent light, often through use of a confocal microscope. TOP RIGHT: Two-dimensional cell preparations can also be cultured and stained in multi-well chamber slides, thereby allowing for the simultaneous testing of different culture conditions, treatment groups, etc. Image created with BioRender.com.

2.14: Confocal microscopy and image analysis

All samples were imaged using the Zeiss LSM880 NLO Confocal Microscope system or the Nikon A1 Confocal Laser Microscope. Images were analyzed and prepared for publication using FIJI software. Cell counts were performed manually using the "Multi-Point" tool and automatically using the "Threshold" and "Analyze Particles" tools. Individuals who conducted manual cell counting of hEpiCs and hHOs were blinded to experimental conditions and at least 5 images were analyzed for each group. For analysis of zebrafish confocal images, at least 3 independent fish from each condition were analyzed. Epicardial cell number was quantified by counting the number of GFP+ cells on the surface of the heart and in the subepicardial space per field of view. To ensure consistency in analysis, each image was taken immediately adjacent to the injured area. The number of h3p+/wt1b+ cells in the epicardial region was normalized to the number of DAPI-stained nuclei. Cardiomyocyte proliferation was quantified by manually counting the number of PCNA+ cells per field of view in the myocardium of the infarct border zone. At least two regions per heart were analyzed. Vascularization was quantified by measuring the GFP+ area within the injury region and dividing that value by the total injured area. In all cases, TNNT2 was utilized as a counterstain to allow for visualization of the cryoinjury. For organoid image analysis, area was measured by manually outlining the hHO with at least 8 samples quantified per condition. The extent of apoptosis after cryoinjury in FlipGFP organoids (Zhang et al., 2019) was determined by dividing the GFP+ area by the total hHO area. Manual and automatic counts of H3P+ and WT1+ nuclei in hHOs were performed using FIJI software as described above.

2.15: Statistical analysis

All graphs were made using GraphPad software. Statistical significance was evaluated with a standard unpaired Student's t-test (2-tailed) when comparing two groups or with a 1-way analysis of variance (ANOVA) with Tukey's or Dunnett's post-test for multiple comparison analysis. Regardless of the test used, a P-value of less than 0.05 was considered statistically significant. All data are presented as mean ± SD or SEM and represent a minimum of 3 independent experiments with at least 3 technical replicates unless otherwise stated. For RNA-seq analysis, a false discovery rate (FDR) was used to determine statistical significance.

Chapter 3: Oxytocin Induces a Pro-Regenerative Phenotype in hiPSC-Derived Epicardial Cells

3.1: Introduction

The brain is critical for maintenance of body homeostasis, as crucial processes such as cardiac output, respiration, energy balance, and thermoregulation are all under some degree of central neural control (Dampney, 2016; Guyenet & Bayliss, 2015; Morrison, 2016; Roh et al., 2016). Coincidentally, heart regeneration is an energetically demanding process that serves to maintain homeostasis (Carvalho & Campos de Carvalho, 2010). There is also evidence that damage to the neural endocrine structures, such as the hypothalamus, inhibits limb regeneration in vertebrates (Zhang et al., 2018). This study suggests that some critical factor, such as a peptide or hormone, is released by this brain region to mediate endogenous regenerative processes. hypothesized that the neuroendocrine system is involved in the process of heart regeneration. Specifically, I focused on brain hormones, knowing that upon secretion, they can be carried through the circulation to reach the heart. To confirm my hypothesis, I started by optimizing a recently described human induced pluripotent stem cell (hiPSC) differentiation protocol that yields pure populations of epicardial cells that can be cultured and expanded long-term while retaining their epithelial nature (Bao et al., 2016, 2017). Throughout this chapter, I will refer to these cells as hEpiCs (human iPSC-derived epicardial cells). First, I modified this protocol such that my hEpiCs would be as mature as possible for experiments. That way, they would resemble cells of the adult epicardium as closely as can be achieved in a two-dimensional in vitro model. I then conducted a systematic screening of 15 candidate neuroendocrine peptides to test for their proliferative effects in hEpiCs. I knew that confirming my hypothesis would require an overwhelming amount of evidence, therefore, I decided to select one primary candidate of interest based on the screening results and conduct an in-depth investigation of its proregenerative potential in hEpiCs. Specifically, I would document its effects on dedifferentiation and proliferation of epicardial progenitor cells, processes that are hallmarks of epicardial activation during heart regeneration. In addition, I would gain mechanistic insight into how my candidate hormone induces this phenotype through bulk RNA sequencing and uncover a few signaling genes and pathways that are altered at the transcriptome level in my model. Finally, I would knock down the receptor for my compound of interest and repeat many of the assays described above. Together, the results of these experiments will demonstrate an effective *in vitro* approach to investigate the effects that the neuroendocrine signaling axis has on the epicardium.

3.2: Results

3.2.1: Differentiation of mature-like epicardial cells from human induced pluripotent stem cells

To produce mature-like epicardial cells from human iPSCs I first derived epicardial progenitor cells using a 3-step Wnt modulation strategy (protocol adopted from (Bao et al., 2016, 2017)). This method utilizes small molecule inhibitors to temporally modulate canonical Wnt signaling pathways at specific timepoints throughout differentiation. An initial exposure to CHIR99021, a glycogen synthase kinase 3 (GSK3) inhibitor, prevents phosphorylation of β -catenin, thereby allowing it to activate transcription of Wnt target genes. This step directs iPSCs down the mesoderm lineage. Exposure to Wnt-C59, a porcupine O-acyltransferase (PORCN) inhibitor, 72 hours later blocks palmitoylation of

Wnt ligands, thereby preventing them from activating target cells. This inactivation of Wnt signaling allows cells to transition into cardiac progenitors. Finally, a second exposure to CHIR99021 on Day 7 of differentiation re-activates the Wnt pathway and directs cells down the epicardial instead of the cardiomyocyte lineage (Figure 3.1). As the hEpiCs progress throughout the protocol, they gradually start to acquire hallmark epithelial cell morphology. By the time they reach their second and third passages, the majority of hEpiCs are well-rounded and display a "cobblestone-like" appearance (Figure 3.2). After ~15-20 days of differentiation, I was successfully able to produce pure populations of epicardial cells with 100 to 200-fold higher expression of epicardial progenitor markers WT1 and TCF21 compared to hiPSCs. In addition, >95% of hEpiCs expressed TCF21 as assessed by immunofluorescence (Figure 3.3). Finally, as hEpiCs aged, time course gRT-PCR data showed that expression of WT1 and CDH1 (epithelial cadherin) gradually increased, suggesting that they further strengthen their cellular identity over time (Figure **3.4**). Clearly, my differentiation protocol reliably and reproducibly yielded epicardial progenitor cells.

Notably, my hEpiCs can be maintained and cultured long term in medium containing Vitamin C (L-ascorbic acid) and supplemented with 2 μ M SB431542 (SB) starting on Day 12. Addition of Vitamin C (Vit. C), an antioxidant, protects cells in culture and promotes the cardiac differentiation of pluripotent stem cells (Cao et al., 2012). SB431542 is a TGF- β type 1 receptor inhibitor that keeps cells in their epicardial state and allows them to continue proliferating. Without this inhibitor, WT1+ epicardial cells spontaneously undergo epithelial-to-mesenchymal transition and lose their WT1 expression (Bao et al., 2016). I found that addition of Vit. C and SB to the culture media

allowed me to passage my hEpiCs at least 20 times, all while retaining their epithelial morphology and WT1 levels (Figure 3.5). However, these compounds also prevented hEpiC maturation. As the epicardium develops, its resident cells transition from a highly proliferative and migratory state to a more mature, quiescent phenotype. Considering that the activation and differentiation of adult EpiPCs is the central focus of this project, I sought to conduct my experiments in cells that most closely recapitulated this phenotype. I hypothesized that removing Vitamin C and SB431542 from the hEpiC media for a short time would allow the cells to mature further in the epicardial lineage and provide a better model to study epicardial activation in vitro. Therefore, I removed these two factors and cultured hEpiCs for 5 days at confluence without passaging. Cells were then assayed for gene expression of common epicardial, smooth muscle, and fibroblast markers to assess potential transdifferentiation into other cell types. Immunofluorescence showed that nearly 100% of hEpiCs stained positive for TJP1 (tight junction protein 1), a highly specific epithelial tight junction protein also known as ZO-1 (zonula occludens 1; Figure 3.5). In addition, qRT-PCR analyses showed no significant difference in expression of smooth muscle marker CNN1 (calponin 1), fibroblast marker VIM (vimentin), and myofibroblast marker ACTA2 (alpha smooth muscle actin) between control and matured hEpiCs Therefore, the cells maintained their epithelial nature and did not (Figure 3.6). spontaneously undergo EMT during the 5 day culture period.

I then explored the effects of removing these components on hEpiC maturation. First, I cultured cells with and without Vit. C and SB and found that cell counts were three times higher with both of them present and two times higher with only one of them present compared to when they were absent (**Figure 3.7**). qRT-PCR for epicardial progenitor

and EMT markers showed that SB removal decreased expression of *WT1*, *TCF21*, and *NT5E* (5'-nucleotidase, an enzyme found in mesenchymal cells) all while increasing expression of mature epithelial marker *CDH1* (**Figure 3.8**). Remarkably, when I tried increasing the length of time hEpiCs were cultured without SB to 12 days, I still observed similar decreases in epicardial and EMT genes (**Figure 3.9**). Taken together, these data suggest that removal of Vitamin C and SB431542 from the hEpiC media decreases their proliferation rates and allows them to adopt a more mature, quiescent transcriptional phenotype, thereby confirming my hypothesis. And even when the cells are cultured in the absence of these components for a longer period of time, they refrain from undergoing EMT and retain their epithelial nature. Therefore, all future experiments with epicardial cells were performed using this final media formulation to ensure that hEpiCs resembled epicardial cells in the adult heart as much as possible.

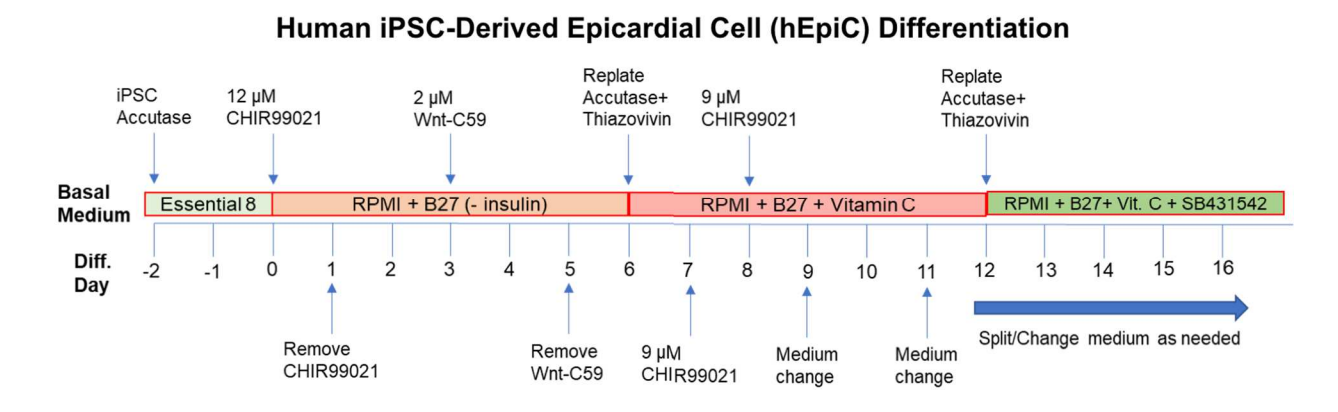


Figure 3.1: Schematic of protocol used for hEpiC differentiation.

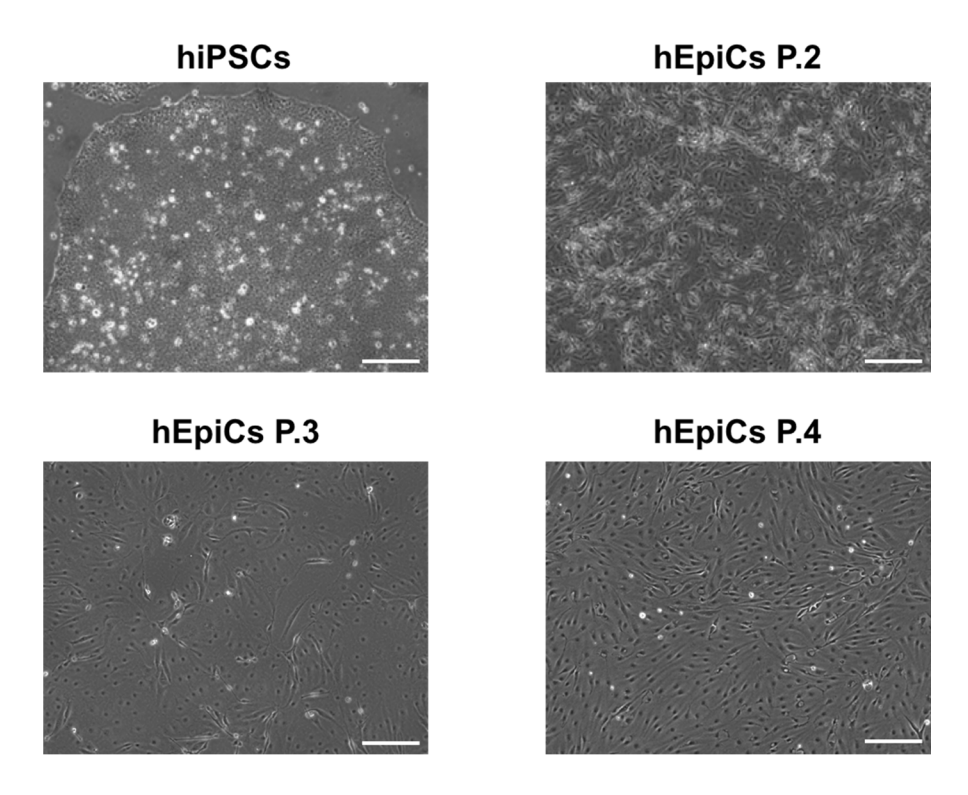


Figure 3.2: hEpiCs display epithelial cell morphology. Brightfield images of hEpiCs through four passages showing the gradual accumulation of the classic epithelial cell cobblestone morphology; scale bar: $500 \ \mu m$.

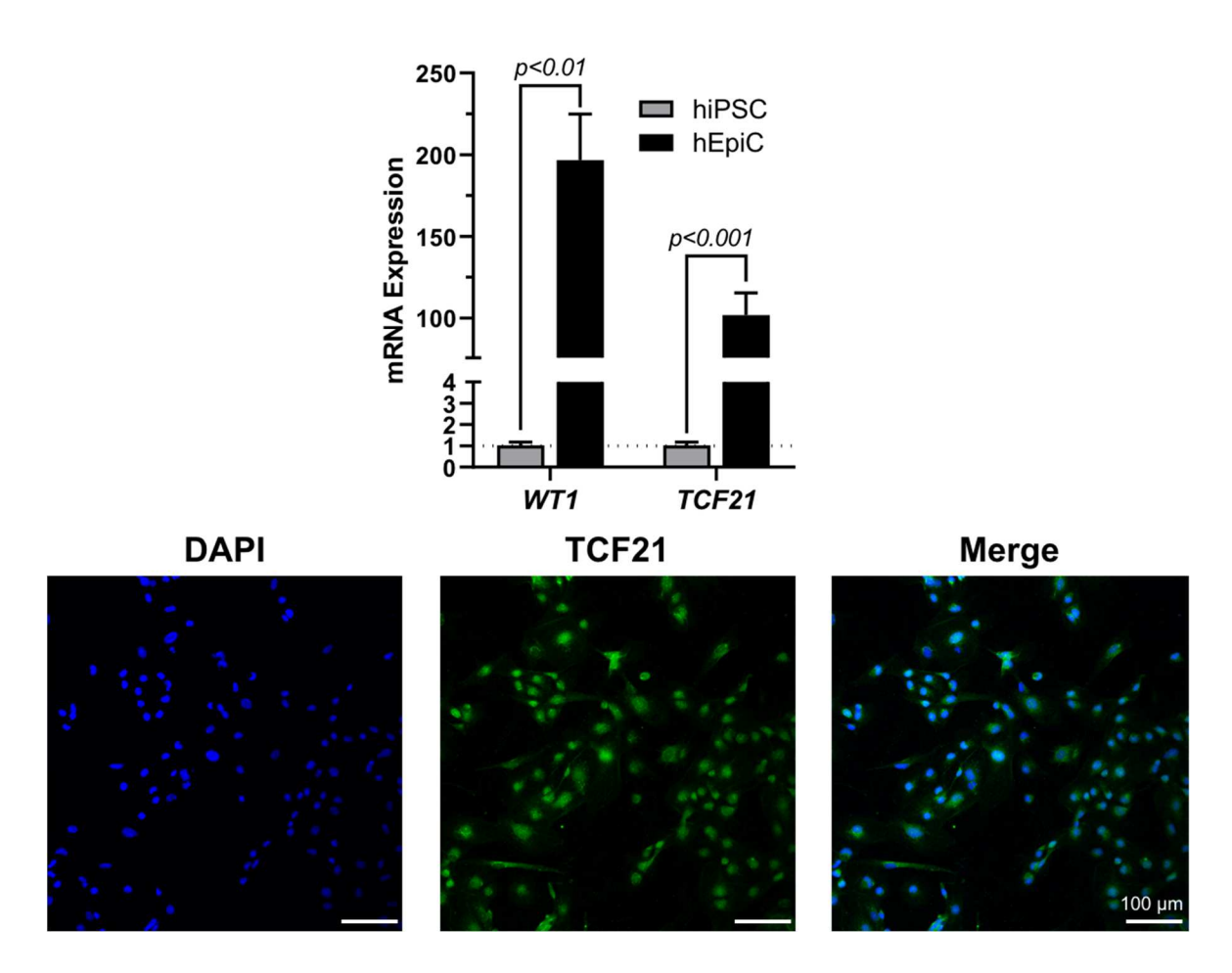


Figure 3.3: hEpiCs express epicardial cell markers. \underline{TOP} : qRT-PCR data for epicardial markers WT1 and TCF21 in hiPSCs and hEpiCs; n=4-6 wells per cell line. \underline{BOTTOM} : Confocal immunofluorescent images for TCF21 (green) and DAPI (blue) showing TCF21 expression in nearly 100% of hEpiC nuclei; scale bar: 100 μ m.

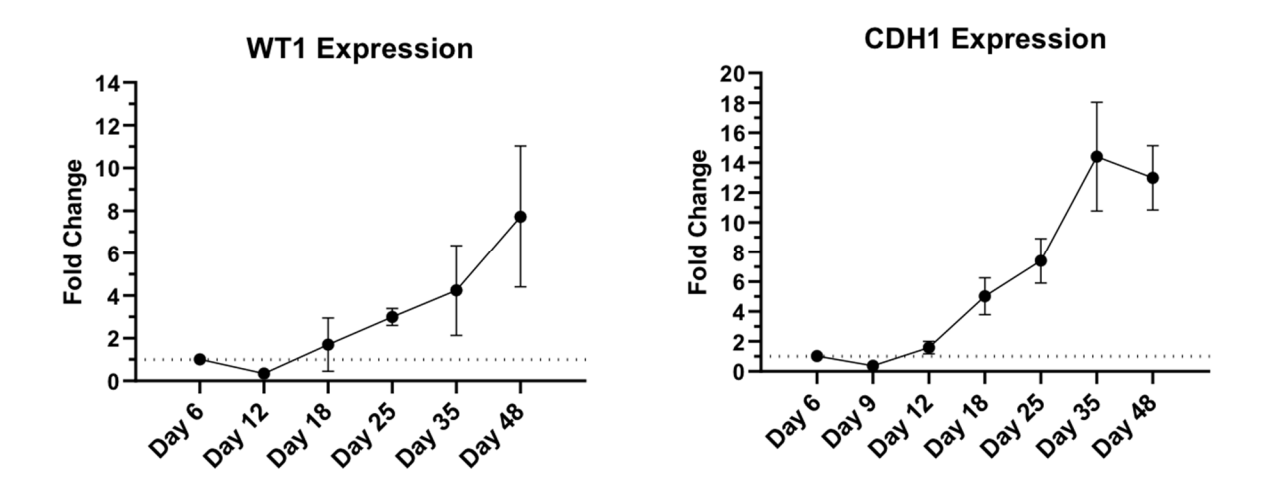


Figure 3.4: Differentiating hEpiCs increase expression of epicardial markers. qRT-PCR data for epicardial (*WT1*) and epithelial (*CDH1*) markers throughout hEpiC differentiation, suggesting an increase in epicardial nature over time; n=3 wells per time point.

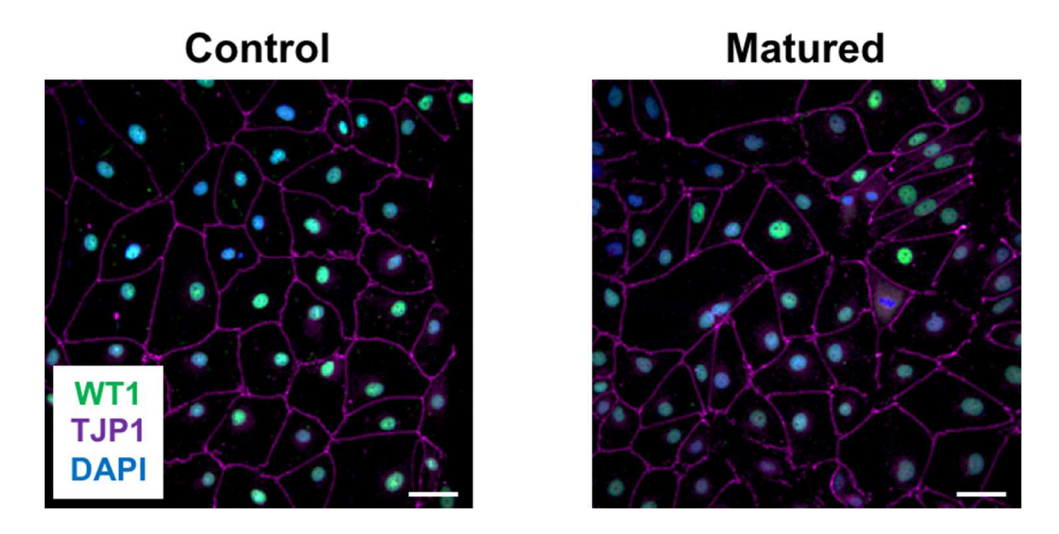


Figure 3.5: Matured hEpiCs retain their epithelial nature. Confocal immunofluorescent images showing robust expression of epithelial markers before (Control) and after (Matured) removal of Vitamin C and SB431542 from the culture media. Epicardial cells are labeled with WT1 (green), epithelial membranes with TJP1 (magenta), nuclei with DAPI (blue); scale bar: $50 \mu m$.

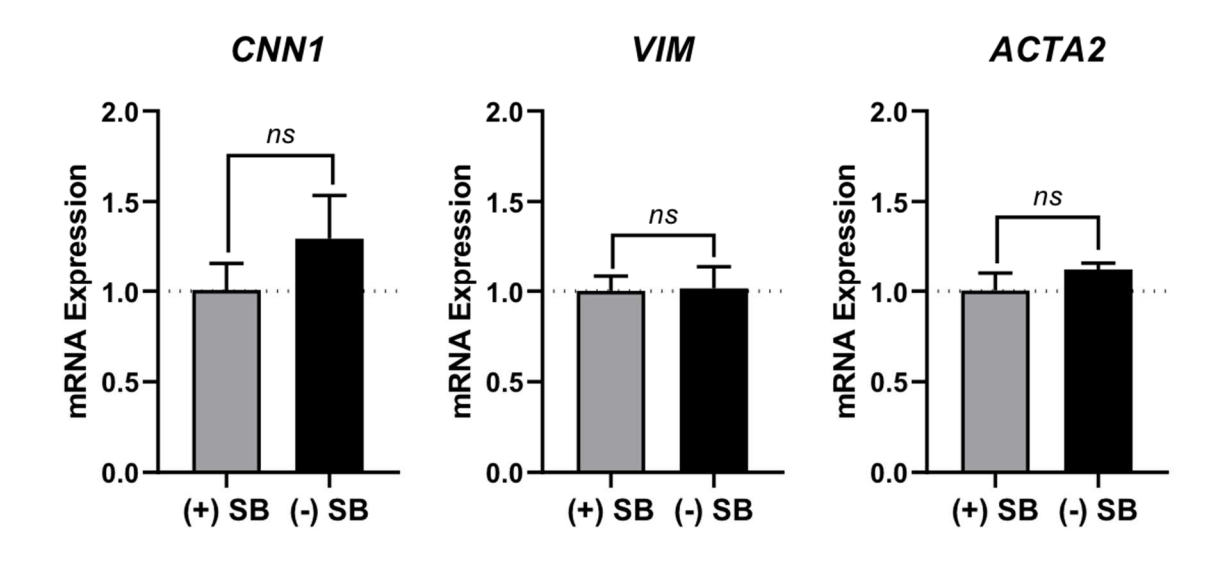


Figure 3.6: Matured hEpiCs do not undergo EMT. qRT-PCR data for hEpiCs in the presence or absence of SB431542, showing no change in smooth muscle (*CNN1*) or fibroblast (*VIM*, *ACTA2*) differentiation; n=3 wells per condition.

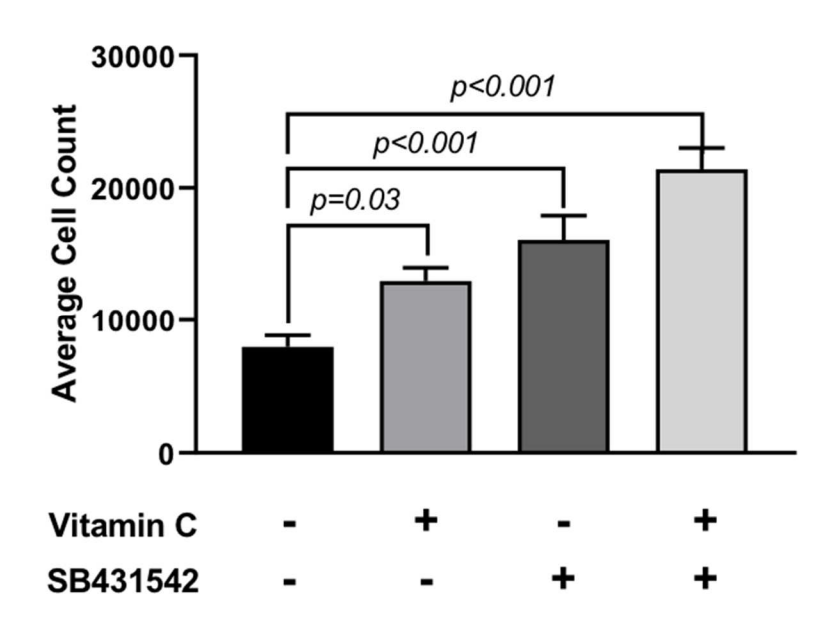


Figure 3.7: Matured hEpiCs decrease their proliferation rates. Number of DAPI-labeled nuclei after exposure to different combinations of Vitamin C and SB431542; n>20 wells per condition.

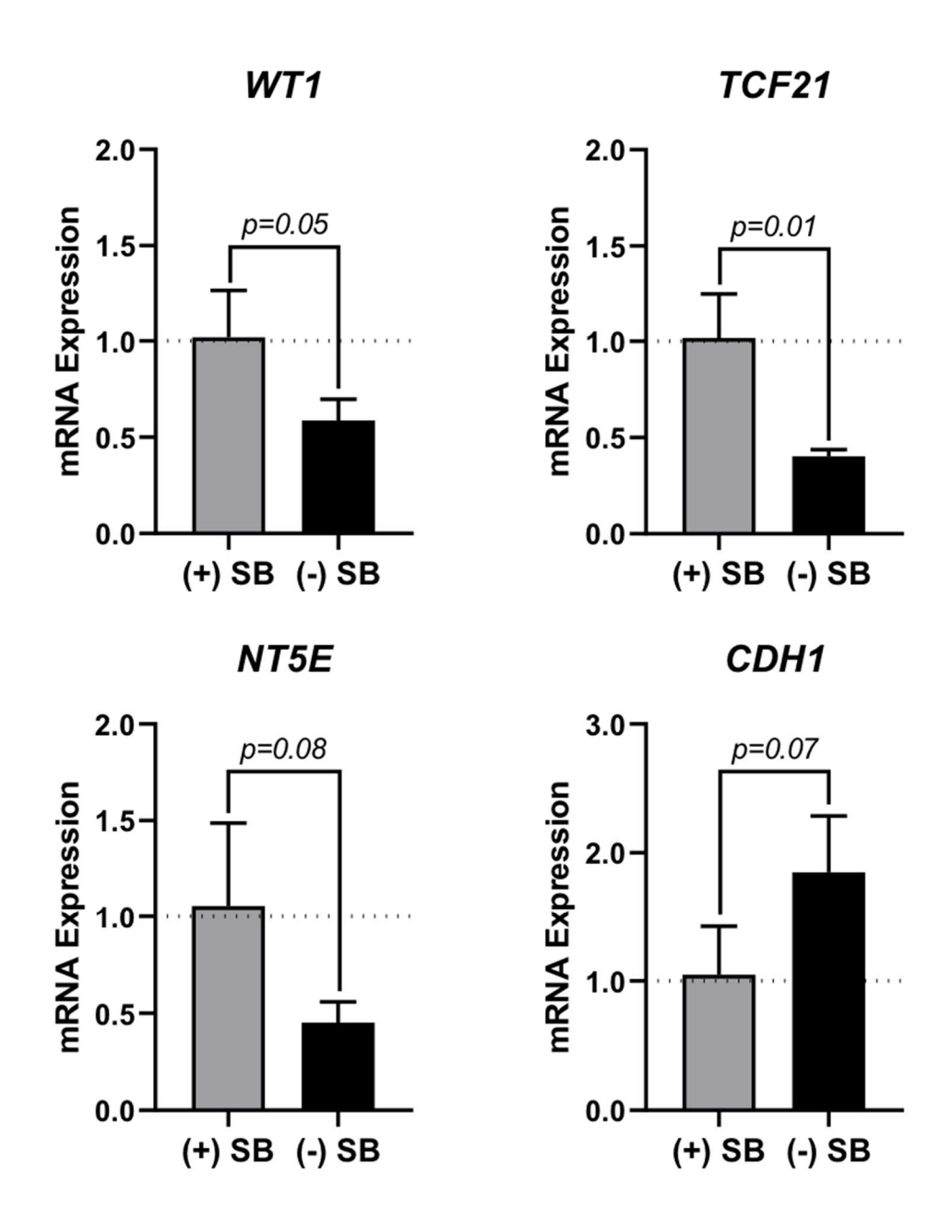


Figure 3.8: Matured hEpiCs display a quiescent transcriptional phenotype short-term. qRT-PCR data for hEpiCs in the presence or absence of SB431542 (SB), showing a decrease in EpiPC (*WT1*, *TCF21*) and mesenchymal (*NT5E*) markers and an increase in epithelial (*CDH1*) markers when this compound is removed from the media for 5 days; n=3 wells per condition.

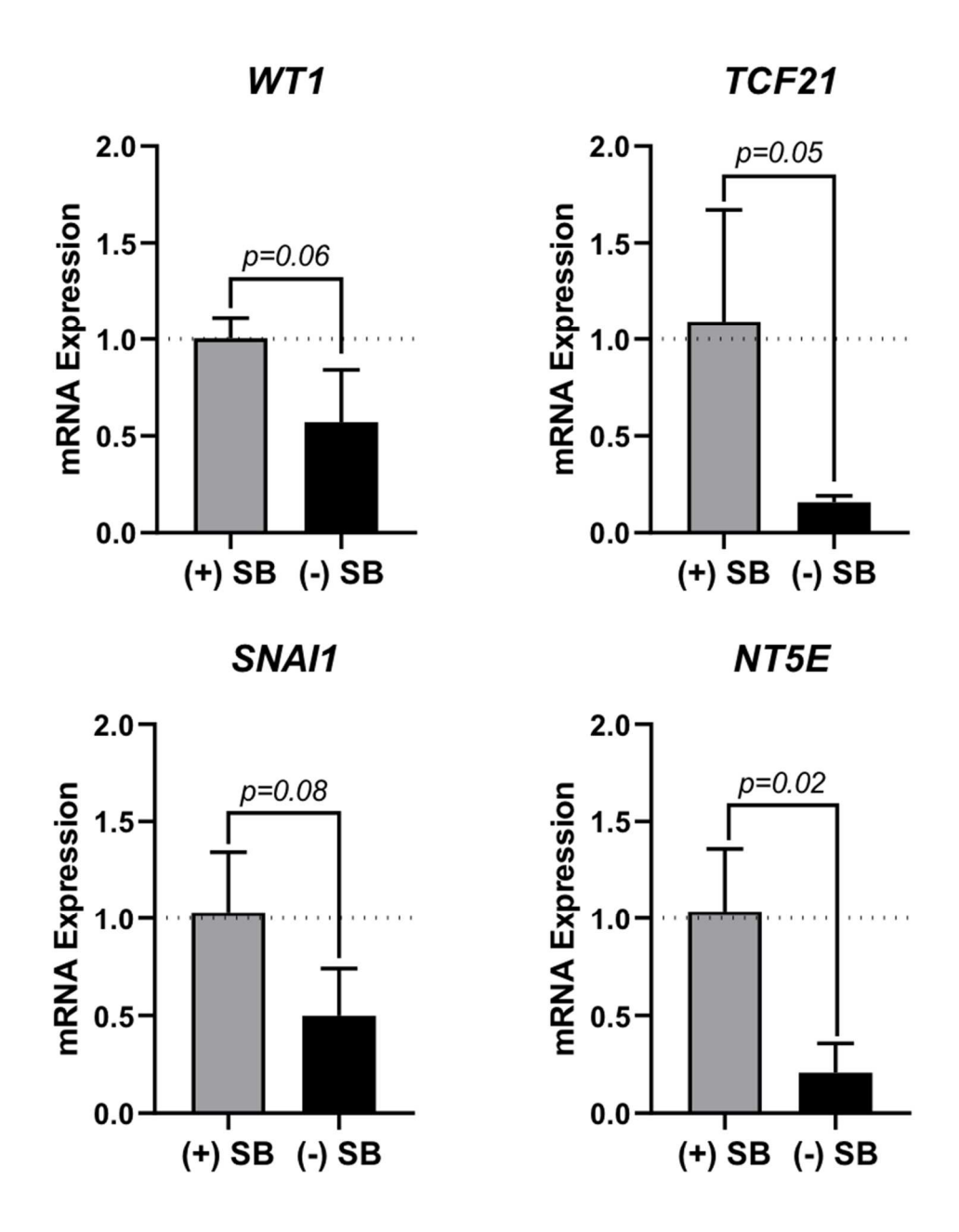


Figure 3.9: Matured hEpiCs display a quiescent transcriptional phenotype long-term. qRT-PCR data for hEpiCs in the presence or absence of SB431542 (SB), showing a decrease in EpiPC (*WT1*, *TCF21*), EMT (*SNAI1*), and mesenchymal (*NT5E*) markers when this compound is removed from the media for 12 days; n=3 wells per condition.

3.2.2: Neuroendocrine candidate screening in hiPSC-derived epicardial cells

To identify potential neuroendocrine hormones that may be involved in epicardial activation and possibly heart regeneration, I first scanned the existing literature to identify candidate peptides. I utilized two main criteria to select my hormones of interest: 1) being involved in the physiological response to stress/injury and 2) being produced and secreted by neuroendocrine tissue. In total, I identified 15 endogenous candidates that met these criteria (**Table 3.1**). To narrow this list of hormones down to one for further analysis, I screened each of them for their proliferative effects on mature hEpiCs in culture. Specifically, I treated cells with each compound for 3 days in a 96-well plate format and stained them with an antibody against phosphorylated histone H3 (H3P) as a putative marker of cellular proliferation. I then used a high-content imaging microscope to count the percentage of H3P+ cells in each well. While growth hormone (GH) and melanin-concentrating hormone (MCH) both produced statistically significant results, oxytocin (OXT) displayed the strongest proliferative effects (~3-fold versus control hEpiCs) and was selected for further downstream analysis (**Figure 3.10**).

Oxytocin (OXT) is a nine amino acid neuropeptide produced by magnocellular neurosecretory cells of the hypothalamus and released into circulation by the posterior pituitary. OXT was first discovered in studies using pituitary extracts in the early 1900s (Dale, 1906; Ott & Scott, 1910; Schafer & Mackenzie, 1911) and its amino acid sequence was identified in the 1950s (Du Vigneaud et al., 1953). The best characterized roles for OXT are in facilitating parturition, lactation, and social bonding. It is especially important for stimulating uterine contractions during childbirth, inducing the milk ejection reflex in lactating mothers, and promoting positive social interactions between individuals

(Argiolas & Gessa, 1991; Kosfeld et al., 2005; Lee et al., 2009). However, oxytocin also has lesser-known roles in the body, including in the cardiovascular system, where it lowers blood pressure, induces negative inotropic and chronotropic effects, and serves as a vasodilator, anti-inflammatory, and anti-oxidant (Gutkowska et al., 2014; Jankowski et al., 2020). In fact, several recent studies have demonstrated the cardioprotective effects of OXT administration. There is ample evidence to suggest that oxytocin improves cardiac function during heart failure. In one report, Garrott et al. experimentally induced left ventricular hypertrophy and heart failure in rats by trans-ascending aortic constriction (TAC) and chronically activated OXT neurons in the hypothalamus using DREADD (designer receptors exclusively activated by designer drugs) receptors. Eight weeks after injury (and after four weeks of chronic OXT administration), the treated animals showed reduced cardiomyocyte hypertrophy and fibrosis accumulation as well as improved contractility (Garrott et al., 2017). In a more recent study, heart failure was again induced in adult rats, with chronic stimulation of OXT neurons in the paraventricular nucleus (PVN) of the hypothalamus being achieved using a combination of DREADDs and optogenetic approaches. The authors found that oxytocin treatment improved cardiac function by increasing the excitation of cardiac vagal neurons in the brainstem, leading to the activation of the parasympathetic neurons that innervate the heart (Dyavanapalli et al., 2020).

While OXT is able to ameliorate heart failure in rodent models, it also has beneficial effects before the injured heart even reaches that point. Indeed, there is evidence that OXT is cardioprotective after experimental MI. For example, studies have shown that pre-treatment with oxytocin directly reduces infarct size after ischemia-reperfusion (I/R)

injury in isolated rat hearts. This is the case both when the hearts are perfused with OXT ex vivo before ischemia (Ondrejcakova et al., 2009) and when the OXT is continuously delivered *in vivo* via osmotic mini-pumps (Ondrejcakova et al., 2012). Perhaps of more clinical relevance, there is also data to suggest that OXT treatment at the onset of cardiac injury has cardioprotective effects. Notably, isolated rat hearts subject to I/R injury show smaller infarct sizes, less cellular apoptosis, increased coronary blood flow, and fewer arrhythmias when OXT is administered during the reperfusion phase compared to controls. These effects are mediated by phosphatidylinositol-3-kinase (PI3K)/Akt and extracellular signal-regulated kinase 1/2 (ERK1/2) signaling (Polshekan et al., 2016) as well as Janus kinase/Signal transducer and activator of transcription-3 (JAK/STAT3) signaling (Polshekan et al., 2019). The same effects hold *in vitro*, as heart-derived H9c2 cells subject to hypoxia-induced ischemia show decreased apoptosis and increased survival when OXT is added to the media at the onset of normoxia/reperfusion (Gonzalez-Reyes et al., 2015).

At the cellular level, the oxytocin peptide has significant regenerative potential, as it can induce proliferation and differentiation of several cell types. Indeed, continuous OXT administration for one week after rat MI leads to a >2-fold increase in expression of proliferating cell nuclear antigen (PCNA) in the infarct zone compared to rats treated with saline (Jankowski et al., 2010). And these effects are reversed when OXT signaling is blocked. Neonatal mice subject to left ventricular apex resection at postnatal day (PND) 1 show ~2-fold decrease in cardiac cell proliferation when they are also administered a short hairpin RNA (shRNA) against the oxytocin receptor at the time of injury. The authors propose that these effects are mediated in part by the c-Myc signaling pathway, as

expression of this protein is ~2-fold lower in shRNA-treated animals than controls (Khori Notably, OXT induces not just cardiac cell proliferation, but also et al., 2021). differentiation. One landmark study conducted in pluripotent P19 embryonic carcinoma cell aggregates demonstrated that oxytocin exposure leads to increased cardiomyocyte differentiation. P19 cells treated with OXT for 10 days showed increased myosin heavy chain (MHC) staining, higher retention levels of rhodamine 123, and earlier beating onset than control cells, findings that are all consistent with a CM phenotype (Paguin et al., 2002). And OXT is able to induce differentiation of more than just cardiomyocytes, as human umbilical vein endothelial cell (HUVEC) spheroids exposed to this hormone display increased capillary sprouting, indicating a pro-angiogenic effect (Cattaneo et al., 2009). Notably, recent evidence suggests that oxytocin is also released into circulation after cardiac injury. In one study, the authors utilized left anterior descending (LAD) coronary artery ligation to induce acute myocardial infarction in rats. 90 minutes after the induction of ischemia, brains were collected and immunolabeled for Fos protein, a marker of neuronal activation. Remarkably, oxytocin neurons in the paraventricular and supraoptic nuclei of the hypothalamus showed a significant increase in Fos expression after injury (Roy et al., 2019). Taken together, the above studies combine to show that OXT has cardioprotective benefits after MI, effects that may be due to its direct release from the hypothalamus. These findings, combined with the fact that injury-induced epicardial activation can be primed by specific signaling factors, such as thymosin β4 (Smart et al., 2007, 2011), suggest that oxytocin may be the critical factor in achieving sufficient EpiPC activation and differentiation to regenerate the lost myocardium after cardiac injury.

Many of the cardiac effects of OXT are mediated by atrial natriuretic peptide (ANP) and nitric oxide (NO) signaling. Experiments using isolated rodent and canine hearts have demonstrated that oxytocin directly induces the cardiac release of ANP and NO, leading to negative inotropic and chronotropic effects (Favaretto et al., 1997; Gutkowska et al., 1997; Mukaddam-Daher et al., 2001). These two factors have well-characterized cardioprotective actions (Jones & Bolli, 2006; Nishikimi et al., 2006). In fact, there is evidence that ANP induces a pro-regenerative phenotype in vitro, as primary human endothelial cells treated with this peptide show increased proliferation and migration (Kook et al., 2003). In addition, treating injured zebrafish hearts with nitrite in a hypoxic environment leads to increased cardiomyocyte proliferation, angiogenesis, and recruitment of immune cells to the site of injury. This finding is important because nitrite is reduced to nitric oxide in hypoxic conditions, suggesting that NO mediates the phenotype observed in this study (Rochon et al., 2020). Clearly, these downstream effectors of OXT can be beneficial to heart function as well. Importantly, these effects are mainly initiated by the oxytocin receptor (OXTR), a 389 amino acid G protein-coupled receptor (GPCR) that is relatively conserved across species (Gimpl & Fahrenholz, 2001). There is only one OXTR in humans, and OXT binding primarily targets phospholipase Cβ (PLC-β) activity, leading to inositol trisphosphate (IP₃) and diacylglycerol (DAG) generation (Jankowski et al., 2020). Increased intracellular IP₃ stimulates the release of calcium from the sarcoplasmic reticulum, which in turn leads to the release of ANP and NO from activated cells. Increased intracellular DAG activates protein kinase C (PKC) signaling and downstream pro-survival pathways, such as ERK (Gutkowska & Jankowski, 2012). Together, OXTR, ANP, and NO activate cyclic guanosine monophosphate

(cGMP), 5' adenosine monophosphate-activated protein kinase (AMPK), and nuclear factor of activated T-cells (NFAT) proteins, among others (Jankowski et al., 2020). These signaling pathways ultimately act together to mediate the cardioprotective effects of OXT discussed above. And my screening data suggest that oxytocin is also able to induce proliferation of human epicardial cells (**Figure 3.10**). Clearly, OXT has significant potential as a compound that can enhance epicardial activation and heart regeneration. And now that I had my model of adult human epicardial cells in place and my screening results in hand, I was able to more thoroughly investigate this hypothesis.

Table 3.1: Neuroendocrine candidate list for screening in hEpiCs.

Name	Abbreviation	Site of Production	Site of Release	Regenerative Effect	References	Screening Concentration
Adrenocorticotropic Hormone	ACTH	Anterior Pituitary	Anterior Pituitary	Cortisol inhibits heart and tailfin regeneration in zebrafish	Sallin and Jazwinska, 2016; Hartig et al., 2016	2 μΜ
Brain-Derived Neurotrophic Factor	BDNF	Many Brain Regions	Many Brain Regions	Stimulates proliferation of neural stem cells (by activating Wnt signaling)	Chen et al., 2013	1.14 µM
Growth Hormone	GН	Anterior Pituitary	Anterior Pituitary	Full limb regeneration in hypophysectimized newts	Landesman and Hessler, 1981; Landesman and Copeland, 1988	0.023 μΜ
Growth Hormone- Releasing Hormone	GHRH	Hypothalamus	Hypothalamus	GHRH agonist increases mitosis and decreases infarct size in rats after MI	Kanashiro-Takeuchi et al., 2012	3.6 µM
Melanin-Concentrating Hormone	мсн	Hypothalamus	Hypothalamus	Stimulates GH secretion and may promote pancreatic islet regeneration	Segal-Lieberman et al., 2006; Pissios et al., 2007	3.9 µM
Neuropeptide Y	NPY	Hypothalamus	Hypothalamus	Promotes mitosis in vascular smooth muscle cell cultures	Pons et al., 2003	2.5 μΜ
Oxytocin	ОХТ	Hypothalamus	Posterior Pituitary	Induces CM differentiation and stimulates muscle regeneration in mice	Paquin et al., 2002; Jankowski et al., 2004; Elabd et al., 2014	10.8 μM
Pituitary Adenylate Cyclase Activating Polypeptide	PACAP	Pituitary Gland	Pituitary Gland	Stimulates axonal regeneration after spinal cord injury in mice	Tsuchida et al., 2014	0.62 μM
Pro-Opiomelanocortin	POMC	Hypo./Pituitary	Cleaved to Peptides	Cleavage products have numerous regenerative effects	N/A	0.214 μM
Prolactin	PRL	Anterior Pituitary	Anterior Pituitary	Promotes tail regeneration in newts and regulates liver regeneration in mice	Liversage et al., 1984; Moreno-Carranza et al., 2013	0.028 μM
Somatostatin	GHIH	Hypothalamus	Hypothalamus	Inhibits limb and tail regeneration in newts	Vethamany-Globus et al., 1977	2.26 µM
Thyroid Stimulating Hormone	TSH	Anterior Pituitary	Anterior Pituitary	Thyroid hormone (TH) surge in mice at PND 15 causes CM proliferation	Naqvi et al., 2014	0.264 μM
Thyrotropin-Releasing Hormone	TRH	Hypothalamus	Hypothalamus	Stimulates epidermal regeneration in tadpole and human skin	Meier et al., 2013	200 μΜ
α-Melanocyte- Stimulating Hormone	α-MSH	POMC/ACTH Cleavage	Hypo./Brainstem	Binds to Mc4r, which is required for tadpole limb regeneration	Zhang et al., 2018	6.6 µM
β-Endorphin	β-End	POMC/ACTH Cleavage	Hypo./Pituitary	Stimulates forelimb regeneration in hypophysectimized newts	Morley and Ensor, 1986	2.5 μΜ

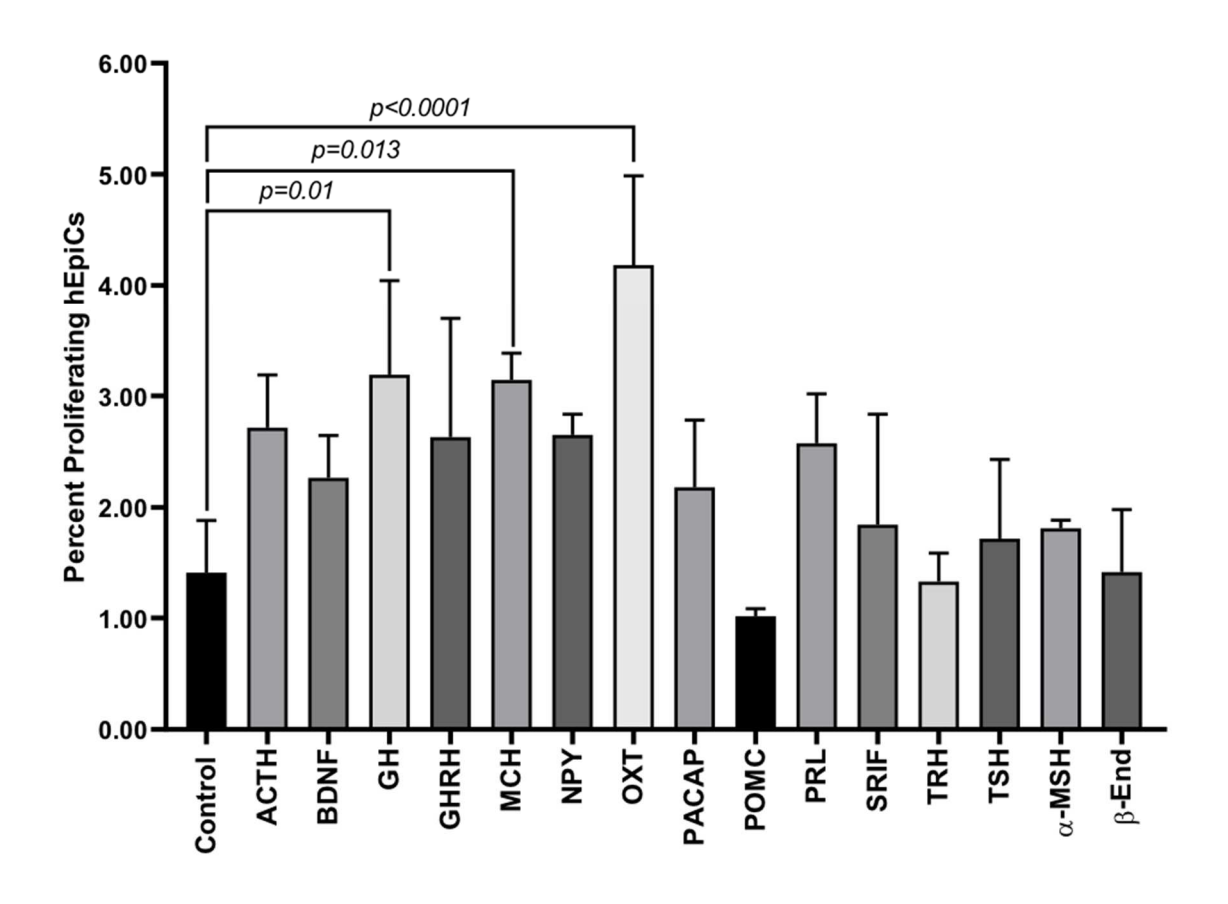


Figure 3.10: Neuroendocrine screening results. Proliferative effects of 15 candidate peptides, shown as the percentage of hEpiCs expressing H3P after exposure to each compound; n=3 wells per condition.

3.2.3: Oxytocin induces proliferation in hiPSC-derived epicardial cells

I next sought to confirm the results of my screening analysis more systematically through immunofluorescence and cell counting assays. I exposed hEpiCs to 100 nM OXT and assessed cell proliferation levels by staining for Ki67, an antigen present in dividing cells. As expected, the percentage of proliferating epicardial cells (defined as nuclei positive for Ki67 and WT1, surrounded by a ring of TJP1 staining) nearly doubled 3 days after oxytocin administration (Figure 3.11). I also assessed proliferation through automated direct cell counting by seeding equal numbers of cells in wells, adding OXT, and labeling them with DAPI, a nuclear dye. I chose to utilize this approach because epicardial cells are mononucleated, meaning that one nucleus equals one cell (Quijada et al., 2020). Again, 3 days after OXT addition, the number of epicardial cells per well increased nearly 2-fold (Figure 3.12). Together, these experiments definitively demonstrate that OXT induces epicardial proliferation. Of significance, I also compared the effects of oxytocin to those of thymosin β4, a short actin sequestering peptide that has been shown to elicit strong epicardial activation in vitro and in vivo in mice (Smart et al., 2007, 2011; Wang et al., 2021). OXT caused a proliferative response that was approximately 2-fold greater than that of the most potent thymosin β4 dose administered (Figure 3.12). To determine the optimal OXT dose, I also counted nuclei after exposure to different OXT concentrations and found that 100 nM induced the greatest increase in proliferation. Therefore, I settled on this value for use in future experiments (Figure 3.13). It should be noted that although I consistently observed a ~1.5-2 fold increase in cell counts in response to OXT treatment in numerous assays, this response was only seen if Vitamin C was not present in the media. Indeed, while oxytocin induced the expected

increase in hEpiC counts in wells lacking Vit. C, this increase did not occur in wells containing Vit. C (**Figure 3.14**). I suspect that because Vitamin C is known to promote proliferation of numerous cell types *in vitro* (Fujisawa et al., 2018; Kouakanou et al., 2020; Zhang et al., 2016), its presence in the hEpiC media masks any proliferative effects of OXT that would be seen otherwise. In addition, ascorbic acid itself has been shown to increase oxytocin secretion *in vitro*, so adding it would prevent me from determining what ultimately causes increases in hEpiC proliferation (Luck & Jungclas, 1987). My findings lend further justification for my use of the maturation conditions presented in Section 3.2.1 and demonstrate that OXT most strongly induces cellular proliferation in more adult-like hEpiCs.

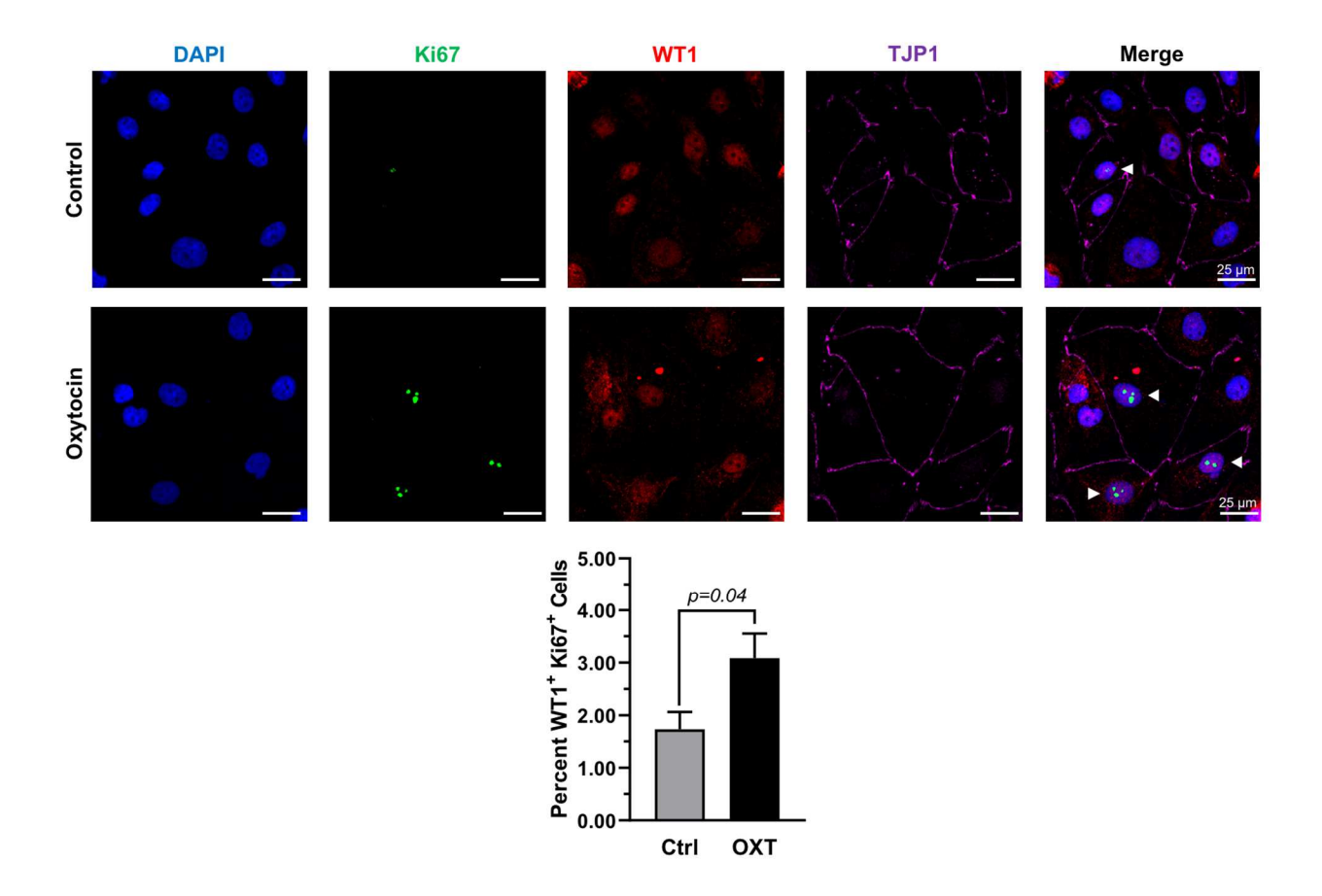


Figure 3.11: OXT induces hEpiC proliferation. Confocal immunofluorescent images and quantification of proliferating hEpiCs after 3 day OXT exposure. Epicardial cells are labeled with WT1 (red), epithelial membranes are labeled with TJP1 (magenta), proliferating cells (arrowheads) are labeled with Ki67 (green), nuclei are labeled with DAPI (blue); n=4 wells per condition, scale bar: $25 \mu m$.

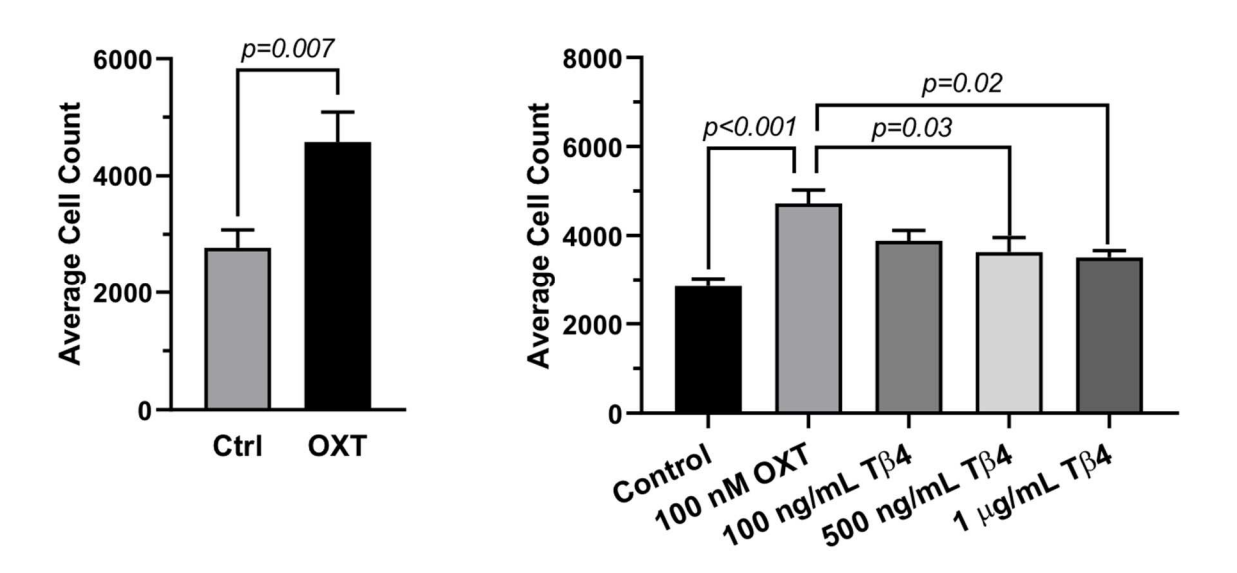


Figure 3.12: OXT displays more potent effects than thymosin β4. Number of DAPI-labeled epicardial cell nuclei after 3 day exposure to OXT (LEFT) or thymosin β4 (RIGHT), a compound previously shown to induce epicardial activation; n≥8 wells per condition.

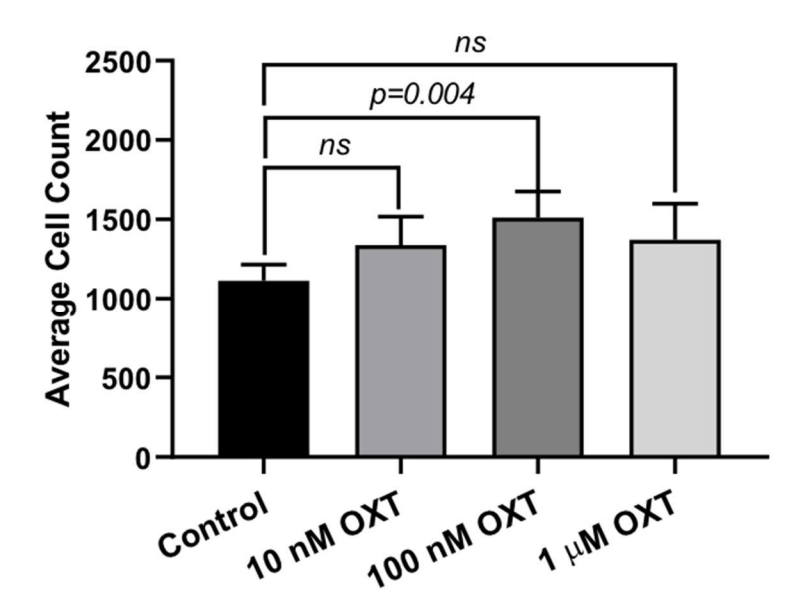


Figure 3.13: 100 nM OXT induces optimal hEpiC proliferation. Number of DAPI-labeled epicardial cell nuclei after 3 day exposure to different concentrations of OXT; n=6 wells per concentration.

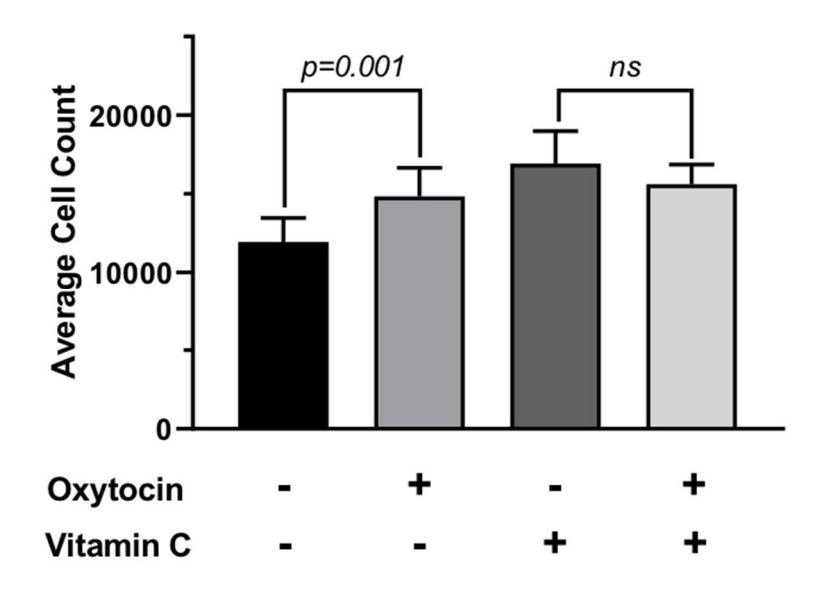


Figure 3.14: Vitamin C masks the proliferative effects of OXT. Number of DAPI-labeled nuclei after exposure to different combinations of oxytocin and Vitamin C; n>10 wells per condition.

3.2.4: Oxytocin induces dedifferentiation of hiPSC-derived epicardial cells to a stem-cell like state

In addition to cellular proliferation, one of the hallmark phenotypes of epicardial activation is the transition of quiescent epicardial cells to a stem-cell like state. In order to form epicardial progenitor cells, mature cells must undergo EMT, which is mediated by a reactivation of the developmental gene program (Quijada et al., 2020; Smits et al., 2018). Indeed, both WT1 and TCF21 have been implicated in regulating EMT (Acharya et al., 2012; Martínez-Estrada et al., 2010; Von Gise et al., 2011). As part of its transition from a dormant to an active state, the epicardium transiently upregulates expression of key genes such as WT1 and TCF21, among others (Huang et al., 2012; Van Wijk et al., 2012; Zhou et al., 2011). Therefore, I tested whether oxytocin administration recapitulates this phenotype in epicardial cells in vitro. Specifically, I treated hEpiCs with 100 nM OXT for 3 days, collected the RNA, and conducted gRT-PCR for EpiPC and EMT markers (Figure 3.15). I found that OXT induced a ~1.5-fold increase in WT1 and TCF21 gene expression. In addition, SNAI1 levels increased by the same amount, which is important because the snail gene family is known to control EMT at the transcriptional level (Von Gise & Pu, 2012). I also observed a nearly 2-fold increase in NT5E levels, used here as a marker of mesenchymal cells. These data all support the notion that OXT induces EMT in hEpiCs. Perhaps of most significance, I observed no changes in expression of CDH1, a cadherin (cell adhesion molecule) found specifically in epithelial cell junctions, between control and OXT treated cells. This finding makes sense, because Wt1 has been shown to activate Snai1 and inactivate Cdh1 in epicardial cells (Martínez-Estrada et al., 2010). In addition, Snail proteins are well-known to directly repress

transcription of E-cadherin (Barrallo-Gimeno & Nieto, 2005; Y. Wang et al., 2013). Taken together, these qRT-PCR data demonstrate that oxytocin administration induces epicardial cell activation to a progenitor-like state by increasing the expression of EpiPC, EMT, and mesenchymal markers without a corresponding change in epithelial markers.

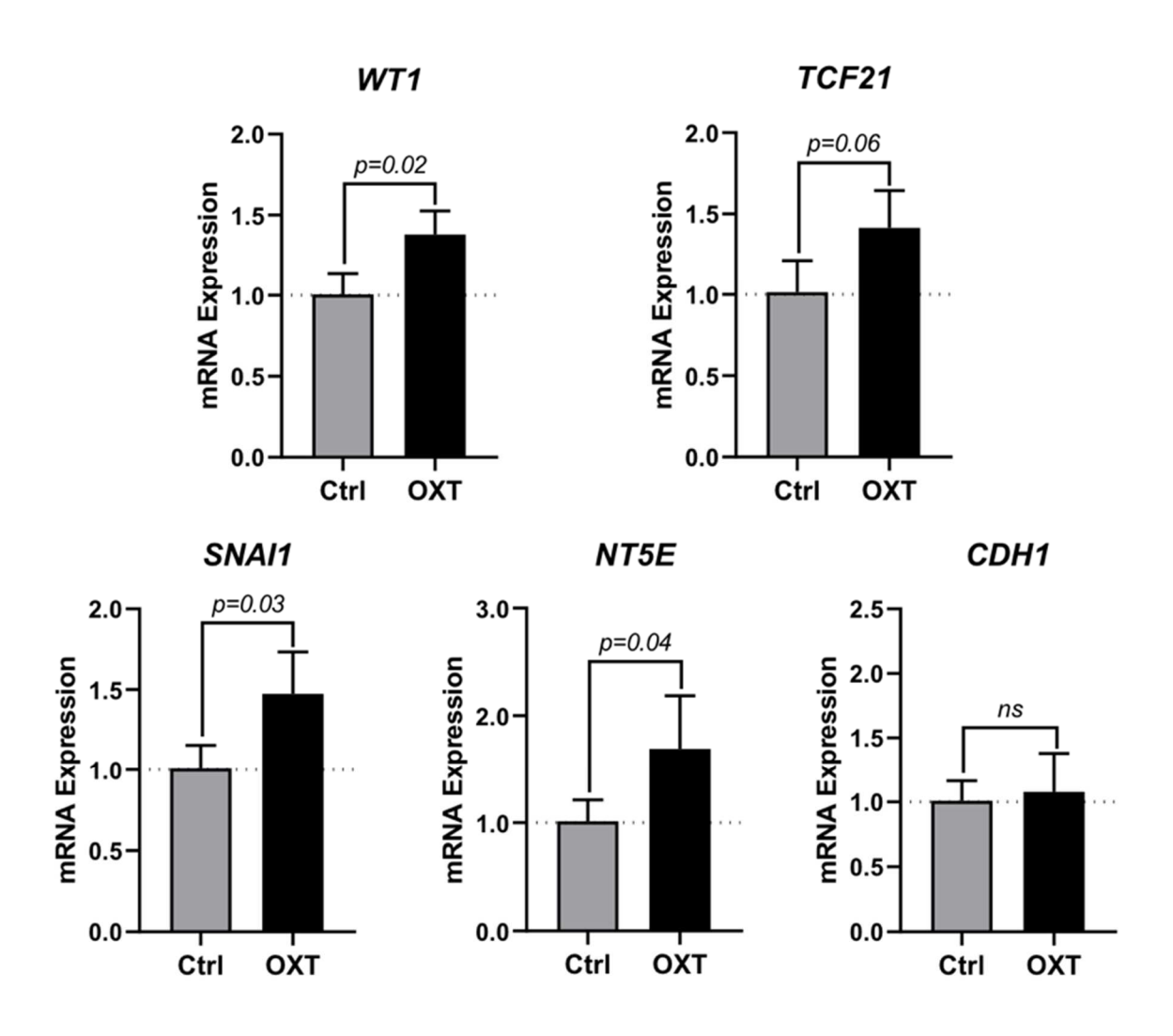


Figure 3.15: OXT induces hEpiC activation. qRT-PCR data for epicardial cells exposed to OXT, showing an increase in EpiPC (WT1, TCF21), EMT (SNAI1), and mesenchymal (NT5E) markers, without a corresponding increase in epithelial (CDH1) markers; n=4 wells per condition.

3.2.5: Transcriptomic analysis reveals a critical role for the TGF-β pathway in mediating the effects of OXT

To uncover additional clues related to the potential mechanism of action driving the effects of oxytocin, I performed bulk RNA sequencing (RNA-seq) on hEpiCs in control and OXT conditions as described above. These transcriptomic data allowed me to obtain a broader transcriptional profile of OXT-treated epicardial cells than qRT-PCR alone. Upon receiving read count data, I first performed differential gene expression analysis and found that oxytocin induced significant widespread transcriptional changes. When comparing the treatment two groups, my analysis revealed 206 genes that had a fold change of at least 1.4 and were statistically significant with a p-value of <0.05 (blue dots in Figure 3.16). I selected these genes for further computational analysis using gene ontology (GO), a resource that associates genes and gene products with controlled terms that describe their functions in cells. My GO analysis identified numerous biological processes and molecular functions that were significantly upregulated and downregulated in hEpiCs after OXT exposure, and these observations were mostly consistent with my previous data (Figure 3.17). For example, processes involved in cell-cell adhesion and epithelial cell development were downregulated, which would be expected based on my proposed model of mature epicardial cells becoming epicardial progenitors upon OXT treatment. In addition, cellular dedifferentiation, proliferation, and EMT functions were all upregulated by OXT.

Of particular interest from the GO analysis was the upregulation of transforming growth factor β (TGF- β) pathway biological processes (**Figure 3.17**, top right). This signaling pathway plays many roles in the body, including in cell growth, proliferation,

differentiation, migration, tissue homeostasis, and regeneration, and its effects are mediated primarily by SMAD proteins (Massagué, 2012). TGF-β ligands have been shown to induce expression of EMT genes and morphological changes consistent with a mesenchymal phenotype in human EpiPCs in culture (Bax et al., 2011). And these effects appear to be conserved across species, as this pathway plays a role in epicardial activation in mice (Dergilev et al., 2021) and its inhibition severely impairs heart regeneration in zebrafish (Chablais & Jaźwińska, 2012). Naturally, the fact that TGF-β signaling genes were upregulated after OXT addition led me to further explore the RNAseg data for specific targets that may be important in my cells. Notably, I found that expression of TGF-β receptor ligands, such as GDF15 (growth differentiation factor 15), INHBB (inhibin subunit beta B), and LEFTY2 (left-right determination factor 2) increased ~1.5-2 fold in OXT hEpiCs. And I observed the same effects when I looked at levels of TMEM100 (transmembrane protein 100), a protein that acts as a downstream effector of the bone morphogenetic protein (BMP) signaling pathway (Figure 3.18). BMP proteins are part of the TGF-β superfamily and control many diverse cellular functions, also through the activity of SMAD proteins (Wang et al., 2014). In addition, this pathway is an essential regulator of zebrafish heart regeneration, although primarily through mediating the activity of cardiomyocytes (Wu et al., 2016). Overall, my RNA sequencing data suggest that oxytocin can promote the expression of genes involved in TGF-β and BMP signaling in the epicardium, leading to EMT and increased epicardial progenitor cell pools that can invade the underlying myocardium (Dronkers et al., 2020). These analyses provide some mechanistic insight behind the phenotypes detailed in previous sections.

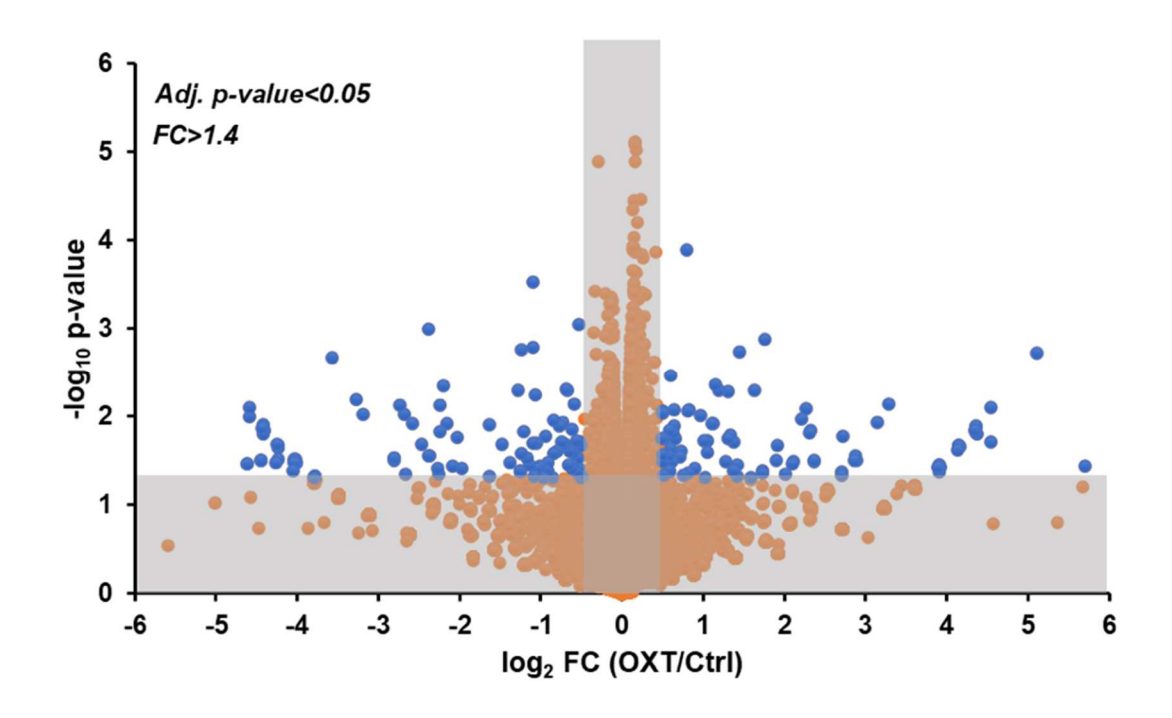
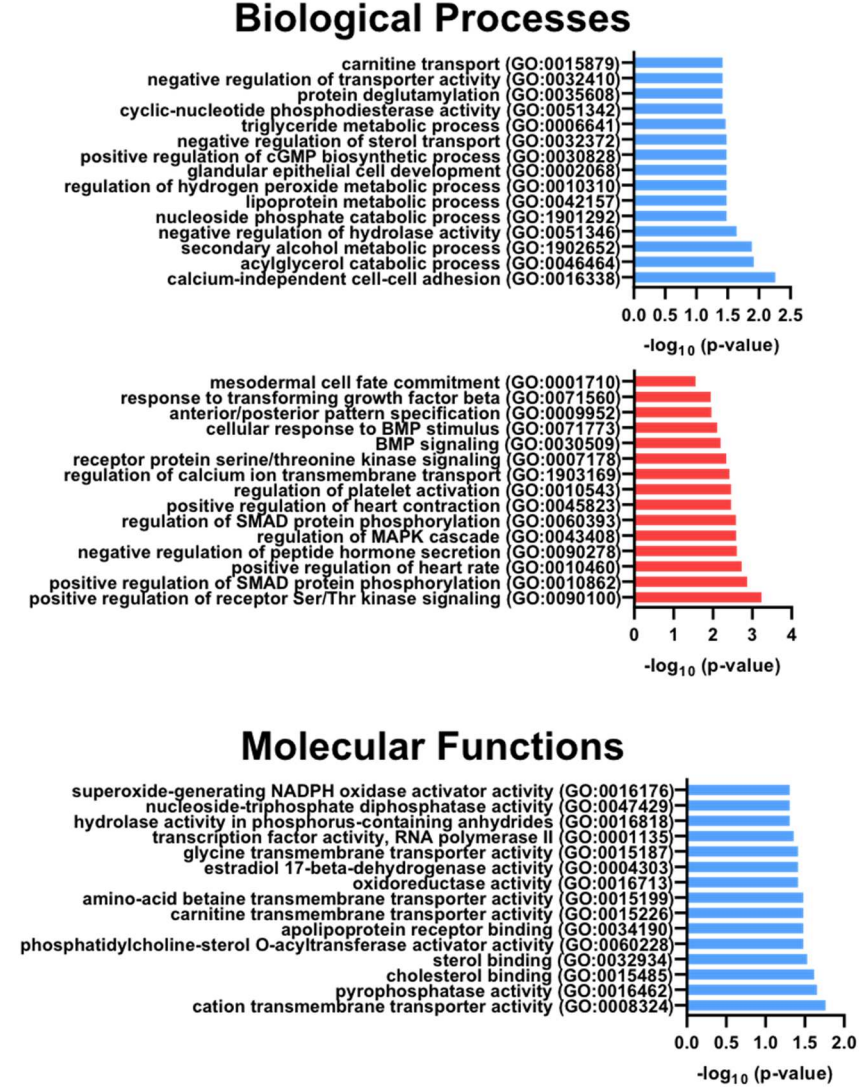


Figure 3.16: Identification of differentially expressed genes. Volcano plot showing relative changes in expression between control and OXT-treated hEpiCs, as determined by RNA sequencing; Blue dots correspond to genes with a fold change \geq 1.4 and a p-value \leq 0.05.



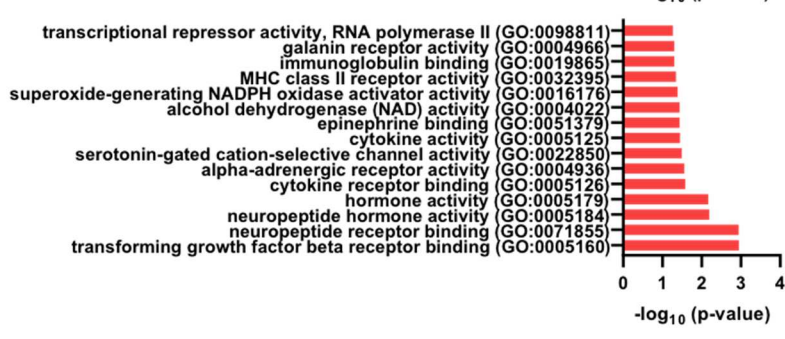


Figure 3.17: Gene ontology analysis. Graphs showing upregulated and downregulated biological processes (TOP) and molecular functions (BOTTOM) after oxytocin exposure in hEpiCs.

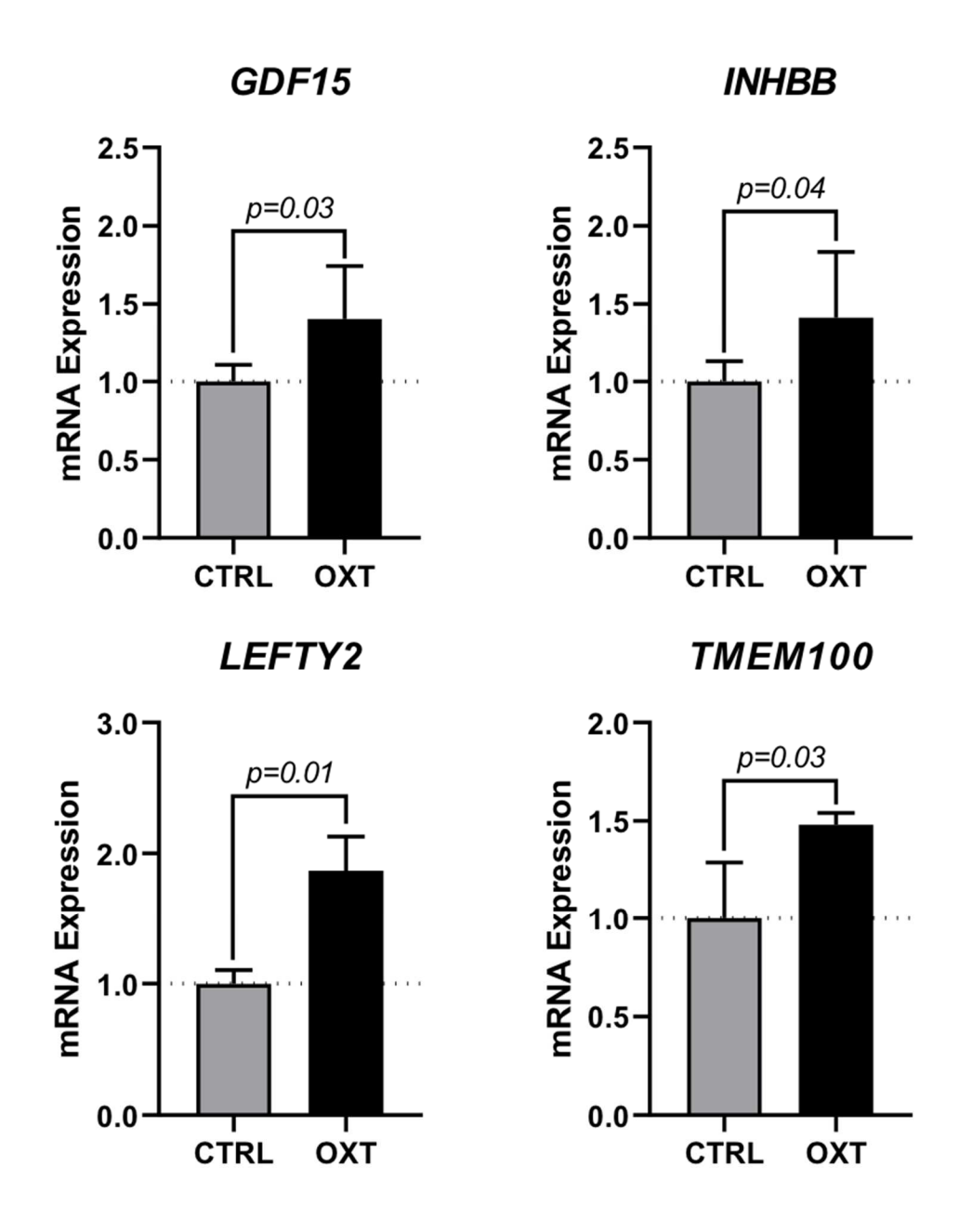


Figure 3.18: OXT increases expression of TGF- β and BMP signaling markers. Relative mRNA expression of ligands for the TGF- β pathway and activators of BMP signaling in control and OXT-treated hEpiCs; n=3 wells per condition.

3.2.6: Oxytocin acts through its receptor to induce epicardial cell activation

One question I sought to answer using hEpiCs is whether oxytocin acts through a receptor-mediated mechanism to exert its effects. There is only one oxytocin receptor in humans (OXTR), and it is a G-protein coupled receptor (GPCR; (Gimpl & Fahrenholz, 2001)). Keeping this information in mind, I first conducted a dose-response experiment by adding successively increasing concentrations of OXT to hEpiCs and performing automated cell counts to quantify epicardial cell proliferation after 3 and 5 days. OXT had a concentration-dependent effect on hEpiC counts at both time points, leading to smooth dose response curves with a maximal response (>2-fold increase in cell count) occurring at 100 nM. These results affirmed my selection of 100 nM OXT as the ideal concentration for experiments, which is reflected throughout the rest of this chapter. In addition, the EC₅₀ for these curves fell in the high pM range (~200-300 pM), numbers that are consistent with a GPCR-mediated response (Figure 3.19). Although there is evidence that OXTR is expressed in both human and rat hearts (Jankowski et al., 2004), the presence of this receptor in the epicardium has not been specifically documented. Therefore, I carried out qRT-PCR assays to confirm that my hEpiCs indeed express OXTR transcripts. I found that after 25 days of differentiation, OXTR levels increase 30fold in hEpiCs compared to undifferentiated hiPSCs (Figure 3.20). Immunostaining and confocal imaging confirmed that the OXTR GPCR is present on the cell membrane and in the cytoplasm of epicardial cells, which may correspond to internalized receptors that are not needed in the absence of ligand (Figure 3.21). While my hEpiCs clearly had oxytocin receptors, they did not express any detectable levels of OXT as assessed by gRT-PCR. In addition to binding its own receptor, OXT can also bind to the arginine

vasopressin (AVP) receptors in humans, albeit with lower affinity than to OXTR (Gimpl & Fahrenholz, 2001). There are three AVP receptor isoforms in humans (*AVPR1A*, *AVPR1B*, *AVPR2*), and I collected hEpiCs at different time points and performed qRT-PCR for all of them. Upon running the reactions, there was no amplification of cDNA and no Ct values recorded, demonstrating that the cells do not express these receptors (**Figure 3.20**).

Confirming that hEpiCs are unlikely to bind to alternative receptors led me to believe that oxytocin acts through OXTR to induce epicardial activation. I therefore created an OXTR knockdown cell line by making a lentivirus containing a short hairpin RNA targeting OXTR and delivering it to hiPSCs. For a more detailed explanation of this method, see Section 2.3. After transduction, I differentiated the hiPSCs to hEpiCs, collected the RNA, and confirmed silencing via qRT-PCR. Indeed, OXTR mRNA expression decreased by >90% after knockdown (shOXTR) compared to scrambled cells (Figure 3.22). Once I had my model in place, I conducted many of the same proliferation and gene expression assays as I had previously. First, I took scrambled and knockdown hEpiCs at Day 25 of differentiation, exposed them to 100 nM OXT for 3 days, and measured epicardial proliferation via Ki67/WT1/TJP1 staining as described in Section 3.2.3. Whereas scrambled cells displayed the expected ~50% increase in Ki67 index when challenged with OXT, shOXTR cells showed no significant response, as I actually saw a slight (~25%) decrease in Ki67 expression (Figure 3.23). Notably, these effects remained in place as the cells aged, as I observed similar trends when I repeated this experiment at Day 65. As an important control experiment, I quantified the percentage of cells that stained positive for WT1 and found that OXTR knockdown did not affect the

efficiency of hEpiC differentiation as nearly 100% of cells expressed this marker in both cell lines (Figure 3.24). Therefore, all hEpiCs that I analyzed were indeed epicardial in nature. I next carried out gene expression analyses to determine if EMT was also affected by OXTR knockdown. I observed the expected 2 to 4-fold increase in hEpiC activation in scrambled cells in response to OXT, as assessed by gRT-PCR for WT1, TCF21, and SNAI1. Remarkably, these effects were entirely prevented in shOXTR cells, suggesting that progenitor activation and EMT do not occur when *OXTR* is silenced (**Figure 3.25**). Overall, because pro-regenerative phenotypes were only observed in cells with intact OXTR signaling, I concluded that oxytocin acts through its own receptor to induce human epicardial cell activation in vitro. Because OXTR is clearly important for epicardial regeneration, utilizing pharmacological strategies to activate it could have significant therapeutic benefits. But using pure oxytocin for this purpose could be problematic due to its short (~5-10 minute) half-life (Morin et al., 2008), insufficient specificity for OXTR, and poor absorption into the bloodstream (Hilfiger et al., 2020). Interestingly, when I added LIT-001, a recently characterized and very potent and specific non-peptide OXTR agonist (Frantz et al., 2018; Hilfiger et al., 2020), to scrambled hEpiCs I observed an even stronger proliferative effect than that of OXT (Figure 3.26). As such, this may be the type of compound that could be administered safely and effectively after cardiac injury in clinical settings in the future.

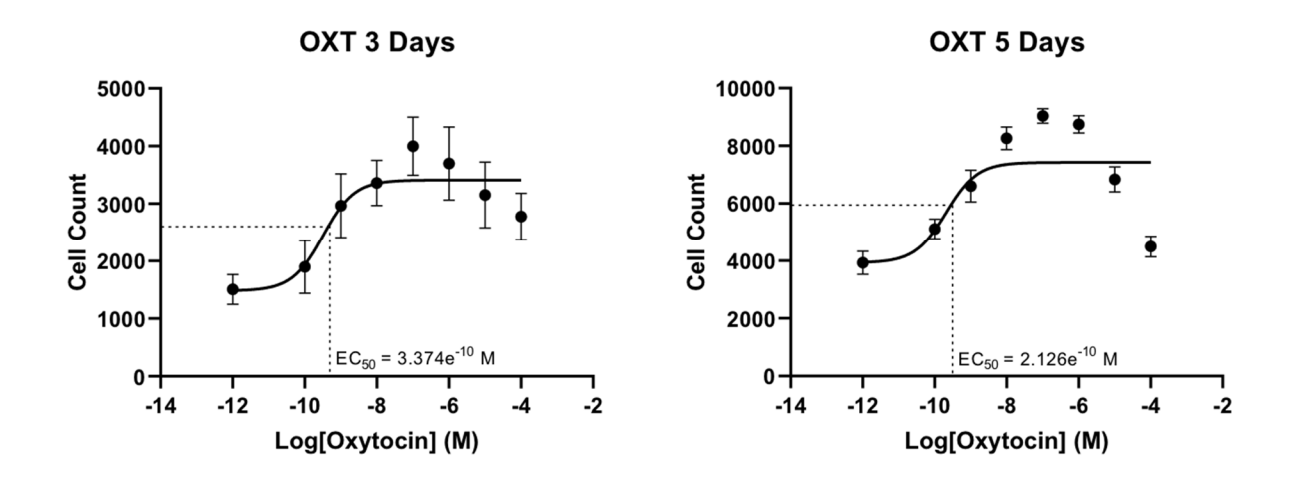


Figure 3.19: OXT acts through a receptor-mediated mechanism. Number of hEpiC nuclei exposed to different concentrations of OXT over the course of 3 and 5 days; n=10 wells per concentration.

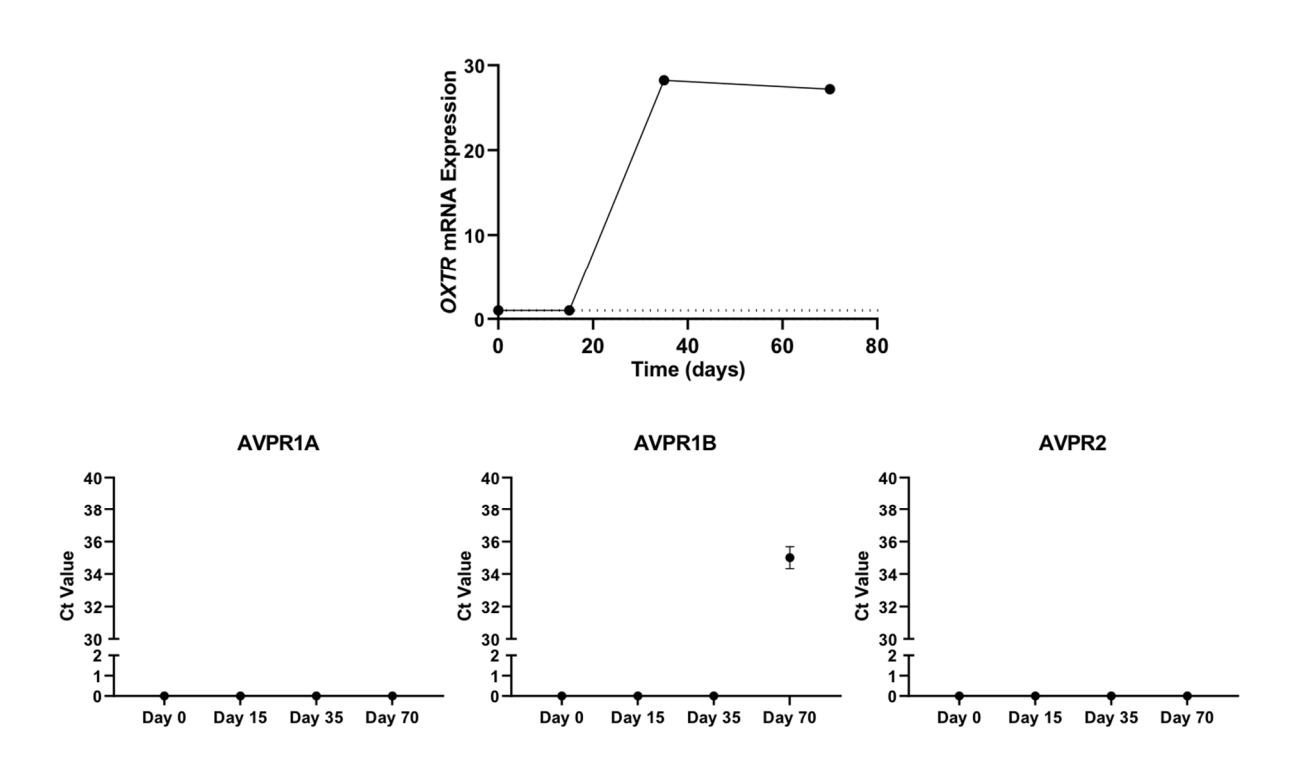


Figure 3.20: hEpiCs do not express AVP receptors. <u>TOP</u>: Time course qRT-PCR data for *OXTR* in hEpiCs showing an increase in expression over time, dashed line corresponds to expression in undifferentiated hiPSCs. <u>BOTTOM</u>: Time course qRT-PCR data for AVP receptors showing no expression in hEpiCs, displayed as Ct (cycle threshold) values.

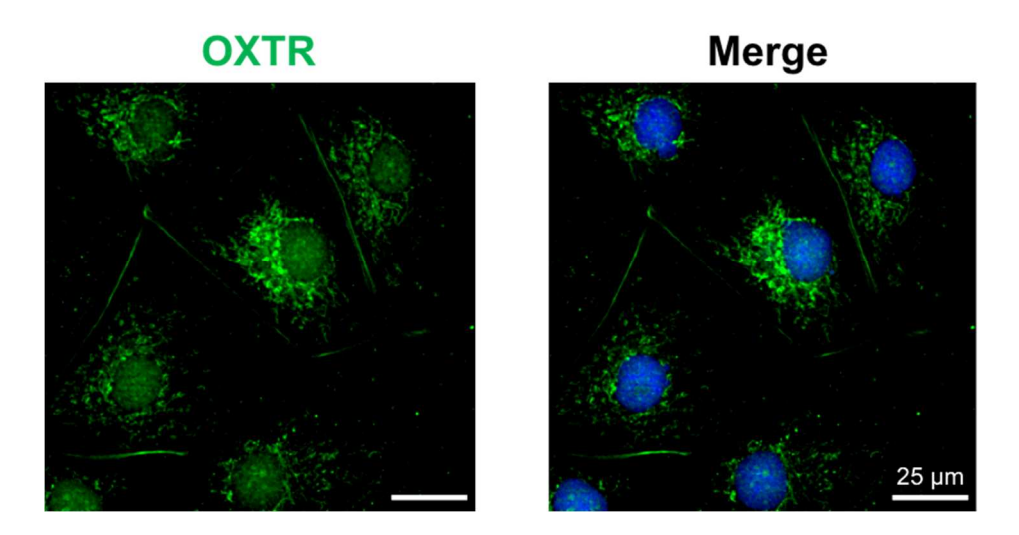


Figure 3.21: hEpiCs express OXT receptor. Confocal immunofluorescent images for OXTR (green) and DAPI (blue) showing oxytocin receptor expression on the cell membrane and in the peri-nuclear region; scale bar: $25 \ \mu m$.

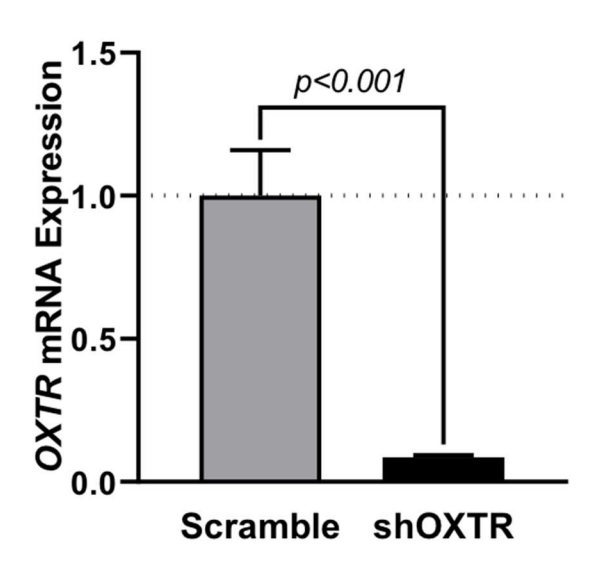


Figure 3.22: Confirmation of successful *OXTR* **knockdown**. qRT-PCR for scrambled and sh*OXTR* hEpiCs showing >90% *OXTR* silencing efficiency; n=6 wells per cell line.

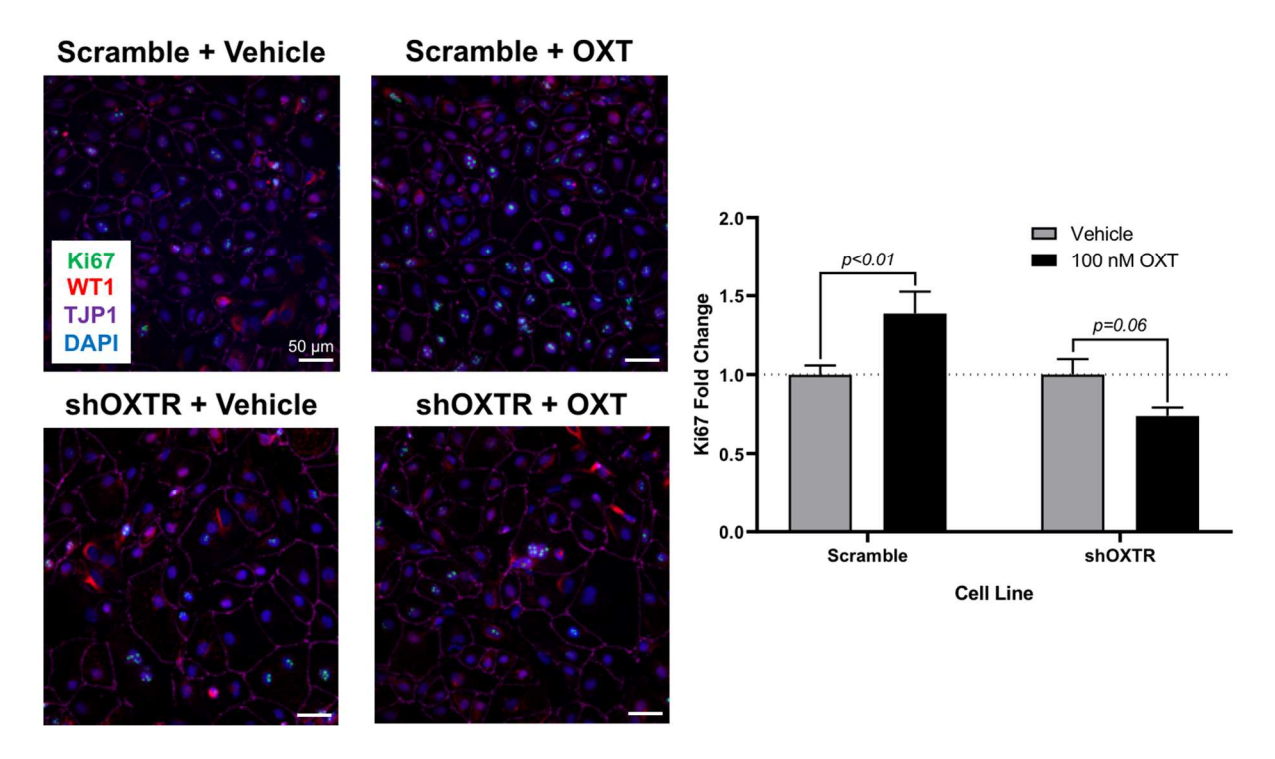


Figure 3.23: *OXTR* knockdown prevents hEpiC proliferation in response to OXT. Confocal immunofluorescent images and quantification of proliferating hEpiCs in scrambled and sh*OXTR* cell lines in the presence and absence of OXT at day 25 of differentiation. Epicardial cells are labeled with WT1 (red), epithelial membranes with TJP1 (magenta), proliferating cells with Ki67 (green), nuclei with DAPI (blue); n=2 wells/10 images per condition, scale bar: $50 \mu m$.

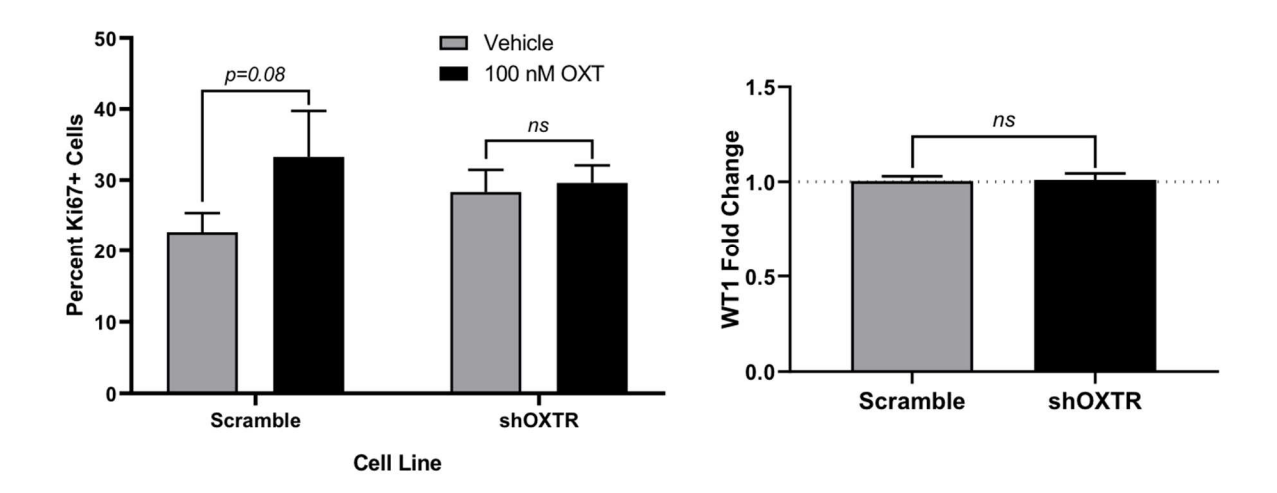


Figure 3.24: *OXTR* **knockdown does not affect hEpiC differentiation efficiency**. <u>LEFT</u>: Quantification of proliferating hEpiCs in scrambled and sh*OXTR* cell lines in the presence and absence of OXT at day 65 of differentiation. <u>RIGHT</u>: hEpiC differentiation efficiency in both cell lines, expressed as percent WT1+ nuclei relative to each other at day 25 of differentiation; n=4 wells/20 images analyzed per cell line.

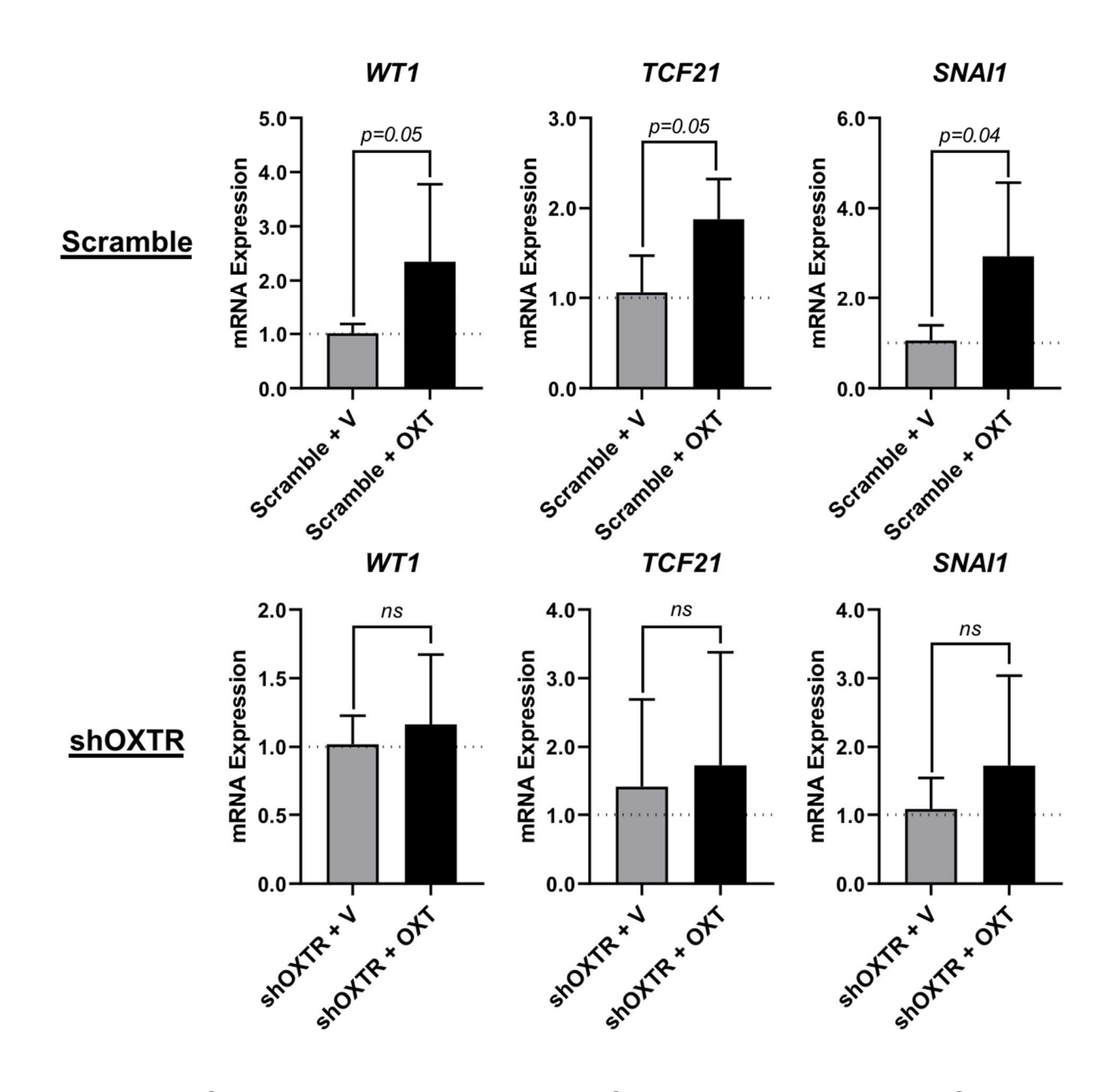


Figure 3.25: *OXTR* **knockdown prevents hEpiC activation in response to OXT**. qRT-PCR data for scrambled (TOP) and sh*OXTR* (BOTTOM) hEpiCs, showing an increase in EpiPC (*WT1*, *TCF21*) and EMT (*SNAI1*) marker expression in control cells that is prevented in knockdown cells; n=6 wells per condition, V: Vehicle.

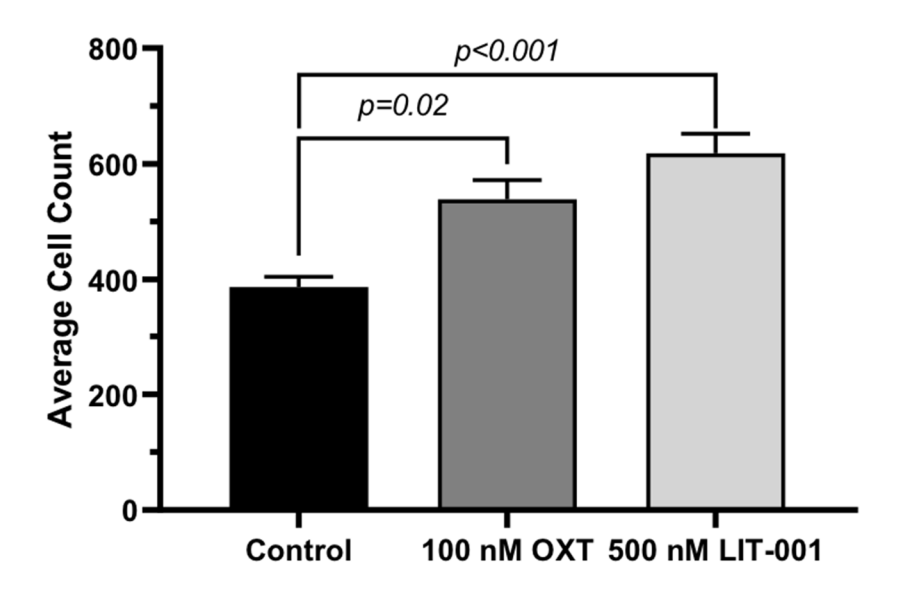


Figure 3.26: OXTR analogs increase hEpiC proliferation. Number of DAPI-labeled nuclei in scrambled hEpiCs exposed to 100 nM OXT and 500 nM LIT-001, a non-peptide OXTR agonist; n=12 wells per condition.

3.3: Discussion

Several pluripotent stem cell-derived models of the human epicardium have been developed in recent years (Bao et al., 2016, 2017; Guadix et al., 2017; Zhao et al., 2017). These cells tend to recapitulate the proepicardium and early embryonic epicardium, as they express high levels of EpiPC markers (WT1, TCF21, TBX18), undergo EMT, and are highly proliferative. While these protocols have proven useful for studying epicardial contributions to the developing heart, they have only limited utility in modeling the adult injury setting. Current efforts to mature hEpiCs *in vitro* are relatively complex, as they involve co-culture with hiPSC-derived cardiomyocytes (Tan et al., 2021). Here, I have shown that I can modify an existing protocol for differentiating epicardial cells (Bao et al., 2016, 2017) and successfully mature them by simply removing two culture components, Vitamin C and SB431542. These mature hEpiCs recapitulate the adult epicardium in

terms of their low rates of proliferation (Figure 3.7) and transcriptional activity (Figures 3.8, 3.9) and serve as the perfect system with which to test my hypothesis that the neuroendocrine axis regulates epicardial activation in heart regeneration. screened my candidate hormones for their proliferative effects in culture, I identified oxytocin as the compound that induced the strongest response, and selected it for further analysis (Figure 3.10). I found that when my hEpiCs were exposed to 100 nM OXT, they increased their proliferation rates (Figures 3.11, 3.12) and adopted an embryonic gene expression profile (Figure 3.15). While the adult epicardium has the innate ability to replenish other cell types after cardiac injury, this contribution is insufficient for any degree of functional regeneration in mammals (Streef & Smits, 2021). Therefore, the concept of a single hypothalamic hormone being able to increase the efficiency of this process, even by a small amount, could have major implications. To date, thymosin β4 is regarded as the gold standard for "priming" epicardial activation, as its administration can induce EpiPC differentiation into vascular progenitor cells and cardiomyocytes (Smart et al., 2007, 2011). Remarkably, OXT induced an even greater proliferative response in hEpiCs than thymosin $\beta4$ (Figure 3.12).

In addition to the above studies, I also conducted RNA sequencing analyses which demonstrated that oxytocin upregulated processes related to TGF-β and BMP signaling, thereby providing some mechanistic insight into how it exerts its effects (**Figure 3.17**). Notably, components of these pathways are known to be active during proepicardial induction, epicardial formation, and EpiPC contribution to the developing heart (Dronkers et al., 2020). There is also some evidence that they are involved in the response to cardiac injury in adults (Bax et al., 2011; Chablais & Jaźwińska, 2012; Peng et al., 2021;

Wu et al., 2016), and it is possible that OXT signaling is upstream of these processes. Finally, I confirmed that oxytocin acts through its own receptor in my system as hEpiCs only express OXTR and not the AVP receptors (Figures 3.20, 3.21), which are similar in sequence and can be bound by OXT (Gimpl & Fahrenholz, 2001). Importantly, loss-of-function experiments demonstrated that the increases in hEpiC proliferation (Figure 3.23) and activation (Figure 3.25) that were seen in scrambled cells were completely abolished in *OXTR* knockdown epicardial cells. In addition, scrambled cells responded to a safe, potent, and specific OXTR agonist with an even greater increase in proliferation than they did to OXT, increasing the potential translatability of my findings (Figure 3.26). Due to its low molecular weight, non-peptide chemical structure, and high specificity for OXTR, LIT-001 may be a promising compound for future clinical use (Gulliver et al., 2019). Overall, the results presented in this chapter are exciting and represent a solid foundation for studying neuroendocrine control of epicardial regeneration in a dish.

3.4: Future Directions

In addition to increasing their transcriptional activity and proliferation rates, epicardial progenitor cells adopt a highly motile phenotype after cardiac injury. This allows them to migrate into the subepicardial space and throughout the myocardium to differentiate into functional new cardiac cells (Quijada et al., 2020; Rao & Spees, 2017; Smits et al., 2018). Future experiments could include transwell migration assays using control and OXT-treated hEpiCs to determine if oxytocin induces the cells to migrate in response to chemoattractants commonly found in the injured heart. In addition, I could further explore the targets uncovered with my RNA sequencing data (Figure 3.18) and test their effects on hEpiC function. Conducting knockdowns of individual genes in much

the same way I did for *OXTR* would allow me to truly dissect the signaling mechanisms that OXT activates or inactivates *in vitro*. Finally, one question worth asking is if the effects that OXT induces in hEpiCs extend to other cell types as well. Differentiating hiPSCs to a variety of cardiac cell types (such as cardiomyocytes, endothelial cells, and cardiac fibroblasts) and repeating my experiments with these models would help to shed light as to whether OXT induces a pro-regenerative phenotype globally or specifically in the epicardium. This is also one of the questions that I sought to answer *in vivo* using zebrafish (Chapter 4).

Chapter 4: Oxytocin Signaling is Necessary for Heart Regeneration in Zebrafish

4.1: Introduction

Ultimately, the most effective way to demonstrate the importance of the brain to heart regeneration is to replicate these findings in a naturally regenerating animal model. The teleost zebrafish (Danio rerio) is a small (~5 cm) fish native to South Asia and naturally found in freshwater habitats, such as streams and ponds (Aleström et al., 2020). It is one of the most powerful regenerating organisms known, with the ability to fully regrow its heart after resection of up to 20% of the ventricle (Beffagna, 2019; Poss et al., 2002). Unlike in mammals, zebrafish cardiomyocytes can dedifferentiate and proliferate, and the majority of heart regeneration occurs via these processes (Jopling et al., 2010). However, there is strong evidence to suggest that the epicardium also plays an important role after cardiac injury in this model (Cao et al., 2016; Kikuchi, Holdway, et al., 2011; Lepilina et al., 2006). Indeed, zebrafish EpiPCs have been shown to contribute to the replacement of perivascular cells (Kikuchi, Gupta, et al., 2011) and cardiac fibroblasts (González-Rosa et al., 2012) and the synthesis of extracellular matrix (Sun et al., 2022; J. Wang et al., 2013) in the injured heart. In addition, the zebrafish epicardium regulates cardiomyocyte proliferation during heart regeneration (Huang et al., 2013). Therefore, it is the perfect in vivo system with which to test my hypothesis that the brain regulates cardiac regeneration. For my experiments in adults, I utilized a well-characterized cardiac cryoinjury model as a means to injure the zebrafish hearts (González-Rosa et al., 2011; González-Rosa & Mercader, 2012). Once this system was in place, I tested whether oxytocin was released from the hypothalamus in response to injury. I then blocked OXTR signaling and measured the subsequent effects on heart regeneration, epicardial

activation, and proliferation of other cell types in the adult heart. I found that all these processes were adversely affected by OXTR inhibition. Finally, I set out to discern whether OXT is important for epicardial development in zebrafish embryos, as the regenerating epicardium largely recapitulates its functions and activities from development (Cao & Poss, 2018; Simões & Riley, 2018). Together, the data in this chapter demonstrate that oxytocin signaling is necessary for proper heart regeneration and development in zebrafish.

4.2: Results

4.2.1: Cardiac cryoinjury induces oxytocin release from the zebrafish hypothalamus

To test if the role oxytocin plays in epicardial activation *in vitro* was conserved *in vivo* during zebrafish heart regeneration, I utilized a previously established cardiac cryoinjury model to induce an infarct of ~25% of the ventricle (González-Rosa et al., 2011; González-Rosa & Mercader, 2012). Remarkably, ~90% of fish survive this procedure and regain normal activity levels only a few hours later. After injury, repair occurs through inflammatory cell-mediated clearance of dead tissue, deposition of new extracellular matrix, and cardiomyocyte proliferation to form a fully regenerated myocardium within 30-60 days (Bise et al., 2020; Chablais et al., 2011). I set out to test if OXT (also known as isotocin in teleosts, such as zebrafish) is released from the hypothalamus in the early stages of this process, within the first week after acute cardiac damage or injury. I cryoinjured fish, harvested their hearts and brains at 1, 3, 5, and 7 days post-injury (dpi), and isolated RNA from these samples for qRT-PCR. I also collected sham (uninjured) fish as controls. While I did not see an immediate increase in *oxt* gene expression in the hypothalamus at 1 dpi, I observed an 18-fold increase in *oxt* mRNA levels at 3 dpi, with

this increase lasting until at least 7 dpi (Figure 4.1). These data suggest that a burst of oxytocin is released from the brain after cardiac injury over a sustained period of time. I then assayed zebrafish hearts for expression of wt1b and tcf21, the orthologous genes to those found in mammals. Remarkably, I observed nearly the same expression patterns as with brain oxt. At 1 dpi, wt1b levels were already increased compared to sham animals, and at 3 dpi, the levels of both genes were significantly increased (~20-fold for wt1b and ~12-fold for tcf21). Again, these increases in mRNA expression lasted until at least 7 dpi (Figure 4.2). While these brain and heart qRT-PCR results are merely correlational, it is interesting that the time course trends are nearly identical. This finding suggests that the oxytocin released from the brain plays a role in activating the epicardium after cardiac injury. Interestingly, I also observed a ~3-fold increase in oxtr levels in the heart at 7 dpi (Figure 4.3). While this time point occurred much later than the maximum increase in brain oxt, it is certainly possible that this upregulation of oxytocin receptor is a direct response to increases in OXT that are sustained over the course of time (Figure **4.1**). Together, these gene expression studies lend strong support to my hypothesis of oxytocin release after cardiac injury.

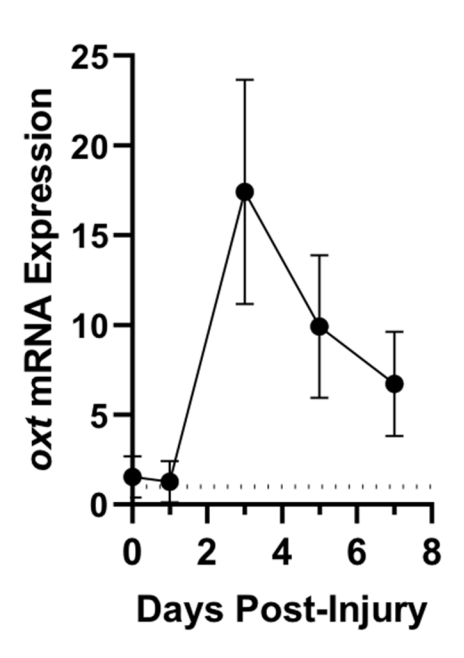


Figure 4.1: Cardiac cryoinjury induces OXT release. Time course qRT-PCR data for *oxt* in zebrafish brains after cardiac cryoinjury; n=3 animals per time point.

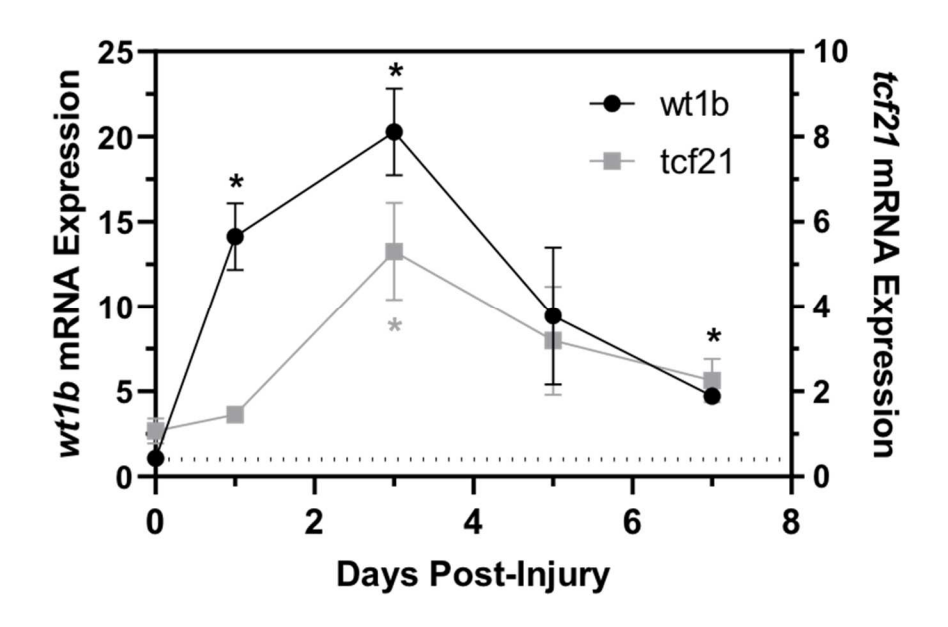


Figure 4.2: Cardiac cryoinjury induces epicardial activation. Time course qRT-PCR data for epicardial markers *wt1b* and *tcf21* in zebrafish hearts after cardiac cryoinjury; *P<0.05 versus sham operated heart; n=3 animals per time point.

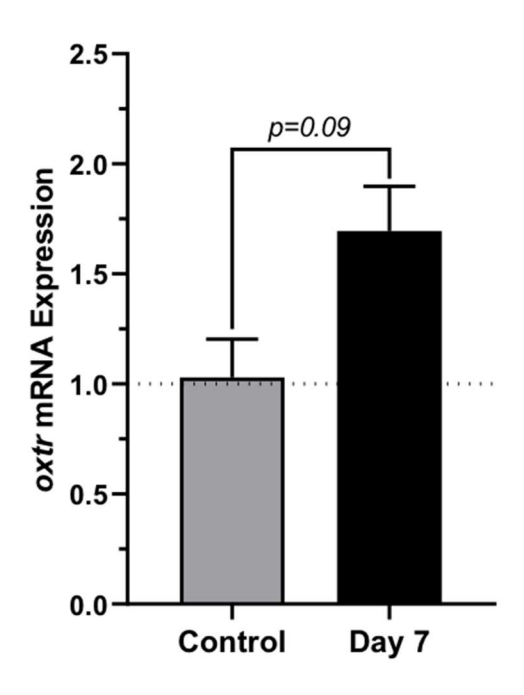


Figure 4.3: Cardiac cryoinjury induces OXTR expression. qRT-PCR data for *oxtr* in zebrafish hearts 7 days after cardiac cryoinjury; n=3 animals per condition.

4.2.2: Inhibition of oxytocin signaling delays heart regeneration in zebrafish

Based on the encouraging results of my initial qRT-PCR data, I sought to investigate the functional significance of this oxytocin burst. To do so, I administered the specific OXTR inhibitor L-368,899 to zebrafish 24 hours after cryoinjury and every 1-2 days thereafter until the end of the experiment. I introduced this compound through manual injections directly into the thoracic cavity, as described previously (Bise & Jaźwińska, 2019). I then collected injured hearts at 3, 7, and 14 dpi and tried to assess regeneration over time through Masson's trichrome staining of control and OXTR inhibited hearts (**Figure 4.4**, top). I quantified these images by measuring the size of the infarcted area relative to the total myocardial area, with a lower value indicating a smaller injury size. At 3 dpi, I observed a slight (~25%) increase in scar area in L-368,899 treated samples compared to controls. This difference increased over time to about 50% at 7 dpi

and to >2-fold (and statistically significant) at 14 dpi. (Figure 4.4, bottom). While these preliminary data do suggest a difference in regenerative capacity between the two groups, a closer look shows that more results are needed to definitively draw this conclusion. Indeed, it is interesting that throughout this experiment, the vehicle-treated animals displayed a consistent injured area of about 10-15% of the myocardium, but the L-368,899 treated animals showed a continuous increase in injured area up to almost 25% at 14 dpi. These data raise two questions that are critical for their interpretation. First of all, it is surprising that the control animals do not display a decrease in scar size over time, because at 14 dpi, hearts would be at an intermediate stage in regeneration, with a scar still present but shrinking as more time passes corresponding to the regrowth of new myocardium (Chablais et al., 2011; Sanz-Morejón & Mercader, 2020). Notably, this does not appear to be the case in the vehicle animals. The second question relates to why scar size continuously increases in OXTR inhibited hearts, instead of merely staying constant between 3 and 14 dpi. It is possible that L-368,899 treatment actually does cause fibrotic tissue to accumulate in the myocardium, thereby leading to larger injury areas over time. It is also feasible that the initial cryoinjuries in the 14 dpi group were larger than those in the 3 dpi group in both control and treated animals. If this were the case, then it would decrease the ability to draw definitive conclusions from these data, as making comparisons between hearts at different time points would not be possible. Overall, it is encouraging that the difference in injury area between control and treated groups increases over time. While these results can be taken with a grain of salt for the time being, they do begin to suggest a delay in regeneration after L-368,899 treatment.

One hallmark of cardiac regeneration is secretion of extracellular matrix (ECM) proteins, such as fibrin, collagen, and fibronectin, by activated fibroblasts in the infarct zone. These proteins protect the heart wall after injury and are necessary for proper regeneration to occur in zebrafish (J. Wang et al., 2013). Eventually, fibroblasts must inactivate and the fibrotic scar must contract in order for new cardiomyocytes to proliferate in its place. These processes typically occur between 7 and 30 dpi (Sanz-Morejón & Mercader, 2020). Keeping the above limitations in mind, I next set out to assess fibrosis accumulation in cryoinjured zebrafish hearts at 14 dpi, right in the middle of this window. I again took control and L-368,899 treated hearts and visualized them with Masson's trichrome staining, which stains ECM proteins blue. High power imaging of heart sections revealed that treated animals had more myocardial fibrosis accumulation than control animals (Figure 4.5). These data could suggest that it takes longer for the fibrotic scar to resolve in treated animals compared to controls and may potentially offer an explanation as to why L-368,899 administered hearts displayed an increase in scar size over time. However, the best way to truly draw conclusions about the effects of OXTR inhibition on cardiac regeneration would be by extending these experiments out to further time points, as full regeneration after cryoinjury typically does not occur until 30-60 dpi (Bise et al., 2020; Chablais et al., 2011). Indeed, it is unlikely that L-368,899 treatment prevents regeneration entirely, and eventually, the treated fish would catch up to the controls. However, inhibiting OXT signaling does appear to at least slow the progression of the early stages of heart regeneration and further studies would provide even more insight into the full extent of this phenotype over time.

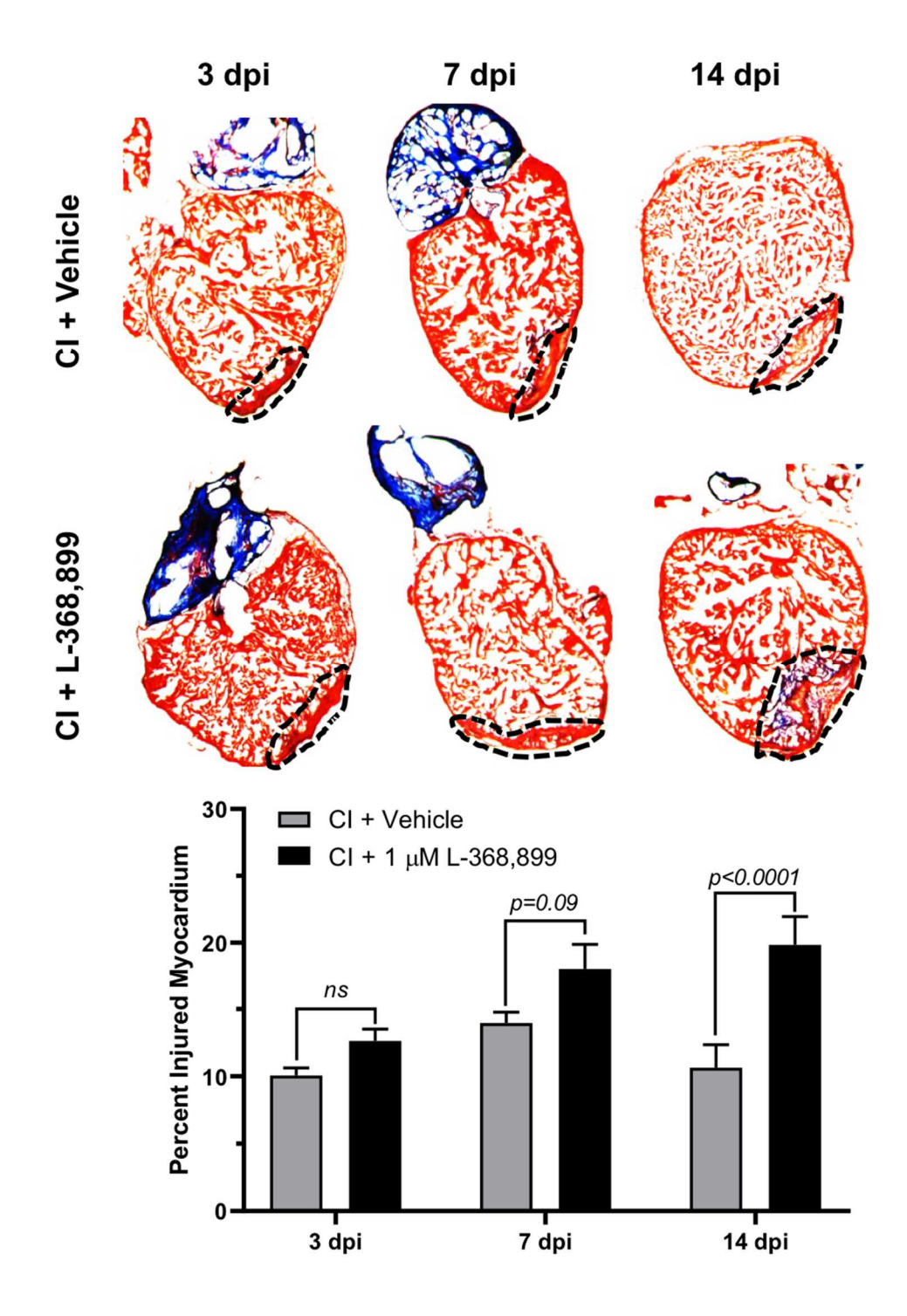


Figure 4.4: OXTR inhibition increases myocardial scar size. Masson's trichrome staining and quantification of cryoinjured zebrafish hearts at 3, 7, and 14 dpi treated with and without 1 μ M L-368,899. Myocardium is stained red, collagen is stained blue, dashed lines demarcate injured area, which is quantified in graph; n=3-5 animals per time point; CI: Cryoinjury, dpi: Days Post-Injury.

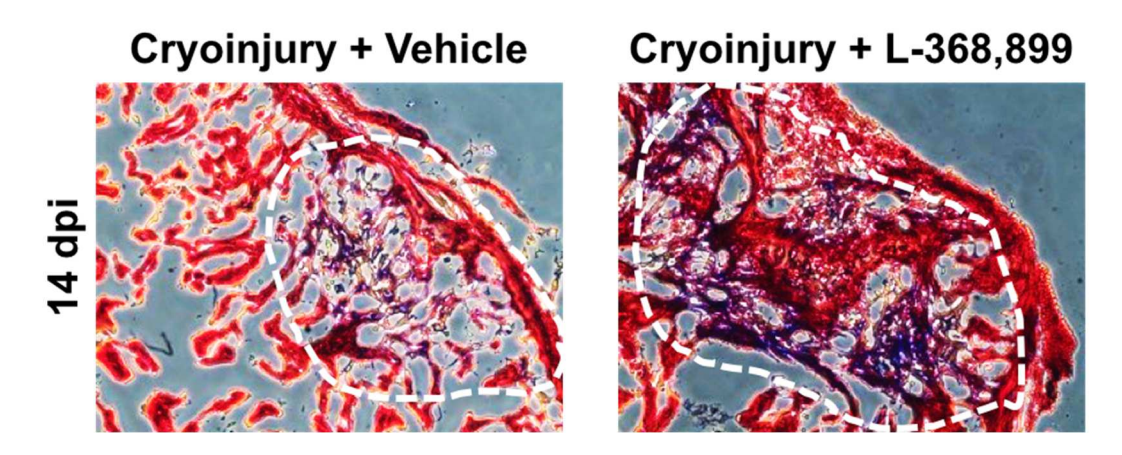


Figure 4.5: OXTR inhibition increases fibrosis accumulation. Representative images of cryoinjured zebrafish myocardium (red) at 14 dpi showing more extracellular matrix deposition (blue) after OXTR inhibition. Dashed lines demarcate fibrotic area; dpi: Days Post-Injury.

4.2.3: Inhibition of oxytocin signaling prevents cryoinjury-induced epicardial activation in zebrafish

I next explored how blocking oxytocin signaling affected epicardial progenitor cell activation in zebrafish. Because one hallmark of EpiPC activation after cardiac injury *in vivo* is upregulation of WT1 and TCF21 levels (Quijada et al., 2020; Schnabel et al., 2011; Smits et al., 2018), I collected cryoinjured hearts to quantify their expression. I chose 3 dpi as my time point of interest because this corresponds to the day I saw maximal hypothalamic *oxt* release and epicardial activation (**Figures 4.1, 4.2**). I found that compared to control tissue, L-368,899 treated samples had significantly lower expression (>2-fold) of *wt1b* and *tcf21* (**Figure 4.6**). I sought to confirm these qRT-PCR data by looking at protein expression in multiple zebrafish strains. First, I utilized transgenic tcf21-nls-eGFP fish with an enhanced green fluorescent protein (eGFP) tag attached to a nuclear localization signal (NLS) for *tcf21* to document EpiPC activation through immunofluorescence (Wang et al., 2011). Staining for GFP revealed a massive

expansion of the subepicardial layer and increase in the number of tcf21+ nuclei covering the myocardial layer of the heart at 3 dpi. Remarkably, when I inhibited OXTR signaling with L-368,899, I found that these responses were almost entirely prevented (**Figure 4.7**, top). Indeed, when I counted the number of tcf21+ EpiPCs per field for each of my conditions, I found a ~4-fold increase after cryoinjury compared to sham animals. L-368,899 treatment subsequently reduced this value by ~2-fold. When I measured the area of the subepicardium (defined as the layer of EpiPCs directly on top of the myocardium), I observed the same trends, with this value being ~2-fold lower in treated hearts than non-treated ones (**Figure 4.7**, bottom). Clearly, OXTR inhibition adversely affects EpiPC dynamics in cryoinjured fish.

I was also interested in specifically documenting the proliferative response of epicardial cells after OXTR inhibition. To do this, I utilized wild-type (AB) zebrafish, cryoinjured them, injected half with 1 μM L-368,899, and stained the hearts for wt1 and h3p, a commonly used marker of cellular proliferation. When I counted the percentage of cells on the surface of the heart that were positive for h3p, I found no difference between control and treated samples. However, the percentage of nuclei that were double positive for h3p and wt1 (proliferating EpiPCs) decreased ~2-fold after OXTR inhibition (**Figure 4.8**, bottom). These results suggest that EpiPC proliferation is decreased by L-368,899 administration. The rest of the h3p+ positive nuclei in the epicardial layer likely correspond to immune cells and fibroblasts, as these populations migrate to the site of injury in the early stages of regeneration (González-Rosa et al., 2017; Sanz-Morejón & Mercader, 2020). It also appears as if EpiPC migration is adversely affected by L-368,899, as treated hearts show far fewer h3p+/wt1+ cells in the

subepicardial and myocardial layers than control hearts (**Figure 4.8**, top). In addition to EpiPC activation, I also wondered whether epithelial-to-mesenchymal transition (EMT) was prevented in OXTR inhibited animals. I again utilized the *snail* gene family as my primary readout for EMT. As expected, qRT-PCR for *snai1a* and *snai2* showed a ~40-50% decrease after L-368,899 administration in cryoinjured hearts (**Figure 4.9**). These results recapitulate my gene expression data for EpiPC markers (**Figure 4.6**). Together, these data demonstrate that several hallmarks of zebrafish heart regeneration such as subepicardial expansion, EMT, and EpiPC proliferation and migration (Cao & Poss, 2018; González-Rosa et al., 2017), are gravely impaired upon L-368,899 treatment. Therefore, I concluded that OXTR inhibition prevents robust activation of the epicardium and its progenitor cell populations after injury, leading to an impaired regenerative response.

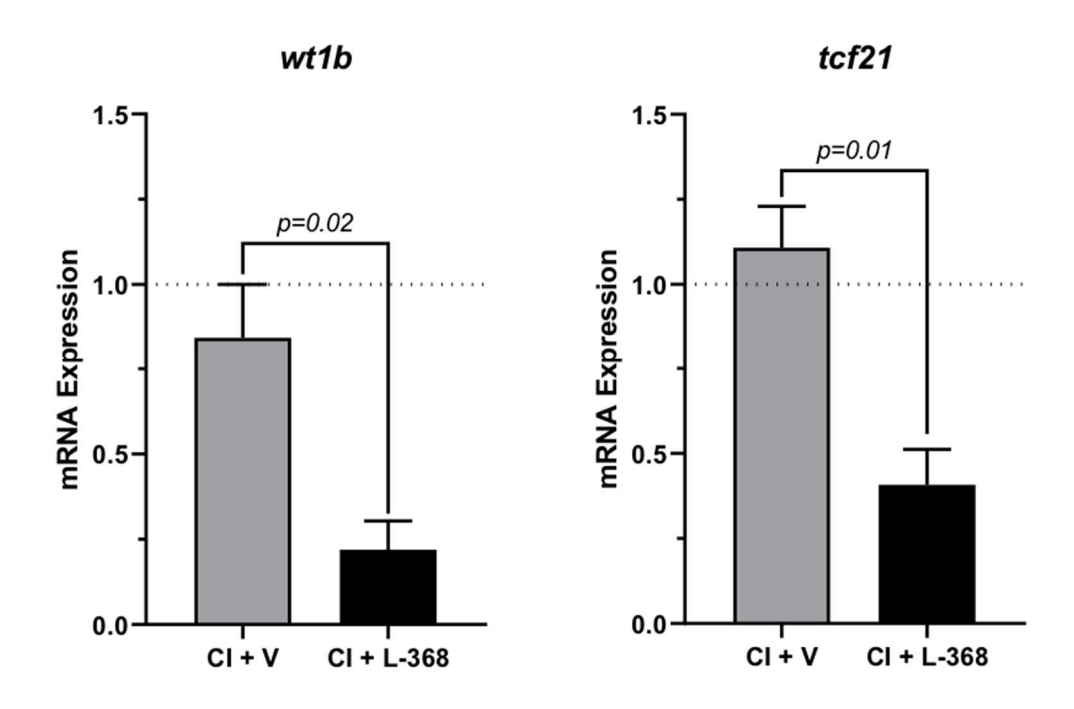


Figure 4.6: OXTR inhibition decreases expression of EpiPC markers. qRT-PCR data for EpiPC markers *wt1b* and *tcf21* in cryoinjured zebrafish hearts at 3 dpi treated with and without 1 μM L-368,899 (L-368); n=4-5 animals per condition; CI: Cryoinjury, V: Vehicle.

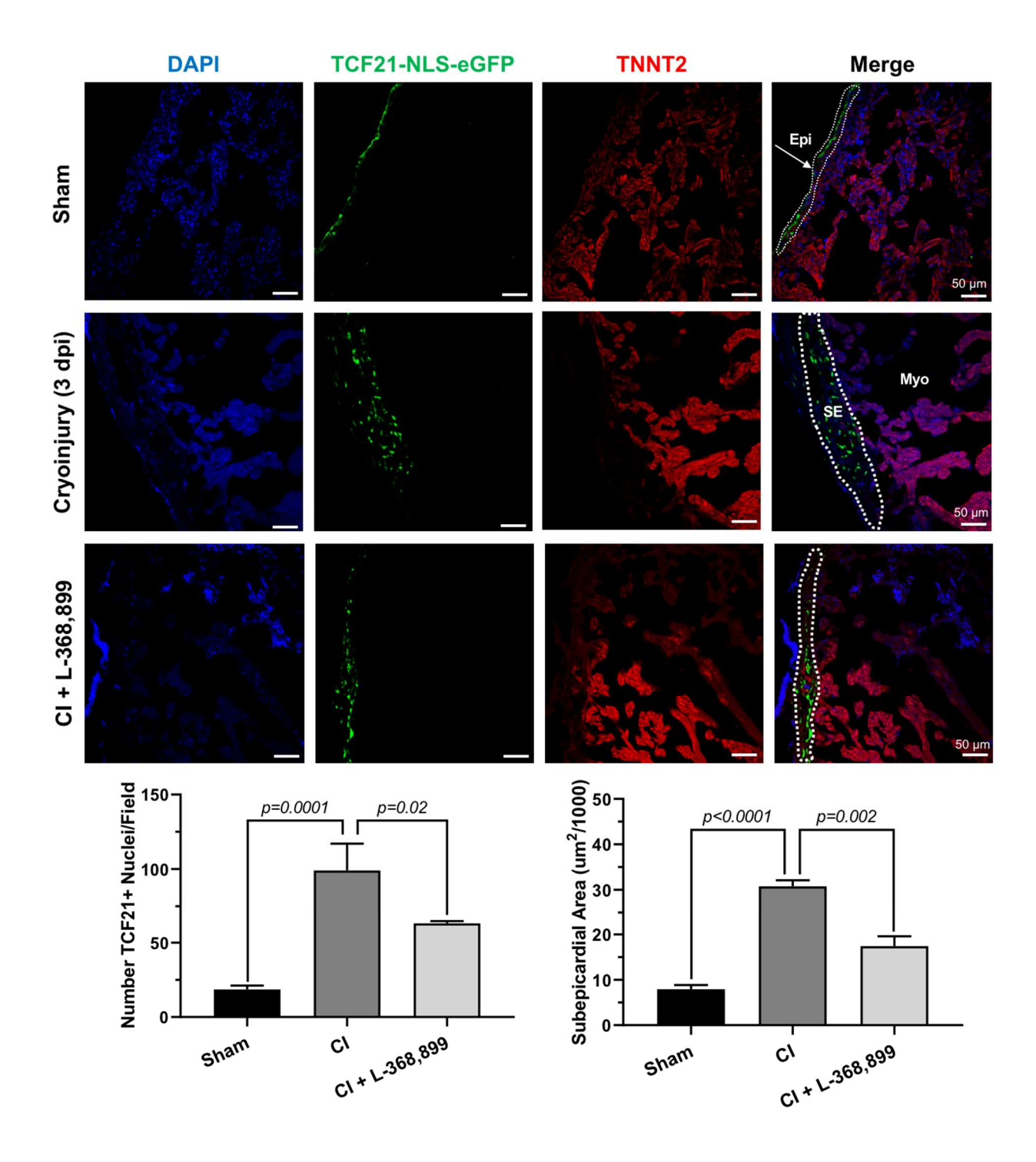


Figure 4.7: OXTR inhibition decreases epicardial activation. Confocal immunofluorescent images and quantification of tcf21-nls-eGFP transgenic zebrafish at 3 dpi showing epicardial activation in sham, cryoinjured, and L-368,899-treated hearts. Epicardial cell nuclei are labeled with GFP (green), cardiomyocytes are labeled with TNNT2 (red), nuclei are labeled with DAPI (blue); n=3-5 animals per condition, scale bar: 50 μ m; CI: Cryoinjury, dpi: Days Post-Injury, Epi: Epicardium, SE: Subepicardium.

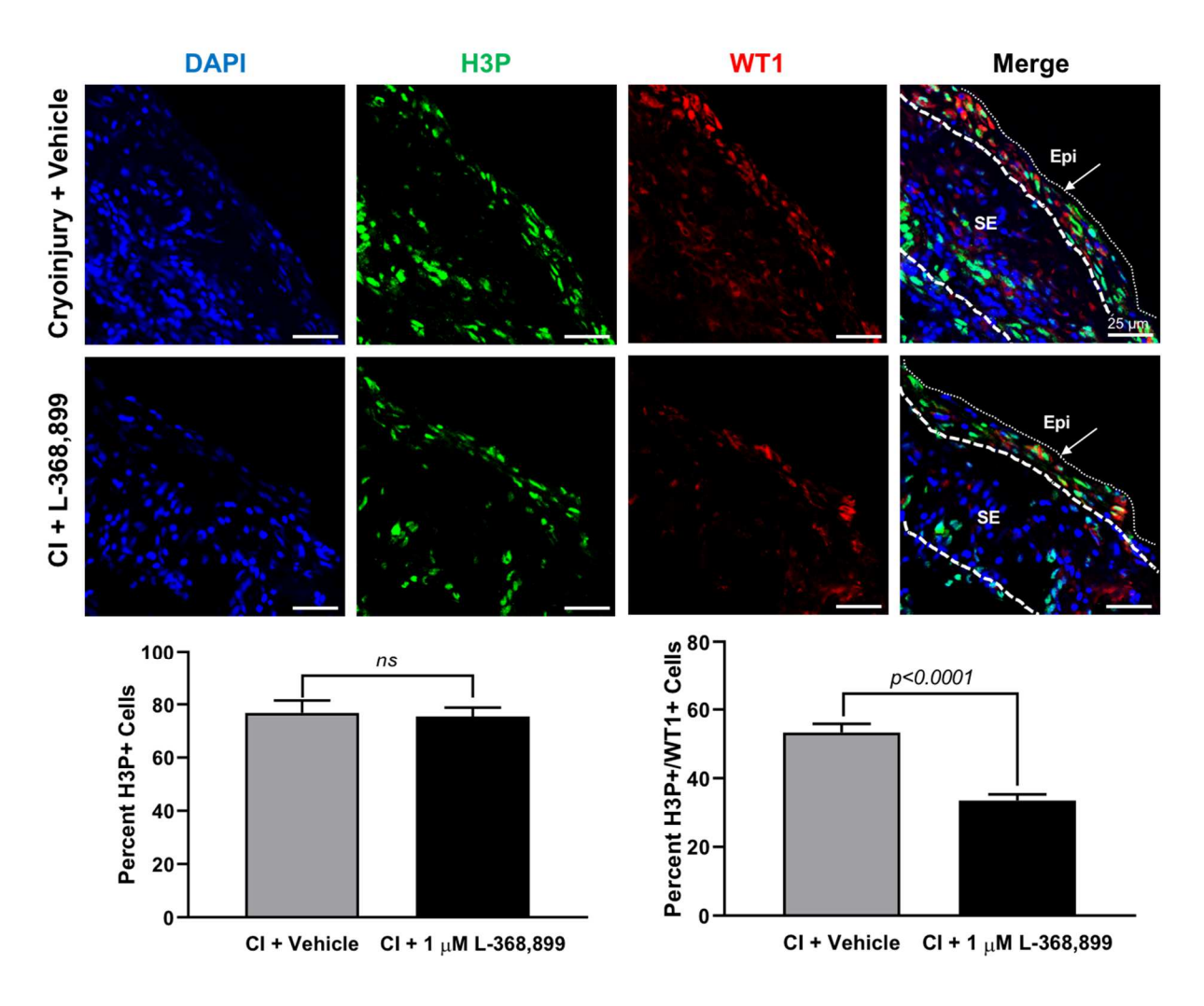


Figure 4.8: OXTR inhibition decreases epicardial proliferation. Confocal immunofluorescent images and quantification of proliferating epicardial cells in cryoinjured zebrafish hearts 3 days after cardiac cryoinjury. Epicardial cells are labeled with WT1 (red), proliferating cells are labeled with H3P (green), nuclei are labeled with DAPI (blue); n=4 animals per condition, scale bar: 25 μ m; CI: Cryoinjury, Epi: Epicardium, SE: Subepicardium.

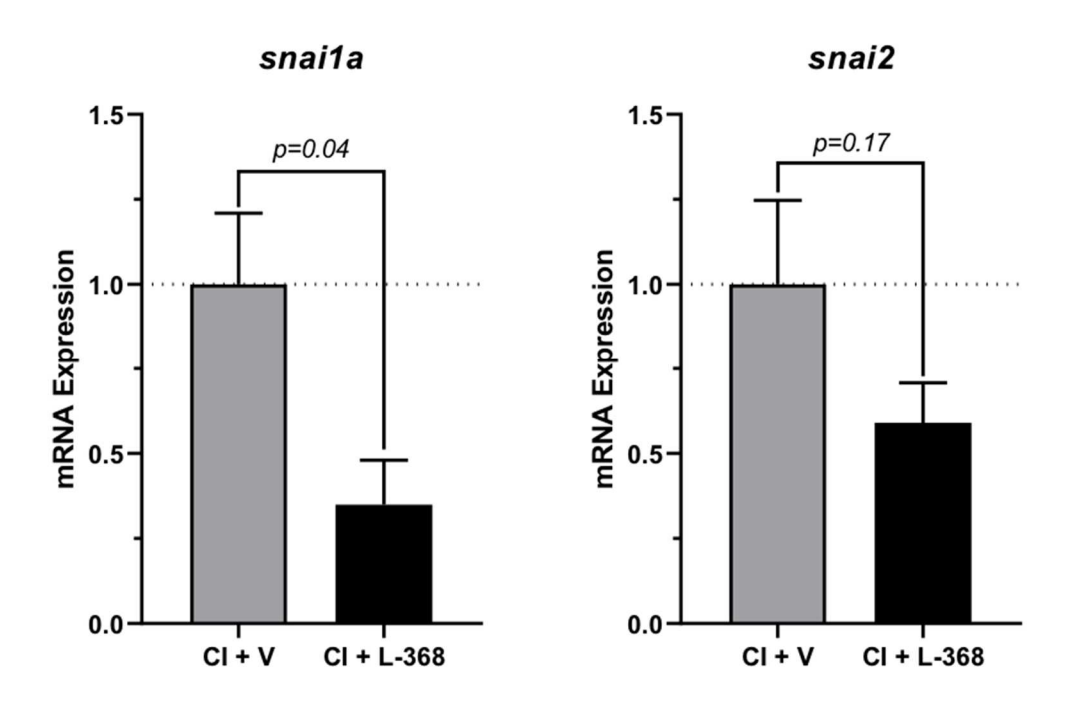


Figure 4.9: OXTR inhibition decreases expression of EMT markers. qRT-PCR data for EMT markers snai1a and snai2 in cryoinjured zebrafish hearts at 3 dpi treated with and without 1 μ M L-368,899 (L-368); n=4-5 animals per condition; CI: Cryoinjury, V: Vehicle.

4.2.4: Inhibition of oxytocin signaling prevents proliferation of other cardiac cell types after zebrafish cryoinjury

Naturally, the heart is made up of many different cell populations, most notably cardiomyocytes, epicardial cells, endocardial cells, cardiac fibroblasts, endothelial cells, and immune cells (Pinto et al., 2016; Zhou & Pu, 2016). While my results suggest that OXTR signaling is necessary for a proper epicardial response after cryoinjury, I wondered what the effects on other cell types would be. Two typical physiological responses observed in zebrafish heart regeneration are cardiomyocyte (CM) proliferation and endothelial cell (EC) revascularization adjacent to the injured area (Jopling et al., 2010; Marín-Juez et al., 2016). Therefore, I further explored these phenotypes after cryoinjury in control and L-368,899 treated hearts at 3 dpi. First, I co-stained injured hearts for pcna

(proliferating cell nuclear antigen), a commonly employed marker of cell proliferation, and tnnt2 (cardiac troponin T), a CM-specific marker, as described previously (Aguirre et al., 2014; Jopling et al., 2010). Upon counting the number of pcna+ cardiomyocytes per field of view, I observed a significant ~3-fold decrease in CM proliferation in the infarct border zone after L-368,899 administration (**Figure 4.10**). I confirmed these results by immunostaining cryoinjured zebrafish hearts for h3p and myh1e (myosin heavy chain 1E), another marker for CMs. Again, I saw a nearly 3-fold decrease in h3p+/myh1e+ CMs in the myocardium in treated hearts (**Figure 4.11**). Clearly, inhibiting oxytocin signaling has a detrimental effect on the ability of cardiomyocytes to proliferate and replenish lost tissue after cardiac cryoinjury.

I also set out to document endothelial cell revascularization of the infarcted area after cryoinjury. To do this, I conducted cryoinjuries in fli1-eGFP zebrafish, a transgenic strain that specifically labels endothelial cells with GFP, thereby serving as a marker for blood vessels (Lawson & Weinstein, 2002). I then stained control and treated tissue sections with gfp and tnnt2 and took images directly surrounding the infarct border zone. While control hearts displayed gfp staining in over 50% of the injured area, L-368,899 treated hearts only showed ~30% coverage (**Figure 4.12**). While not quite statistically significant, this nearly 2-fold difference in EC formation suggests that revascularization of the wound after cryoinjury is slowed by OXTR inhibition. Therefore, oxytocin signaling is necessary for both CM proliferation and blood vessel growth during heart regeneration. It is conceivable that the deleterious effects of L-368,899 on these phenotypes may be indirect and ultimately mediated by the epicardium. Activated epicardial cells have been shown to promote CM cycling and endothelial revascularization during heart development

and regeneration through secretion of paracrine factors such as fibroblast growth factor (FGF; (Lavine et al., 2005)), platelet-derived growth factor (PDGF; (Kim et al., 2010)), insulin-like growth factor (IGF; (Li et al., 2011)), and various glycoproteins (EI-Sammak et al., 2022; Lowe et al., 2019). These studies suggest that epicardial signaling plays a central role in inducing the numerous anti-regenerative phenotypes observed after L-368,899 administration. Finally, one more notable experiment I conducted was qRT-PCR for *oxt* mRNA in zebrafish brains 3 days after cardiac cryoinjury. Interestingly, I observed a ~10-fold increase in *oxt* expression in OXTR inhibited brains compared to controls (**Figure 4.13**). While this finding is preliminary, it suggests that the hypothalamus increases its production and release of oxytocin to compensate for inhibition of its receptor. If this is truly the case, then these data provide further evidence that the epicardial regeneration process depends on brain-derived OXT to a large extent.

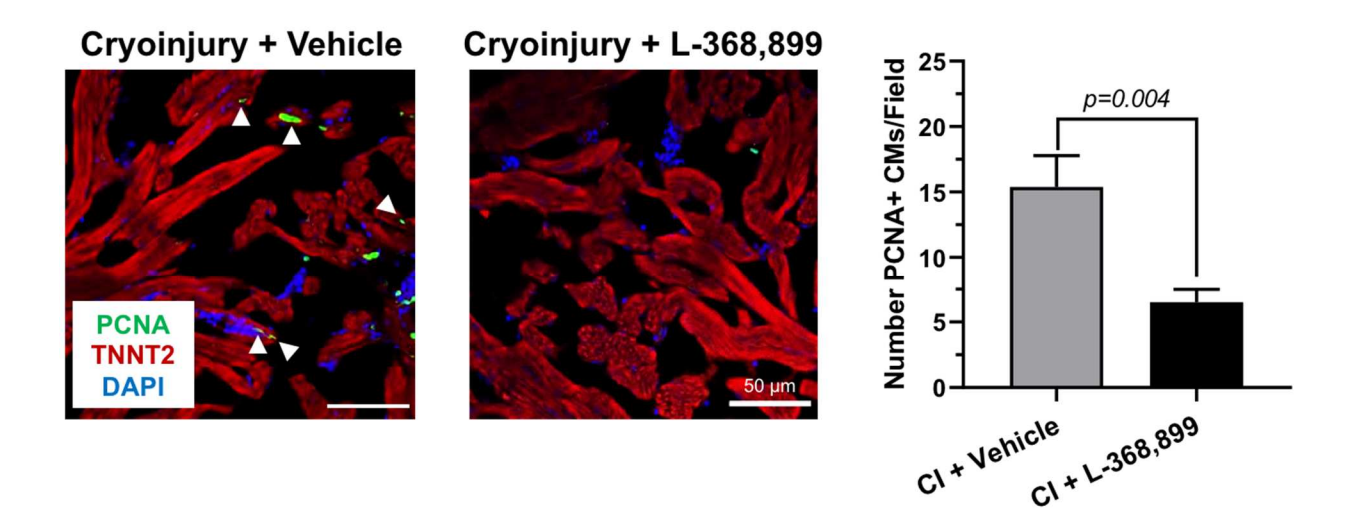


Figure 4.10: OXTR inhibition decreases cardiomyocyte proliferation. Confocal immunofluorescent images and quantification of proliferating CMs in cryoinjured zebrafish hearts at 3 dpi. Cardiomyocytes are labeled with TNNT2 (red), proliferating cells (arrowheads) with PCNA (green), nuclei with DAPI (blue); Images are high magnification of myocardium immediately adjacent to the injured area; n=4 animals per condition, scale bar: 50 μ m; CI: Cryoinjury, CM: Cardiomyocyte.

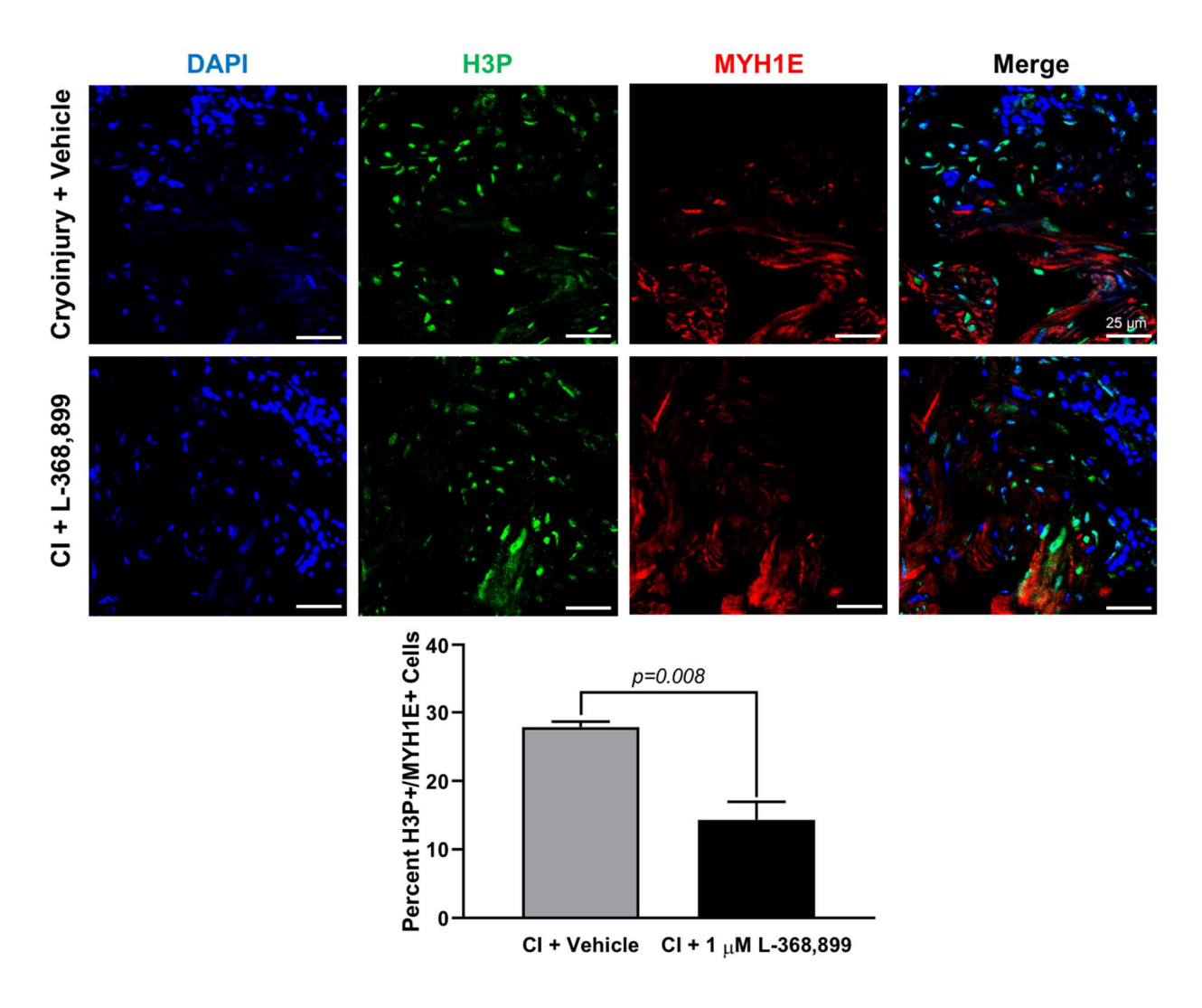


Figure 4.11: OXTR inhibition decreases cardiomyocyte proliferation. Confocal immunofluorescent images and quantification of proliferating CMs in cryoinjured zebrafish hearts 3 days after cardiac cryoinjury. Cardiomyocytes are labeled with MYH1E (red), proliferating cells are labeled with H3P (green), nuclei are labeled with DAPI (blue); n=3 animals per condition, scale bar: 25 μ m; CI: Cryoinjury, CM: Cardiomyocyte.

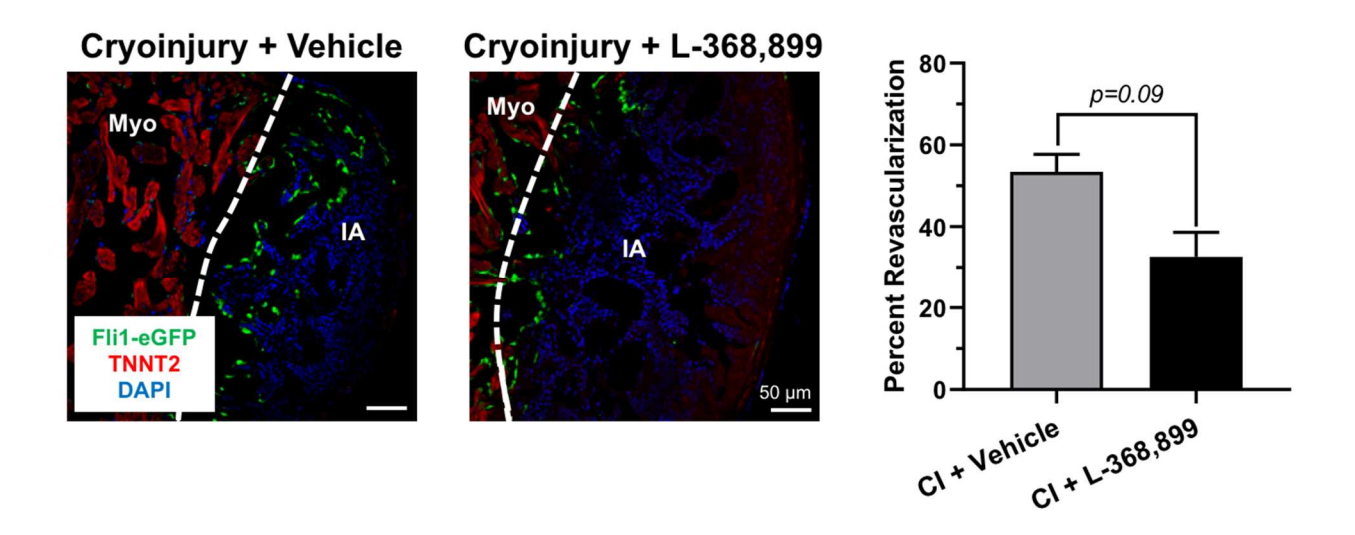


Figure 4.12: OXTR inhibition decreases vasculature formation. Confocal immunofluorescent images and quantification of *fli1-eGFP* transgenic zebrafish at 3 dpi showing endothelial revascularization in cryoinjured and L-368,899-treated hearts. Endothelial cells are labeled with GFP (green), cardiomyocytes with TNNT2 (red), nuclei with DAPI (blue); n=3-4 animals per condition, scale bar: 50 μ m; CI: Cryoinjury, IA: Injured Area, Myo: Myocardium.

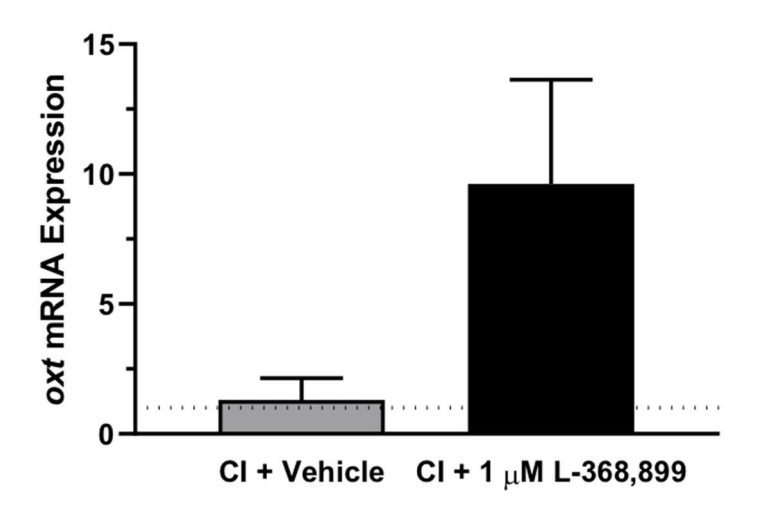


Figure 4.13: OXTR inhibition increases oxytocin release. qRT-PCR data for *oxt* in zebrafish brains 3 days after cardiac cryoinjury suggesting a compensatory oxytocin release after treatment with 1 μ M L-368,899 (L-368); n=3 animals per condition; CI: Cryoinjury.

4.2.5: Oxytocin signaling is required for epicardium development in zebrafish embryos

My data from adult zebrafish suggest that OXT plays an important role in epicardial function during regeneration. Since a regenerating heart recapitulates many of the phenotypes it had during development (high activity levels, increased gene transcription, EMT, EpiPC migration; (Cao & Poss, 2018; Simões & Riley, 2018)), I hypothesized that OXT signaling might be important during cardiac development as well. I therefore sought to determine if OXTR inhibition would have deleterious effects on epicardium formation in developing zebrafish embryos. The epicardium derives from an extra-cardiac cell cluster originating in the splanchnic mesoderm called the proepicardial organ (PEO). Once the PEO forms, it contributes new cells to the developing heart by migration into the epicardial and subepicardial spaces (Peralta et al., 2014). Most of these cells adhere to the surface of the heart to form the epicardium, while a subset undergo EMT to form EpiPCs, which can then differentiate into other cardiac cell types (Smits et al., 2018). I

bred double transgenic myl7-DsRed2, tcf21-nls-eGFP zebrafish embryos for my experiments. These animals express a dsRed2 fluorescent protein in cardiomyocytes, as myl7 is specific for this cell type in the heart (Kikuchi et al., 2010). They also express an eGFP tag in epicardial cell and EpiPC nuclei, due to the presence of the nuclear localization signal and specificity of tcf21 for these cell types (Wang et al., 2011). This model allowed me to visualize the development of the epicardium and myocardium in real time via fluorescence microscopy, thereby providing a perfect system with which to conduct my experiments.

Upon breeding these transgenic fish and collecting their eggs, I dissolved different concentrations of L-368,899 into the embryo medium and imaged epicardium formation at 3, 5, and 7 days post-fertilization (dpf). I quantified epicardium development by counting the number of tcf21-positive (green) cells covering the surface of the atrial and ventricular myocardium (red). At 3 dpf, a time point shortly after PEO formation when the epicardial layer is just starting to cover the surface of the heart, I observed statistically significant decreases in the number of epicardial cells on the ventricle at higher L-368,899 doses (Figure 4.14). And these differences only intensified with time, as imaging at 5 dpf revealed dose-dependent and statistically significant decreases in ventricular coverage, with a maximal inhibition of ~2-fold after treatment with 100 µM L-368,899 (Figure 4.15). Finally, at 7 dpf, a time point when epicardial formation should be mostly complete, I observed statistically significant differences between control and L-368,899 treated ventricles, regardless of concentration (Figure 4.16). Clearly, OXTR inhibition resulted in a massive delay in epicardial coverage of the developing zebrafish ventricle. Interestingly, I observed a more modest response to L-368,899 when I counted tcf21+

cells overlying the atrium. While imaging at 5 dpf did reveal a maximal decrease in atrial cells of ~2-fold at 100 μ M L-368,899, imaging at 7 dpf only resulted in a small (~15-30%) reduction in atrial counts at all concentrations (**Figure 4.17**). In general, proepicardial clusters tend to form closer to the ventricle than the atrium, causing the atrial epicardium to form later in development with a lower final cell count (Peralta et al., 2013, 2014). This may explain why decreases in atrial epicardial counts were more modest than ventricular counts. Regardless, the formation of the epicardium on both chambers is clearly adversely affected by L-368,899 treatment.

I confirmed the above findings by repeating my zebrafish embryo experiments with atosiban, a competitive OXTR antagonist. Again, at 3 dpf, I observed a ~2-fold, statistically significant decrease in the number of epicardial cells covering the surface of the heart after treatment with 100 µM atosiban (Figure 4.18). These findings provide further evidence that oxytocin receptor inhibition disrupts epicardial formation in zebrafish. This delay could be due to defects in proepicardial cell migration to the surface of the developing heart, as it appears that the proepicardial cluster is farther from the myocardium in atosiban-treated embryos than in control embryos (Figure 4.18). Alternatively, it could be due to a defect in epicardial cell proliferation after PEO cells have already adhered to the myocardial surface, as suggested by my previous in vitro and in *vivo* data. The observed phenotype could also be due to a combination of both factors. And it is entirely possible that OXTR inhibition has a detrimental effect on more than just epicardium formation. Indeed, further inspection of my fluorescent images revealed that myocardium development also may be affected, as atosiban-treated hearts appear much more linear in shape whereas control hearts display the ventricle and the atrium side-byside at 3 dpf (**Figure 4.18**). This observation suggests a delay in heart looping, a process that transforms the shape of the embryonic heart from a tube-like structure into a chambered organ (Andrés-Delgado & Mercader, 2016; Noël & Bakkers, 2017). While further investigation would be required to confirm this hypothesis, overall, my zebrafish embryo data strongly suggest that oxytocin signaling is vital for proper heart development.

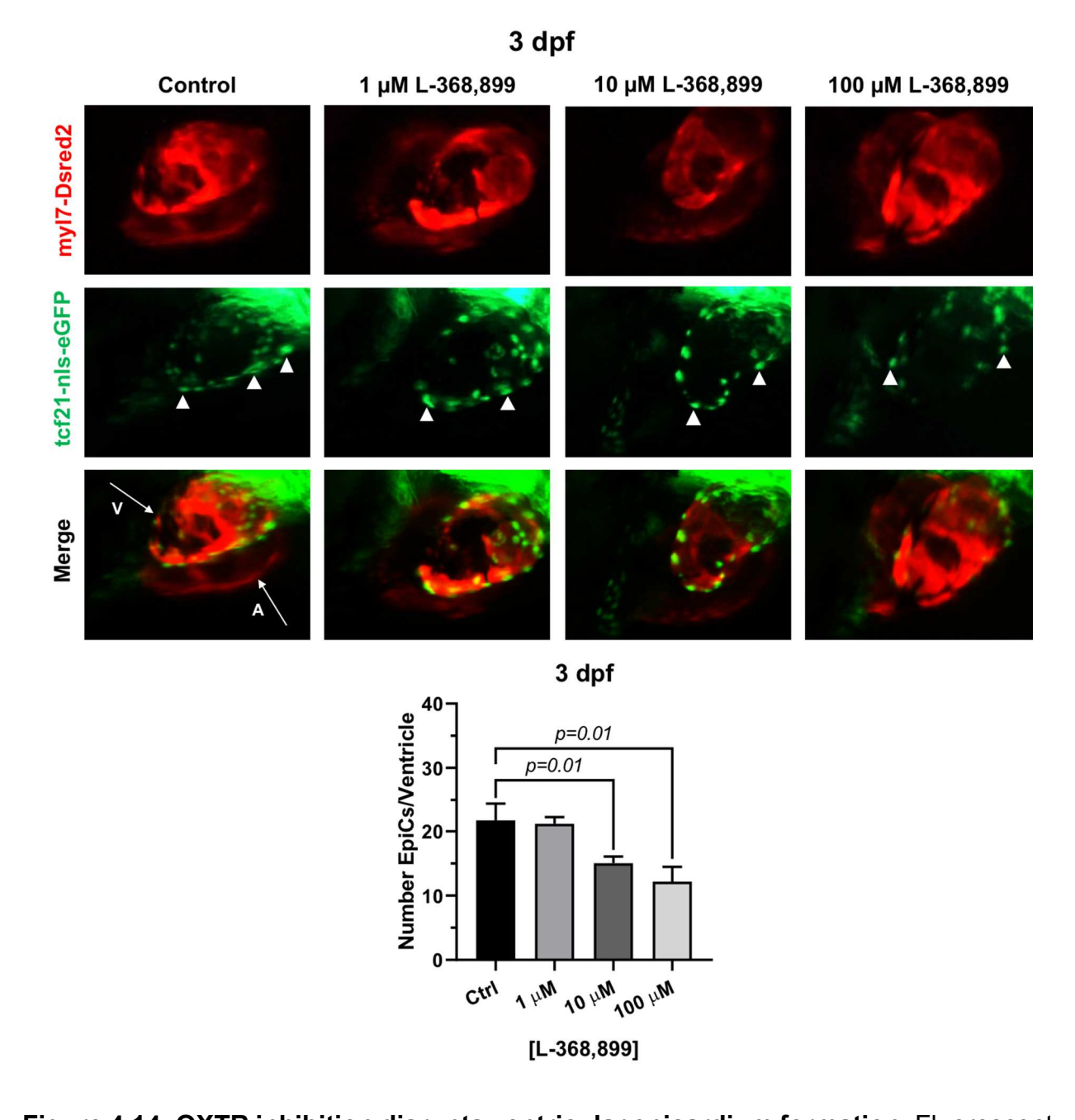


Figure 4.14: OXTR inhibition disrupts ventricular epicardium formation. Fluorescent images and epicardial cell counts per ventricle of developing zebrafish embryos at 3 dpf treated with different concentrations of L-368,899. Proepicardial and epicardial cells are labeled with GFP (green dots, arrowheads), myocardium is labeled with DsRed2 (red); n≥5 embryos per condition for each time point; A: Atrium, dpf: Days Post-Fertilization, EpiCs: Epicardial Cells, V: Ventricle.

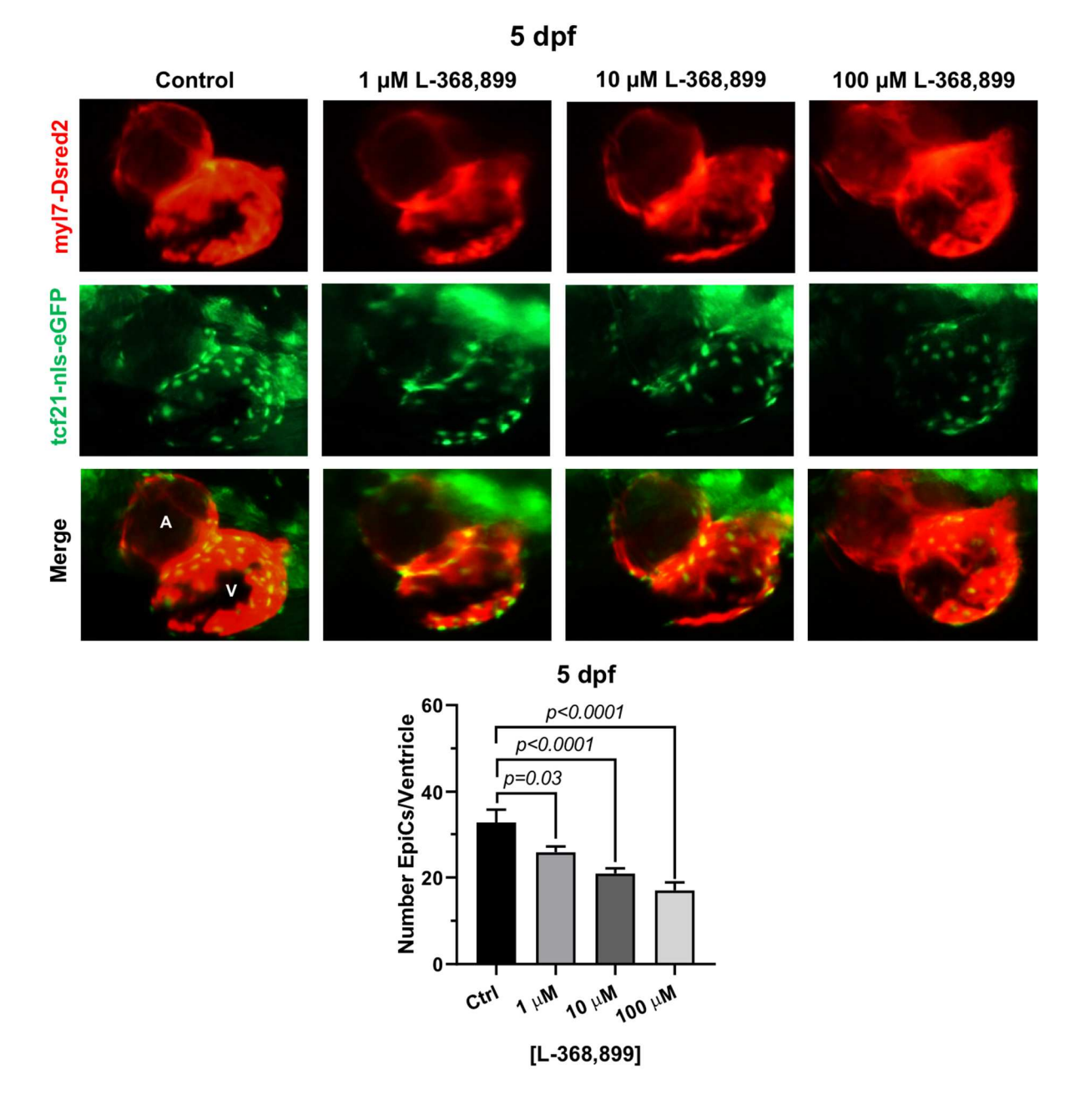


Figure 4.15: OXTR inhibition disrupts ventricular epicardium formation. Fluorescent images and epicardial cell counts per ventricle of developing zebrafish embryos at 5 dpf treated with different concentrations of L-368,899. Epicardial cells are labeled with GFP (green dots), myocardium is labeled with DsRed2 (red); n≥5 embryos per condition for each time point; A: Atrium, dpf: Days Post-Fertilization, EpiCs: Epicardial Cells, V: Ventricle.

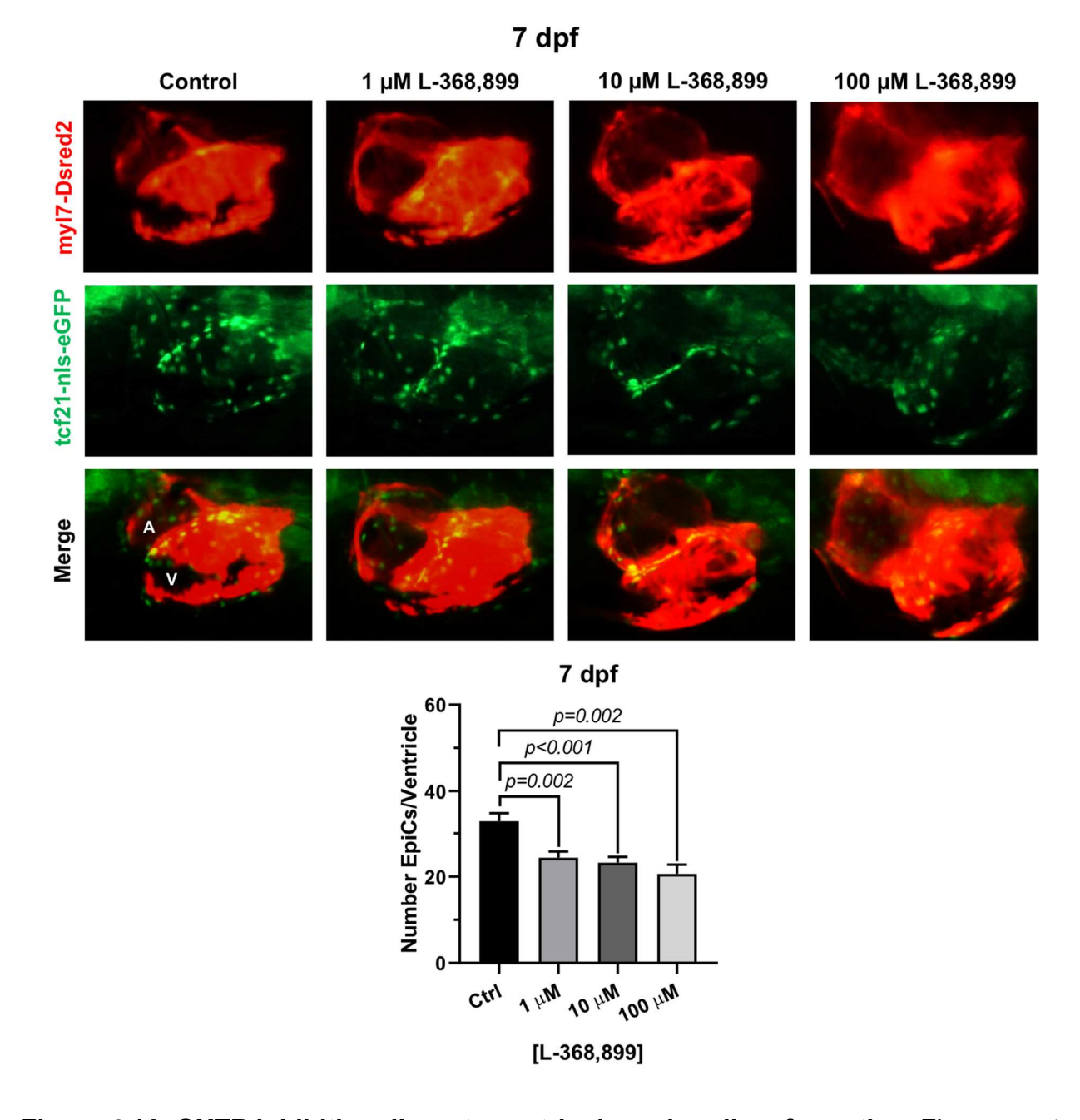


Figure 4.16: OXTR inhibition disrupts ventricular epicardium formation. Fluorescent images and epicardial cell counts per ventricle of developing zebrafish embryos at 7 dpf treated with different concentrations of L-368,899. Epicardial cells are labeled with GFP (green dots), myocardium is labeled with DsRed2 (red); n≥5 embryos per condition for each time point; A: Atrium, dpf: Days Post-Fertilization, EpiCs: Epicardial Cells, V: Ventricle.

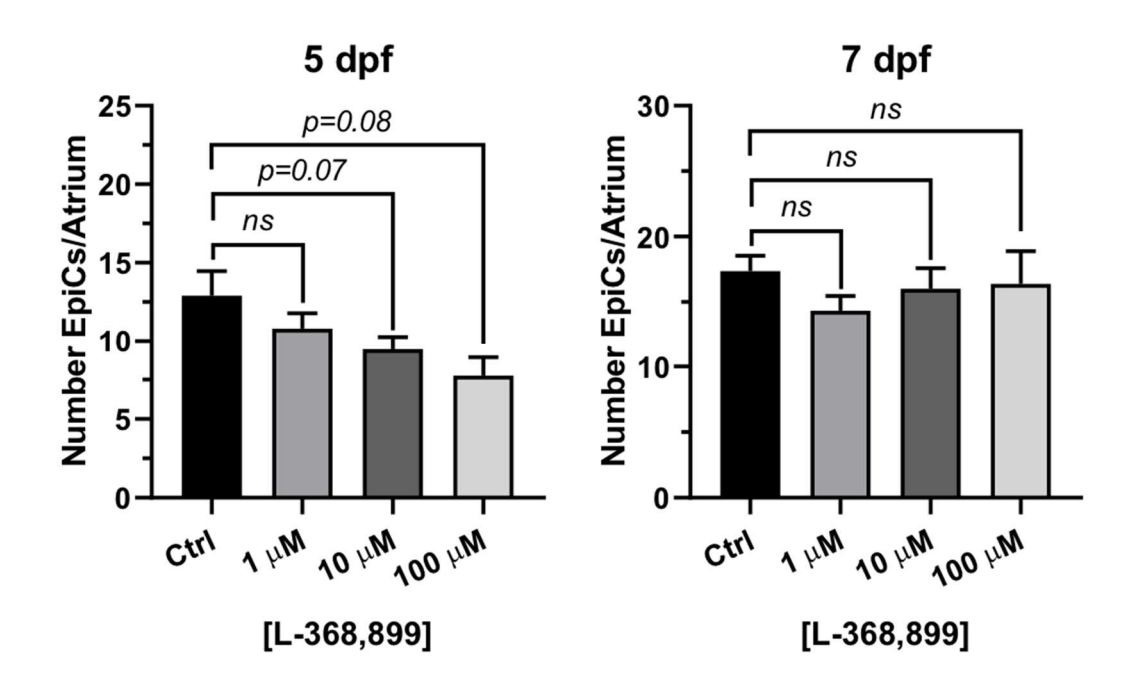


Figure 4.17: OXTR inhibition disrupts atrial epicardium formation. Epicardial cell counts per atrium of developing zebrafish embryos at 5 and 7 dpf treated with different concentrations of L-368,899; n≥5 embryos per condition for each time point; dpf: Days Post-Fertilization, EpiCs: Epicardial Cells.

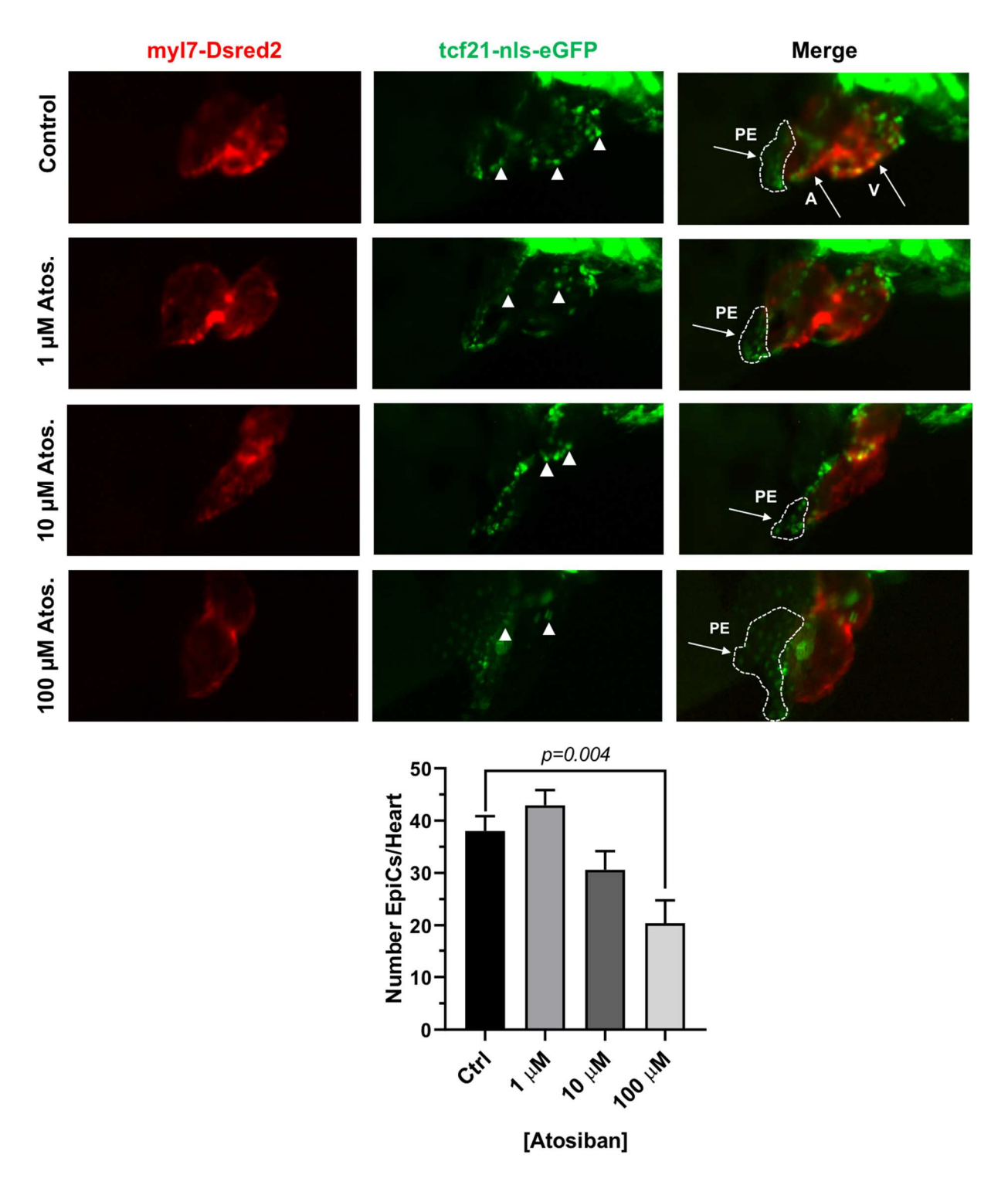


Figure 4.18: OXTR inhibition disrupts epicardium formation. Fluorescent images and epicardial cell counts per heart of developing zebrafish embryos at 3 dpf treated with different concentrations of atosiban. Proepicardial and epicardial cells are labeled with GFP (green dots, arrowheads), myocardium is labeled with DsRed2 (red), dashed lines

Figure 4.18 (cont'd)

demarcate proepicardial organ; n≥8 embryos per condition; A: Atrium, EpiCs: Epicardial Cells, PE: Proepicardium, V: Ventricle.

4.3: Discussion

To date, there is no evidence of brain-derived hormones directly regulating regeneration after cardiac injury. However, studies show that both the sympathetic (White et al., 2015) and parasympathetic (Mahmoud et al., 2015) branches of the autonomic nervous system are important for proper heart regeneration in neonatal mice and zebrafish. It is reasonable to infer that the central nervous system may play a role in these processes as well, especially since several brain-induced peripheral hormones, such as estrogen (Xu et al., 2020), thyroid hormone (Hirose et al., 2019), and cortisol (Sallin & Jaźwińska, 2016), have been implicated in regulating heart regeneration. In this chapter, I have taken these findings one step further and demonstrated that oxytocin, a hormone secreted by the neuroendocrine system, is released after cardiac cryoinjury in a naturally regenerating animal model. I found that brain oxt levels maximally increased at 3 dpi (Figure 4.1), with a corresponding increase seen in wt1b and tcf21 expression in the heart (Figure 4.2). These results suggest that OXT is released from the hypothalamus into circulation, where it travels to the heart to induce epicardial activation, a phenomenon that has not been described previously. Indeed, heart regeneration is a coordinated effort that involves communication between multiple organs (Filosa & Sawamiphak, 2021), and my studies strongly indicate that the brain is right at the center of this network.

In order to demonstrate the importance of central OXT release after cardiac cryoinjury, I utilized a pharmacological approach to inhibit OXT receptor signaling and

studied the effects on several aspects of regeneration. When cryoinjured zebrafish were administered L-368,899 they displayed a significantly larger myocardial injury area (Figure 4.4) and more myocardial fibrosis accumulation (Figure 4.5). While more time points would be necessary to be able to draw thorough conclusions, the difference in injury area between control and L-368,899 treated animals appeared to reach a maximum between 7 and 14 dpi. At this point, epicardial and endothelial cells have been activated, extracellular matrix proteins have accumulated, and cardiomyocytes have started to dedifferentiate and proliferate to fill the injured area (Bise et al., 2020; Sanz-Morejón & Mercader, 2020). Therefore, I investigated the activity of several cell types at 3 dpi to see if they were responsible for the differences in scar size I observed at later time points. I found that EpiPC activation and proliferation were greatly impaired by OXTR inhibition (Figures 4.7, 4.8). In addition, L-368,899 treatment after cryoinjury almost entirely prevented cardiomyocyte proliferation (Figure 4.10) and endothelial cell revascularization of the injured area (Figure 4.12). These data demonstrate that OXTR signaling is important for a proper regenerative response throughout the entire heart. The fact that oxytocin has global effects instead of just regulating one cell type is important because evidence suggests that the EpiPC contribution to new CMs in naturally regenerating animals is ~15% (Eroglu et al., 2022). Clearly, new cardiac cells arise from more than just EpiPC transdifferentiation, and OXT appears to be important for regeneration of all cell types after cryoinjury. Finally, I also observed that OXTR inhibition significantly delays development of the epicardium during zebrafish embryogenesis (Figures 4.14-4.16), likely through adverse effects on PEO migration and epicardial cell proliferation (Figure 4.18). The EpiPC contribution to CMs has been estimated as high as 18% in

developing hearts (Zhou et al., 2008), so the deficiencies in epicardial formation seen after L-368,899 treatment may extend to the myocardium as well, a theory supported by my images (**Figure 4.18**). Therefore, oxytocin is necessary for proper epicardial function through the entire lifespan of the zebrafish. The results presented here are an exciting first step towards establishing a causative link between neuroendocrine signaling and heart regeneration *in vivo*.

4.4: Future Directions

It important to note that my studies in Section 4.2.1 represent gene expression data. Indeed, just because transcription of one gene increases, it does not necessarily mean that levels of its corresponding protein increase. It is entirely possible that the newly synthesized mRNA is transient and degraded before it is even translated to functional protein (Shyu et al., 2008). Therefore, I could utilize ELISA (enzyme-linked immunosorbent assay) to confirm that oxytocin protein expression in tissue and blood samples also increases after cardiac cryoinjury. ELISA would be a beneficial technique because it has been successfully used to quantify OXT expression across multiple species (Bienboire-Frosini et al., 2017; Gnanadesikan et al., 2021). However, this approach does have its drawbacks. First, ELISA is a labor-intensive assay that involves numerous wash steps and takes a long time to complete. Just the sheer amount of manual manipulation that the plate undergoes could lead to large variation across wells and mask any changes in protein levels that would otherwise be seen. In addition, many kits have the potential for high background due to so many reagents being present in the wells at once. Cross-reactivity between substrates could increase absorbance signals to the point where they cannot be accurately measured (Sakamoto et al., 2018). If these

potential obstacles prevent me from quantifying OXT peptide, there are certainly alternative approaches I could take. One option is a western blot, although I would not be able to use this method with pure OXT, as it is a small (~1 kilodalton) peptide that would likely just run off a gel. However, I could perform a western blot for oxytocin bound to its natural carrier protein, neurophysin I, as shown previously (Rapacz-Leonard et al., 2020; Sarn et al., 2021). Another alternative approach would be OXT immunohistochemistry in fish brains after cryoinjury (Roy et al., 2019). Hopefully, these experiments would provide further evidence to confirm that oxytocin is indeed released into circulation after heart injury.

Although L-368,899 is specific for the oxytocin receptor (Pettibone et al., 1993), to fully demonstrate that the phenotypes I observed are not due to off-target effects, I could utilize a genetic approach. Specifically, I could generate an *oxtr* knockout zebrafish line through CRISPR-Cas9. To accomplish this task, I can utilize a "codon-optimized" Tol2 transposase-based system to ensure that the CRISPR reagents are effectively delivered into the host genome (Kawakami, 2007; Kwan et al., 2007; Mackey et al., 2020). I can introduce these sequences via microinjections into one-cell stage fish embryos (to ensure ubiquitous expression) directly into the yolk sac, as described previously (Rosen et al., 2009). Growing these knockout animals to adulthood and subsequently performing cryoinjuries would allow me to study the effects of oxytocin signaling on zebrafish heart regeneration with even greater precision. My hypothesis is that oxytocin is released from the brain into the bloodstream after cardiac injury to facilitate epicardial regeneration. While my qRT-PCR data showing an upregulation of *oxt*, *wt1b*, and *tcf21* mRNA levels after cryoinjury are encouraging correlational findings, it is possible that this increase in

epicardial activation could be due to local effects, as the heart is able to produce some OXT on its own (Gutkowska et al., 2000; Jankowski et al., 1998). To confirm that my results due to hypothalamic OXT release. could utilize are the Nitroreductase/Metronidazole (NTR/Mtz) system (Curado et al., 2007, 2008) to selectively ablate cells of the paraventricular nucleus, the main site of OXT production. By preventing the brain from synthesizing oxytocin, I could more thoroughly elucidate how important systemic hormone release is to heart regeneration. I can then further study the effects on EpiPCs and other cardiac cell types such as cardiomyocytes, endothelial cells, cardiac fibroblasts, and immune cells. Together, these techniques and methods would provide even more insight into the role OXT plays in epicardial activity in zebrafish.

Chapter 5: Oxytocin Induces a Pro-Regenerative Phenotype in Three-Dimensional Human Heart Organoids

5.1: Introduction

To this point, I have presented in vitro and in vivo data to demonstrate that oxytocin enhances heart regeneration by activating the epicardium. My hiPSC-derived epicardial cells provide convincing evidence to support this claim using a model of human origin, but lack the three-dimensional structure that is a hallmark feature of the human heart. My results from zebrafish suggest that OXTR signaling is necessary for cardiac regeneration in a naturally regenerating animal model, but ultimately, using fish to draw conclusions about human biology can only go so far. To bridge the gap between these model systems, I need a source of human cardiac cells that can be studied in three dimensions. Organoids (literally "resembling an organ") are miniature versions of whole organs produced in vitro that recapitulate the histological and anatomical features of the structures they represent (Kim et al., 2020; Lancaster & Knoblich, 2014). applications are numerous, as they can be utilized for developmental studies, disease modeling, drug discovery/toxicity screening, and regenerative medicine, among others (Corrò et al., 2020; Lancaster & Knoblich, 2014). In general, organoids are made from adult or pluripotent stem cells, theoretically allowing for any three-dimensional structure found in the body to be modeled in vitro (Clevers, 2016). The earliest attempts to generate organoids were focused on the intestine (Sato et al., 2009), brain (Lancaster et al., 2013), and kidney (Takasato et al., 2015), however, progress in cardiac organoid fabrication has lagged behind. This could be due to the complex nature of heart morphogenesis as well as challenges in ensuring adequate nutrient delivery and protocol

reproducibility in a dish (Kim et al., 2022; Miyamoto et al., 2021; Zhao et al., 2021). However, significant progress has been made in the last ~2-3 years to overcome these obstacles, as several recent reports detailing the generation of human heart organoids (hHOs) have greatly expanded the field of *in vitro* cardiac modeling (Drakhlis et al., 2021; Hofbauer et al., 2021; Lewis-Israeli, Volmert, et al., 2021; Lewis-Israeli, Wasserman, Gabalski, et al., 2021; Mills et al., 2017; Richards et al., 2020; Silva et al., 2021).

In general, hHOs are fabricated by one of two approaches, directed assembly and self-organization. In directed assembly, pre-differentiated stem cells are co-cultured and seeded onto a scaffold or bioengineered device that allows them to develop their threedimensional structure. In self-organization, stem cells differentiate, aggregate, and organize autonomously, with minimal exogenous intervention, due to the presence of morphogens and growth factors in the media (Cho et al., 2022; Lewis-Israeli, Wasserman, While both methodologies have their benefits and drawbacks, & Aguirre, 2021). organoids generated by self-assembly tend to more closely recapitulate the physiological complexity of the human heart (Lewis-Israeli, Wasserman, & Aguirre, 2021). Therefore, we developed a protocol to generate hHOs by this approach (Lewis-Israeli, Volmert, et al., 2021), and are currently utilizing them for disease modeling, maturation studies, and toxicity testing. We found that these "miniature hearts" self-organized into beating structures complete with cardiac chamber-like features, the entire array of cell types found in the heart, vascularization, and cardiac functional activity (Lewis-Israeli, Wasserman, Gabalski, et al., 2021). It should be noted that at the end of the 15 day differentiation protocol, these hHOs tended to resemble the human fetal heart transcriptionally and morphologically. Naturally, to model the cardiac injury setting, I wanted to ensure that my

organoids were as adult-like as possible. Therefore, I grew the hHOs in fatty acidcontaining "maturation medium" (Yang et al., 2014, 2019) for 10 days prior to experiments to ensure that they recapitulated the adult heart as closely as they could. Studies show that exposure to these culture components allows cardiomyocytes to increase their size, force generation, calcium handling dynamics, and respiratory capacity, features that are all consistent with a more mature phenotype (Yang et al., 2019). Therefore, matured hHOs provided the perfect platform with which to conduct my regeneration studies. First, I developed and characterized a cardiac injury model in organoids by modification of existing cryoinjury protocols (Hofbauer et al., 2021; Voges et al., 2017). I then differentiated scrambled and OXTR knockdown hiPSCs (see Section 2.3) into hHOs and studied the effects on epicardial activation after cryoinjury. While these results are preliminary and would greatly benefit from additional experimentation, I found that knockdown hHOs were unable to respond to OXT, which is similar to the case observed in hEpiCs. Overall, I show here that oxytocin signaling may be necessary for a proregenerative phenotype in cryoinjured human heart organoids.

5.2: Results

5.2.1: Development and characterization of a cardiac injury model in three-dimensional human heart organoids

To uncover the effects of oxytocin on regeneration *in vitro*, I first needed a reliable method to induce injury in hHOs. I chose cryoinjury, as it is a well-accepted myocardial infarction model in animals (Chablais et al., 2011; González-Rosa et al., 2011; Polizzotti et al., 2016; Van den Bos et al., 2005). In addition, it is relatively easy to carry out, as the cryoprobe can be constructed from inexpensive materials (González-Rosa & Mercader,

2012). I induced cryoinjury at the end of the hHO maturation protocol (differentiation Day 30) by applying a liquid nitrogen cooled metal probe directly to the organoid surface, as described in Section 2.5. Remarkably, the vast majority of organoids are able to survive this procedure, and regain relatively normal morphology and beating patterns within 1 day. In order to characterize the extent of cryoinjury, I first set out to confirm that the hHOs were indeed injured by visual means. To accomplish this goal, I added Cyanine 3 (Cy3), a bright fluorescent dye that is commonly used to label nucleic acids, directly to the medium post-cryoinjury. Importantly, this dye also colors the hHOs pink, thereby providing contrast to an otherwise colorless structure. After cryoinjury, I observed small holes in the hHOs, corresponding to areas where the cryoprobe made contact. Brightfield imaging confirmed that the probe was damaging the surface of the organoids (Figure **5.1**). I then stained my hHOs with NucBlue, a modified version of the nuclear counterstain Hoechst 33342 that allows for imaging of live cells. Before cryoinjury, organoids displayed consistent nuclear staining on their surfaces. I found that the same organoids appeared to contain less nuclei after cryoinjury, suggesting that the procedure was causing some cells to die off (Figure 5.2). Next, I expanded upon these data by utilizing trypan blue, a cell-impermeant stain frequently used to assess cell viability. This assay works based on the principle of dye exclusion, with live cells (with intact membranes) excluding the dye and dead cells (with compromised cell membranes) letting it in. Once the trypan blue gets into dead cells, it stains the cytoplasm blue (Strober, 2001). I again cryoinjured hHOs and added trypan blue to the wells. When looking at whole organoids, I observed far more blue staining on injured samples than sham samples (Figure 5.3). It should be noted that the above imaging experiments were all conducted within 30-60

minutes after cryoinjury, meaning that cell loss occurs immediately upon exposure to the freezing temperatures. Together, they provide qualitative evidence that the hHO cryoinjury procedure produces the desired results.

As a natural follow-up, I sought to quantitatively determine the magnitude of the increase in cell death due to cryoinjury. To do this, I dissociated cryoinjured hHOs, diluted them in trypan blue, and pipetted them onto a hemocytometer. This device is commonly used to count individual cells, which can simply be observed under a microscope. Both sham and injured organoids contained >80% live cells approximately 1 hour after cryoinjury, which makes sense seeing as the protocol is not lethal to the hHOs. Notably, I observed a ~2-fold increase in dead cells in cryoinjured hHOs (nearly 20% versus ~10%), thereby providing quantitative evidence that the protocol decreases cell viability (Figure 5.4). However, this difference was not statistically significant between the groups, suggesting that more hHO samples were needed or alternative readouts for cell death would be required. On that note, I next looked to determine whether cryoinjured cells were dying due to apoptosis. I utilized a transgenic hiPSC line expressing FlipGFP, a marker commonly employed as a reporter for apoptosis. In healthy cells, the GFP variant is engineered to be non-fluorescent. In apoptotic cells, activation of caspase activity flips one of the β-strands of the GFP protein to a more stable structure, allowing for the emission of fluorescence (Zhang et al., 2019). I differentiated FlipGFP hiPSCs to hHOs, cryoinjured them, and documented fluorescence levels over time. I found that injured organoids at 1 and 3 dpi (days post-injury) displayed ~2-fold greater GFP+ area compared to controls (Figure 5.5). This increase in apoptosis may have played a role in sham samples consistently measuring ~20-30% larger than injured samples at 1, 3, and

7 dpi (**Figure 5.6**). Clearly, organoid cryoinjury induces programmed cell death, a finding that aligns with previous cryoinjury studies (Chablais et al., 2011; Voges et al., 2017). Finally, I also wondered if extracellular matrix and fibrosis accumulate in the hHO myocardium after cryoinjury, as would be expected during the early stages of regeneration (Bise et al., 2020; Uygur & Lee, 2016). Therefore, I took injured hHOs at 3 dpi, sectioned them, and stained them with Masson's trichrome reagents. Notably, I detected minimal blue staining in all the sections, suggesting that fibrosis levels did not increase at this time point (**Figure 5.7**). Further characterization (more time points, immunofluorescence for ECM proteins, etc.) would be required to more thoroughly document the "regenerative" response of the organoids to cryoinjury.

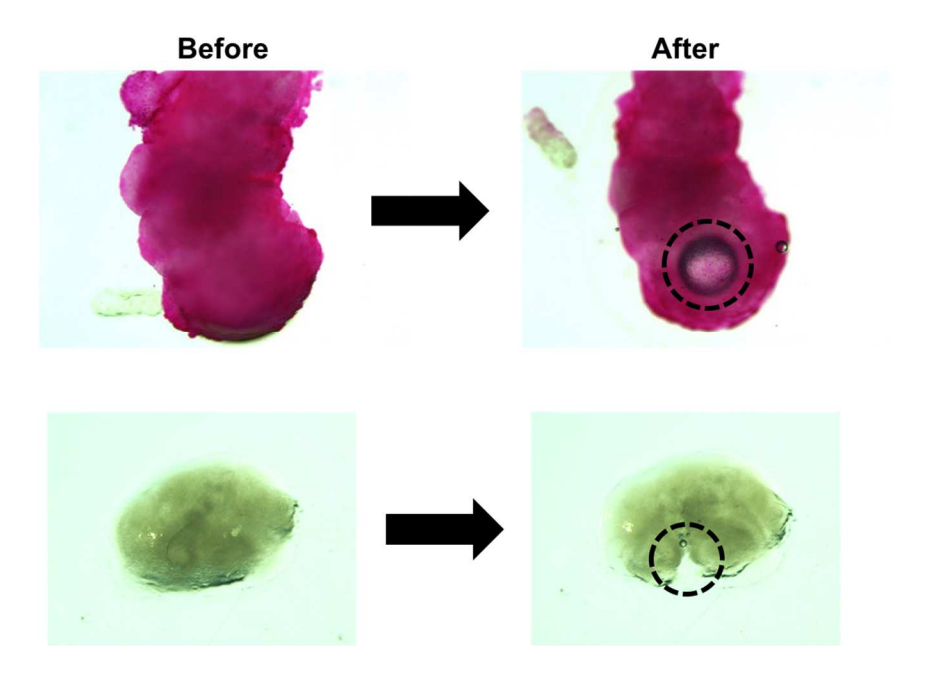


Figure 5.1: Visualization of cryoinjured organoids. Images of whole hHOs stained with Cy3 (TOP) and under brightfield (BOTTOM) before and after cryoinjury. Dashed lines demarcate areas where the cryoprobe made contact with the organoid surface.

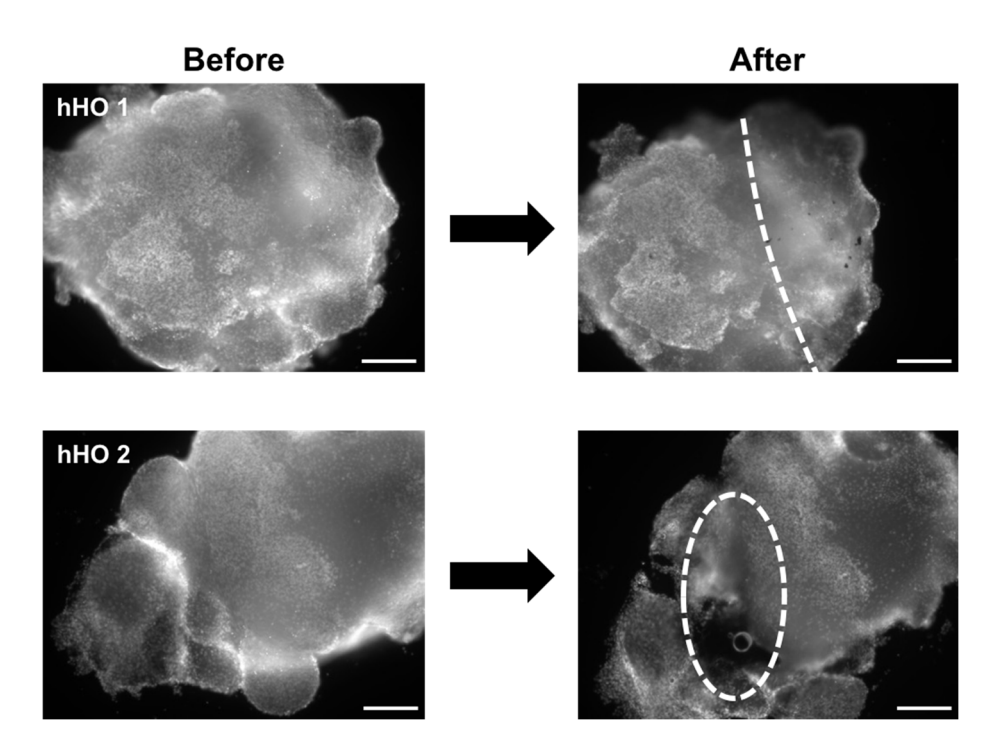


Figure 5.2: Cryoinjury decreases nuclei staining in hHOs. Live imaging of hHOs stained with Hoechst 33342 showing less cells on the surface of the organoid after cryoinjury. Dashed lines demarcate areas where the cryoprobe made contact with the hHO; Scale bar: 200 μ m.

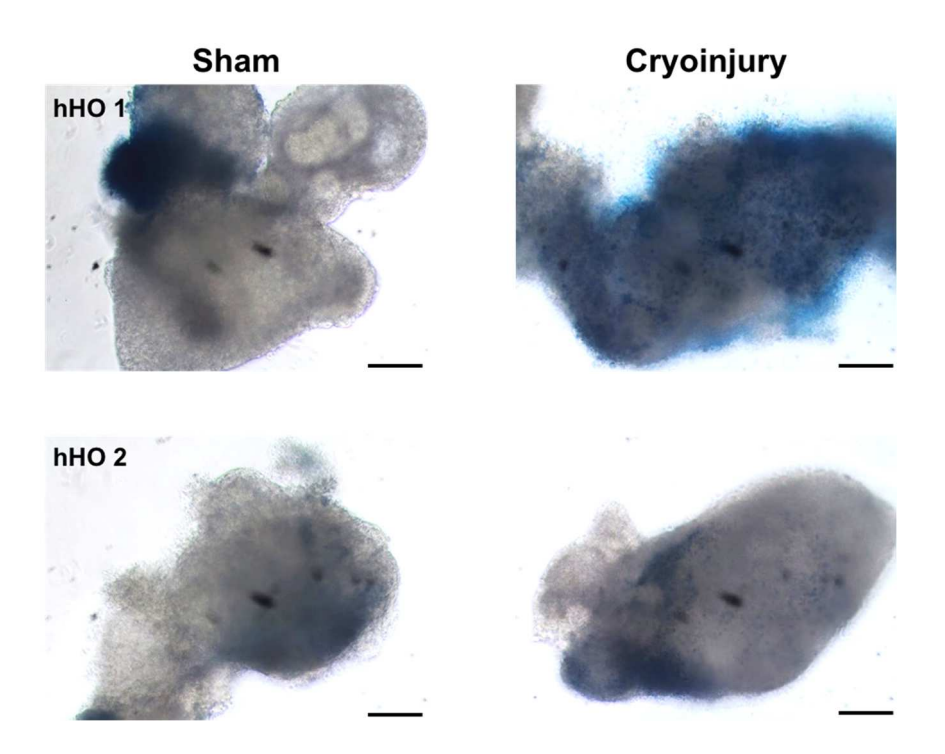


Figure 5.3: Cryoinjury increases trypan blue staining in hHOs. Live imaging of whole hHOs stained with trypan blue showing more dye accumulation after cryoinjury; Scale bar: $200 \ \mu m$.

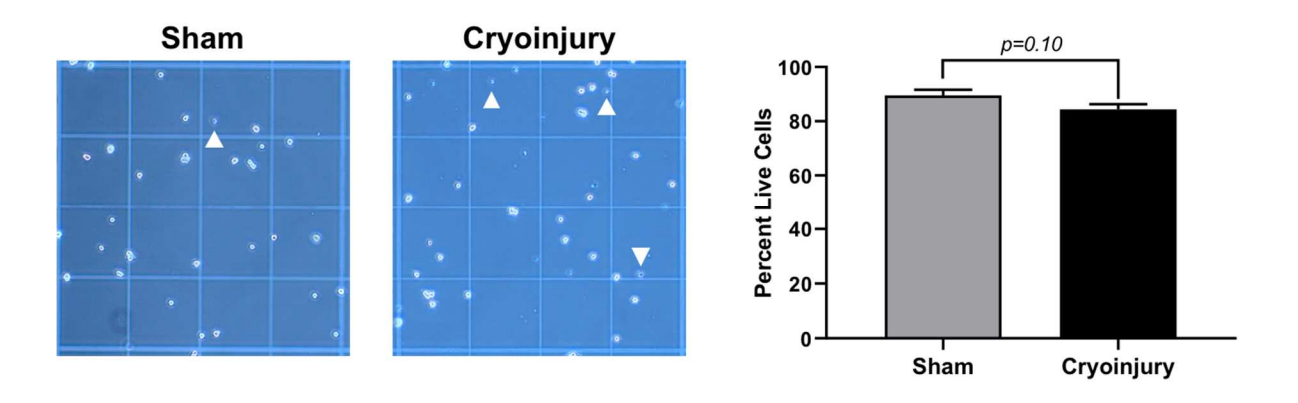


Figure 5.4: Cryoinjury decreases cellular viability in hHOs. Hemocytometer images and quantification of dissociated hHOs after cryoinjury. Arrowheads indicate dead or compromised cells stained with trypan blue; n=6 hHOs per condition.

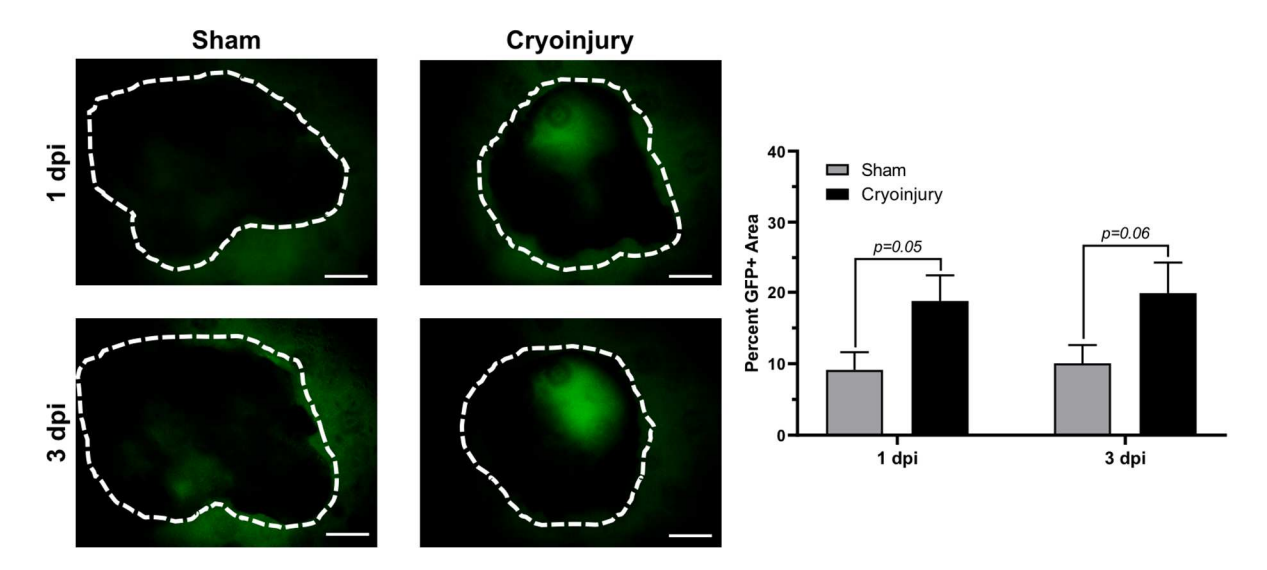


Figure 5.5: Cryoinjury increases cellular apoptosis in hHOs. Fluorescent images and quantification of cryoinjured FlipGFP hHOs at 1 and 3 dpi showing an increase in apoptosis (green fluorescence) after the procedure. Dashed lines demarcate hHO perimeter; n≥8 hHOs per time point, scale bar: 200 μm; dpi: Days Post-Injury.

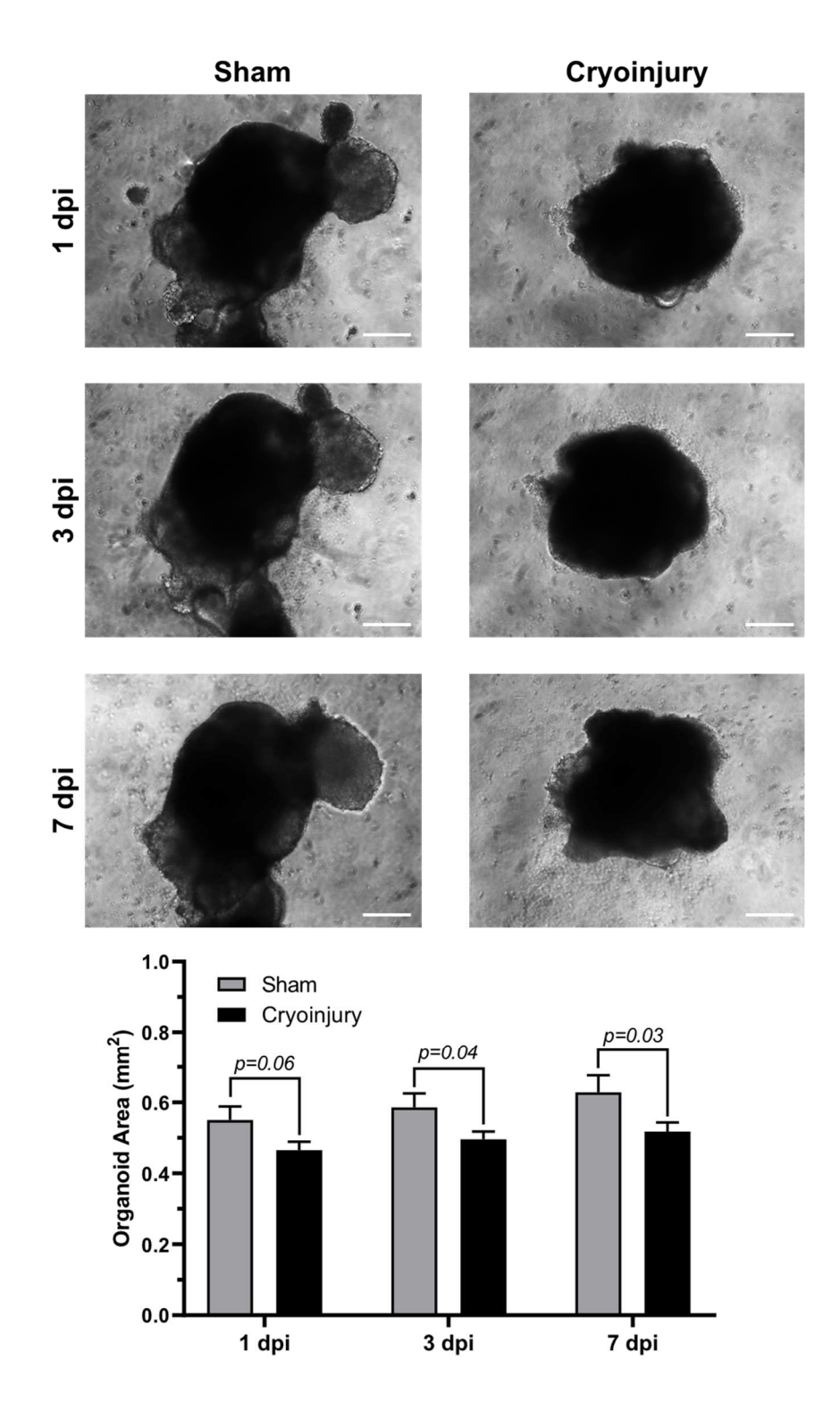


Figure 5.6: Cryoinjury decreases hHO size. Brightfield images and quantification of FlipGFP hHO area at 1, 3, and 7 days after cryoinjury; n≥8 hHOs per time point, scale bar: 200 μm; dpi: Days Post-Injury.

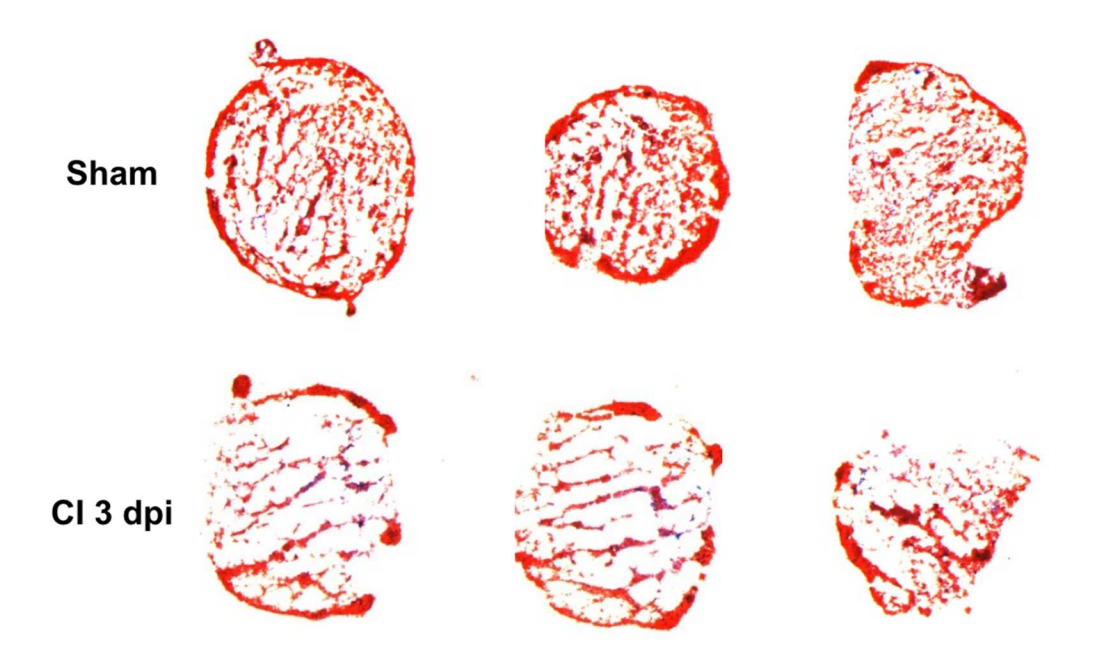


Figure 5.7: Cryoinjury does not affect extracellular matrix deposition in hHOs. Masson's trichrome staining of cryoinjured hHOs at 3 dpi showing minimal fibrosis accumulation at this time point; CI: Cryoinjury, dpi: Days Post-Injury.

5.2.2: Knockdown of the oxytocin receptor prevents epicardial activation in threedimensional human heart organoids

Once my cryoinjury model was in place, I set out to investigate the effects oxytocin signaling has on epicardial activation in hHOs. Just as I did in hEpiCs (see Section 3.2.6), I took scrambled and *OXTR* knockdown hiPSCs and differentiated them to organoids. I then compared several features between the two hHO lines. When looking at gross morphology, I noticed that *OXTR* silenced (sh*OXTR*) hHOs were much smaller than scrambled ones on differentiation Day 30. Quantification of hHO area revealed this difference to be ~50%. In addition, brightfield imaging showed that sh*OXTR* organoids had large amounts of dead cells and debris sloughing off the edge of the tissue (**Figure 5.8**). They were also much more fragile in nature than scrambled organoids. These analyses and observations suggest that *OXTR* knockdown affects hHO development and

differentiation, effects that are consistent with my findings in Chapter 4 showing that OXTR signaling is necessary for proper heart development. I also wondered whether receptor silencing had an effect on epicardial activity after cryoinjury. To investigate, I cryoinjured scrambled and shOXTR hHOs, collected RNA, and carried out qRT-PCR for several EpiPC, EMT, and mesenchymal markers (Figure 5.9). Notably, WT1 and TCF21 expression were >2-fold lower in knockdown organoids, suggesting that EpiPC activation after injury is more efficient when OXTR signaling is intact. I observed the same effects when I looked at SNAI1 levels. These qRT-PCR data demonstrate that EMT processes are impaired in knockdown organoids, as WT1 and TCF21 regulate the activity of Snail proteins, which facilitate EMT by repression of epithelial markers and upregulation of mesenchymal markers (Acharya et al., 2012; Braitsch & Yutzey, 2013; Martínez-Estrada et al., 2010; Von Gise & Pu, 2012). Indeed, I found ~2-fold lower expression of VIM in shOXTR hHOs, used here as a readout for mesenchymal cells (Figure 5.9). One alternative explanation for these qRT-PCR data is that the observed decreases in gene expression are simply due to the fact that knockdown hHOs are smaller, and therefore produce less of each transcript than scrambled hHOs. Therefore, controlling for organoid size would be critical to demonstrating how important the oxytocin receptor is for a proper epicardial response to cryoinjury in vitro.

I next sought to systematically assess the extent of EpiPC proliferation and activation in response to OXT. For each organoid line, I utilized four conditions: sham, sham + 1 μM OXT, cryoinjury, and cryoinjury + 1 μM OXT. Three days after cryoinjury, I collected and fixed several hHOs per condition and stained them for H3P to quantify proliferating cells and WT1 to quantify activated EpiPCs. I manually counted the number

of H3P+ and WT1+ nuclei in each organoid and divided these values by the total number of nuclei to obtain percentages for my readouts of interest. As expected, the percentage of H3P+ cells increased by ~40-60% in the scrambled line in response to OXT in both sham and cryoinjured hHOs (Figure 5.10). These values fall in line with my results from scrambled hEpiCs presented in Chapter 3. In the shOXTR line, this response to OXT was completely abolished after sham procedure. But interestingly, I observed a ~2-fold (not statistically significant) decrease in cellular proliferation in cryoinjured hHOs after OXT administration, a result that was unexpected (Figure 5.11). Regardless, I then set out to see if I could recapitulate these results in organoids stained for WT1. In addition to manual nuclei counts, I also quantified the percentage of hHO area covered by WT1+ immunoreactivity, thereby providing two readouts for epicardial activation. In scrambled hHOs, I again saw a ~1.5-2 fold increase in WT1 area in response to OXT, with a more modest (~20-30%) increase as assessed by nuclei counts. Although the fold changes did not quite reach statistical significance, these trends were consistent in both healthy and injured hHOs (Figure 5.12). Remarkably, knockdown organoids were once again unable to respond to OXT challenge, regardless of injury status or quantification method utilized (Figure 5.13), results mostly consistent with the H3P analysis described above.

Although these immunofluorescence data seem to suggest a function for OXTR in epicardial proliferation before and after cryoinjury, it should be noted that in general, the response to oxytocin in scrambled hHOs was somewhat lower in magnitude than that observed in two-dimensional epicardial cells. In addition, none of the results reached statistical significance and therefore should not be overstated too greatly. Indeed, the sample sizes for these experiments are relatively low (~3-4 hHOs per condition) and

would need to be higher before further conclusions can be drawn. As it stands right now, it is possible that the differences I documented between groups could have been due to random chance or even observer bias. Therefore, these data currently lack enough statistical power to definitively interpret them. However, I did find it interesting that my organoids did not respond as strongly to oxytocin as hEpiCs did. Outside of the limitations discussed above, this observation could simply be due to the fact that the threedimensional hHOs are more complex, and therefore displayed a less robust epicardial response after OXT administration. Alternatively, it could be because my organoids make their own oxytocin. Indeed, while hHOs contain negligible OXT transcripts through Day 19 of differentiation (see Gene Expression Omnibus entry GSE153185), once exposed to the maturation protocol, their oxytocin expression increases exponentially. In fact, gRT-PCR analyses in hHOs showed that compared to Day 19, OXT expression increased ~2-fold at Day 25 and nearly 4-fold at Day 30 (Figure 5.14). Clearly, matured organoids synthesize their own OXT, and the presence of this endogenous peptide could partially mask the effects of exogenous OXT administration in scrambled hHOs. At a minimum, my results do suggest that shOXTR hHOs are unable to muster even a modest response after OXT addition. Therefore, I can conclude that intact OXTR signaling at least plays a role in oxytocin-induced epicardial activation in human heart organoids, and future work could reveal how vital that role truly is to a proper regenerative response.

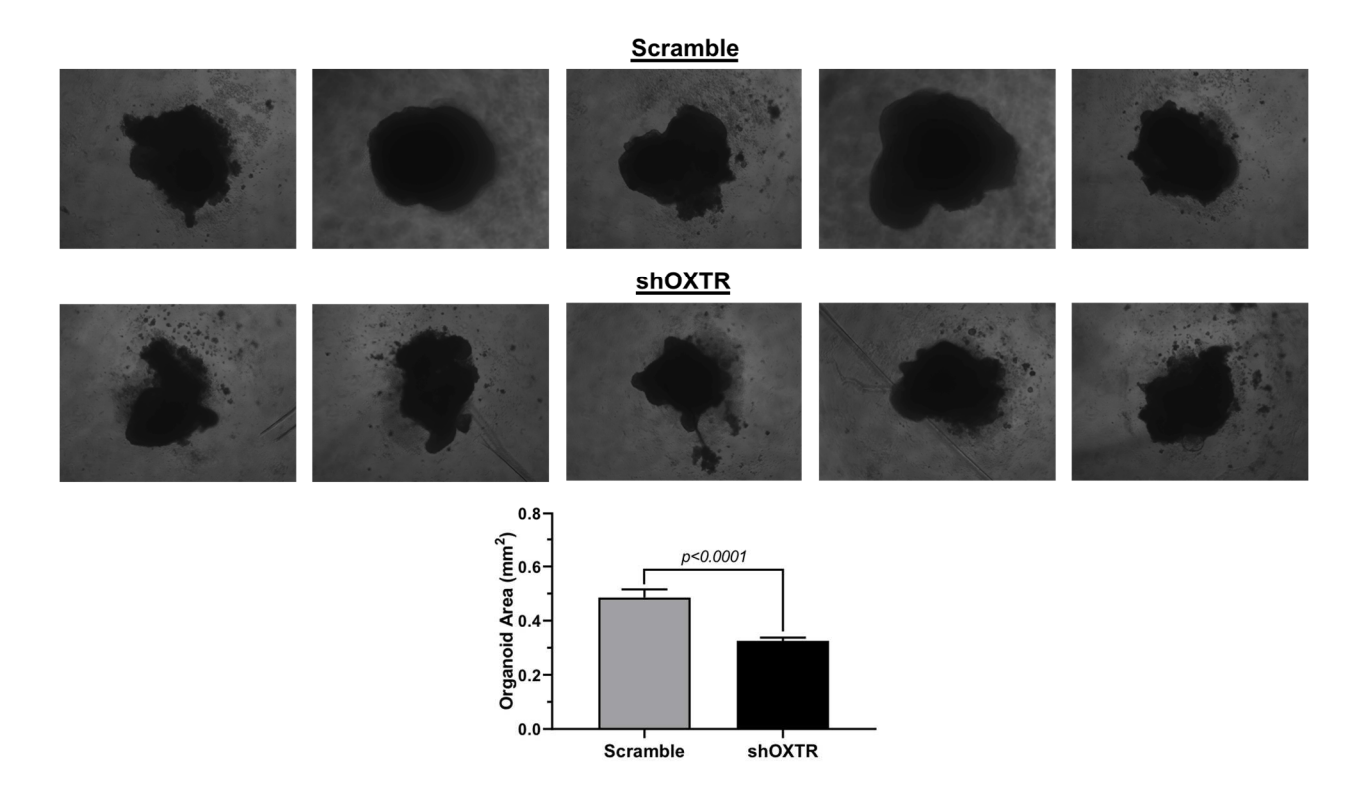


Figure 5.8: OXTR knockdown decreases hHO size. Brightfield images and quantification of scrambled and sh*OXTR* hHO area at Day 30 of differentiation; n=16 hHOs per cell line.

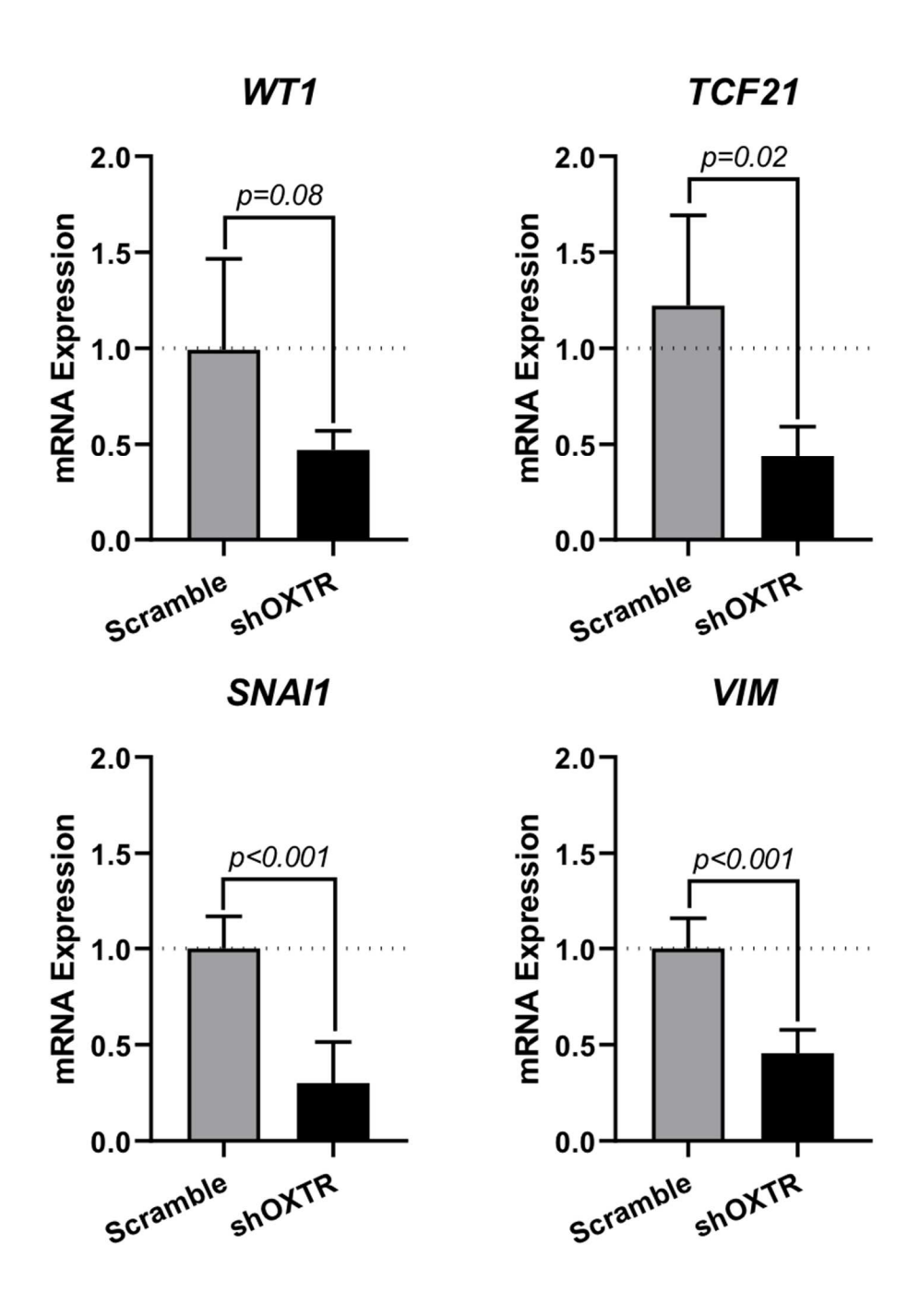


Figure 5.9: *OXTR* knockdown decreases epicardial activity after cryoinjury. qRT-PCR data for scrambled and shOXTR hHOs 3 days after cryoinjury, showing a decrease in epicardial (*WT1*, *TCF21*), EMT (*SNAI1*), and mesenchymal (*VIM*) markers when OXTR signaling is silenced; n=4-5 hHOs per cell line.

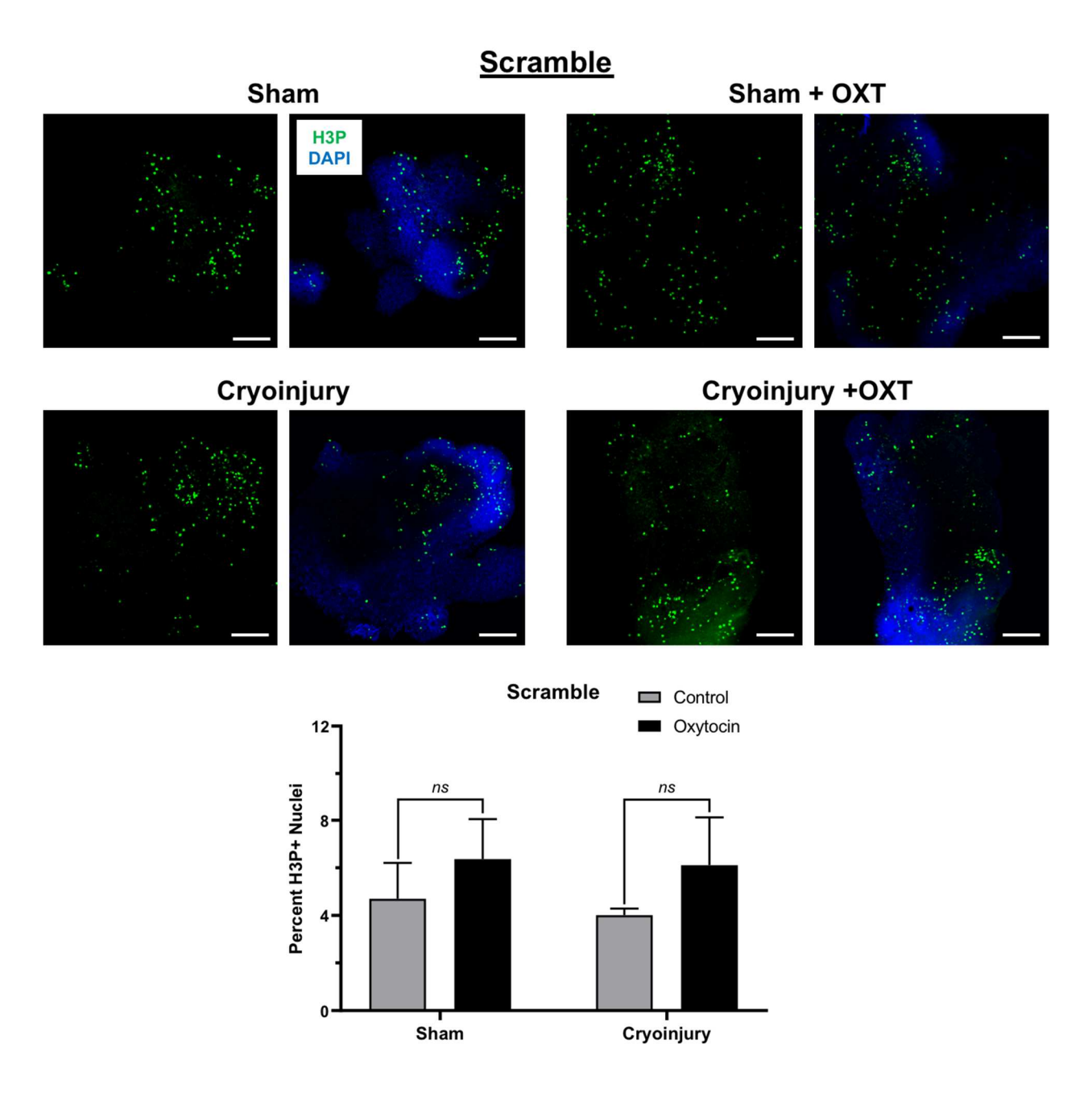


Figure 5.10: OXT induces modest cellular proliferation before OXTR knockdown. Confocal immunofluorescent images and quantification of cellular proliferation in scrambled hHOs in the presence and absence of OXT 3 days after cryoinjury or sham procedure. Proliferating cells are labeled with H3P (green), nuclei are labeled with DAPI (blue); n=3-4 hHOs per condition, scale bar: 200 μ m.

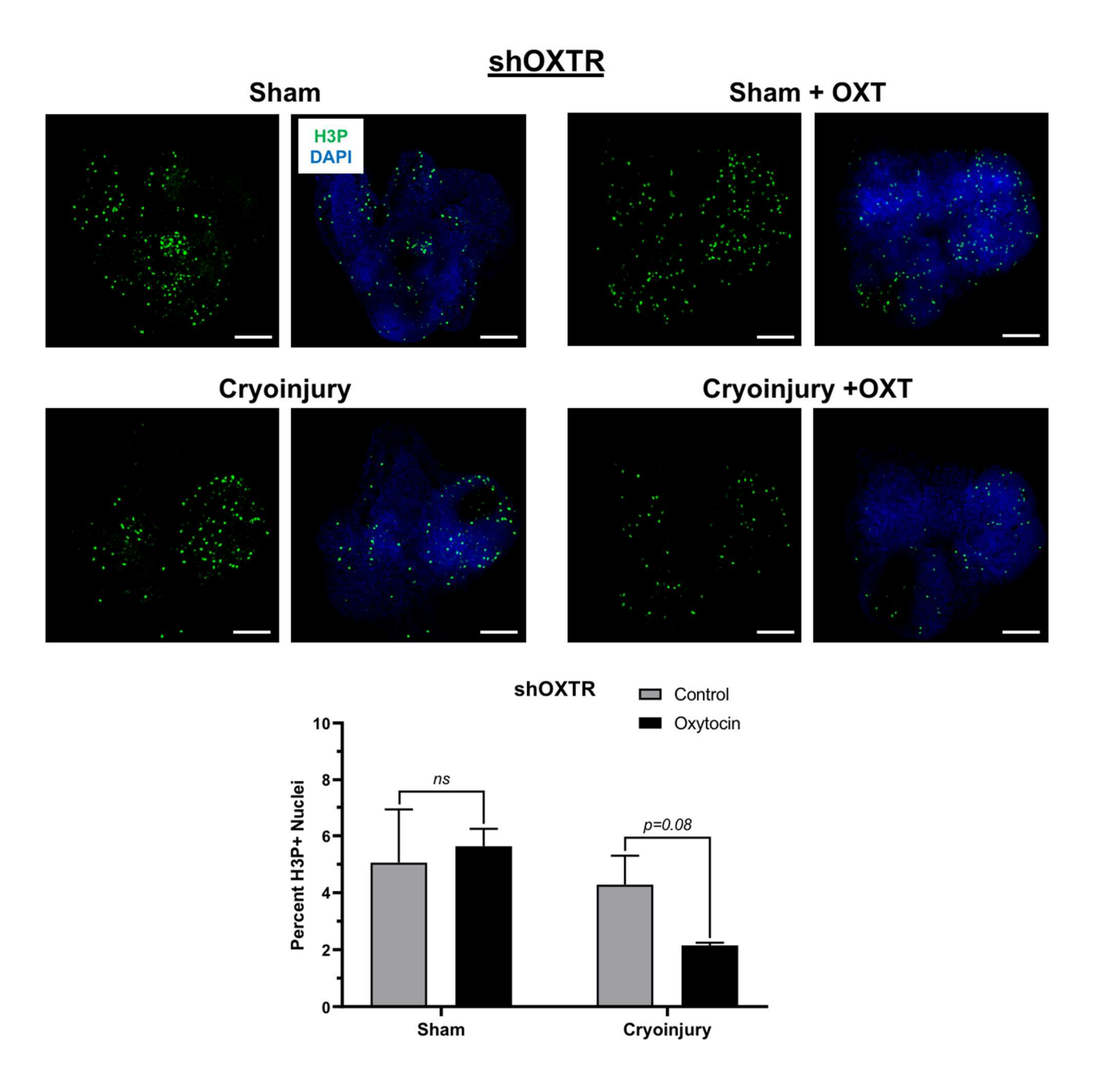


Figure 5.11: OXT does not induce cellular proliferation after OXTR knockdown. Confocal immunofluorescent images and quantification of cellular proliferation in shOXTR hHOs in the presence and absence of OXT 3 days after cryoinjury or sham procedure. Proliferating cells are labeled with H3P (green), nuclei are labeled with DAPI (blue); n=3-4 hHOs per condition, scale bar: 200 μ m.

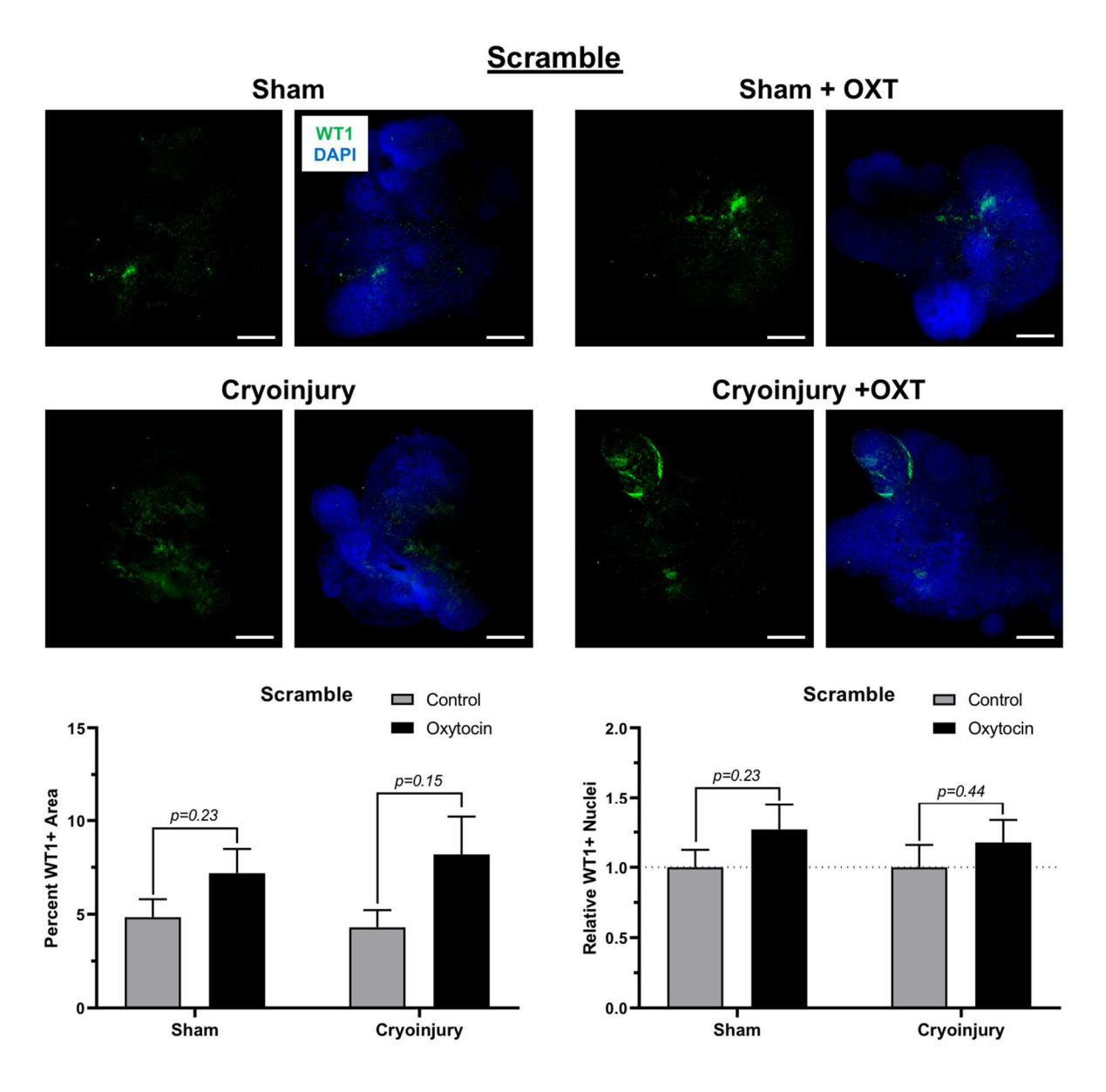


Figure 5.12: OXT induces modest epicardial activation before OXTR knockdown. Confocal immunofluorescent images and quantification of epicardial activation in scrambled hHOs in the presence and absence of OXT 3 days after cryoinjury or sham procedure. EpiPCs are labeled with WT1 (green), nuclei are labeled with DAPI (blue); n=3-12 hHOs per condition, scale bar: 200 μ m.

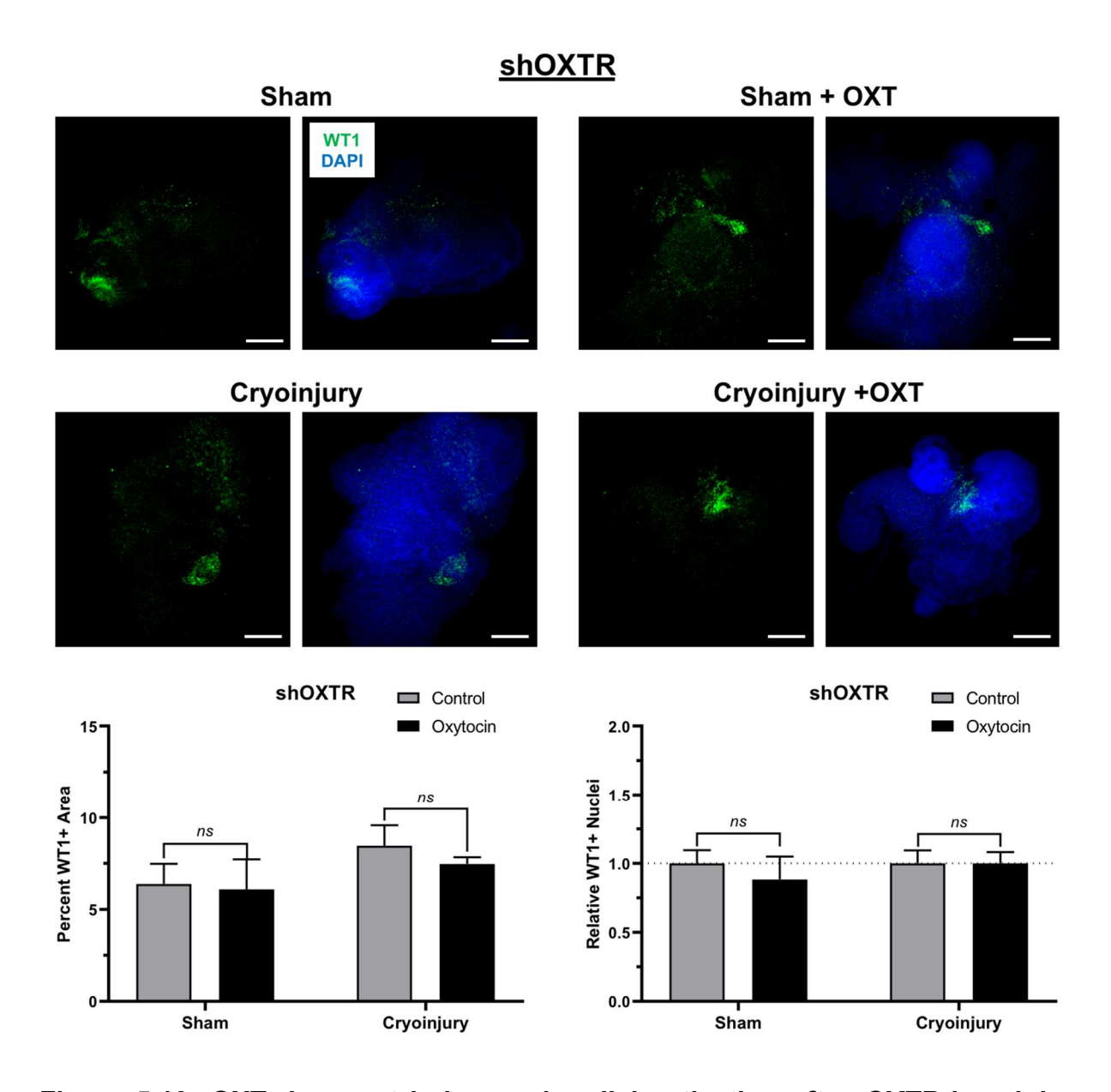


Figure 5.13: OXT does not induce epicardial activation after OXTR knockdown. Confocal immunofluorescent images and quantification of epicardial activation in shOXTR hHOs in the presence and absence of OXT 3 days after cryoinjury or sham procedure. EpiPCs are labeled with WT1 (green), nuclei are labeled with DAPI (blue); n=3-12 hHOs per condition, scale bar: 200 μ m.

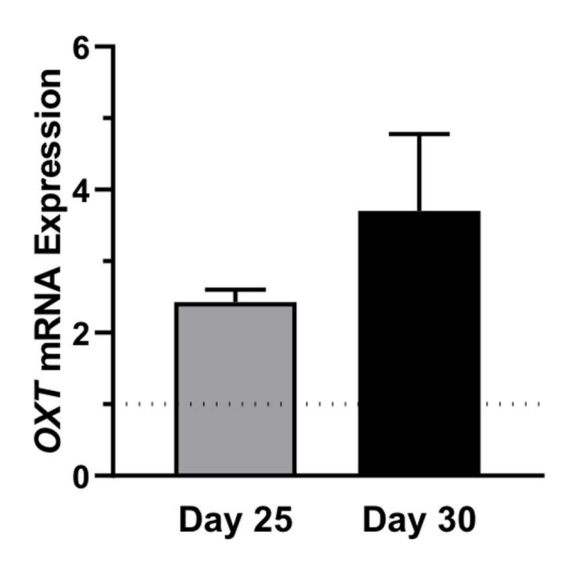


Figure 5.14: hHO maturation increases OXT production. qRT-PCR for *OXT* at Day 25 and 30 of hHO differentiation showing an increase in oxytocin expression as organoids mature. Dotted line indicates *OXT* expression at Day 19; n=2 hHOs per time point.

5.3: Discussion

Here, I have further expanded upon my previous findings from hEpiCs and zebrafish with a three-dimensional, human stem cell-derived model of the heart. I used these organoids to elucidate the importance of the epicardium to heart regeneration in a dish. First, I adapted and characterized a cryoinjury protocol and employed it as a myocardial infarction model in hHOs. Previous organoid injury methods utilized hypoxia chambers to induce oxygen diffusion gradients, thereby mimicking the infarct, border, and remote zones that develop after MI. While this was an elegant approach, it induced more of a global response, as exposing the hHOs to low oxygen levels affected the whole structure (Richards et al., 2020). Seeing as a typical human MI affects only up to ~25% of the myocardium (Laflamme & Murry, 2011), I decided that cryoinjury would be the best method to control the extent of damage to my organoids. As expected, I found that hHO cryoinjury caused a partial decrease in cell viability (Figures 5.3, 5.4). It appears that

these cells died off due to programmed cell death, as I observed a significant increase in GFP fluorescence after cryoinjury in an apoptosis reporter line (Figure 5.5). Once my cryoinjury model was characterized, I explored the effects of OXTR silencing in matured organoids. Knockdown hHOs were smaller, more fragile, and displayed less epicardial activity after cryoinjury (Figures 5.8, 5.9). Indeed, oxytocin is important for several aspects of human heart development such as cellular proliferation (Noiseux et al., 2012), cardiomyocyte differentiation (Danalache et al., 2007; Paquin et al., 2002), and angiogenesis (Cattaneo et al., 2009), so knockdown of its receptor should affect hHO development as well. Importantly, my cryoinjury model is the first that can be used to study the innate epicardial response to MI in vitro, as earlier cryoinjury protocols utilized hHOs that had no epicardium (Voges et al., 2017) or contained epicardial aggregates that were added exogenously after hHO formation (Hofbauer et al., 2021). Whereas injured and uninjured scrambled hHOs were able to respond to OXT administration with a modest increase in cellular proliferation and epicardial activation, these processes were prevented entirely in shOXTR hHOs (Figures 5.10-5.13). Clearly, organoids are unable to adopt a pro-regenerative phenotype when necessary if OXTR signaling is silenced.

5.4: Future Directions

While my results represent an exciting step towards studying epicardial regeneration *in vitro*, I acknowledge that these data are preliminary and have their limitations. My findings could surely benefit from larger sample sizes as well as additional experimentation. Specifically, histological stains could be used to document regeneration over time and qRT-PCR and immunofluorescence assays could be used to quantify the expression of more targets in more cell types in all my conditions. In addition, my data

suggests that hHOs produce their own oxytocin as differentiation proceeds (**Figure 5.14**), and inhibiting this endogenous production may allow me to more fully uncover the importance of OXT to the phenotypes described above. And conducting these types of studies in other three-dimensional systems could prove useful as well. Indeed, an organotypic model of the epicardium would allow me to document the activity specifically of EpiPCs after cardiac injury and in response to OXT administration. Interestingly, an ex *vivo* porcine tissue culture protocol has recently been developed to study epicardial cell dynamics in real time (Maselli et al., 2022). Ultimately though, the most translationally relevant model with which to prove that oxytocin induces epicardial activation during cardiac regeneration is a human-derived system. In this respect, hHOs offer great potential, as they are *bona fide*, three-dimensional, "miniature hearts" that will drive the field of pre-clinical cardiac research to heights it has never seen before.

Chapter 6: Conclusions and Perspectives

6.1: Main Findings

I originally set out to test my hypothesis that oxytocin is released from the hypothalamus after cardiac injury, leading to activation of epicardial stem cells and regeneration of damaged cardiac tissue. To do this, I took three approaches, each via the use of a different model system. First, I differentiated human induced pluripotent stem cells into two-dimensional epicardial cells and investigated the pro-regenerative phenotype that OXT has on these hEpiCs, and explored its mechanism of action. I then utilized zebrafish, a powerful naturally regenerating model organism, inhibited OXT signaling, and documented the subsequent effects on heart regeneration and epicardial activation. Finally, I brought all of my previous data together via the use of threedimensional, hiPSC-derived human heart organoids. I conducted many of the same experiments in hHOs that I had in hEpiCs and zebrafish to fully characterize the importance OXT has to epicardial regeneration in a model of the human heart. Overall, I found that of all the candidate neuroendocrine peptides tested, oxytocin had the strongest effect on the epicardium. Indeed, administration of this peptide to cardiac cells in vitro induced proliferation, EMT, and dedifferentiation to a progenitor-like state, thereby priming EpiPCs to assist with regeneration down the road. Conversely, inhibition of OXT signaling slowed heart regeneration in vivo, likely through effects on the epicardium. These processes appear to be mediated primarily through OXT binding to its receptor, as EpiPC activation is adversely affected after OXTR silencing in hEpiCs and cryoinjured organoids as well as pharmacological OXTR inhibition in zebrafish. Therefore, OXT treatment induces a pro-regenerative phenotype in vitro and its removal interferes with

heart regeneration *in vivo*. Remarkably, OXT levels increased after cardiac cryoinjury in zebrafish, with a corresponding increase seen in epicardial activity in the heart (Wasserman et al., 2022). Together, my data demonstrate that this release of oxytocin by the neuroendocrine system is critical for ensuring proper regeneration of the heart. For an overview of my proposed model, see **Figure 6.1**.

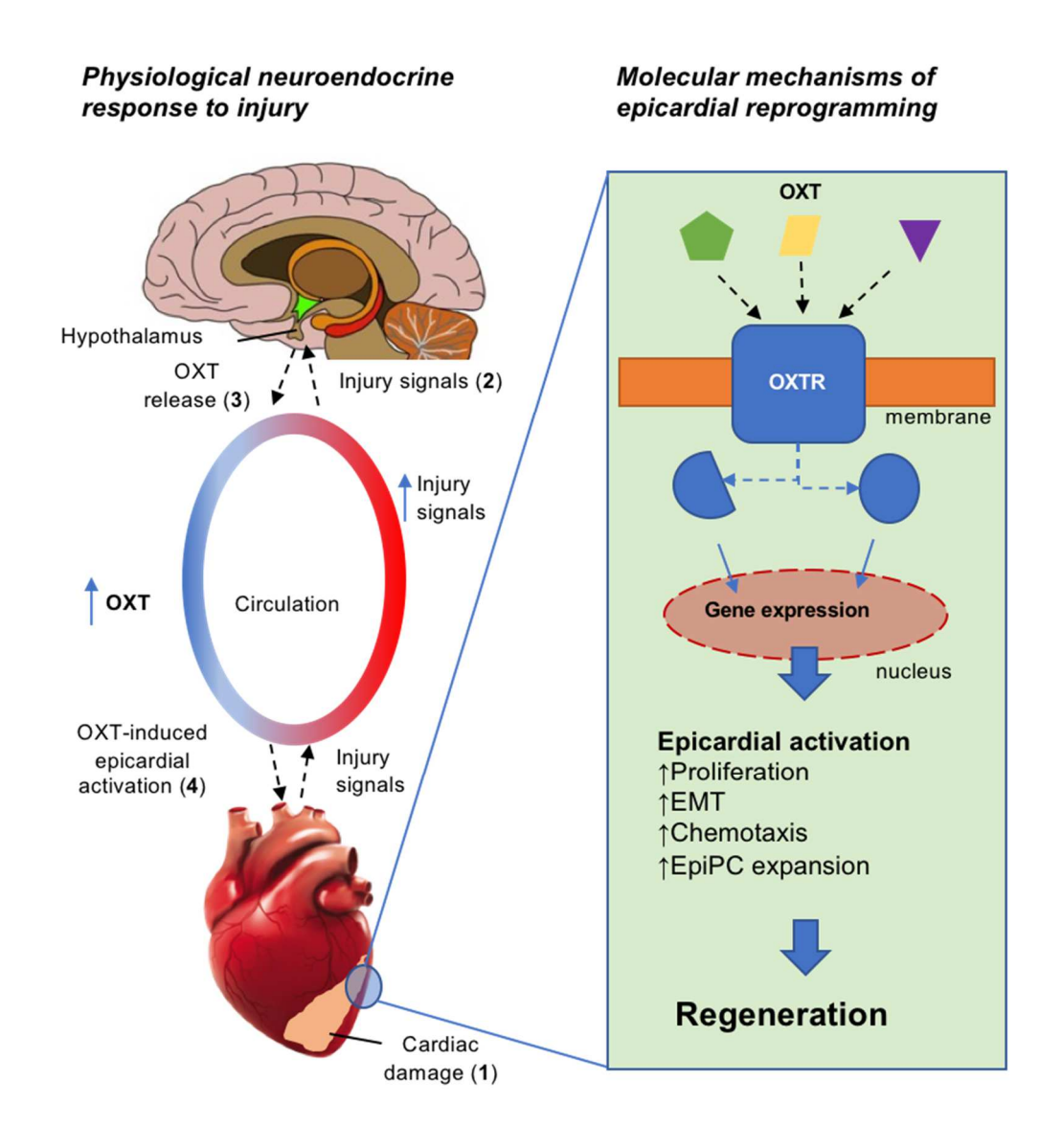


Figure 6.1: Proposed model for neuroendocrine reprogramming of the epicardium in heart regeneration. After injury, oxytocin released from the hypothalamus reaches the heart and triggers epicardial conversion into epicardial progenitor cells. Numbers in bold

Figure 6.1 (cont'd)

indicate order of events. The preliminary data in human epicardial cells, zebrafish, and human heart organoids presented here strongly support this hypothesis; EMT: Epithelial-to-Mesenchymal Transition, EpiPC: Epicardium-Derived Progenitor Cell, OXT: Oxytocin, OXTR: Oxytocin Receptor.

6.2: Limitations

Although the results of my studies are novel and intriguing on their own, there are always ways to improve and build upon solid data. At its core, the foundations upon which this project rests are human stem cells and zebrafish. The next logical step with which to further expand my findings would be mice. Although mice have limited cardiac regenerative capacity, rodent models are a commonly-used, translationally relevant system to study the innate mammalian response to heart disease. Conducting cardiac injuries in mice and administering oxytocin immediately after would be an effective means of testing my hypothesis in vivo. Several injury models exist in rodents that can be used to simulate acute myocardial infarction, many of which are surgical in nature. One simpler approach is a chemically-induced injury through the use of isoproterenol (isoprenaline), a β-adrenergic receptor agonist and analog of epinephrine. In fact, several studies have shown that subcutaneous injections of isoproterenol can induce an infarct-like myocardial injury, complete with fibrosis accumulation, cellular hypertrophy, and impaired cardiac function (Brooks & Conrad, 2009; Grimm et al., 1998). Clearly, utilizing this system could prove beneficial to my research. With that said, my use of hHOs has provided me with a three-dimensional, human derived model of the heart with which to conduct my studies (discussed at length in Chapter 5). Overall, these hHO data should complement any data obtained from rodent injury models quite nicely, and could be used to tell an impactful scientific story in the future. One more piece of the puzzle that this project has overlooked

to this point is the initial cause of oxytocin release from the hypothalamus. It is likely that after injury, pro-regenerative signals are released from the heart and travel to the brain to instruct it to produce more OXT. These factors could include immune cells and cytokines, hormones, or other endocrine molecules. Further elucidation of the nature of these signals would go a long way towards helping to paint a more complete picture covering all the steps involved in OXT-induced epicardial regeneration.

6.3: Significance and Broader Implications

Here, I demonstrate for the first time a neuroendocrine-mediated mechanism that induces epicardial activation and regeneration after heart injury. I have shown that oxytocin is a critical brain-derived hormone that can "prime" these processes and make them more efficient, both in human stem-cell derived cardiac cells and in a naturally regenerating animal model. I concede it is unlikely that OXT is the sole regulator of epicardial activation, as it is likely part of much larger physiological systems that the brain and heart utilize to maintain homeostasis after cardiac injury. At its core, heart regeneration occurs through a complex, coordinated set of steps that involve release of numerous hormones, peptides, and other factors and manipulation of several signaling cascades (Laflamme & Murry, 2011; Sadek & Olson, 2020; Vujic et al., 2020). While OXT is undoubtedly an essential part of this process, regeneration ultimately depends upon the synergistic effects of OXT signaling acting in conjunction with other pathways. Regardless, the results I have presented here will prove highly innovative and significant to the cardiac research field. I have provided novel evidence to support the notion that cardiac regeneration is under central hormonal control. Specifically, I established a previously uncharacterized causative mechanism where OXT, a hormone best-known for

its roles outside of the cardiovascular system, is released after cardiac injury and facilitates regeneration. To accomplish this goal, I utilized cutting edge techniques and methodologies, such as human iPSC culture, three-dimensional human heart organoid models, zebrafish cardiac cryoinjury, transgenic animals, RNA interference, and innovative imaging tools to investigate cellular reprogramming processes. I feel that ultimately, my findings will prove important and relevant to the treatment of human cardiovascular disease. They present exciting drug discovery opportunities surrounding OXT and other clinically available analogs that can aid in the recovery from cardiac injuries and prevent progression to heart failure. In addition, my research lays the foundation for new therapeutic approaches for the treatment of CVD via reprogramming of endogenous epicardial cells to functional cardiomyocytes without a need for stem cell therapy or organ transplant. Together, these advances will lead to an increase in both average lifespan and health span in the U.S. and worldwide.

REFERENCES

- Acharya, A., Baek, S. T., Huang, G., Eskiocak, B., Goetsch, S., Sung, C. Y., Banfi, S., Sauer, M. F., Olsen, G. S., Duffield, J. S., Olson, E. N., & Tallquist, M. D. (2012). The bHLH transcription factor Tcf21 is required for lineage-specific EMT of cardiac fibroblast progenitors. *Development*, 139(12), 2139–2149. https://doi.org/10.1242/dev.079970
- Aguirre, A., Montserrat, N., Zacchigna, S., Nivet, E., Hishida, T., Krause, M. N., Kurian, L., Ocampo, A., Vazquez-Ferrer, E., Rodriguez-Esteban, C., Kumar, S., Moresco, J. J., Yates, J. R., Campistol, J. M., Sancho-Martinez, I., Giacca, M., & Izpisua Belmonte, J. C. (2014). In vivo activation of a conserved microRNA program induces mammalian heart regeneration. *Cell Stem Cell*, *15*(5), 589–604. https://doi.org/10.1016/j.stem.2014.10.003
- Aleström, P., D'Angelo, L., Midtlyng, P. J., Schorderet, D. F., Schulte-Merker, S., Sohm, F., & Warner, S. (2020). Zebrafish: Housing and husbandry recommendations. *Laboratory Animals*, *54*(3), 213–224. https://doi.org/10.1177/0023677219869037
- Amram, A. V., Cutie, S., & Huang, G. N. (2021). Hormonal control of cardiac regenerative potential. *Endocrine Connections*, *10*(1), R25–R35. https://doi.org/10.1530/EC-20-0503
- Andersen, D. C., Ganesalingam, S., Jensen, C. H., & Sheikh, S. P. (2014). Do neonatal mouse hearts regenerate following heart apex resection? *Stem Cell Reports*, *2*(4), 406–413. https://doi.org/10.1016/j.stemcr.2014.02.008
- Andrés-Delgado, L., & Mercader, N. (2016). Interplay between cardiac function and heart development. *Biochimica et Biophysica Acta*, *1863*(7), 1707–1716. https://doi.org/10.1016/j.bbamcr.2016.03.004
- Argiolas, A., & Gessa, G. L. (1991). Central functions of oxytocin. *Neuroscience and Biobehavioral Reviews*, *15*(2), 217–231. https://doi.org/10.1016/S0149-7634(05)80002-8
- Bao, X., Lian, X., Hacker, T. A., Schmuck, E. G., Qian, T., Bhute, V. J., Han, T., Shi, M., Drowley, L., Plowright, A. T., Wang, Q. D., Goumans, M. J., & Palecek, S. P. (2016). Long-term self-renewing human epicardial cells generated from pluripotent stem cells under defined xeno-free conditions. *Nature Biomedical Engineering*, 1, 1–12. https://doi.org/10.1038/s41551-016-0003
- Bao, X., Lian, X., Qian, T., Bhute, V. J., Han, T., & Palecek, S. P. (2017). Directed differentiation and long-term maintenance of epicardial cells derived from human pluripotent stem cells under fully defined conditions. *Nature Protocols*, *12*(9), 1890–1900. https://doi.org/10.1038/nprot.2017.080

- Barrallo-Gimeno, A., & Nieto, M. A. (2005). The Snail genes as inducers of cell movement and survival: Implications in development and cancer. *Development*, 132(14), 3151–3161. https://doi.org/10.1242/dev.01907
- Bax, N. A. M., Van Oorschot, A. A. M., Maas, S., Braun, J., Van Tuyn, J., De Vries, A. A. F., Gittenberger-De Groot, A. C., & Goumans, M. J. (2011). In vitro epithelial-to-mesenchymal transformation in human adult epicardial cells is regulated by TGFβ-signaling and WT1. Basic Research in Cardiology, 106(5), 829–847. https://doi.org/10.1007/s00395-011-0181-0
- Becker, R. O., Chapin, S., & Sherry, R. (1974). Regeneration of the ventricular myocardium in amphibians. *Nature*, *248*(5444), 145–147. https://doi.org/10.1038/248145a0
- Beffagna, G. (2019). Zebrafish as a Smart Model to Understand Regeneration After Heart Injury: How Fish Could Help Humans. *Frontiers in Cardiovascular Medicine*, 6(August), 1–8. https://doi.org/10.3389/fcvm.2019.00107
- Bellin, M., Marchetto, M. C., Gage, F. H., & Mummery, C. L. (2012). Induced pluripotent stem cells: The new patient? *Nature Reviews Molecular Cell Biology*, *13*(11), 713–726. https://doi.org/10.1038/nrm3448
- Bergmann, O., Bhardwaj, R. D., Bernard, S., Zdunek, S., Barnabé-Heider, F., Walsh, S., Zupicich, J., Alkass, K., Buchholz, B. A., Druid, H., Jovinge, S., & Frisén, J. (2009). Evidence for Cardiomyocyte Renewal in Humans. *Science*, *324*(5923), 98–102. https://doi.org/10.1126/science.1164680
- Bergmann, O., Zdunek, S., Felker, A., Salehpour, M., Alkass, K., Bernard, S., Sjostrom, S. L., Szewczykowska, M., Jackowska, T., Dos Remedios, C., Malm, T., Andrä, M., Jashari, R., Nyengaard, J. R., Possnert, G., Jovinge, S., Druid, H., & Frisén, J. (2015). Dynamics of Cell Generation and Turnover in the Human Heart. *Cell*, 161(7), 1566–1575. https://doi.org/10.1016/j.cell.2015.05.026
- Bienboire-Frosini, C., Chabaud, C., Cozzi, A., Codecasa, E., & Pageat, P. (2017). Validation of a commercially available enzyme immunoassay for the determination of oxytocin in plasma samples from seven domestic animal species. *Frontiers in Neuroscience*, *11*, 1–16. https://doi.org/10.3389/fnins.2017.00524
- Bise, T., & Jaźwińska, A. (2019). Intrathoracic injection for the study of adult zebrafish heart. *Journal of Visualized Experiments*, *147*, 1–10. https://doi.org/10.3791/59724
- Bise, T., Sallin, P., Pfefferli, C., & Jaźwińska, A. (2020). Multiple cryoinjuries modulate the efficiency of zebrafish heart regeneration. *Scientific Reports*, *10*, 1–15. https://doi.org/10.1038/s41598-020-68200-1
- Braitsch, C. M., & Yutzey, K. E. (2013). Transcriptional control of cell lineage

- development in epicardium-derived cells. *Journal of Developmental Biology*, *1*(2), 92–111. https://doi.org/10.3390/jdb1020092
- Brooks, W. W., & Conrad, C. H. (2009). Isoproterenol-induced myocardial injury and diastolic dysfunction in mice: Structural and functional correlates. *Comparative Medicine*, *59*(4), 339–343.
- Cai, C.-L., Martin, J. C., Sun, Y., Cui, L., Wang, L., Ouyang, J., Yang, L., Bu, L., Xingqun, L., Zhang, X., Stallcup, W. B., Denton, C. P., McCulloch, A., Chen, J., & Evans, S. M. (2008). A myocardial lineage derives from Tbx18 epicardial cells. *Nature*, *454*(7200), 104–108. https://doi.org/10.1038/nature06969.A
- Cai, W., Tan, J., Yan, J., Zhang, L., Cai, X., Wang, H., Liu, F., Ye, M., & Cai, C. L. (2019). Limited Regeneration Potential with Minimal Epicardial Progenitor Conversions in the Neonatal Mouse Heart after Injury. *Cell Reports*, *28*(1), 190–201. https://doi.org/10.1016/j.celrep.2019.06.003
- Cao, J., Navis, A., Cox, B. D., Dickson, A. L., Gemberling, M., Karra, R., Bagnat, M., & Poss, K. D. (2016). Single epicardial cell transcriptome sequencing identifies caveolin 1 as an essential factor in zebrafish heart regeneration. *Development*, 143, 232–243. https://doi.org/10.1242/dev.130534
- Cao, J., & Poss, K. D. (2018). The epicardium as a hub for heart regeneration. *Nature Reviews Cardiology*, *15*(10), 631–647. https://doi.org/10.1038/s41569-018-0046-4
- Cao, N., Liu, Z., Chen, Z., Wang, J., Chen, T., Zhao, X., Ma, Y., Qin, L., Kang, J., Wei, B., Wang, L., Jin, Y., & Yang, H. T. (2012). Ascorbic acid enhances the cardiac differentiation of induced pluripotent stem cells through promoting the proliferation of cardiac progenitor cells. *Cell Research*, 22(1), 219–236. https://doi.org/10.1038/cr.2011.195
- Carmona, R., Guadix, J. A., Cano, E., Ruiz-Villalba, A., Portillo-Sánchez, V., Pérez-Pomares, J. M., & Muñoz-Chápuli, R. (2010). The embryonic epicardium: An essential element of cardiac development. *Journal of Cellular and Molecular Medicine*, *14*(8), 2066–2072. https://doi.org/10.1111/j.1582-4934.2010.01088.x
- Carvalho, A. B., & Campos de Carvalho, A. C. (2010). Heart regeneration: Past, present and future. *World Journal of Cardiology*, 2(5), 107–111. https://doi.org/10.4330/wjc.v2.i5.107
- Cattaneo, M. G., Lucci, G., & Vicentini, L. M. (2009). Oxytocin stimulates in vitro angiogenesis via a Pyk-2/Src-dependent mechanism. *Experimental Cell Research*, 315(18), 3210–3219. https://doi.org/10.1016/j.yexcr.2009.06.022
- Chablais, F., & Jaźwińska, A. (2012). The regenerative capacity of the zebrafish heart is dependent on TGFβ signaling. *Development*, *139*(11), 1921–1930.

- https://doi.org/10.1242/dev.078543
- Chablais, F., Veit, J., Rainer, G., & Jawiska, A. (2011). The zebrafish heart regenerates after cryoinjury-induced myocardial infarction. *BMC Developmental Biology*, *11*(21), 1–13. https://doi.org/10.1186/1471-213X-11-21
- Cho, J., Lee, H., Rah, W., Chang, H. J., & Yoon, Y. (2022). From engineered heart tissue to cardiac organoid. *Theranostics*, *12*(6), 2758–2772. https://doi.org/10.7150/thno.67661
- Christoffels, V. M., Grieskamp, T., Norden, J., Mommersteeg, M. T. M., Rudat, C., & Kispert, A. (2009). Tbx18 and the fate of epicardial progenitors. *Nature*, *458*(7240), E8–E10. https://doi.org/10.1038/nature07916
- Clevers, H. (2016). Modeling Development and Disease with Organoids. *Cell*, *165*(7), 1586–1597. https://doi.org/10.1016/j.cell.2016.05.082
- Corrò, C., Novellasdemunt, L., & Li, V. S. W. (2020). A brief history of organoids. *American Journal of Physiology - Cell Physiology*, *319*(1), C151–C165. https://doi.org/10.1152/ajpcell.00120.2020
- Cramer, J. A. (2002). Effect of partial compliance on cardiovascular medication effectiveness. *Heart*, 88(2), 203–206. https://doi.org/10.1136/heart.88.2.203
- Crane, A. M., Kramer, P., Bui, J. H., Chung, W. J., Li, X. S., Gonzalez-Garay, M. L., Hawkins, F., Liao, W., Mora, D., Choi, S., Wang, J., Sun, H. C., Paschon, D. E., Guschin, D. Y., Gregory, P. D., Kotton, D. N., Holmes, M. C., Sorscher, E. J., & Davis, B. R. (2015). Targeted correction and restored function of the CFTR gene in cystic fibrosis induced pluripotent stem cells. *Stem Cell Reports*, *4*(4), 569–577. https://doi.org/10.1016/j.stemcr.2015.02.005
- Curado, S., Anderson, R. M., Jungblut, B., Mumm, J., Schroeter, E., & Stainier, D. Y. R. (2007). Conditional targeted cell ablation in zebrafish: A new tool for regeneration studies. *Developmental Dynamics*, *236*(4), 1025–1035. https://doi.org/10.1002/dvdy.21100
- Curado, S., Stainier, D. Y. R., & Anderson, R. M. (2008). Nitroreductase-mediated cell/tissue ablation in zebrafish: A spatially and temporally controlled ablation method with applications in developmental and regeneration studies. *Nature Protocols*, *3*(6), 948–954. https://doi.org/10.1038/nprot.2008.58
- Dale, H. H. (1906). On some physiological actions of ergot. *The Journal of Physiology*, 34(3), 163–206. https://doi.org/10.1113/jphysiol.1906.sp001148
- Dampney, R. A. L. (2016). Central neural control of the cardiovascular system: Current perspectives. *Advances in Physiology Education*, *40*(3), 283–296.

- https://doi.org/10.1152/advan.00027.2016
- Danalache, B. A., Paquin, J., Donghao, W., Grygorczyk, R., Moore, J. C., Mummery, C. L., Gutkowska, J., & Jankowski, M. (2007). Nitric Oxide Signaling in Oxytocin-Mediated Cardiomyogenesis. *Stem Cells*, *25*(3), 679–688. https://doi.org/10.1634/stemcells.2005-0610
- Deinsberger, J., Reisinger, D., & Weber, B. (2020). Global trends in clinical trials involving pluripotent stem cells: a systematic multi-database analysis. *NPJ Regenerative Medicine*, *5*, 1–13. https://doi.org/10.1038/s41536-020-00100-4
- Dergilev, K. V., Tsokolaeva, Z. I., Beloglazova, I. B., Ratner, E. I., & Parfenova, E. V. (2021). Transforming Growth Factor Beta (TGF-β1) Induces Pro-Reparative Phenotypic Changes in Epicardial Cells in Mice. *Bulletin of Experimental Biology and Medicine*, *170*(4), 565–570. https://doi.org/10.1007/s10517-021-05107-5
- Derks, W., & Bergmann, O. (2020). Polyploidy in cardiomyocytes: Roadblock to heart regeneration? *Circulation Research*, *126*(4), 552–565. https://doi.org/10.1161/CIRCRESAHA.119.315408
- Drakhlis, L., Biswanath, S., Farr, C.-M., Lupanow, V., Teske, J., Ritzenhoff, K., Franke, A., Manstein, F., Bolesani, E., Kempf, H., Liebscher, S., Schenke-Layland, K., Hegermann, J., Nolte, L., Meyer, H., de la Roche, J., Thiemann, S., Wahl-Schott, C., Martin, U., & Zweigerdt, R. (2021). Human heart-forming organoids recapitulate early heart and foregut development. *Nature Biotechnology*, *39*(6), 737–746. https://doi.org/10.1038/s41587-021-00815-9
- Dronkers, E., Wauters, M. M. M., Goumans, M. J., & Smits, A. M. (2020). Epicardial TGFβ and BMP signaling in cardiac regeneration: What lesson can we learn from the developing heart? *Biomolecules*, *10*(3), 1–25. https://doi.org/10.3390/biom10030404
- Du Vigneaud, V., Ressler, C., & Trippett, S. (1953). The sequence of amino acids in oxytocin, with a proposal for the structure of oxytocin. *The Journal of Biological Chemistry*, 205(2), 949–957. https://doi.org/10.1016/s0021-9258(18)49238-1
- Dyavanapalli, J., Rodriguez, J., Rocha dos Santos, C., Escobar, J. B., Dwyer, M. K., Schloen, J., Lee, K. min, Wolaver, W., Wang, X., Dergacheva, O., Michelini, L. C., Schunke, K. J., Spurney, C. F., Kay, M. W., & Mendelowitz, D. (2020). Activation of Oxytocin Neurons Improves Cardiac Function in a Pressure-Overload Model of Heart Failure. *JACC: Basic to Translational Science*, 5(5), 484–497. https://doi.org/10.1016/j.jacbts.2020.03.007
- El-Sammak, H., Yang, B., Guenther, S., Chen, W., Marín-Juez, R., & Stainier, D. Y. R. (2022). A Vegfc-Emilin2a-Cxcl8a Signaling Axis Required for Zebrafish Cardiac Regeneration. *Circulation Research*, *130*(7), 1014–1029.

- https://doi.org/10.1161/CIRCRESAHA.121.319929
- Eroglu, E., Yen, C. Y. T., Tsoi, Y. L., Witman, N., Elewa, A., Joven Araus, A., Wang, H., Szattler, T., Umeano, C. H., Sohlmér, J., Goedel, A., Simon, A., & Chien, K. R. (2022). Epicardium-derived cells organize through tight junctions to replenish cardiac muscle in salamanders. *Nature Cell Biology*, *24*(5), 645–658. https://doi.org/10.1038/s41556-022-00902-2
- Fan, D., Takawale, A., Lee, J., & Kassiri, Z. (2012). Cardiac fibroblasts, fibrosis and extracellular matrix remodeling in heart disease. *Fibrogenesis & Tissue Repair*, *5*, 1–13. https://doi.org/10.1186/1755-1536-5-15
- Favaretto, A. L. V., Ballejo, G. O., Albuquerque-Araújo, W. I. C., Gutkowska, J., Antunes-Rodrigues, J., & McCann, S. M. (1997). Oxytocin releases atrial natriuretic peptide from rat atria in vitro that exerts negative inotropic and chronotropic action. *Peptides*, *18*(9), 1377–1381. https://doi.org/10.1016/S0196-9781(97)00209-X
- Filosa, A., & Sawamiphak, S. (2021). Heart development and regeneration-a multiorgan effort. *The FEBS Journal*, 1–18. https://doi.org/10.1111/febs.16319
- Frantz, M. C., Pellissier, L. P., Pflimlin, E., Loison, S., Gandiá, J., Marsol, C., Durroux, T., Mouillac, B., Becker, J. A. J., Le Merrer, J., Valencia, C., Villa, P., Bonnet, D., & Hibert, M. (2018). LIT-001, the First Nonpeptide Oxytocin Receptor Agonist that Improves Social Interaction in a Mouse Model of Autism. *Journal of Medicinal Chemistry*, *61*(19), 8670–8692. https://doi.org/10.1021/acs.jmedchem.8b00697
- Fujisawa, K., Hara, K., Takami, T., Okada, S., Matsumoto, T., Yamamoto, N., & Sakaida, I. (2018). Evaluation of the effects of ascorbic acid on metabolism of human mesenchymal stem cells. *Stem Cell Research and Therapy*, 9(1), 1–12. https://doi.org/10.1186/s13287-018-0825-1
- Garrott, K., Dyavanapalli, J., Cauley, E., Dwyer, M. K., Kuzmiak-Glancy, S., Wang, X., Mendelowitz, D., & Kay, M. W. (2017). Chronic activation of hypothalamic oxytocin neurons improves cardiac function during left ventricular hypertrophy-induced heart failure. *Cardiovascular Research*, *113*(11), 1318–1328. https://doi.org/10.1093/cvr/cvx084
- Gimpl, G., & Fahrenholz, F. (2001). The oxytocin receptor system: Structure, function, and regulation. *Physiological Reviews*, *81*(2), 629–683. https://doi.org/10.1152/physrev.2001.81.2.629
- Gnanadesikan, G. E., Hammock, E. A. D., Tecot, S. R., Carter, C. S., & MacLean, E. L. (2021). Specificity of plasma oxytocin immunoassays: A comparison of commercial assays and sample preparation techniques using oxytocin knockout and wildtype mice. *Psychoneuroendocrinology*, *132*, 1–9. https://doi.org/10.1016/j.psyneuen.2021.105368

- Gonzalez-Reyes, A., Menaouar, A., Yip, D., Danalache, B., Plante, E., Noiseux, N., Gutkowska, J., & Jankowski, M. (2015). Molecular mechanisms underlying oxytocin-induced cardiomyocyte protection from simulated ischemia-reperfusion. *Molecular and Cellular Endocrinology*, *412*, 170–181. https://doi.org/10.1016/j.mce.2015.04.028
- González-Rosa, J. M., Burns, C. E., & Burns, C. G. (2017). Zebrafish heart regeneration: 15 years of discoveries. *Regeneration*, *4*(3), 105–123. https://doi.org/10.1002/reg2.83
- González-Rosa, J. M., Martín, V., Peralta, M., Torres, M., & Mercader, N. (2011). Extensive scar formation and regression during heart regeneration after cryoinjury in zebrafish. *Development*, *138*(9), 1663–1674. https://doi.org/10.1242/dev.060897
- González-Rosa, J. M., & Mercader, N. (2012). Cryoinjury as a myocardial infarction model for the study of cardiac regeneration in the zebrafish. *Nature Protocols*, 7(4), 782–788. https://doi.org/10.1038/nprot.2012.025
- González-Rosa, J. M., Peralta, M., & Mercader, N. (2012). Pan-epicardial lineage tracing reveals that epicardium derived cells give rise to myofibroblasts and perivascular cells during zebrafish heart regeneration. *Developmental Biology*, 370(2), 173–186. https://doi.org/10.1016/j.ydbio.2012.07.007
- Gordan, R., Gwathmey, J. K., & Xie, L.-H. (2015). Autonomic and endocrine control of cardiovascular function. *World Journal of Cardiology*, 7(4), 204–214. https://doi.org/10.4330/wjc.v7.i4.204
- Grimm, D., Elsner, D., Schunkert, H., Pfeifer, M., Griese, D., Bruckschlegel, G., Muders, F., Riegger, G. A. J., & Kromer, E. P. (1998). Development of heart failure following isoproterenol administration in the rat: role of the renin-angiotensin system. *Cardiovascular Research*, *37*(1), 91–100. https://doi.org/10.1016/S0008-6363(97)00212-5
- Guadix, J. A., Orlova, V. V., Giacomelli, E., Bellin, M., Ribeiro, M. C., Mummery, C. L., Pérez-Pomares, J. M., & Passier, R. (2017). Human Pluripotent Stem Cell Differentiation into Functional Epicardial Progenitor Cells. *Stem Cell Reports*, *9*(6), 1754–1764. https://doi.org/10.1016/j.stemcr.2017.10.023
- Gulliver, D., Werry, E., Reekie, T. A., Katte, T. A., Jorgensen, W., & Kassiou, M. (2019). Targeting the Oxytocin System: New Pharmacotherapeutic Approaches. *Trends in Pharmacological Sciences*, *40*(1), 22–37. https://doi.org/10.1016/j.tips.2018.11.001
- Gutkowska, J., & Jankowski, M. (2012). Oxytocin Revisited: Its Role in Cardiovascular Regulation. *Journal of Neuroendocrinology*, *24*(4), 599–608. https://doi.org/10.1111/j.1365-2826.2011.02235.x

- Gutkowska, J., Jankowski, M., & Antunes-Rodrigues, J. (2014). The role of oxytocin in cardiovascular regulation. *Brazilian Journal of Medical and Biological Research*, 47(3), 206–214. https://doi.org/10.1590/1414-431X20133309
- Gutkowska, J., Jankowski, M., Mukaddam-Daher, S., & McCann, S. M. (2000). Oxytocin is a cardiovascular hormone. *Brazilian Journal of Medical and Biological Research*, 33(6), 625–633. https://doi.org/10.1590/S0100-879X2000000600003
- Gutkowska, Jolanta, Jankowski, M., Lambert, C., Mukaddam-Daher, S., Zingg, H. H., & McCann, S. M. (1997). Oxytocin releases atrial natriuretic peptide by combining with oxytocin receptors in the heart. *Proceedings of the National Academy of Sciences of the United States of America*, *94*(21), 11704–11709. https://doi.org/10.1073/pnas.94.21.11704
- Guyenet, P. G., & Bayliss, D. A. (2015). Neural Control of Breathing and CO2 Homeostasis. *Neuron*, 87(5), 946–961. https://doi.org/10.1016/j.neuron.2015.08.001
- Heidenreich, P. A., Trogdon, J. G., Khavjou, O. A., Butler, J., Dracup, K., Ezekowitz, M. D., Finkelstein, E. A., Hong, Y., Johnston, S. C., Khera, A., Lloyd-Jones, D. M., Nelson, S. A., Nichol, G., Orenstein, D., Wilson, P. W. F., & Woo, Y. J. (2011). Forecasting the future of cardiovascular disease in the United States: A policy statement from the American Heart Association. *Circulation*, *123*(8), 933–944. https://doi.org/10.1161/CIR.0b013e31820a55f5
- Heusch, G. (2020). Myocardial ischaemia–reperfusion injury and cardioprotection in perspective. *Nature Reviews Cardiology*, *17*(12), 773–789. https://doi.org/10.1038/s41569-020-0403-v
- Hilfiger, L., Zhao, Q., Kerspern, D., Inquimbert, P., Andry, V., Goumon, Y., Darbon, P., Hibert, M., & Charlet, A. (2020). A Nonpeptide Oxytocin Receptor Agonist for a Durable Relief of Inflammatory Pain. *Scientific Reports*, 10(1), 1–10. https://doi.org/10.1038/s41598-020-59929-w
- Hinderer, S., & Schenke-Layland, K. (2019). Cardiac fibrosis A short review of causes and therapeutic strategies. *Advanced Drug Delivery Reviews*, *146*, 77–82. https://doi.org/10.1016/j.addr.2019.05.011
- Hirose, K., Payumo, A. Y., Cutie, S., Hoang, A., Zhang, H., Guyot, R., Lunn, D., Bigley, R. B., Yu, H., Wang, J., Smith, M., Gillett, E., Muroy, S. E., Schmid, T., Wilson, E., Field, K. A., Reeder, D. A. M., Maden, M., Yartsev, M. M., ... Huang, G. N. (2019). Evidence for hormonal control of heart regenerative capacity during endothermy acquisition. *Science*, *364*(6436), 184–188. https://doi.org/10.1126/science.aar2038
- Hofbauer, P., Jahnel, S. M., Papai, N., Giesshammer, M., Deyett, A., Schmidt, C., Penc, M., Tavernini, K., Grdseloff, N., Meledeth, C., Ginistrelli, L. C., Ctortecka, C., Šalic,

- Š., Novatchkova, M., & Mendjan, S. (2021). Cardioids reveal self-organizing principles of human cardiogenesis. *Cell*, *184*(12), 3299–3317. https://doi.org/10.1016/j.cell.2021.04.034
- Huang, G. N., Thatcher, J. E., McAnally, J., Kong, Y., Qi, X., Tan, W., DiMaio, J. M., Amatruda, J. F., Gerard, R. D., Hill, J. A., Bassel-Duby, R., & Olson, E. N. (2012). C/EBP transcription factors mediate epicardial activation during heart development and injury. *Science*, 338(6114), 1599–1603. https://doi.org/10.1126/science.1229765
- Huang, Y., Harrison, M. R., Osorio, A., Kim, J., Baugh, A., Duan, C., Sucov, H. M., & Lien, C.-L. (2013). Igf Signaling is Required for Cardiomyocyte Proliferation during Zebrafish Heart Development and Regeneration. *PLoS ONE*, 8(6), 1–11. https://doi.org/10.1371/journal.pone.0067266
- lacobellis, G. (2015). Local and systemic effects of the multifaceted epicardial adipose tissue depot. *Nature Reviews Endocrinology*, *11*(6), 363–371. https://doi.org/10.1038/nrendo.2015.58
- Jankowski, M., Bissonauth, V., Gao, L., Gangal, M., Wang, D., Danalache, B., Wang, Y., Stoyanova, E., Cloutier, G., Blaise, G., & Gutkowska, J. (2010). Anti-inflammatory effect of oxytocin in rat myocardial infarction. *Basic Research in Cardiology*, 105(2), 205–218. https://doi.org/10.1007/s00395-009-0076-5
- Jankowski, M., Broderick, T. L., & Gutkowska, J. (2020). The Role of Oxytocin in Cardiovascular Protection. *Frontiers in Psychology*, *11*, 1–17. https://doi.org/10.3389/fpsyg.2020.02139
- Jankowski, M., Danalache, B., Wang, D., Bhat, P., Hajjar, F., Marcinkiewicz, M., Paquint, J., McCann, S. M., & Gutkowska, J. (2004). Oxytocin in cardiac ontogeny. *Proceedings of the National Academy of Sciences of the United States of America*, 101(35), 13074–13079. https://doi.org/10.1073/pnas.0405324101
- Jankowski, M., Hajjar, F., Al Kawas, S., Mukaddam-Daher, S., Hoffman, G., Mccann, S. M., & Gutkowska, J. (1998). Rat heart: A site of oxytocin production and action. *Proceedings of the National Academy of Sciences of the United States of America*, 95(24), 14558–14563. https://doi.org/10.1073/pnas.95.24.14558
- Jeon, K., Lim, H., Kim, J. H., Van Thuan, N., Park, S. H., Lim, Y. M., Choi, H. Y., Lee, E. R., Kim, J. H., Lee, M. S., & Cho, S.-G. (2012). Differentiation and transplantation of functional pancreatic beta cells generated from induced pluripotent stem cells derived from a type 1 diabetes mouse model. *Stem Cells and Development*, *21*(14), 2642–2655. https://doi.org/10.1089/scd.2011.0665
- Jia, B., Chen, S., Zhao, Z., Liu, P., Cai, J., Qin, D., Du, J., Wu, C., Chen, Q., Cai, X., Zhang, H., Yu, Y., Pei, D., Zhong, M., & Pan, G. (2014). Modeling of hemophilia A

- using patient-specific induced pluripotent stem cells derived from urine cells. *Life Sciences*, 108(1), 22–29. https://doi.org/10.1016/j.lfs.2014.05.004
- Jiang, H., Ren, Y., Yuen, E. Y., Zhong, P., Ghaedi, M., Hu, Z., Azabdaftari, G., Nakaso, K., Yan, Z., & Feng, J. (2012). Parkin controls dopamine utilization in human midbrain dopaminergic neurons derived from induced pluripotent stem cells. *Nature Communications*, 3, 1–9. https://doi.org/10.1038/ncomms1669
- Jones, S. P., & Bolli, R. (2006). The ubiquitous role of nitric oxide in cardioprotection. *Journal of Molecular and Cellular Cardiology*, *40*(1), 16–23. https://doi.org/10.1016/j.yjmcc.2005.09.011
- Jopling, C., Sleep, E., Raya, M., Marti, M., Raya, A., & Izpisua Belmonte, J. C. (2010). Zebrafish heart regeneration occurs by cardiomyocyte dedifferentiation and proliferation. *Nature*, *176*(12), 139–148. https://doi.org/10.1038/nature08899.Zebrafish
- Kawakami, K. (2007). Tol2: A versatile gene transfer vector in vertebrates. *Genome Biology*, 8(SUPPL 1), 1–10. https://doi.org/10.1186/gb-2007-8-s1-s7
- Kazuki, Y., Hiratsuka, M., Takiguchi, M., Osaki, M., Kajitani, N., Hoshiya, H., Hiramatsu, K., Yoshino, T., Kazuki, K., Ishihara, C., Takehara, S., Higaki, K., Nakagawa, M., Takahashi, K., Yamanaka, S., & Oshimura, M. (2010). Complete genetic correction of iPS cells from duchenne muscular dystrophy. *Molecular Therapy*, *18*(2), 386–393. https://doi.org/10.1038/mt.2009.274
- Khori, V., Mohammad Zadeh, F., Tavakoli-Far, B., Alizadeh, A. M., Khalighfard, S., Ghandian Zanjan, M., Gharghi, M., Khodayari, S., Khodayari, H., & Keshavarz, P. (2021). Role of oxytocin and c-Myc pathway in cardiac remodeling in neonatal rats undergoing cardiac apical resection. *European Journal of Pharmacology*, 908, 1–7. https://doi.org/10.1016/j.ejphar.2021.174348
- Kikuchi, K., Gupta, V., Wang, J., Holdway, J. E., Wills, A. A., Fang, Y., & Poss, K. D. (2011). Tcf21+ epicardial cells adopt non-myocardial fates during zebrafish heart development and regeneration. *Development*, *138*(14), 2895–2902. https://doi.org/10.1242/dev.067041
- Kikuchi, K., Holdway, J. E., Major, R. J., Blum, N., Dahn, R. D., Begemann, G., & Poss, K. D. (2011). Retinoic Acid Production by Endocardium and Epicardium Is an Injury Response Essential for Zebrafish Heart Regeneration. *Developmental Cell*, *20*(3), 397–404. https://doi.org/10.1016/j.devcel.2011.01.010
- Kikuchi, K., Holdway, J. E., Werdich, A. A., Anderson, R. M., Fang, Y., Egnaczyk, G. F., Evans, T., MacRae, C. A., Stainier, D. Y. R., & Poss, K. D. (2010). Primary contribution to zebrafish heart regeneration by gata4+ cardiomyocytes. *Nature*, 464(7288), 601–605. https://doi.org/10.1038/nature08804

- Kim, H., Kamm, R. D., Vunjak-Novakovic, G., & Wu, J. C. (2022). Progress in multicellular human cardiac organoids for clinical applications. *Cell Stem Cell*, 29(4), 503–514. https://doi.org/10.1016/j.stem.2022.03.012
- Kim, Jieun, Wu, Q., Zhang, Y., Wiens, K. M., Huang, Y., Rubin, N., Shimada, H., Handin, R. I., Chao, M. Y., Tuan, T. L., Starnes, V. A., & Lien, C. L. (2010). PDGF signaling is required for epicardial function and blood vessel formation in regenerating zebrafish hearts. *Proceedings of the National Academy of Sciences of the United States of America*, 107(40), 17206–17210. https://doi.org/10.1073/pnas.0915016107
- Kim, Jihoon, Koo, B. K., & Knoblich, J. A. (2020). Human organoids: model systems for human biology and medicine. *Nature Reviews Molecular Cell Biology*, *21*(10), 571–584. https://doi.org/10.1038/s41580-020-0259-3
- Kiskinis, E., & Eggan, K. (2010). Progress toward the clinical application of patient-specific pluripotent stem cells. *Journal of Clinical Investigation*, *120*(1), 51–59. https://doi.org/10.1172/JCI40553
- Knapper, J. T., Ghasemzadeh, N., Khayata, M., Patel, S. P., Quyyumi, A. A., Mendis, S., Mensah, G. A., Taubert, K., & Sperling, L. S. (2015). Time to Change Our Focus: Defining, Promoting, and Impacting Cardiovascular Population Health. *Journal of the American College of Cardiology*, 66(8), 960–971. https://doi.org/10.1016/j.jacc.2015.07.008
- Kook, H., Itoh, H., Choi, B. S., Sawada, N., Doi, K., Hwang, T. J., Kim, K. K., Arai, H., Baik, Y. H., & Nakao, K. (2003). Physiological concentration of atrial natriuretic peptide induces endothelial regeneration in vitro. *American Journal of Physiology Heart and Circulatory Physiology*, 284(4), 1388–1397. https://doi.org/10.1152/ajpheart.00414.2002
- Kosfeld, M., Heinrichs, M., Zak, P. J., Fischbacher, U., & Fehr, E. (2005). Oxytocin increases trust in humans. *Nature*, *435*(7042), 673–676. https://doi.org/10.1038/nature03701
- Kouakanou, L., Xu, Y., Peters, C., He, J., Wu, Y., Yin, Z., & Kabelitz, D. (2020). Vitamin C promotes the proliferation and effector functions of human γδ T cells. *Cellular and Molecular Immunology*, *17*(5), 462–473. https://doi.org/10.1038/s41423-019-0247-8
- Kwan, K. M., Fujimoto, E., Grabher, C., Mangum, B. D., Hardy, M. E., Campbell, D. S., Parant, J. M., Yost, H. J., Kanki, J. P., & Chien, C. Bin. (2007). The Tol2kit: A multisite gateway-based construction Kit for Tol2 transposon transgenesis constructs. *Developmental Dynamics*, 236(11), 3088–3099. https://doi.org/10.1002/dvdy.21343

- Laflamme, M. A., & Murry, C. E. (2011). Heart Regeneration. *Nature*, *473*(7347), 326–335. https://doi.org/10.1038/nature10147.Heart
- Lancaster, M. A., & Knoblich, J. A. (2014). Organogenesisin a dish: Modeling development and disease using organoid technologies. *Science*, *345*(6194), 1–10. https://doi.org/10.1126/science.1247125
- Lancaster, M. A., Renner, M., Martin, C.-A., Wenzel, D., Bicknell, L. S., Hurles, M. E., Homfray, T., Penninger, J. M., Jackson, A. P., & Knoblich, J. A. (2013). Cerebral organoids model human brain development and microcephaly. *Nature*, *501*(7467), 373–379. https://doi.org/10.1038/nature12517
- Lavine, K. J., Yu, K., White, A. C., Zhang, X., Smith, C., Partanen, J., & Ornitz, D. M. (2005). Endocardial and epicardial derived FGF signals regulate myocardial proliferation and differentiation in vivo. *Developmental Cell*, 8(1), 85–95. https://doi.org/10.1016/j.devcel.2004.12.002
- Lawson, N. D., & Weinstein, B. M. (2002). In vivo imaging of embryonic vascular development using transgenic zebrafish. *Developmental Biology*, 248(2), 307–318. https://doi.org/10.1006/dbio.2002.0711
- Lee, H. J., Macbeth, A. H., Pagani, J. H., & Scott Young, W. (2009). Oxytocin: The great facilitator of life. *Progress in Neurobiology*, *88*(2), 127–151. https://doi.org/10.1016/j.pneurobio.2009.04.001
- Lengner, C. J. (2010). IPS cell technology in regenerative medicine. *Annals of the New York Academy of Sciences*, 1192, 38–44. https://doi.org/10.1111/j.1749-6632.2009.05213.x
- Lepilina, A., Coon, A. N., Kikuchi, K., Holdway, J. E., Roberts, R. W., Burns, C. G., & Poss, K. D. (2006). A Dynamic Epicardial Injury Response Supports Progenitor Cell Activity during Zebrafish Heart Regeneration. *Cell*, *127*(3), 607–619. https://doi.org/10.1016/j.cell.2006.08.052
- Lewis-Israeli, Y. R., Volmert, B. D., Gabalski, M. A., Huang, A. R., & Aguirre, A. (2021). Generating Self-Assembling Human Heart Organoids Derived from Pluripotent Stem Cells. *Journal of Visualized Experiments*, *175*, 1–18. https://doi.org/10.3791/63097
- Lewis-Israeli, Y. R., Wasserman, A. H., & Aguirre, A. (2021). Heart organoids and engineered heart tissues: Novel tools for modeling human cardiac biology and disease. *Biomolecules*, *11*(9), 1–14. https://doi.org/10.3390/biom11091277
- Lewis-Israeli, Y. R., Wasserman, A. H., Gabalski, M. A., Volmert, B. D., Ming, Y., Ball, K. A., Yang, W., Zou, J., Ni, G., Pajares, N., Chatzistavrou, X., Li, W., Zhou, C., & Aguirre, A. (2021). Self-assembling human heart organoids for the modeling of

- cardiac development and congenital heart disease. *Nature Communications*, *12*(1), 1–16. https://doi.org/10.21203/rs.3.rs-132349/v1
- Li, N., Rignault-Clerc, S., Bielmann, C., Bon-Mathier, A. C., Déglise, T., Carboni, A., Ducrest, M., & Rosenblatt-Velin, N. (2020). Increasing heart vascularisation after myocardial infarction using brain natriuretic peptide stimulation of endothelial and WT1+ epicardial cells. *ELife*, *9*, 1–28. https://doi.org/10.7554/eLife.61050
- Li, P., Cavallero, S., Gu, Y., Chen, T. H. P., Hughes, J., Hassan, A. B., Brüning, J. C., Pashmforoush, M., & Sucov, H. M. (2011). IGF signaling directs ventricular cardiomyocyte proliferation during embryonic heart development. *Development*, 138(9), 1795–1805. https://doi.org/10.1242/dev.054338
- Liao, S., Dong, W., Lv, L., Guo, H., Yang, J., Zhao, H., Huang, R., Yuan, Z., Chen, Y., Feng, S., Zheng, X., Huang, J., Huang, W., Qi, X., & Cai, D. (2017). Heart regeneration in adult Xenopus tropicalis after apical resection. *Cell and Bioscience*, 7(70), 1–16. https://doi.org/10.1186/s13578-017-0199-6
- Limana, F., Bertolami, C., Mangoni, A., Di Carlo, A., Avitabile, D., Mocini, D., Iannelli, P., De Mori, R., Marchetti, C., Pozzoli, O., Gentili, C., Zacheo, A., Germani, A., & Capogrossi, M. C. (2010). Myocardial infarction induces embryonic reprogramming of epicardial c-kit+ cells: Role of the pericardial fluid. *Journal of Molecular and Cellular Cardiology*, *48*(4), 609–618. https://doi.org/10.1016/j.yjmcc.2009.11.008
- Limana, F., Zacheo, A., Mocini, D., Mangoni, A., Borsellino, G., Diamantini, A., De Mori, R., Battistini, L., Vigna, E., Santini, M., Loiaconi, V., Pompilio, G., Germani, A., & Capogrossi, M. C. (2007). Identification of myocardial and vascular precursor cells in human and mouse epicardium. *Circulation Research*, *101*(12), 1255–1265. https://doi.org/10.1161/CIRCRESAHA.107.150755
- Liu, H., Kim, Y., Sharkis, S., Marchionni, L., & Jang, Y.-Y. (2011). In vivo liver regeneration potential of human induced pluripotent stem cells from diverse origins. *Science Translational Medicine*, *3*(82), 1–19. https://doi.org/10.1126/scitranslmed.3002376
- Lowe, V., Wisniewski, L., Sayers, J., Evans, I., Frankel, P., Mercader-Huber, N., Zachary, I. C., & Pellet-Many, C. (2019). Neuropilin 1 mediates epicardial activation and revascularization in the regenerating zebrafish heart. *Development*, *146*(13), 1–13. https://doi.org/10.1242/dev.174482
- Luck, M. R., & Jungclas, B. (1987). Catecholamines and ascorbic acid as stimulators of bovine ovarian oxytocin secretion. *The Journal of Endocrinology*, *114*(3), 423–430. https://doi.org/10.1677/joe.0.1140423
- Mackey, A. S., Redd, P. S., DeLaurier, A., & Hancock, C. N. (2020). Codon optimized Tol2 transposase results in increased transient expression of a crystallin-GFP

- transgene in zebrafish. *MicroPublication Biology*, 2020, 2011–2014. https://doi.org/10.17912/micropub.biology.000268
- Mahmoud, A. I., O'Meara, C. C., Gemberling, M., Zhao, L., Bryant, D. M., Zheng, R., Gannon, J. B., Cai, L., Choi, W. Y., Egnaczyk, G. F., Burns, C. E., Burns, C. G., MacRae, C. A., Poss, K. D., & Lee, R. T. (2015). Nerves Regulate Cardiomyocyte Proliferation and Heart Regeneration. *Developmental Cell*, *34*(4), 387–399. https://doi.org/10.1016/j.devcel.2015.06.017
- Marín-Juez, R., Marass, M., Gauvrit, S., Rossi, A., Lai, S. L., Materna, S. C., Black, B. L., & Stainier, D. Y. R. (2016). Fast revascularization of the injured area is essential to support zebrafish heart regeneration. *Proceedings of the National Academy of Sciences of the United States of America*, 113(40), 11237–11242. https://doi.org/10.1073/pnas.1605431113
- Martínez-Estrada, O. M., Lettice, L. A., Essafi, A., Guadix, J. A., Slight, J., Velecela, V., Hall, E., Reichmann, J., Devenney, P. S., Hohenstein, P., Hosen, N., Hill, R. E., Műoz-Chapuli, R., & Hastie, N. D. (2010). Wt1 is required for cardiovascular progenitor cell formation through transcriptional control of Snail and E-cadherin. *Nature Genetics*, *42*(1), 89–93. https://doi.org/10.1038/ng.494
- Maselli, D., Matos, R. S., Johnson, R. D., Chiappini, C., Camelliti, P., & Campagnolo, P. (2022). Epicardial slices: an innovative 3D organotypic model to study epicardial cell physiology and activation. *NPJ Regenerative Medicine*, 7(1), 1–16. https://doi.org/10.1038/s41536-021-00202-7
- Massagué, J. (2012). TGFβ signalling in context. *Nature Reviews Molecular Cell Biology*, *13*(10), 616–630. https://doi.org/10.1038/nrm3434
- Masters, M., & Riley, P. R. (2014). The epicardium signals the way towards heart regeneration. *Stem Cell Research*, *13*(3), 683–692. https://doi.org/10.1016/j.scr.2014.04.007
- Masumoto, H., Ikuno, T., Takeda, M., Fukushima, H., Marui, A., Katayama, S., Shimizu, T., Ikeda, T., Okano, T., Sakata, R., & Yamashita, J. K. (2014). Human iPS cell-engineered cardiac tissue sheets with cardiomyocytes and vascular cells for cardiac regeneration. *Scientific Reports*, *4*, 1–7. https://doi.org/10.1038/srep06716
- Mattis, V. B., Svendsen, S. P., Ebert, A., Svendsen, C. N., King, A. R., Casale, M., Winokur, S. T., Batugedara, G., Vawter, M., Donovan, P. J., Lock, L. F., Thompson, L. M., Zhu, Y., Fossale, E., Atwal, R. S., Gillis, T., Mysore, J., Li, J. H., Seong, I., ... Arjomand, J. (2012). Induced pluripotent stem cells from patients with huntington's disease show CAG repeat expansion associated phenotypes. *Cell Stem Cell*, 11(2), 264–278. https://doi.org/10.1016/j.stem.2012.04.027
- Mills, R. J., Titmarsh, D. M., Koenig, X., Parker, B. L., Ryall, J. G., Quaife-Ryan, G. A.,

- Voges, H. K., Hodson, M. P., Ferguson, C., Drowley, L., Plowright, A. T., Needham, E. J., Wang, Q.-D., Gregorevic, P., Xin, M., Thomas, W. G., Parton, R. G., Nielsen, L. K., Launikonis, B. S., ... Hudson, J. E. (2017). Functional screening in human cardiac organoids reveals a metabolic mechanism for cardiomyocyte cell cycle arrest. *Proceedings of the National Academy of Sciences of the United States of America*, 114(40), E8372–E8381. https://doi.org/10.1073/pnas.1707316114
- Miyamoto, M., Nam, L., Kannan, S., & Kwon, C. (2021). Heart organoids and tissue models for modeling development and disease. *Seminars in Cell and Developmental Biology*, *118*, 119–128. https://doi.org/10.1016/j.semcdb.2021.03.011
- Moretti, A., Bellin, M., Welling, A., Jung, C. B., Lam, J. T., Bott-Flügel, L., Dorn, T., Goedel, A., Höhnke, C., Hofmann, F., Seyfarth, M., Sinnecker, D., Schömig, A., & Laugwitz, K.-L. (2010). Patient-specific induced pluripotent stem-cell models for long-QT syndrome. *The New England Journal of Medicine*, 363(15), 1397–1409. https://doi.org/10.1056/NEJMoa0908679
- Morin, V., Del Castillo, J. R. E., Authier, S., Ybarra, N., Otis, C., Gauvin, D., Gutkowska, J., & Troncy, E. (2008). Evidence for non-linear pharmacokinetics of oxytocin in anesthetizetized rat. *Journal of Pharmacy and Pharmaceutical Sciences*, *11*(4), 12–24. https://doi.org/10.18433/j3pk5x
- Morrison, S. F. (2016). Central control of body temperature. *F1000Research*, *5*, 1–10. https://doi.org/10.12688/F1000RESEARCH.7958.1
- Mukaddam-Daher, S., Yin, Y. L., Roy, J., Gutkowska, J., & Cardinal, R. (2001). Negative inotropic and chronotropic effects of oxytocin. *Hypertension*, 38(2), 292–296. https://doi.org/10.1161/01.HYP.38.2.292
- Nishikimi, T., Maeda, N., & Matsuoka, H. (2006). The role of natriuretic peptides in cardioprotection. *Cardiovascular Research*, 69(2), 318–328. https://doi.org/10.1016/j.cardiores.2005.10.001
- Noël, E. S., & Bakkers, J. (2017). Twists and turns. *ELife*, *6*, 1–3. https://doi.org/10.7554/eLife.32709
- Noiseux, N., Borie, M., Desnoyers, A., Menaouar, A., Stevens, L. M., Mansour, S., Danalache, B. A., Roy, D. C., Jankowski, M., & Gutkowska, J. (2012). Preconditioning of stem cells by oxytocin to improve their therapeutic potential. *Endocrinology*, *153*(11), 5361–5372. https://doi.org/10.1210/en.2012-1402
- Nori, S., Okada, Y., Yasuda, A., Tsuji, O., Takahashi, Y., Kobayashi, Y., Fujiyoshi, K., Koike, M., Uchiyama, Y., Ikeda, E., Toyama, Y., Yamanaka, S., Nakamura, M., & Okano, H. (2011). Grafted human-induced pluripotent stem-cell-derived neurospheres promote motor functional recovery after spinal cord injury in mice.

- Proceedings of the National Academy of Sciences of the United States of America, 108(40), 16825–16830. https://doi.org/10.1073/pnas.1108077108
- Ondrejcakova, M., Barancik, M., Bartekova, M., Ravingerova, T., & Jezova, D. (2012). Prolonged oxytocin treatment in rats affects intracellular signaling and induces myocardial protection against infarction. *General Physiology and Biophysics*, *31*(3), 261–270. https://doi.org/10.4149/gpb 2012 030
- Ondrejcakova, M., Ravingerova, T., Bakos, J., Pancza, D., & Jezova, D. (2009). Oxytocin exerts protective effects on in vitro myocardial injury induced by ischemia and reperfusion. *Canadian Journal of Physiology and Pharmacology*, 87(2), 137–142. https://doi.org/10.1139/Y08-108
- Ott, I., & Scott, J. C. (1910). The action of infundibulin upon the mammary secretion. *Experimental Biology and Medicine*, 8(2), 48–49. https://doi.org/10.3181/00379727-8-27
- Page, A., Messer, S., & Large, S. R. (2018). Heart transplantation from donation after circulatory determined death. *Annals of Cardiothoracic Surgery*, 7(1), 75–81. https://doi.org/10.21037/acs.2018.01.08
- Palma, J.-A., & Benarroch, E. E. (2014). Neural control of the heart: recent concepts and clinical correlations. *Neurology*, *83*(3), 261–271. https://doi.org/10.1212/WNL.000000000000000
- Paquin, J., Danalache, B. A., Jankowski, M., McCann, S. M., & Gutkowska, J. (2002). Oxytocin induces differentiation of P19 embryonic stem cells to cardiomyocytes. *Proceedings of the National Academy of Sciences of the United States of America*, 99(14), 9550–9555. https://doi.org/10.1073/pnas.152302499
- Park, I. H., Arora, N., Huo, H., Maherali, N., Ahfeldt, T., Shimamura, A., Lensch, M. W., Cowan, C., Hochedlinger, K., & Daley, G. Q. (2008). Disease-Specific Induced Pluripotent Stem Cells. *Cell*, *134*(5), 877–886. https://doi.org/10.1016/j.cell.2008.07.041
- Patel, V. B., Shah, S., Verma, S., & Oudit, G. Y. (2017). Epicardial adipose tissue as a metabolic transducer: role in heart failure and coronary artery disease. *Heart Failure Reviews*, 22(6), 889–902. https://doi.org/10.1007/s10741-017-9644-1
- Peng, Y., Wang, W., Fang, Y., Hu, H., Chang, N., Pang, M., Hu, Y. F., Li, X., Long, H., Xiong, J. W., & Zhang, R. (2021). Inhibition of TGF-β/Smad3 Signaling Disrupts Cardiomyocyte Cell Cycle Progression and Epithelial–Mesenchymal Transition-Like Response During Ventricle Regeneration. *Frontiers in Cell and Developmental Biology*, 9, 1–14. https://doi.org/10.3389/fcell.2021.632372
- Peralta, M., González-Rosa, J. M., Marques, I. J., & Mercader, N. (2014). The

- epicardium in the embryonic and adult zebrafish. *Journal of Developmental Biology*, 2(2), 101–116. https://doi.org/10.3390/jdb2020101
- Peralta, M., Steed, E., Harlepp, S., González-Rosa, J. M., Monduc, F., Ariza-Cosano, A., Cortés, A., Rayón, T., Gómez-Skarmeta, J. L., Zapata, A., Vermot, J., & Mercader, N. (2013). Heartbeat-driven pericardiac fluid forces contribute to epicardium morphogenesis. *Current Biology*, *23*(18), 1726–1735. https://doi.org/10.1016/j.cub.2013.07.005
- Pettibone, D. J., Clineschmidt, B. V., Guidotti, M. T., Lis, E. V., Reiss, D. R., Woyden, C. J., Bock, M. G., Evans, B. E., Freidinger, R. M., Hobbs, D. W., Veber, D. F., Williams, P. D., Chiu, S. -H L., Thompson, K. L., Schorn, T. W., Siegl, P. K. S., Kaufman, M. J., Cukierski, M. A., Haluska, G. J., ... Novy, M. J. (1993). L-368,899, a potent orally active oxytocin antagonist for potential use in preterm labor. *Drug Development Research*, 30(3), 129–142. https://doi.org/10.1002/ddr.430300305
- Pinto, A. R., Ilinykh, A., Ivey, M. J., Kuwabara, J. T., D'Antoni, M. L., Debuque, R., Chandran, A., Wang, L., Arora, K., Rosenthal, N. A., & Tallquist, M. D. (2016). Revisiting Cardiac Cellular Composition. *Circulation Research*, *118*(3), 400–409. https://doi.org/10.1161/CIRCRESAHA.115.307778
- Polizzotti, B. D., Ganapathy, B., Haubner, B. J., Penninger, J. M., & Kühn, B. (2016). A cryoinjury model in neonatal mice for cardiac translational and regeneration research. *Nature Protocols*, *11*(3), 542–552. https://doi.org/10.1038/nprot.2016.031
- Polshekan, M., Jamialahmadi, K., Khori, V., Alizadeh, A. M., Saeidi, M., Ghayour-Mobarhan, M., Jand, Y., Ghahremani, M. H., & Yazdani, Y. (2016). RISK pathway is involved in oxytocin postconditioning in isolated rat heart. *Peptides*, *86*, 55–62. https://doi.org/10.1016/j.peptides.2016.10.001
- Polshekan, M., Khori, V., Alizadeh, A. M., Ghayour-Mobarhan, M., Saeidi, M., Jand, Y., Rajaei, M., Farnoosh, G., & Jamialahmadi, K. (2019). The SAFE pathway is involved in the postconditioning mechanism of oxytocin in isolated rat heart. *Peptides*, *111*, 142–151. https://doi.org/10.1016/j.peptides.2018.04.002
- Porrello, E. R., Mahmoud, A. I., Simpson, E., Hill, J. A., Richardson, J. A., Olson, E. N., & Sadek, H. A. (2011). Transient regenerative potential of the neonatal mouse heart. *Science*, 331(6020), 1078–1080. https://doi.org/10.1126/science.1200708
- Porrello, E. R., Mahmoud, A. I., Simpson, E., Johnson, B. A., Grinsfelder, D., Canseco, D., Mammen, P. P., Rothermel, B. A., Olson, E. N., & Sadek, H. A. (2013). Regulation of neonatal and adult mammalian heart regeneration by the miR-15 family. *Proceedings of the National Academy of Sciences of the United States of America*, 110(1), 187–192. https://doi.org/10.1073/pnas.1208863110
- Poss, K. D., Wilson, L. G., & Keating, M. T. (2002). Heart regeneration in zebrafish.

- Science, 298(5601), 2188–2190. https://doi.org/10.1126/science.1077857
- Quijada, P., Trembley, M. A., & Small, E. M. (2020). The Role of the Epicardium during Heart Development and Repair. *Circulation Research*, *126*, 377–394. https://doi.org/10.1161/CIRCRESAHA.119.315857
- Rao, K. S., Aronshtam, A., McElory-Yaggy, K. L., Bakondi, B., VanBuren, P., Sobel, B. E., & Spees, J. L. (2015). Human epicardial cell-conditioned medium contains HGF/IgG complexes that phosphorylate RYK and protect against vascular injury. *Cardiovascular Research*, *107*(2), 277–286. https://doi.org/10.1093/cvr/cvv168
- Rao, K. S., & Spees, J. L. (2017). Harnessing Epicardial Progenitor Cells and Their Derivatives for Rescue and Repair of Cardiac Tissue After Myocardial Infarction. *Current Molecular Biology Reports*, *3*(3), 149–158. https://doi.org/10.1016/j.physbeh.2017.03.040
- Rapacz-Leonard, A., Leonard, M., Chmielewska-Krzesińska, M., Siemieniuch, M., & Janowski, T. E. (2020). The oxytocin-prostaglandins pathways in the horse (Equus caballus) placenta during pregnancy, physiological parturition, and parturition with fetal membrane retention. *Scientific Reports*, *10*(1), 1–12. https://doi.org/10.1038/s41598-020-59085-1
- Rhee, S. S., & Pearce, E. N. (2011). The Endocrine System and the Heart: A Review. *Revista Española de Cardiología (English Edition)*, *64*(3), 220–231. https://doi.org/10.1016/j.rec.2010.10.016
- Richards, D. J., Li, Y., Kerr, C. M., Yao, J., Beeson, G. C., Coyle, R. C., Chen, X., Jia, J., Damon, B., Wilson, R., Starr Hazard, E., Hardiman, G., Menick, D. R., Beeson, C. C., Yao, H., Ye, T., & Mei, Y. (2020). Human cardiac organoids for the modelling of myocardial infarction and drug cardiotoxicity. *Nature Biomedical Engineering*, 4(4), 446–462. https://doi.org/10.1038/s41551-020-0539-4
- Riley, P. R. (2012). An Epicardial Floor Plan for Building and Rebuilding the Mammalian Heart. *Current Topics in Developmental Biology*, 100, 233–251. https://doi.org/10.1016/B978-0-12-387786-4.00007-5
- Rochon, E. R., Missinato, M. A., Xue, J., Tejero, J., Tsang, M., Gladwin, M. T., & Corti, P. (2020). Nitrite Improves Heart Regeneration in Zebrafish. *Antioxidants and Redox Signaling*, 32(6), 363–377. https://doi.org/10.1089/ars.2018.7687
- Rodgers, L. S., Lalani, S., Runyan, R. B., & Camenisch, T. D. (2008). Differential growth and multicellular villi direct proepicardial translocation to the developing mouse heart. *Developmental Dynamics*, 237(1), 145–152. https://doi.org/10.1002/dvdy.21378
- Roh, E., Song, D. K., & Kim, M. S. (2016). Emerging role of the brain in the homeostatic

- regulation of energy and glucose metabolism. *Experimental and Molecular Medicine*, 48(3), 1–12. https://doi.org/10.1038/emm.2016.4
- Romito, A., & Cobellis, G. (2016). Pluripotent Stem Cells: Current Understanding and Future Directions. *Stem Cells International*, *2016*, 1–20. https://doi.org/10.1155/2016/9451492
- Rosen, J. N., Sweeney, M. F., & Mably, J. D. (2009). Microinjection of zebrafish embryos to analyze gene function. *Journal of Visualized Experiments*, *25*, 1–5. https://doi.org/10.3791/1115
- Roy, R. K., Augustine, R. A., Brown, C. H., & Schwenke, D. O. (2019). Acute myocardial infarction activates magnocellular vasopressin and oxytocin neurones. *Journal of Neuroendocrinology*, *31*(12), 1–10. https://doi.org/10.1111/jne.12808
- Rudat, C., & Kispert, A. (2012). Wt1 and epicardial fate mapping. *Circulation Research*, 111(2), 165–169. https://doi.org/10.1161/CIRCRESAHA.112.273946
- Russell, J. L., Goetsch, S. C., Gaiano, N. R., Hill, J. A., Olson, E. N., & Schneider, J. W. (2011). A dynamic notch injury response activates epicardium and contributes to fibrosis repair. *Circulation Research*, *108*(1), 51–59. https://doi.org/10.1161/CIRCRESAHA.110.233262
- Sadek, H., & Olson, E. N. (2020). Toward the Goal of Human Heart Regeneration. *Cell Stem Cell*, 26(1), 7–16. https://doi.org/10.1016/j.stem.2019.12.004
- Sakamoto, S., Putalun, W., Vimolmangkang, S., Phoolcharoen, W., Shoyama, Y., Tanaka, H., & Morimoto, S. (2018). Enzyme-linked immunosorbent assay for the quantitative/qualitative analysis of plant secondary metabolites. *Journal of Natural Medicines*, 72(1), 32–42. https://doi.org/10.1007/s11418-017-1144-z
- Sallin, P., & Jaźwińska, A. (2016). Acute stress is detrimental to heart regeneration in zebrafish. *Open Biology*, 6, 1–15. https://doi.org/10.1098/rsob.160012
- Sanz-Morejón, A., & Mercader, N. (2020). Recent insights into zebrafish cardiac regeneration. *Current Opinion in Genetics and Development*, *64*, 37–43. https://doi.org/10.1016/j.gde.2020.05.020
- Sarn, N., Thacker, S., Lee, H., & Eng, C. (2021). Germline nuclear-predominant Pten murine model exhibits impaired social and perseverative behavior, microglial activation, and increased oxytocinergic activity. *Molecular Autism*, *12*(1), 1–19. https://doi.org/10.1186/s13229-021-00448-4
- Sato, T., Vries, R. G., Snippert, H. J., Van De Wetering, M., Barker, N., Stange, D. E., Van Es, J. H., Abo, A., Kujala, P., Peters, P. J., & Clevers, H. (2009). Single Lgr5 stem cells build crypt-villus structures in vitro without a mesenchymal niche. *Nature*,

- 459(7244), 262–265. https://doi.org/10.1038/nature07935
- Schafer, E. A., & Mackenzie, K. (1911). The action of animal extracts on milk secretion. *Proceedings of the Royal Society of London, Series B*, 84(568), 16–22. https://doi.org/10.1098/rspb.1911.0042
- Schnabel, K., Wu, C. C., Kurth, T., & Weidinger, G. (2011). Regeneration of cryoinjury induced necrotic heart lesions in zebrafish is associated with epicardial activation and cardiomyocyte proliferation. *PLoS ONE*, *6*(4), 1–11. https://doi.org/10.1371/journal.pone.0018503
- Senyo, S. E., Steinhauser, M. L., Pizzimenti, C. L., Yang, V. K., Cai, L., Wang, M., Wu, T. Di, Guerquin-Kern, J. L., Lechene, C. P., & Lee, R. T. (2013). Mammalian heart renewal by pre-existing cardiomyocytes. *Nature*, *493*(7432), 433–436. https://doi.org/10.1038/nature11682
- Shi, Y., Inoue, H., Wu, J. C., & Yamanaka, S. (2017). Induced pluripotent stem cell technology: A decade of progress. *Nature Reviews Drug Discovery*, *16*(2), 115–130. https://doi.org/10.1038/nrd.2016.245
- Shyu, A.-B., Wilkinson, M. F., & van Hoof, A. (2008). Messenger RNA regulation: To translate or to degrade. *EMBO Journal*, 27(3), 471–481. https://doi.org/10.1038/sj.emboj.7601977
- Silva, A. C., Matthys, O. B., Joy, D. A., Kauss, M. A., Natarajan, V., Lai, M. H., Turaga, D., Blair, A. P., Alexanian, M., Bruneau, B. G., & McDevitt, T. C. (2021). Coemergence of cardiac and gut tissues promotes cardiomyocyte maturation within human iPSC-derived organoids. *Cell Stem Cell*, 28(12), 2137–2152. https://doi.org/10.1016/j.stem.2021.11.007
- Simões, F. C., & Riley, P. R. (2018). The ontogeny, activation and function of the epicardium during heart development and regeneration. *Development*, *145*(7), 1–13. https://doi.org/10.1242/dev.155994
- Singh, V. K., Kalsan, M., Kumar, N., Saini, A., & Chandra, R. (2015). Induced pluripotent stem cells: Applications in regenerative medicine, disease modeling, and drug discovery. *Frontiers in Cell and Developmental Biology*, 3, 1–18. https://doi.org/10.3389/fcell.2015.00002
- Smart, N., Bollini, S., Dubé, K. N., Vieira, J. M., Zhou, B., Davidson, S., Yellon, D., Riegler, J., Price, A. N., Lythgoe, M. F., Pu, W. T., & Riley, P. R. (2011). De novo cardiomyocytes from within the activated adult heart after injury. *Nature*, *474*(7353), 640–644. https://doi.org/10.1038/nature10188
- Smart, N., Risebro, C. A., Clark, J. E., Ehler, E., Miquerol, L., Rossdeutsch, A., Marber, M. S., & Riley, P. R. (2010). Thymosin β4 facilitates epicardial neovascularization of

- the injured adult heart. *Annals of the New York Academy of Sciences*, 1194, 97–104. https://doi.org/10.1111/j.1749-6632.2010.05478.x
- Smart, N., Risebro, C. A., Melville, A. A. D., Moses, K., Schwartz, R. J., Chien, K. R., & Riley, P. R. (2007). Thymosin β4 induces adult epicardial progenitor mobilization and neovascularization. *Nature*, *445*(7124), 177–182. https://doi.org/10.1038/nature05383
- Smits, A. M., Dronkers, E., & Goumans, M. J. (2018). The epicardium as a source of multipotent adult cardiac progenitor cells: Their origin, role and fate. *Pharmacological Research*, 127, 129–140. https://doi.org/10.1016/j.phrs.2017.07.020
- Streef, T. J., & Smits, A. M. (2021). Epicardial Contribution to the Developing and Injured Heart: Exploring the Cellular Composition of the Epicardium. *Frontiers in Cardiovascular Medicine*, *8*, 1–16. https://doi.org/10.3389/fcvm.2021.750243
- Strober, W. (2001). Trypan blue exclusion test of cell viability. *Current Protocols in Immunology*, *Appendix 3*, 1–2. https://doi.org/10.1002/0471142735.ima03bs21
- Sun, J., Peterson, E. A., Wang, A. Z., Ou, J., Smith, K. E., Poss, K. D., & Wang, J. (2022). hapln1 Defines an Epicardial Cell Subpopulation Required for Cardiomyocyte Expansion During Heart Morphogenesis and Regeneration. *Circulation*, *146*, 48–63. https://doi.org/10.1161/CIRCULATIONAHA.121.055468
- Takahashi, K. (2010). Direct reprogramming 101. *Development Growth and Differentiation*, 52(3), 319–333. https://doi.org/10.1111/j.1440-169X.2010.01169.x
- Takahashi, K., Tanabe, K., Ohnuki, M., Narita, M., Ichisaka, T., Tomoda, K., & Yamanaka, S. (2007). Induction of Pluripotent Stem Cells from Adult Human Fibroblasts by Defined Factors. *Cell*, *131*(5), 861–872. https://doi.org/10.1016/j.cell.2007.11.019
- Takahashi, K., & Yamanaka, S. (2006). Induction of Pluripotent Stem Cells from Mouse Embryonic and Adult Fibroblast Cultures by Defined Factors. *Cell*, *126*(4), 663–676. https://doi.org/10.1016/j.cell.2006.07.024
- Takasato, M., Er, P. X., Chiu, H. S., Maier, B., Baillie, G. J., Ferguson, C., Parton, R. G., Wolvetang, E. J., Roost, M. S., De Sousa Lopes, S. M. C., & Little, M. H. (2015). Kidney organoids from human iPS cells contain multiple lineages and model human nephrogenesis. *Nature*, *526*(7574), 564–568. https://doi.org/10.1038/nature15695
- Tan, J. J., Guyette, J. P., Miki, K., Xiao, L., Kaur, G., Wu, T., Zhu, L., Hansen, K. J., Ling, K. H., Milan, D. J., & Ott, H. C. (2021). Human iPS-derived pre-epicardial cells direct cardiomyocyte aggregation expansion and organization in vitro. *Nature Communications*, *12*(1), 1–19. https://doi.org/10.1038/s41467-021-24921-z

- Tanaka, A., Yuasa, S., Mearini, G., Egashira, T., Seki, T., Kodaira, M., Kusumoto, D., Kuroda, Y., Okata, S., Suzuki, T., Inohara, T., Arimura, T., Makino, S., Kimura, K., Kimura, A., Furukawa, T., Carrier, L., Node, K., & Fukuda, K. (2014). Endothelin-1 induces myofibrillar disarray and contractile vector variability in hypertrophic cardiomyopathy-induced pluripotent stem cell-derived cardiomyocytes. *Journal of the American Heart Association*, 3(6), 1–25. https://doi.org/10.1161/JAHA.114.001263
- Tedesco, F. S., Gerli, M. F. M., Perani, L., Benedetti, S., Ungaro, F., Cassano, M., Antonini, S., Tagliafico, E., Artusi, V., Longa, E., Tonlorenzi, R., Ragazzi, M., Calderazzi, G., Hoshiya, H., Cappellari, O., Mora, M., Schoser, B., Schneiderat, P., Oshimura, M., ... Cossu, G. (2012). Transplantation of genetically corrected human iPSC-derived progenitors in mice with limb-girdle muscular dystrophy. *Science Translational Medicine*, *4*(140), 1–13. https://doi.org/10.1126/scitranslmed.3003541
- Thygesen, K., Alpert, J. S., Jaffe, A. S., Chaitman, B. R., Bax, J. J., Morrow, D. A., White, H. D., Corbett, S., Chettibi, M., Hayrapetyan, H., Roithinger, F. X., Aliyev, F., Sujayeva, V., Claeys, M. J., Smajić, E., Kala, P., Iversen, K. K., Hefny, E. El, Marandi, T., ... Parkhomenko, A. (2018). Fourth Universal Definition of Myocardial Infarction (2018). In *Circulation* (Vol. 138, Issue 20). https://doi.org/10.1161/CIR.00000000000000017
- Tzahor, E., & Poss, K. D. (2017). Cardiac regeneration strategies: Staying young at heart. *Science*, *356*(6342), 1035–1039. https://doi.org/10.1126/science.aam5894
- Uygur, A., & Lee, R. T. (2016). Mechanisms of Cardiac Regeneration. *Developmental Cell*, 36(4), 362–374. https://doi.org/10.1016/j.devcel.2016.01.018
- Van den Bos, E. J., Mees, B. M. E., de Waard, M. C., de Crom, R., & Duncker, D. J. (2005). A novel model of cryoinjury-induced myocardial infarction in the mouse: A comparison with coronary artery ligation. *American Journal of Physiology Heart and Circulatory Physiology*, 289(3), H1291–H1300. https://doi.org/10.1152/ajpheart.00111.2005
- Van Wijk, B., Gunst, Q. D., Moorman, A. F. M., & van den Hoff, M. J. B. (2012). Cardiac Regeneration from Activated Epicardium. *PLoS ONE*, 7(9), 1–14. https://doi.org/10.1371/journal.pone.0044692
- Virani, S. S., Alonso, A., Benjamin, E. J., Bittencourt, M. S., Callaway, C. W., Carson, A. P., Chamberlain, A. M., Chang, A. R., Cheng, S., Delling, F. N., Djousse, L., Elkind, M. S. V., Ferguson, J. F., Fornage, M., Khan, S. S., Kissela, B. M., Knutson, K. L., Kwan, T. W., Lackland, D. T., ... Heard, D. G. (2020). Heart disease and stroke statistics—2020 update: A report from the American Heart Association. *Circulation*, 141, E139–E596. https://doi.org/10.1161/CIR.00000000000000757
- Voges, H. K., Mills, R. J., Elliott, D. A., Parton, R. G., Porrello, E. R., & Hudson, J. E.

- (2017). Development of a human cardiac organoid injury model reveals innate regenerative potential. *Development*, *144*(6), 1118–1127. https://doi.org/10.1242/dev.143966
- Von Gise, A., & Pu, W. T. (2012). Endocardial and epicardial epithelial to mesenchymal transitions in heart development and disease. *Circulation Research*, *110*(12), 1628–1645. https://doi.org/10.1161/CIRCRESAHA.111.259960
- Von Gise, A., Zhou, B., Honor, L. B., Ma, Q., Petryk, A., & Pu, W. T. (2011). WT1 regulates epicardial epithelial to mesenchymal transition through β-catenin and retinoic acid signaling pathways. *Developmental Biology*, *356*(2), 421–431. https://doi.org/10.1016/j.ydbio.2011.05.668
- Vujic, A., Natarajan, N., & Lee, R. T. (2020). Molecular mechanisms of heart regeneration. *Seminars in Cell and Developmental Biology*, *100*, 20–28. https://doi.org/10.1016/j.semcdb.2019.09.003
- Wang, J., Cao, J., Dickson, A. L., & Poss, K. D. (2015). Epicardial regeneration is guided by cardiac outflow tract and Hedgehog signalling. *Nature*, *522*(7555), 226–230. https://doi.org/10.1038/nature14325
- Wang, J., Karra, R., Dickson, A. L., & Poss, K. D. (2013). Fibronectin is deposited by injury-activated epicardial cells and is necessary for zebrafish heart regeneration. *Developmental Biology*, 382(2), 427–435. https://doi.org/10.1016/j.ydbio.2013.08.012
- Wang, J., Panáková, D., Kikuchi, K., Holdway, J. E., Gemberling, M., Burris, J. S., Singh, S. P., Dickson, A. L., Lin, Y. F., Khaled Sabeh, M., Werdich, A. A., Yelon, D., MacRae, C. A., & Poss, K. D. (2011). The regenerative capacity of zebrafish reverses cardiac failure caused by genetic cardiomyocyte depletion. *Development*, 138(16), 3421–3430. https://doi.org/10.1242/dev.068601
- Wang, R. N., Green, J., Wang, Z., Deng, Y., Qiao, M., Peabody, M., Zhang, Q., Ye, J., Yan, Z., Denduluri, S., Idowu, O., Li, M., Shen, C., Hu, A., Haydon, R. C., Kang, R., Mok, J., Lee, M. J., Luu, H. L., & Shi, L. L. (2014). Bone Morphogenetic Protein (BMP) signaling in development and human diseases. *Genes and Diseases*, *1*(1), 87–105. https://doi.org/10.1016/j.gendis.2014.07.005
- Wang, Y. L., Yu, S. N., Shen, H. R., Wang, H. J., Wu, X. P., Wang, Q. L., Zhou, B., & Tan, Y. Z. (2021). Thymosin β4 released from functionalized self-assembling peptide activates epicardium and enhances repair of infarcted myocardium. *Theranostics*, 11(9), 4262–4280. https://doi.org/10.7150/THNO.52309
- Wang, Y., Shi, J., Chai, K., Ying, X., & Zhou, B. (2013). The Role of Snail in EMT and Tumorigenesis. *Current Cancer Drug Targets*, *13*(9), 963–972. https://doi.org/10.2174/15680096113136660102

- Wasserman, A. H., Huang, A. R., Lewis-Israeli, Y. R., Dooley, M. D., Mitchell, A. L., Venkatesan, M., & Aguirre, A. (2022). Oxytocin promotes epicardial cell activation and heart regeneration after cardiac injury. *Frontiers in Cell and Developmental Biology*, 10, 1–19. https://doi.org/10.3389/fcell.2022.985298
- Wei, K., Serpooshan, V., Hurtado, C., Diez-Cunado, M., Zhao, M., Maruyama, S., Zhu, W., Fajardo, G., Noseda, M., Nakamura, K., Tian, X., Liu, Q., Wang, A., Matsuura, Y., Bushway, P., Cai, W., Savchenko, A., Mahmoudi, M., Schneider, M. D., ... Ruiz-Lozano, P. (2015). Epicardial FSTL1 reconstitution regenerates the adult mammalian heart. *Nature*, *525*(7570), 479–485. https://doi.org/10.1038/nature15372
- White, I. A., Gordon, J., Balkan, W., & Hare, J. M. (2015). Sympathetic reinnervation is required for mammalian cardiac regeneration. *Circulation Research*, *117*(12), 990–994. https://doi.org/10.1161/CIRCRESAHA.115.307465
- Wills, A. A., Holdway, J. E., Major, R. J., & Poss, K. D. (2008). Regulated addition of new myocardial and epicardial cells fosters homeostatic cardiac growth and maintenance in adult zebrafish. *Development*, 135(1), 183–192. https://doi.org/10.1242/dev.010363
- Witman, N., Murtuza, B., Davis, B., Arner, A., & Morrison, J. I. (2011). Recapitulation of developmental cardiogenesis governs the morphological and functional regeneration of adult newt hearts following injury. *Developmental Biology*, 354, 67–76. https://doi.org/10.1016/j.ydbio.2011.03.021
- Wu, C. C., Kruse, F., Vasudevarao, M. D., Junker, J. P., Zebrowski, D. C., Fischer, K., Noël, E. S., Grün, D., Berezikov, E., Engel, F. B., Van Oudenaarden, A., Weidinger, G., & Bakkers, J. (2016). Spatially Resolved Genome-wide Transcriptional Profiling Identifies BMP Signaling as Essential Regulator of Zebrafish Cardiomyocyte Regeneration. *Developmental Cell*, 36(1), 36–49. https://doi.org/10.1016/j.devcel.2015.12.010
- Xu, S., Xie, F., Tian, L., Fallah, S., Babaei, F., Manno, S. H. C., Manno, F. A. M., Zhu, L., Wong, K. F., Liang, Y., Ramalingam, R., Sun, L., Wang, X., Plumb, R., Gethings, L., Lam, Y. W., & Cheng, S. H. (2020). Estrogen accelerates heart regeneration by promoting the inflammatory response in zebrafish. *Journal of Endocrinology*, 245(1), 39–51. https://doi.org/10.1530/JOE-19-0413
- Yagi, T., Ito, D., Okada, Y., Akamatsu, W., Nihei, Y., Yoshizaki, T., Yamanaka, S., Okano, H., & Suzuki, N. (2011). Modeling familial Alzheimer's disease with induced pluripotent stem cells. *Human Molecular Genetics*, *20*(23), 4530–4539. https://doi.org/10.1093/hmg/ddr394
- Yamaguchi, Y., Cavallero, S., Patterson, M., Shen, H., Xu, J., Kumar, S. R., & Sucov, H. M. (2015). Adipogenesis and epicardial adipose tissue: A novel fate of the

- epicardium induced by mesenchymal transformation and PPARγ activation. *Proceedings of the National Academy of Sciences of the United States of America*, 112(7), 2070–2075. https://doi.org/10.1073/pnas.1417232112
- Yang, X., Rodriguez, M. L., Leonard, A., Sun, L., Fischer, K. A., Wang, Y., Ritterhoff, J., Zhao, L., Kolwicz, S. C., Pabon, L., Reinecke, H., Sniadecki, N. J., Tian, R., Ruohola-Baker, H., Xu, H., & Murry, C. E. (2019). Fatty Acids Enhance the Maturation of Cardiomyocytes Derived from Human Pluripotent Stem Cells. Stem Cell Reports, 13(4), 657–668. https://doi.org/10.1016/j.stemcr.2019.08.013
- Yang, X., Rodriguez, M., Pabon, L., Fischer, K. A., Reinecke, H., Regnier, M., Sniadecki, N. J., Ruohola-Baker, H., & Murry, C. E. (2014). Tri-iodo-I-thyronine promotes the maturation of human cardiomyocytes-derived from induced pluripotent stem cells. *Journal of Molecular and Cellular Cardiology*, 72, 296–304. https://doi.org/10.1016/j.yjmcc.2014.04.005
- Zangi, L., Lui, K. O., Von Gise, A., Ma, Q., Ebina, W., Ptaszek, L. M., Später, D., Xu, H., Tabebordbar, M., Gorbatov, R., Sena, B., Nahrendorf, M., Briscoe, D. M., Li, R. A., Wagers, A. J., Rossi, D. J., Pu, W. T., & Chien, K. R. (2013). Modified mRNA directs the fate of heart progenitor cells and induces vascular regeneration after myocardial infarction. *Nature Biotechnology*, 31(10), 898–907. https://doi.org/10.1038/nbt.2682
- Zangi, L., Oliveira, M. S., Ye, L. Y., Ma, Q., Sultana, N., Hadas, Y., Chepurko, E., Später, D., Zhou, B., Chew, W. L., Ebina, W., Abrial, M., Wang, Q. D., Pu, W. T., & Chien, K. R. (2017). Insulin-like growth factor 1 receptor-dependent pathway drives epicardial adipose tissue formation after myocardial injury. *Circulation*, *135*(1), 59–72. https://doi.org/10.1161/CIRCULATIONAHA.116.022064
- Zhang, M., Chen, Y., Xu, H., Yang, L., Yuan, F., Li, L., Xu, Y., Chen, Y., Zhang, C., & Lin, G. (2018). Melanocortin Receptor 4 Signaling Regulates Vertebrate Limb Regeneration. *Developmental Cell*, *46*(4), 397–409. https://doi.org/10.1016/j.devcel.2018.07.021
- Zhang, P., Li, J., Qi, Y., Zou, Y., Liu, L., Tang, X., Duan, J., Liu, H., & Zeng, G. (2016). Vitamin C promotes the proliferation of human adipose-derived stem cells via p53-p21 pathway. *Organogenesis*, *12*(3), 143–151. https://doi.org/10.1080/15476278.2016.1194148
- Zhang, Q., Schepis, A., Huang, H., Yang, J., Ma, W., Torra, J., Zhang, S. Q., Yang, L., Wu, H., Nonell, S., Dong, Z., Kornberg, T. B., Coughlin, S. R., & Shu, X. (2019). Designing a Green Fluorogenic Protease Reporter by Flipping a Beta Strand of GFP for Imaging Apoptosis in Animals. *Journal of the American Chemical Society*, 141(11), 4526–4530. https://doi.org/10.1021/jacs.8b13042
- Zhao, D., Lei, W., & Hu, S. (2021). Cardiac organoid a promising perspective of

- preclinical model. *Stem Cell Research and Therapy*, *12*(1), 1–10. https://doi.org/10.1186/s13287-021-02340-7
- Zhao, J., Cao, H., Tian, L., Huo, W., Zhai, K., Wang, P., Ji, G., & Ma, Y. (2017). Efficient Differentiation of TBX18+/WT1+ Epicardial-Like Cells from Human Pluripotent Stem Cells Using Small Molecular Compounds. *Stem Cells and Development*, *26*(7), 528–540. https://doi.org/10.1089/scd.2016.0208
- Zhou, B., Honor, L. B., He, H., Qing, M., Oh, J. H., Butterfield, C., Lin, R. Z., Melero-Martin, J. M., Dolmatova, E., Duffy, H. S., Von Gise, A., Zhou, P., Hu, Y. W., Wang, G., Zhang, B., Wang, L., Hall, J. L., Moses, M. A., McGowan, F. X., & Pu, W. T. (2011). Adult mouse epicardium modulates myocardial injury by secreting paracrine factors. *Journal of Clinical Investigation*, *121*(5), 1894–1904. https://doi.org/10.1172/JCI45529
- Zhou, B., Honor, L. B., Ma, Q., Oh, J. H., Lin, R. Z., Melero-Martin, J. M., von Gise, A., Zhou, P., Hu, T., He, L., Wu, K. H., Zhang, H., Zhang, Y., & Pu, W. T. (2012). Thymosin beta 4 treatment after myocardial infarction does not reprogram epicardial cells into cardiomyocytes. *Journal of Molecular and Cellular Cardiology*, 52, 43–47. https://doi.org/10.1016/j.yjmcc.2011.08.020
- Zhou, B., Ma, Q., Rajagopal, S., Wu, S. M., Domian, I., Rivera-Feliciano, J., Jiang, D., Von Gise, A., Ikeda, S., Chien, K. R., & Pu, W. T. (2008). Epicardial progenitors contribute to the cardiomyocyte lineage in the developing heart. *Nature*, *454*(7200), 109–113. https://doi.org/10.1038/nature07060
- Zhou, P., & Pu, W. T. (2016). Recounting cardiac cellular composition. *Circulation Research*, *118*(3), 368–370. https://doi.org/10.1161/CIRCRESAHA.116.308139